Polly Roy (Ed.)

Reoviruses: Entry, Assembly and Morphogenesis

Springer

309
Current Topics in Microbiology and Immunology

Polly Roy (Ed.)

Reoviruses: Entry, Assembly and Morphogenesis

With 42 Figures and 4 Tables

Springer

Polly Roy, M.Sc., Ph.D.

Department of Infectious and Tropical Diseases
London School of Hygiene and Tropical Medicine
Keppel Street
London WC1E 7HT
UK

e-mail: polly.roy@lshtm.ac.uk

Cover Illustration:
Composite of Fig. 1C of chapter 6 (Patton and collegues) and Fig. 2A of chapter 1 (Dermody and collegues).

Library of Congress Catalog Number 72-152360

ISSN 0070-217X
ISBN-10 3-540-30772-9 Springer Berlin Heidelberg New York
ISBN-13 978-3-540-30772-3 Springer Berlin Heidelberg New York

Springer is a part of Springer Science+Business Media
springeronline.com

Printed in Germany

Editor: Simon Rallison, Heidelberg
Desk editor: Anne Clauss, Heidelberg
Production editor: Nadja Kroke, Leipzig
Cover design: design & production GmbH, Heidelberg
Typesetting: LE-TEX Jelonek, Schmidt & Vöckler GbR, Leipzig
Printed on acid-free paper SPIN 11316497 27/3150/YL – 5 4 3 2 1 0

Preface

Reoviridae family members are large, complex viruses that infect humans, animals, plants and insects. They are unique in that they lack lipid envelopes and package their genomes of discrete double-stranded segments of RNA within multi-layered capsids. Lack of a lipid envelope has allowed three-dimensional structures of these large complex viruses (diameter, ~600–1,000) to be obtained. Indeed the atomic structure of one of these viruses was the first large, highly complex structure ever solved, and subsequently has served as a model for other similar structures.

The capsids of these viruses undergo cell entry and uncoating, the enzymatic functions necessary for transcription of the genome, and are later involved in egress from host cells. Recent years have seen an increase in our knowledge of the structure of these viruses coupled with substantial progress in unravelling the molecular details of these processes. Intriguingly, despite their diversity in hosts, structures and modes of transmission, striking parallels have emerged in the molecular interactions necessary for the essential processes of virus entry, assembly and release.

Mammalian reovirus had been the major focus for molecular understanding of the *Reoviridae* and has served as a model system for the other members of the family. Indeed, most of our initial understanding of molecular biology and processes involved in virus replication and pathogenesis for the members of the family was generated from reovirus studies. With this platform, two other members of the family causing disease in humans and/or animals have gained in prominence, and the molecular interactions from a structural level through to host–virus interactions as well as the function of the structural and nonstructural proteins in the virus life cycle have been investigated in detail.

This book reviews our current understanding of *Reoviridae* entry, disassembly/assembly and egress in addition to updating high-resolution structures of virus proteins and capsids from three different genera of the family. Two of the nine chapters cover current molecular mechanisms of mammalian reovirus entry and assembly. One chapter (by K.M. Guglielmi et al.) deals with the high-resolution structures of individual components of the reovirus outer capsid and a viral receptor and provides insight into the roles of these molecules in viral entry, disassembly and pathogenesis. The second chap-

ter (by K.M. Coombs) is a comprehensive review of the assembly of a mature infectious reovirus. In it, high-resolution structures of many reovirus proteins are combined with the complete genomic sequence and sequence lesions in temperature-sensitive assembly-defective reovirus mutants to provide an overall picture of the molecular interactions that promote or abrogate reovirus capsid assembly. An additional chapter (by J. Benavente and J. Martnez-Costas), provides an authoritative review of an avian reovirus that causes considerable economic losses in poultry farming, complementing the various stages of reovirus replication, from virus entry mechanism, assembly to a possible route of virus morphogenesis.

Four chapters are dedicated to Rotaviruses, the cause of severe diarrheal disease in infants and young children, which may cause up to 600,000 deaths worldwide annually. Its importance to childhood health has fueled substantial progress in our understanding of the structural and functional aspects of a variety of the molecular processes that are involved in the rotavirus life cycle. One chapter (by S. Lopez and C. Arias) discusses the complex nature of rotavirus entry into the host cell, which involves several cell surface receptors and several domains of the viral outer layer proteins. The authors then describe the sequential interactions between the cellular receptors and viral proteins that occur, probably in glycosphingolipid-enriched lipid microdomains. Although the exact roles played by individual cell surface molecules, their conformational changes and the mechanism of virus internalization are not completely understood, the authors discuss the likelihood that cooperative actions among multiple cell surface molecules in lipid rafts may decide the cell and tissue tropism of these viruses. The following stages of virus life cycle, rotavirus replication and assembly, each of which possesses several unique and intriguing features, are summarized in a second chapter (by J.T. Patton et al.). This review focuses on virus inclusion bodies known as viroplasms and how these structures act as the major centres for virus replication, assembly and morphogenesis. The third rotavirus chapter (by J.B. Pesavento et al.) deals mainly with the structural features of the viral capsids, viral proteins and genomic organization and the overall impact of these structural features on virus replication, assembly and morphogenesis. The last chapter (by S. Chwetzoff and G. Trugnan) on rotavirus release discusses very recent observations regarding how the final steps of rotavirus assembly take place in the cytosol but not in the endoplasmic reticulum and how a rotavirus structural protein takes advantage of lipid raft trafficking pathways for nonlytic virus release and thus by-passes the classical exocytic route.

Two chapters are dedicated to orbiviruses. Like other members of the *Reoviridae*, bluetongue virus, the type species of the *Orbivirus* genus, faces the same constraints on structure and assembly that are imposed by a large

dsRNA genome. The chapter by P. Roy and R. Noad focuses on the current understanding of BTV capsid protein assembly pathways and highlights the host–virus interactions that govern virus assembly and morphogenesis. However, since it is arthropod-transmitted, BTV must have assembly pathways that are sufficiently flexible to allow it to replicate in evolutionarily distant hosts. With this background, it is perhaps not surprising that BTV interacts with highly conserved cellular pathways during morphogenesis and trafficking. Perhaps the most intriguing discovery has been that the pathways involved in the entry and egress of nonenveloped BTV are similar to those used by enveloped viruses. In addition, recent studies with the protein that is the major component of the BTV viroplasm have revealed how the assembly and, as importantly, the disassembly of this structure may be controlled. The second chapter on orbiviruses (D.I. Stuart and J.M. Grimes) summarizes various aspects of the organization and structure of the BTV capsids, as revealed by X-ray and electron microscopy analyses. The atomic structure of the BTV core particle, the first structure for the members of the family resolved at atomic level, not only revealed the complex organization of the core proteins but also provided a plausible model for the organization of the dsRNA viral genome and the arrangement of the viral transcriptase complex. Electron cryomicroscopy on the viral particle has shown how the two viral proteins VP2 and VP5 are arranged to form the outer capsid, with distinct packing arrangements between them and the core. The authors also propose a more detailed model of these structures and relate this to possible mechanisms of cell entry. Overall, these chapters demonstrate that the integration of structural, biochemical and molecular data is necessary to fully understand the assembly and replication of these complex RNA viruses.

I am grateful to each of the contributors for undertaking the task of writing their various chapters with great enthusiasm. I am also indebted to Dr. Ulrich Desselberger, who meticulously reviewed every chapter and provided highly constructive criticisms that have improved the quality of the book. He also provided a fitting tribute to Jean Cohen, whose untimely recent loss is mourned by all in the field. Dr. Cohen was a major investigator in Rotavirus research, enormously respected by his peers and will be sadly missed.

Finally, I am grateful to Dr. Peter Vogt, who persuaded me to draw this book together. Without his encouragement I may never have been minded to put together the great scientific achievements that work on these viruses has achieved in recent years.

London, UK, 2006 *Polly Roy*

Jean Cohen, PhD, 1941–2004† A Pioneer in Rotavirus Research

After a prolonged illness, from which he was recovering, Jean Cohen suddenly and prematurely passed away on November 11, 2004.

After studying physics and biochemistry and earning a PhD at the Université d'Orsay, Paris, Jean entered the Institut National de la Recherche Agronomique (INRA) at Thiverval-Grignon in 1969. In 1984 he became Directeur de Recherche. In the late 1980s, INRA moved to a large research facility in Jouy-en-Josas. In 2003, Jean's group transferred to the Institut National de la Recherche Scientifique (CNRS), Gif-sur-Yvette, to form a Unit Mixte de Recherche (UMR), Virologie Molculaire et Structurale, with Flix Reys group.

Jean Cohen devoted nearly his entire professional life to the research on rotaviruses (RV). Between 1975 and 2004 he published or co-published over 100 scientific papers in peer-refereed journals.

Early in his career, Jean made the important discovery that purified RV subviral particles (double-layered particles, DLPs) have transcriptase activity in vitro [1, 2]. Similar data had been obtained with infectious pancreatic necrosis virus of the *Birnaviridae* family, described in his first publication [3], and before with reovirus [4] and bluetongue virus [5]. The first two papers are still frequently cited after 25years. Another classic study [6] demonstrated that RV cores can be prepared from purified DLPs, but have then lost their transcriptase activity. Jean's interest in RV structures became apparent at an early stage of his career, when he correctly deduced the number of capsomers and the triangulation number of the capsid structure from high-quality electron micrographs of freeze-dried RV particles [7].

Expression of single or multiple RV genes in recombinant baculovirus-infected insect cells [8–12] led to studies on virus-like particles (VLPs) of different composition [9, 12–15], but also to novel structure–function data, e.g., the production of chimeric group A/C RV particles [12], or the reconstitution in vitro of RV transcriptase activity by reacting purified native viral cores with baculovirus recombinant-expressed VP6 [16]. The transcriptase activity of DLPs can be inhibited in vitro with VP6-specific monoclonal antibodies (Mabs) [17]. The molecular mechanism of this effect was later elucidated at the structural level by elegant studies from Elisabeth Hewat's group [18].

The RV core as the molecular machine [19] of the virus attracted Jean's particular interest early on. In collaboration with Mary Estes' group, core particles were characterized morphologically (by electron microscopy) in detail [13], and VP1/VP2 complexes were identified as the minimal replicase-active entity [15], also as complexes with NSP2 [20], and binding nucleic acid [21]. Early structure–function studies of NSP5 pointed toward the importance of this protein in early morphogenesis [22], exerting, among other functions, a strong affinity for VP2 [23]. NSP3, the RV protein involved in initiation of virus-specific translation, was intensely investigated [24–28] and led to the identification of a novel cellular protein (RoXaN; [29, 30]), interacting with NSP3, by his collaborator Didier Poncet who now has his own research team.

The construction of RV VLPs carrying 120 molecules of VP2 fused to green fluorescent protein (GFP) allowed infections to be followed in real time [31], including quantitation of viral propagation in single living cells [32]. This reagent has become very popular and is used by various research groups throughout the world. Two examples may suffice: in collaboration with Soizick Le Guyaders and Albert Boschs groups, GFP-labeled VP2/6 VLPs were applied as tracers for tracking viral transmission pathways in the environment [33, 34], and Manuel Franco's group used them to determine which cells of the immune system interact with RVs [35].

The collaboration with Flix Rey's group was very productive and, as a highlight, solved the atomic structure of the VP6 protein [36–40]. Knowledge of the VP6 structure permitted a rational approach to studies on VP6 assembly (with Jean Lepault, [38, 39]) and on VP6/VP2 interactions (with B. Venkataram Prasad, [41]). Studies on VP6/VP7 and VP6/VP4 interactions were planned by Jean and are now in progress. In the absence of crystal-derived structures of viral cores, structural implications of the core architecture were deduced from elegant studies on DLP variants and defined at the molecular level [42, 43].

The outer membrane proteins VP7 and VP4, their interactions with cellular membranes, as well as unusual intracellular transport mechanisms were intensely investigated, and the results were published in a large number of papers, many of them in collaboration with the groups of Fabian Michelangeli and Marie Christine Ruiz [44–51] and Germain Trugnan and Cathrine Sapin [52–56].

Jean was keen to connect RV molecular research with the exploration of immune responses in animal model studies. Thus, in collaboration with a number of other groups, the antigenicity and immunogenicity of isolated RV proteins and various VLPs were studied [57–61]. In addition, this work drew attention to the possibilities of developing VLP-based, safe RV vaccines. In collaboration with Claude Andrieux' group, RV infection and diarrhea in germfree rats were established as a heterologous animal model [62, 63], later

expanded by Max Ciarlet et al. [64]. Following Harry Greenberg's discovery that VP6-specific IgA antibodies can provide protection from infection in mice [65], it was found, in collaboration with Isabelle Schwartz-Cornil, that transcytosis of mucosal immunoglobulins is a prerequisite for this effect [66].

Jean's closest collaborator, Annie Charpilienne, worked with him as an engineer for 27years and is a coauthor on many of his papers. On a personal note, as a Visiting Research Fellow in Jean's laboratory in 2003–2004, I was enabled to pursue ideas on a reverse genetics (*gntique inverse*) system for rotaviruses in a free and highly interactive, enjoyably manner. Jean did not live to see the resolution of this problem of great interest to him and his laboratory.

Jean's research was rich in major achievements which have met with wide international recognition. His work was driven by his many original and creative ideas and an ever-searching mind, and was supported by his exceptional skills at the bench. He was enthusiastic for his work and was an inspiration to all those who knew and worked with him. In his unassuming way, he was enormously generous with his time for other researchers' questions and problems, and his advice and collaboration were in great demand. He listened carefully, engaged ideas, and sought and enjoyed hardy debates. He was widely read and possessed a deep sense of humour. He is sorely missed by his family, friends, and colleagues. Finally, his death is an enormous loss for the science of rotavirus research.

References

1. Cohen J (1977) Ribonucleic acid polymerase activity associated with purified calf rotavirus. J Gen Virol 36:395–402
2. Cohen J, Laporte J, Charpilienne A, Scherrer R (1979) Activation of rotavirus RNA polymerase by calcium chelation. Arch Virol 60:177–186
3. Cohen J (1975) Ribonucleic acid polymerase activity in purified infectious pancreatic necrosis virus of trout. Biochem Biophys Res Commun 62:689–695
4. Skehel JJ, Joklik WK (1969) Studies on the in vitro transcription of reovirus RNA catalyzed by reovirus cores. Virology 39:822–831
5. Verwoerd DW, Huismans H (1972) Studies on the in vitro and in vivo transcription of the bluetongue virus genome. Onderstepoort J Vet Res 39:185–192
6. Bican P, Cohen J, Charpilienne A, Scherrer R (1982) Purification and characterization of bovine rotavirus cores. J Virol 43:1113–1117
7. Roseto A, Escaig J, Delain E, Cohen J, Scherrer R (1979) Structure of rotaviruses as studied by the freeze-drying technique. Virology 98:471–475
8. Cohen J, Charpilienne A, Chilmonczyk S, Estes MK (1989) Nucleotide sequence of bovine rotavirus gene 1 and expression of the gene product in baculovirus. Virology 171:131–140

9. Labb M, Charpilienne A, Crawford SE, Estes MK, Cohen J (1991) Expression of rotavirus VP2 produces empty corelike particles. J Virol 65:2946–2952
10. Dharakul T, Labb M, Cohen J, Bellamy AR, Street JE, Mackow ER, Fiore L, Rott L, Greenberg HB (1991) Immunization with baculovirus-expressed recombinant proteins VP1, VP4, VP6, and VP7 induces CD8+ T lymphocytes that mediate clearance of chronic rotavirus infection in SCID mice. J Virol 65:5928–5932
11. Brottier P, Nandi P, Bremont M, Cohen J (1992) Bovine rotavirus segment 5 protein expressed in the baculovirus system interacts with zinc and RNA. J Gen Virol .73:1931–1938
12. Tosser G, Labb M, Bremont M, Cohen J (1992) Expression of the major capsid protein VP6 of group C rotavirus and synthesis of chimeric single-shelled particles by using recombinant baculoviruses. J Virol 66:5825–5831
13. Zeng CQ, Labb M, Cohen J, Prasad BV, Chen D, Ramig RF, Estes MK (1994) Characterization of rotavirus VP2 particles. Virology 201:55–65
14. Crawford SE, Labb M, Cohen J, Burroughs MH, Zhou YJ, Estes MK (1994) Characterization of virus-like particles produced by the expression of rotavirus capsid proteins in insect cells. J Virol 68:5945–5952
15. Zeng CQ, Wentz MJ, Cohen J, Estes MK, Ramig RF (1996) Characterization and replicase activity of double-layered and single-layered rotavirus-like particles expressed from baculovirus recombinants. J Virol 70:2736–2742
16. Kohli E, Pothier P, Tosser G, Cohen J, Sandino AM, Spencer E (1993) In vitro reconstitution of rotavirus transcriptional activity using viral cores and recombinant baculovirus expressed VP6. Arch Virol 133:451–458
17. Kohli E, Pothier P, Tosser G, Cohen J, Sandino AM, Spencer E (1994) Inhibition of in vitro reconstitution of rotavirus transcriptionally active particles by anti-VP6 monoclonal antibodies. Arch Virol 135:193–200
18. Thouvenin E, Schoehn G, Rey F, Petitpas I, Mathieu M, Vaney MC, Cohen J, Kohli E, Pothier P, Hewat E (2001) Antibody inhibition of the transcriptase activity of the rotavirus DLP: a structural view. J Mol Biol 307:161–172
19. Bamford D, Mindich L (eds) (2004) Viral molecular machines: replication systems within the inner cores of dsRNA viruses. Virus Res 101:1–100
20. Aponte C, Poncet D, Cohen J (1996) Recovery and characterization of a replicase complex in rotavirus-infected cells by using a monoclonal antibody against NSP2. J Virol 70:985–991
21. Labb M, Baudoux P, Charpilienne A, Poncet D, Cohen J (1994) Identification of the nucleic acid binding domain of the rotavirus VP2 protein. J Gen Virol 75:3423–3430
22. Poncet D, Lindenbaum P, L'Haridon R, Cohen J (1997) In vivo and in vitro phosphorylation of rotavirus NSP5 correlates with its localization in viroplasms. J Virol 71:34–41
23. Berois M, Sapin C, Erk I, Poncet D, Cohen J (2003) Rotavirus nonstructural protein NSP5 interacts with major core protein VP2. J Virol 77:1757–1763
24. Mattion NM, Cohen J, Aponte C, Estes MK (1992) Characterization of an oligomerization domain and RNA-binding properties on rotavirus nonstructural protein NS34. Virology 190:68–83
25. Poncet D, Aponte C, Cohen J (1993) Rotavirus protein NSP3 (NS34) is bound to the 3 – end consensus sequence of viral mRNAs in infected cells. J Virol 67:3159–3165

26. Poncet D, Laurent S, Cohen J (1994) Four nucleotides are the minimal requirement for RNA recognition by rotavirus non-structural protein NSP3. EMBO J 13:4165–4173
27. Poncet D, Aponte C, Cohen J (1996) Structure and function of rotavirus nonstructural protein NSP3. Arch Virol 12 [Suppl]:29–35
28. Piron M, Vende P, Cohen J, Poncet D (1998) Rotavirus RNA-binding protein NSP3 interacts with eIF4GI and evicts the poly(A) binding protein from eIF4F. EMBO J 17:5811–5821
29. Poncet D (2003) Translation of rotavirus mRNA in the infected cell. In: Desselberger U, Gray J (eds) Viral gastroenteritis. Elsevier, Amsterdam, pp185–205
30. Vitour D, Lindenbaum P, Vende P, Becker MM, Poncet D (2004) RoXaN, a novel cellular protein containing TPR, LD, and zinc finger motifs, forms a ternary complex with eukaryotic initiation factor 4G and rotavirus NSP3. J Virol 78:3851–3862
31. Charpilienne A, Nejmeddine M, Berois M, Parez N, Neumann E, Hewat E, Trugnan G, Cohen J (2001) Individual rotavirus-like particles containing 120 molecules of fluorescent protein are visible in living cells. J Biol Chem 276:29361–29367
32. Dundr M, McNally JG, Cohen J, Misteli T (2002) Quantitation of GFP-fusion proteins in single living cells. J Struct Biol 140:92–99
33. Caballero S, Abad FX, Loisy F, Le Guyader FS, Cohen J, Pinto RM, Bosch A (2004) Rotavirus-like particles as surrogates in environmental persistence and inactivation studies. Appl Environ Microbiol 70:3904–3909
34. Loisy F, Atmar RL, Cohen J, Bosch A, Le Guyader FS (2004) Rotavirus VP2/6: a new tool for tracking rotavirus in the marine environment. Res Microbiol 155:575–578
35. Gonzalez AM, Jaimes MC, Cajiao I, Rojas OL, Cohen J, Pothier P, Kohli E, Butcher EC, Greenberg HB, Angel J, Franco MA (2003) Rotavirus-specific B cells induced by recent infection in adults and children predominantly express the intestinal homing receptor alpha4beta7. Virology 305:93–105
36. Petitpas I, Lepault J, Vachette P, Charpilienne A, Mathieu M, Kohli E, Pothier P, Cohen J, Rey FA (1998) Crystallization and preliminary X-ray analysis of rotavirus protein VP6. J Virol 72:7615–7619
37. Mathieu M, Petitpas I, Navaza J, Lepault J, Kohli E, Pothier P, Prasad BV, Cohen J, Rey FA (2001) Atomic structure of the major capsid protein of rotavirus: implications for the architecture of the virion. EMBO J 20:1485–1497
38. Lepault J, Petitpas I, Erk I, Navaza J, Bigot D, Dona M, Vachette P, Cohen J, Rey FA (2001) Structural polymorphism of the major capsid protein of rotavirus. EMBO J 20:1498–1507
39. Erk I, Huet JC, Duarte M, Duquerroy S, Rey F, Cohen J, Lepault J (2003) A zinc ion controls assembly and stability of the major capsid protein of rotavirus. J Virol 77:3595–3601
40. Rey FA, Lepault J, Cohen J (2003) The three-dimensional structure of rotavirus VP6. In: Desselberger U, Gray J (eds) Viral gastroenteritis. Elsevier, Amsterdam, pp129–141
41. Lawton JA, Zeng CQ, Mukherjee SK, Cohen J, Estes MK, Prasad BV (1997) Three-dimensional structural analysis of recombinant rotavirus-like particles with intact and amino-terminal-deleted VP2: implications for the architecture of the VP2 capsid layer. J Virol 71:7353–7360

42. Charpilienne A, Lepault J, Rey F, Cohen J (2002) Identification of rotavirus VP6 residues located at the interphase with VP2 that are essential for capsid assembly and transcriptase activity. J Virol 76:7822–7831
43. Zeng CQ, Estes MK, Charpilienne A, Cohen J (1998) The N terminus of rotavirus VP2 is necessary for encapsidation of VP1 and VP3. J Virol 72:201–208
44. Ruiz MC, Charpilienne A, Liprandi F, Gajardo R, Michelangeli F, Cohen J (1996) The concentration of Ca2+ that solubilizes outer capsid proteins from rotavirus particles is dependent on the strain. J Virol 70:4877–4883
45. Gajardo R, Vende P, Poncet D, Cohen J (1997) Two proline residues are essential in the calcium-binding activity of rotavirus VP7 outer capsid protein. J Virol 71:2211–2216
46. Ruiz MC, Cohen J, Michelangeli F (2000) Role of Ca2+ in the replication and pathogenesis of rotavirus and other viral infections. Review. Cell Calcium 28:137–149
47. Nandi P, Charpilienne A, Cohen J (1992) Interaction of rotavirus particles with liposomes. J Virol 66:3363–3367
48. Ruiz MC, Alonso-Torre SR, Charpilienne A, Vasseur M, Michelangeli F, Cohen J, Alvarado F (1994) Rotavirus interaction with isolated membrane vesicles. J Virol 68:4009–4016
49. Charpilienne A, Abad MJ, Michelangeli F, Alvarado F, Vasseur M, Cohen J, Ruiz MC (1997) Solubilized and cleaved VP7, the outer glycoprotein of rotavirus, induces permeabilization of cell membrane vesicles. J Gen Virol 78:1367–1371
50. Liprandi F, Moros Z, Gerder M, Ludert JE, Pujol FH, Ruiz MC, Michelangeli F, Charpilienne A, Cohen J (1997) Productive penetration of rotavirus in cutured cells induces coentry of the translation inhibitor alpha-sarcin. Virology 237:430–438
51. Ruiz MC, Abad MJ, Charpilienne A, Cohen J, Michelangeli F (1997) Cell lines susceptible to infection are permeabilized by cleaved and solubilized outer layer proteins of rotavirus. J Gen Virol 78:2883–2893
52. Nejmeddine M, Trugnan G, Sapin C, Kohli E, Svensson L, Lopez S, Cohen J (2000) Rotavirus spike protein VP4 is present at the plasma membrane and is associated with microtubules in infected cells. J Virol 74:3313–3320
53. Sapin C, Colard O, Delmas O, Tessier C, Breton M, Enouf V, Chwetzoff S, Ouanich J, Cohen J, Wolf C, Trugnan G (2002) Rafts promote assembly and atypical targeting of a nonenveloped virus, rotavirus, in Caco-2 cells. J Virol 76:4591–4602
54. Enouf V, Chwetzoff S, Trugnan G, Cohen J (2003) Interactions of rotavirus VP4 spike protein with the endosomal protein Rab5 and the prenylated Rab acceptor PRA1. J Virol 77:7041–7047
55. Delmas O, Gardet A, Chwetzoff S, Breton M, Cohen J, Colard O, Sapin C, Trugnan G (2004) Different ways to reach the top of a cell. Analysis of rotavirus assembly and targeting in human intestinal cells reveals an original raft-dependent, Golgi-independent apical targeting pathway. Virology 327:157–161
56. Delmas O, Durand-Schneider AM, Cohen J, Colard O, Trugnan G (2004) Spike protein VP4 assembly with maturing rotavirus requires a postendoplasmic reticulum event in polarized Caco-2 cells. J Virol 78:10987–10994

57. Conner ME, Crawford SE, Barone C, O'Neal C, Zhou YJ, Fernandez F, Parwani A, Saif LJ, Cohen J, Estes MK (1996) Rotavirus subunit vaccines. Arch Virol 12 [Suppl]:199–200
58. Crawford SE, Estes MK, Ciarlet M, Barone C, O'Neal CM, Cohen J, Conner ME (1999) Heterotypic protection and induction of a broad heterotypic neutralization response by rotavirus-like particles. J Virol 73:4813–4822
59. Coste A, Sirard JC, Johanson K, Cohen J, Kraehenbuhl JP (2000) Nasal immunization of mice with virus-like particles protects offspring against rotavirus diarrhea. J Virol 74:8966–8971
60. Coste A, Cohen J, Reinhardt M, Kraehenbuhl JP, Sirard JC (2001) Nasal immunization with Salmonella typhimurium producing rotavirus VP2 and VP6 antigens stimulates specific antibody response in serum and milk but fails to protect offspring. Vaccine 19:4167–4174
61. Fromantin C, Jamot B, Cohen J, Piroth L, Pothier P, Kohli E (2001) Rotavirus 2/6 virus-like particles administered intranasally in mice, with or without the mucosal adjuvants cholera toxin and Escherichia coli heat-labile toxin, induce a Th1/Th2-like immune response. J Virol 75:11010–11016
62. Gurin-Danan C, Meslin JC, Lambre F, Charpilienne A, Serezat M, Bouley C, Cohen J, Andrieux C (1998) Development of a heterologous model in germfree suckling rats for studies of rotavirus diarrhea. J Virol 72:9298–9302
63. Gurin-Danan C, Meslin JC, Chambard A, Charpilienne A, Relano P, Bouley C, Cohen J, Andrieux C (2001) Food supplementation with milk fermented by Lactobacillus casei DN-114 001 protects suckling rats from rotavirus-associated diarrhea. J Nutr 131:111–117
64. Ciarlet M, Conner ME, Finegold MF, Estes MK (2002) Group A rotavirus infection and age-dependent diarrhoeal disease in rats: a new animal model to study the pathophysiology of rotavirus infection. J Virol 76:41–57
65. Burns JW, Siadat-Pajouh M, Krishnaney AA, Greenberg HB (1996) Protective effect of rotavirus VP6-specific IgA monoclonal antibodies that lack neutralizing activity. Science 272:104–107
66. Schwartz-Cornil I, Benureau Y, Greenberg H, Hendrickson BA, Cohen J (2002) Heterologous protection induced by the inner capsid proteins of rotavirus requires transcytosis of mucosal immunoglobulins. J Virol 76:8110–8117

(A complete list of Jean Cohen's publications is available upon request.)

Trieste, November 2005 *Ulrich Desselberger*

List of Contents

List of Contributors

(Addresses stated at the beginning of respective chapters)

CTMI (2006) 309:1–38

Attachment and Cell Entry of Mammalian Orthoreovirus

K. M. Guglielmi[1,3] · E. M. Johnson[1,3] · T. Stehle[2,3,4] · T. S. Dermody[1,3,4] (✉)

[1]Departments of Microbiology and Immunology, and Pediatrics[4], Vanderbilt University School of Medicine, Nashville, TN 37232, USA

[2]Interfakultäres Institut für Biochemie, Eberhard-Karls Universität Tübingen, 72076 Tübingen, Germany

[3]Lamb Center for Pediatric Research, D7235 MCN, Vanderbilt University School of Medicine, Nashville, TN 37232, USA
terry.dermody@vanderbilt.edu.

Abstract Mammalian orthoreoviruses (reoviruses) serve as a tractable model system for studies of viral pathogenesis. Reoviruses infect virtually all mammals, but cause disease only in the very young. Prototype strains of the three reovirus serotypes differ in pathogenesis following infection of newborn mice. Reoviruses are nonenveloped, icosahedral particles that consist of ten segments of double-stranded RNA encapsidated within two protein shells, the inner core and outer capsid. High-resolution structures of individual components of the reovirus outer capsid and a single viral receptor have been solved and provide insight into the functions of these molecules in viral attachment, entry, and pathogenesis. Attachment of reovirus to target cells is mediated by the reovirus σ1 protein, a filamentous trimer that projects from the outer capsid. Junctional adhesion molecule-A is a serotype-independent receptor for reovirus, and sialic acid is a coreceptor for serotype 3 strains. After binding to receptors on the cell surface, reovirus is internalized via receptor-mediated endocytosis. Internalization is followed by stepwise disassembly of the viral outer capsid in the endocytic compartment. Uncoating events, which require acidic pH and endocytic proteases, lead to removal of major outer-capsid protein σ3, resulting in exposure of membrane-penetration mediator μ1 and a conformational change in attachment protein σ1. After penetration of endosomes by uncoated particles, the transcriptionally active viral core is released into the cytoplasm, where replication proceeds. Despite major advances in defining reovirus attachment and entry mechanisms, many questions remain. Ongoing research is aimed at understanding serotype-dependent differences in reovirus tropism, viral cell-entry pathways, the individual and corporate roles of acidic pH and proteases in viral entry, and μ1 function in membrane penetration.

1 Introduction

Mammalian orthoreoviruses (called reoviruses here) serve as highly tractable models for studies of viral pathogenesis. Reoviruses are nonenveloped, icosahedral viruses that contain a genome of ten double-stranded (ds) RNA gene segments. There are three reovirus serotypes, which can be differentiated by the capacity of anti-reovirus antisera to neutralize viral infectivity and inhibit hemagglutination [120, 126]. The three serotypes are each represented by a prototype strain isolated from a human host: type 1 Lang (T1L), type 2 Jones (T2J), and type 3 Dearing (T3D). Reoviruses have a wide geographic distribution, and virtually all mammals, including humans, serve as hosts for infection [146]. However, reovirus is rarely associated with disease, except in the very young [89, 142].

Newborn mice are exquisitely sensitive to reovirus infection and have been used as the preferred experimental system for studies of reovirus pathogenesis [151]. Following oral or intramuscular inoculation of newborn mice, strains of serotype 1 and serotype 3 reoviruses invade the central nervous sys-

tem (CNS), yet by different routes and with distinct pathologic consequences. Serotype 1 reovirus spreads to the CNS hematogenously and infects ependymal cells [147, 155], resulting in hydrocephalus [153]. In contrast, serotype 3 reovirus spreads to the CNS by neural routes and infects neurons [99, 147, 155], causing lethal encephalitis [142, 153]. Studies using T1L x T3D reassortant viruses have shown that the pathways of viral spread [147] and tropism for neural tissues [45, 155] segregate with the viral S1 gene, which encodes attachment protein σ1 [83, 154]. T1L x T3D reassortant viruses also were used to demonstrate that serotype-specific differences in virus binding to primary cultures of ependymal cells and neurons are determined by the S1 gene [45, 141]. These studies suggest that σ1 dictates the CNS cell types that serve as targets for reovirus infection, presumably by its capacity to bind to receptors expressed by specific CNS cells.

In addition to conferring viral attachment, engagement of reovirus receptors also induces postbinding signaling events that may influence disease pathogenesis. Reovirus induces apoptosis in cultured cells [32, 36, 119, 148] and in vivo [38, 109]. Strain T3D induces apoptosis to a greater extent than strain T1L in murine L929 (L) cells [148], Madin-Darby canine kidney cells [119], and human HeLa cells [34]. Differences in the capacity of these strains to induce apoptosis are determined primarily by the S1 gene [34, 119, 148], suggesting a critical role for receptor-linked signaling in the apoptotic response elicited by reovirus. However, viral disassembly steps that occur following cell attachment are also required for the induction of apoptosis by reovirus [35].

Following attachment to host cells, reovirus particles must penetrate cell membranes and uncoat to activate the viral transcription machinery. Mechanisms underlying these events are dependent on receptor-mediated endocytosis, host-cell proteases resident in the endocytic pathway, and a novel membrane penetration process that requires stepwise disassembly of the viral outer capsid. The σ3 protein is the outermost capsid component and acts as a protective cap for the μ1 protein, which facilitates membrane penetration. Following removal of σ3 by endocytic proteases [50, 68], μ1 undergoes a conformational rearrangement to facilitate entry of the core particle into the cytoplasm [26].

Here we review mechanisms of reovirus attachment and cell entry. Studies of these reovirus replication steps have been significantly advanced by the availability of high-resolution structures of the viral outer-capsid proteins and at least one of the viral receptors. This work, coupled with biochemical and genetic analyses of the reovirus attachment and entry process, has allowed an enhanced understanding of how viral protein structure and function relate to viral disease.

2
Structure and Function of Reovirus Attachment Protein σ1

2.1
Structure of the σ1 Trimer

Reovirus particles are approximately 850 Å in diameter [104]. The ten segments of dsRNA that compose the reovirus genome are encapsidated within two concentric protein shells, the outer capsid and inner core. Together, the outer capsid and core are composed of eight structural proteins. The bulk of the outer capsid consists of the tightly associated μ1 and σ3 proteins [86]. In addition, there are turrets at each of the 12 icosahedral vertices of the virion formed by the pentameric λ2 protein, from which the viral attachment protein, σ1, extends [8, 29, 47, 60, 61].

The σ1 protein is a fibrous, trimeric molecule about 480 Å in length with distinct head-and-tail morphology [60, 61] (Fig. 1). Discrete regions of the molecule mediate binding to cell-surface receptors. Sequences in the N-terminal σ1 tail bind to carbohydrate, which is known to be sialic acid in either α2,3 or α2,6 linkages for serotype 3 reoviruses [29, 30, 43, 64, 116]. The C-terminal σ1 head binds to junctional adhesion molecule-A (JAM-A, previously called JAM1) [8]. The σ1 tail partially inserts into the virion, while the head projects away from the virion surface [46, 61]. Insertion of the trimeric σ1 protein into a pentameric λ2 base results in an unusual symmetry mismatch. Such symmetry mismatches often produce interactions of limited strength or specificity and indicate a strong potential to undergo structural rearrangement.

Structural analysis of the C-terminal half of T3D σ1 (residues 246–455) reveals a trimeric structure, in which each monomer is composed of a slender tail and a compact head [31] (Fig. 2). The C-terminal residues that form the head domain (310–455) consist of two Greek-key motifs that fold into a β-barrel. Loops connecting the individual strands of the β-barrel are short with the exception of the loop that connects β-strands D and E, which contains a 3_{10} helix (Fig. 2). N-terminal residues in the crystallized fragment form a portion of the tail, residues 246–309, which consists of three β-spiral repeats. Each repeat is composed of two short β-strands connected by a four-residue β-turn that has either a proline or a glycine residue at its third position [31]. A surface-exposed, variable loop links successive repeats, and trimerization generates an unusual triple β-spiral motif that has been observed in only one other molecule to date, the adenovirus attachment protein, fiber [150]. The σ1 trimer features a distinct bend between the three-fold axes of the head and tail domains. Although this bend is most likely introduced by crystal packing forces, it indicates that the σ1 trimer possesses a high degree of flexibility. The region

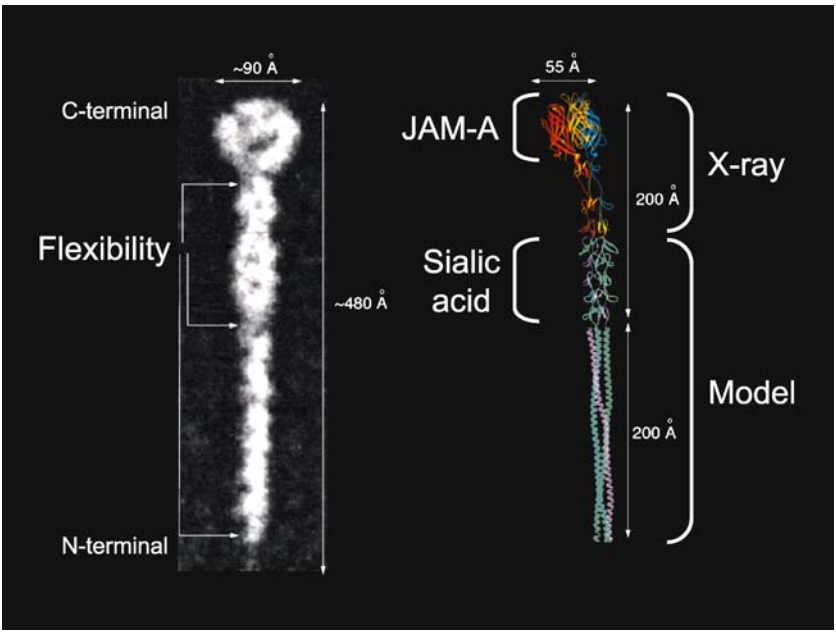

Fig. 1 Structure of reovirus σ1. *Left:* Computer-processed electron micrograph of σ1 showing regions of flexibility and approximate molecular dimensions. Image adapted from Fraser et al. [60]. *Right*: Full-length model of reovirus σ1 generated by adding five β-spiral repeats, followed by a trimeric coiled coil formed by elongating an existing coiled-coil structure [156], to the N-terminus of the crystallized fragment of σ1 [31]. Regions of the molecule that interact with JAM-A and sialic acid, and approximate molecular dimensions are indicated. This model was prepared using RIBBONS [22]

of flexibility is located between the second and third β-spiral repeats in the tail and corresponds to a four-residue insertion, amino acids 291–294 [31] (Fig. 2).

Sequence analysis has facilitated the development of a model of full-length σ1 [31]. The σ1 tail is thought to contain an N-terminal α-helical coiled-coil followed by eight β-spiral repeats (Fig. 1). Sequences predicted to form the α-helical coiled coil are required for trimer stability [29, 84, 138, 159]. Electron microscopic (EM) images of full-length σ1 show flexibility at three regions of the molecule, a region near the N-terminus, a region that correlates with the transition from the predicted α-helical coiled-coil to the triple β-spiral, and a region that corresponds to the insertion between β-spiral repeats 2 and 3 of the crystallized portion of T3D σ1 [31, 60] (Fig. 1). These regions of flexibility could facilitate interactions with receptors or enable structural rearrangements during viral assembly or disassembly (see also Sect. 1.9).

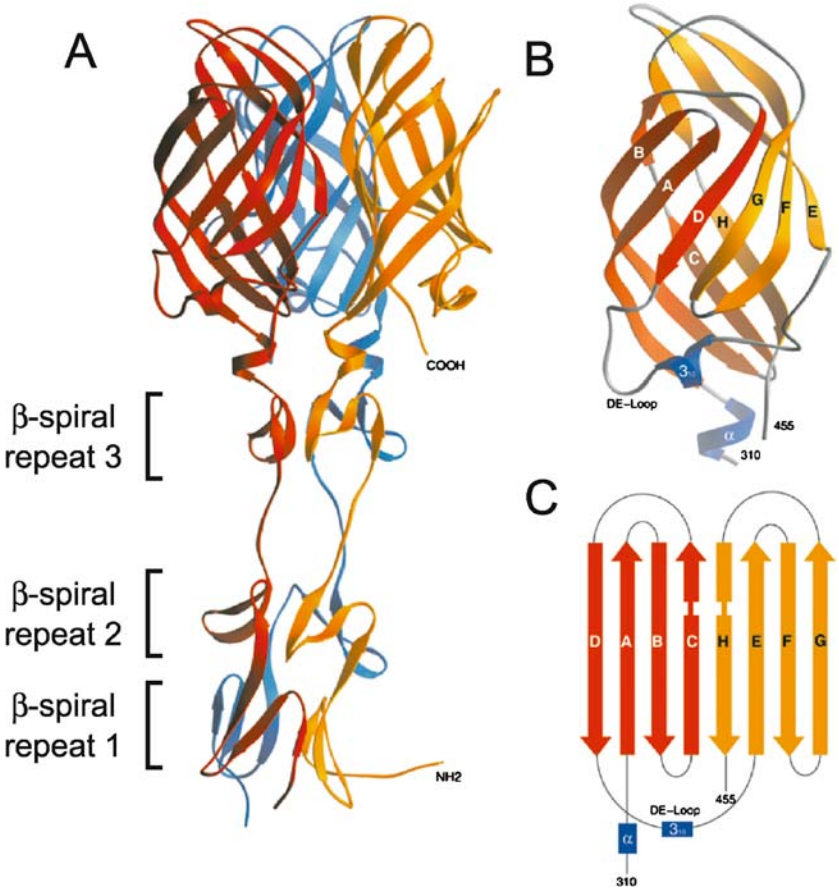

Fig. 2A–C Crystal structure of reovirus σ1. **A** Ribbon drawing of the σ1 trimer with σ1 monomers shown in *red*, *orange*, and *blue*. Each monomer consists of a head domain formed by a compact β-barrel and a fibrous tail with three β-spiral repeats. **B** Enlarged view of the σ1 head domain monomer. The two Greek-key motifs, shown in *red* and *orange*, form a compact, cylindrical β-sheet that contains eight β-strands (*A*–*H*). The head domain also contains two short helices, shown in *blue*: one 3_{10} and one α-helix. **C** Schematic view of the β-strand arrangement in the σ1 head domain. Colors are as in **B**. (Image adapted from Chappell et. al [31])

2.2 Interactions of σ1 with Sialic Acid

Reoviruses exhibit the capacity to agglutinate erythrocytes of several mammalian species [85]. For serotype 3 reoviruses, hemagglutination is mediated

by interactions of the σ1 protein with terminal α-linked sialic acid residues on several glycosylated erythrocyte proteins such as glycophorin A [65, 115]. The carbohydrate receptors for other serotypes of reovirus have not been well characterized. Sialic acid binding is required for reovirus attachment and infection of certain cell types, including murine erythroleukemia (MEL) cells [30, 122]. Although not all serotype 3 strains are capable of binding to sialic acid, the majority bind to this carbohydrate and produce hemagglutination. Sequence polymorphism within the σ1 tail determines the capacity of field-isolate reovirus strains to bind to sialic acid and infect MEL cells [42, 122]. Furthermore, non-sialic acid-binding serotype 3 variants can be adapted to growth in MEL cells during serial passage. These variants have gained the capacity to bind to sialic acid and contain sequence changes within a discrete region of the σ1 tail (residues 198–204) predicted to form a β-spiral [30]. Residues in this vicinity may form part of a sialic acid-binding site [31, 135]. Experiments using expressed σ1 truncation mutants and chimeric molecules derived from T1L and T3D σ1 proteins have confirmed that the sialic acid-binding domain of serotype 3 σ1 is contained within this predicted β-spiral region of the σ1 tail [29] (Fig. 1).

Serotype 1 reoviruses also appear to bind to sialic acid in some contexts. T1L, but not T3D, binds to the apical surface of microfold (M) cells, but not to enterocytes, in tissue sections of rabbit Peyer's patches [71]. Binding is inhibited by preincubation of the tissue sections with neuraminidase or with lectins that specifically recognize α2–3-linked sialic acid. The capacity of T1L to bind to the apical surface of M cells was shown to segregate with the S1 gene using reassortant genetics and with reovirus particles recoated with recombinant σ1 protein. The interaction between T1L σ1 and sialic acid is especially intriguing as serotype 1 reoviruses are incapable of infecting MEL cells, a property dependent on sialic acid binding that segregates with the S1 gene [123], and are insensitive to the growth-inhibitory effects of neuraminidase treatment of L cells [107].

2.3 Interactions of σ1 with JAM-A

Substantial evidence has accumulated to suggest that the σ1 head also binds to receptors on the cell surface [11, 49, 107, 145]. Neutralization-resistant variants of T3D selected using σ1-specific monoclonal antibody 9BG5 contain mutations in the σ1 head that segregate genetically with alterations in neural tropism [11, 75, 133, 134]. This finding suggests a role for the σ1 head in receptor binding. Truncated forms of σ1 containing only the head domain are capable of specific cell interactions [48, 49]. Concordantly, proteolysis of T3D

virions leads to release of a C-terminal receptor-binding fragment of σ1 and a resultant loss in infectivity [107]. These findings indicate that the σ1 head promotes receptor interactions that are distinct from interactions with sialic acid mediated by the σ1 tail.

A flow cytometry-based expression-cloning approach was employed to identify a receptor bound by the σ1 head [8]. A non-sialic acid-binding strain of reovirus that contains a serotype 3 σ1 was used as an affinity ligand to avoid the potential complication of isolating heavily glycosylated molecules that might not interact specifically with σ1. A neural precursor cell (NT2) cDNA library was selectively enriched for cDNAs that confer binding of fluoresceinated virions to transfected cells. Four clones were identified that conferred virus binding. Each encoded JAM-A, a member of the immunoglobulin superfamily postulated to regulate formation of intercellular tight junctions [87, 92, 158]. Three lines of evidence support the contention that JAM-A is a functional reovirus receptor [8]. First, JAM-A-specific monoclonal antibodies inhibit reovirus binding and infection. Second, expression of JAM-A in nonpermissive cells allows reovirus growth. Third and most convincingly, the σ1 protein binds directly to JAM-A with an apparent K_D of approximately 6×10^{-8} M. Together, these findings indicate that JAM-A serves as a receptor for the σ1 head. Surprisingly, JAM-A serves as a receptor for both prototype and field-isolate strains of all three reovirus serotypes [8, 165]. Therefore, utilization of JAM-A as a receptor does not appear to explain the serotype-dependent differences in reovirus tropism observed in the CNS. Variation in the affinity of σ1 for JAM-A among reoviruses or interactions with receptors other than JAM-A, possibly including carbohydrate-based coreceptors, may influence reovirus pathogenesis.

3
Structure of the JAM-A Ectodomain

Reovirus receptor JAM-A is an important component of barriers known as the zonula occludens or tight junctions that form between endothelial and epithelial cells [87, 92, 114]. Tight junctions constitute a semipermeable barrier to the transport of water and solutes between cells, help to establish distinct apical and basolateral regions in polarized epithelia, and serve as critical sites for vesicle targeting and signaling [5, 164]. Tight junctions are composed of complex networks of interacting fibrils that encircle the lateral portion of a polarized epithelial cell toward its apical end and seal the paracellular space. Occludin and members of the claudin family are concentrated in the fibrils and make important contributions to tight junction barrier func-

tion [144]. JAM-A interacts with several proteins. The extracellular domain of JAM-A interacts with the leukocyte function-associated antigen-1 (LFA-1, integrin αLβ2) [113]. Cytosolic proteins known to bind to tight junction components, including zonula occludens (ZO)-1 [13, 53], AF-6 [53], multi-PDZ-domain protein 1 (MUPP1) [70, 149], and partitioning-defective protein (PAR)-3 [54, 72], interact with the JAM-A cytoplasmic tail in a PDZ-domain-dependent manner. JAM-A appears to influence the migration of leukocytes across endothelial and epithelial barriers during the course of an inflammatory response [39, 82], although mechanisms by which JAM-A regulates transendothelial migration are not known.

The capacity of reovirus to interact with tight junctions via JAM-A may make important contributions to the pathogenesis of reovirus infection. Reovirus gains access to the basolateral surface of intestinal cells by transport through M cells [162], which would allow virus exposure to the area of highest JAM-A expression. It is also possible that transient disruptions of the tight junction barrier, such as those that occur during migration of immune and inflammatory cells, permit reovirus access to JAM-A from the intestinal lumen. In addition to reovirus, several other viruses bind to receptors expressed at regions of cell–cell contact [132]. Like JAM-A, the coxsackievirus and adenovirus receptor CAR [14] is expressed at tight junctions [33], and nectins, which serve as receptors for herpes simplex virus [67, 152], are expressed at adherens junctions [140, 163]. Interestingly, each of these viruses is capable of i (TJ)nfecting both epithelial surfaces and neurons in some types of hosts. Reovirus interactions with JAM-A may induce tight junction dysregulation, enhancing viral shedding and transmission. After spreading from the intestine, reovirus interactions with JAM-A may lead to a destabilization of tight junctions in CNS endothelium, which could promote breakdown of the blood–brain barrier and permit cerebral edema and neural inflammation, conditions evident in reovirus encephalitis [151].

JAM-A is a member of a family of related proteins. The proteins most closely related to JAM-A are JAM-B (JAM2) and JAM-C (JAM3), which share 44% and 32% amino acid identity with JAM-A, respectively [2, 37, 55]. Each protein consists of two extracellular immunoglobulin-like domains, a short transmembrane region, and a cytoplasmic tail containing a PDZ-domain-binding motif [14, 92, 131, 158]. Crystal structures are available for the extracellular regions of the human and murine homologues of JAM-A [80, 117] (Fig. 3), which both serve as reovirus receptors [8]. Unlike JAM-A, JAM-B and JAM-C do not serve as receptors for reovirus [117, 165].

JAM-A crystallizes as a homodimer in which monomers engage in an "arm-wrestling grip" via the membrane-distal, or D1, domain [80, 117] (Fig. 3A, B). This dimeric structure is maintained by a highly unusual interface that is

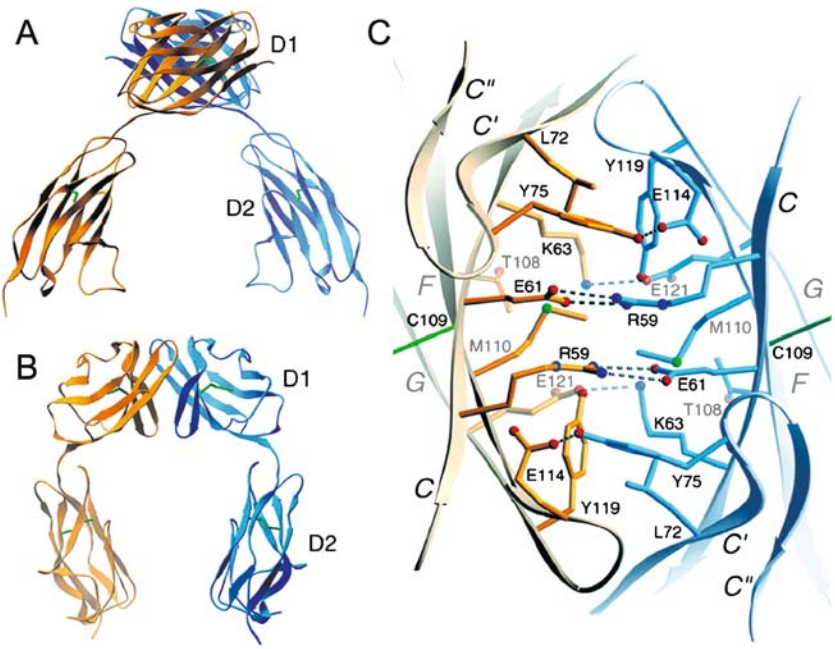

Fig. 3A–C Crystal structure of the hJAM-A extracellular domain. **A, B** Ribbon drawings of the hJAM-A dimer, with one monomer shown in *orange* and the other in *blue*. Two orthogonal views are displayed. Disulfide bonds are shown in *green*. **C** View of the interface between two hJAM-A monomers. The interface is formed by residues on the GFCC' faces of two membrane-distal (D1) domains. The view is along a crystallographic dyad. Hydrogen bonds and salt bridges are represented by broken cylinders. Amino acids are labeled in single-letter code. (Image from Prota et. al [117])

rich in charged residues [117] (Fig. 3C). The principal means of association between JAM-A monomers involves four salt bridges at the center of the interface. These interactions are mediated by the side chains of Arg59, Glu61, Lys63, and Glu121, all of which are buried and solvent-inaccessible [117]. Protein–protein contacts are often mediated by hydrophobic or polar residues, whereas charged amino acids are more typically found at solvent-exposed areas. Although formation of salt bridges is generally viewed as energetically favorable, the stability of these interactions depends very much on the nature of the surrounding environment. Apolar surroundings increase the energy gained by salt bridge formation, whereas highly polar surroundings or low pH values decrease the stability of these contacts. Of note, JAM-A dimers can dissociate into monomers under conditions of moderately high ionic strength or when exposed to low pH [12]. This dynamic nature of the JAM-A interface

may facilitate efficient binding of the viral attachment protein [59]. Sequence alignments show that most of the residues mediating dimer formation are conserved in JAM-B and JAM-C, which has led to the suggestion that these two molecules form similar dimeric structures [80, 117].

4 Model of σ1-JAM-A Interactions

Although structural data for a σ1-JAM-A complex are not yet available, experimental results suggest that σ1 engages monomeric JAM-A. Chemical cross-linking of the JAM-A dimer diminishes the capacity of reovirus to bind to JAM-A in vitro and on cells and negates the competitive effects of soluble JAM-A on reovirus attachment [59]. These observations suggest that the virus cannot interact with a covalently linked dimer, but can recognize a monomeric version of the receptor. Sequences required for reovirus binding have been defined in part by mutating several solvent-accessible residues covering most of the JAM-A D1 surface. Residues selected for this analysis are conserved in human and murine homologues of JAM-A, which both serve as reovirus receptors [8, 117]. Assaying the mutant constructs for the capacity to bind to reovirus in vitro identified residues Ser57 and Tyr75 as especially important for efficient reovirus attachment [59]. Tyr75 is located at the JAM-A dimer interface and forms a hydrogen bond with Glu114 [117] (Fig. 3C). Thus, Tyr75 would not be accessible to ligand in the context of dimeric JAM-A. Ser57 is located close to Tyr75, at the edge of the JAM-A dimer interface. Together, these results provide strong evidence that reovirus σ1 engages a monomeric form of JAM-A, most likely via residues located at or in the vicinity of the JAM-A dimer interface.

Structural observations and sequence analysis also support a model of the σ1-JAM-A interaction in which σ1 engages monomeric JAM-A via the dimer interface. The JAM-A dimer interface is concave and composed of four β-strands (C', C, F, and G). The structure of the monomeric reovirus σ1 head domain features a solvent-exposed surface that is similarly concave and also composed of four β-strands (B, A, D, and G). In fact, the concave β-sheets C'CFG of JAM-A and BADG of σ1 are so similar that they can be superimposed with low root mean square deviations [136]. Sequence analysis of prototype strains of the three reovirus serotypes, which each use JAM-A as a receptor [165], identifies a cluster of conserved residues at the lower edge of the BADG sheet of σ1, including several residues that form the loop connecting β-strands D and E (Fig. 2) [31]. Therefore, it is possible that the σ1 surface mimics features of the JAM-A dimer interface and engages JAM-A in

a manner similar to that used to form JAM-A dimers. Structural analysis of a σ1-JAM-A complex is ongoing to test this hypothesis.

5 Adhesion-Strengthening Mechanism of Stable Reovirus Attachment to Cells

Monoreassortant viruses containing the σ1-encoding S1 gene of either non-sialic acid-binding strain T3C44 ($T3SA^-$) or sialic acid-binding strain T3C44-MA ($T3SA^+$) in a T1L background have been used to study the contribution of sialic acid to stable reovirus attachment to cells [7]. $T3SA^-$ and $T3SA^+$ vary by a single amino acid residue at position 204 (leucine for $T3SA^-$ and proline for $T3SA^+$), which correlates with the capacity to bind to sialic acid [30]. $T3SA^+$ binds to sialic acid with an apparent K_D of approximately 5×10^{-9} M, while $T3SA^-$ displays no specific interaction with this carbohydrate [7]. While the steady-state avidity of these strains for L cells, as determined by competition binding assays, is nearly equivalent (K_D ~3×10^{-11} M), the avidity of $T3SA^+$ for HeLa cells is fivefold higher than that of $T3SA^-$ [7]. Kinetic assessments of binding indicate that the capacity to engage sialic acid functions primarily to increase the k_{on} value of virus attachment to HeLa cells.

The enhanced infectivity of $T3SA^+$ is mediated by the interaction of σ1 with cell-surface sialic acid, since preincubation of virus with sialyllactose (SLL) dramatically reduces the efficiency of $T3SA^+$ infection, yet has no effect on $T3SA^-$ infectivity [7]. However, sialic acid-mediated enhancement of $T3SA^+$ infection occurs only during the initial phases of virus–cell interaction, since SLL does not inhibit productive binding of $T3SA^+$ after the first 30 min of virus adsorption. In contrast, Fab fragments of a monoclonal antibody directed to the σ1 head (9BG5) neutralize $T3SA^+$ infection efficiently, even when added at late times during adsorption [7].

Results of the binding studies performed using $T3SA^+$ and $T3SA^-$ suggest that reovirus attaches to cells using an adhesion-strengthening mechanism, in which initial low-affinity binding to sialic acid facilitates secondary higher-affinity binding to JAM-A (Fig. 4A). For sialic acid-binding reovirus strains, the initial interaction between the virus and the host cell is likely mediated by sialic acid because of the high surface concentration of this carbohydrate. By virtue of its rapid association rate, virus binding to sialic acid would adhere the virion to the cell surface, thereby enabling it to diffuse laterally until it encounters JAM-A. Such lateral diffusion has been reported for influenza virus [127] and phage T4 [161]. After attachment, interactions between reovirus and additional proteins on the cell surface may be required for internalization.

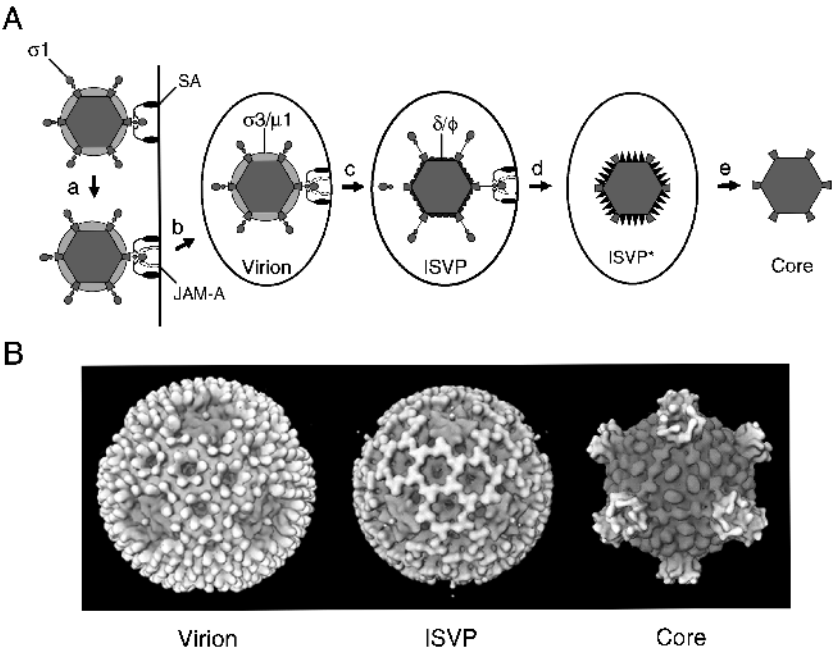

Fig. 4A, B Stepwise disassembly of reovirus. **A** Schematic of the reovirus disassembly steps. (*a*) Following attachment to cell-surface carbohydrate (α-linked sialic acid [SA] for type 3 reoviruses) and junctional adhesion molecule-A (JAM-A), reovirus virions enter cells by receptor-mediated endocytosis (*b*). Within an endocytic compartment, the viral outer-capsid undergoes acid-dependent proteolysis. (*c*) The first disassembly intermediate is the ISVP, which is characterized by loss of σ3 and cleavage of μ1C into particle-associated fragments δ and φ. (*d*) The ISVP then undergoes further conformational changes to form the ISVP*. The ISVP* is characterized by conformational rearrangements of the μ1 fragments to expose hydrophobic residues, release of μ1N, and loss of attachment protein σ1. (*e*) The μ1 cleavage fragments mediate penetration through the endosomal membrane releasing the transcriptionally active core into the cytoplasm. **B** Structure of reovirus virions, ISVPs, and cores. Surface-shaded representations of cryo-EM image reconstructions of reovirus are shown, as viewed along a twofold axis of symmetry. Density, representing σ1, can bee seen extending from turrets of λ2 at the icosahedral axes of virions and ISVPs. Cores lack σ1. (Image adapted from Dryden et. al [46])

6 Overview of Entry Steps

Following attachment to cell-surface receptors, reovirus virions are delivered into the endocytic pathway (Fig. 4A). Although conclusive evidence

for the mechanism of internalization is lacking, current data support a role for clathrin-dependent endocytosis in reovirus cell entry. Thin-section EM images show virions in structures that appear to be clathrin-coated pits on the cell surface and in clathrin-coated vesicles in the cytoplasm [17, 18, 122, 139], suggesting clathrin-dependent uptake. This finding was confirmed by using video fluorescence microscopy in which reovirus virions and clathrin were observed to colocalize during internalization [56]. While these results are interesting, the involvement of clathrin-dependent uptake in functional reovirus entry (i.e., leading to productive reovirus infection) has not been demonstrated.

Vesicles containing internalized reovirus virions are transported via microtubules [66] and accumulate in late endosomes [17, 18, 66, 122, 139]. In the endocytic compartment, reovirus virions undergo stepwise disassembly forming sequential disassembly intermediates, the first of which is the infectious subvirion particle (ISVP) (Fig. 4). ISVPs are characterized by the loss of outer-capsid protein σ3, a conformational change in attachment protein σ1, and cleavage of outer-capsid protein μ1 to form particle-associated fragments, δ and φ. Following further processing, ISVP-like particles (called ISVP*s) penetrate through the endosomal membrane, leading to release of transcriptionally active core particles, which lack μ1 and σ1, into the cytoplasm. Thus, the disassembly process consists of a highly coordinated series of events that are dependent on host cell functions that act upon discrete components of the viral outer capsid.

7
Cellular Factors That Facilitate Reovirus Disassembly

7.1
Reovirus Disassembly in Some Cell Types Requires Acidic pH and Endocytic Proteases

Treatment of murine L cells [21, 90, 139] or rat insulinoma cells [21, 90, 139] with the weak base ammonium chloride (AC), which raises the pH of endosomes and lysosomes [95, 111], blocks growth of reovirus when infection is initiated with virions. However, ISVPs generated in vitro by treatment of virions with chymotrypsin or trypsin can infect AC-treated cells [139]. This finding indicates that the block to reovirus growth mediated by AC occurs following internalization but prior to disassembly. Concordantly, treatment of L cells with inhibitors of vacuolar proton ATPase activity, such as bafilomycin A1 and concanamycin A, blocks infection by virions but not by ISVPs [91]. Thus, acidic pH is required for reovirus disassembly in some types of cells.

Pharmacologic treatments also have been used to demonstrate an important function for endocytic proteases in reovirus disassembly. Treatment of L cells with E64, an inhibitor of cysteine proteases [6], blocks growth of reovirus virions. Similar to findings made in studies using acidification inhibitors, ISVPs generated in vitro can infect E64-treated cells [3, 25, 52, 73], suggesting that one or more endocytic cysteine proteases can catalyze reovirus disassembly. However, pepstatin A, an inhibitor of aspartyl proteases, is incapable of blocking reovirus infection and uncoating in multiple cell types [81]. Moreover, in vitro treatment of reovirus virions with cathepsin D, an aspartyl protease, does not lead to generation of ISVPs [81]. Thus, aspartyl proteases appear to be incapable of mediating virion-to-ISVP conversion.

Proteolytic enzymes are required for reovirus infection when mice are infected by the peroral route [10, 15]. Virions are converted to ISVPs in the intestinal lumen by the resident proteases chymotrypsin and trypsin. ISVPs produced in this fashion infect intestinal M cells to gain entry into the host [1]. ISVPs generated by chymotrypsin or trypsin in vitro or in the gut lumen [10, 15] are similar to ISVPs generated in the endocytic compartment of cells [4, 51].

7.2 Studies of Persistent Reovirus Infections Provide Clues About the Identity of Proteases That Catalyze Disassembly

Support for a critical role of cysteine proteases in reovirus disassembly comes from studies of persistent reovirus infections in cultured cells. Although usually cytolytic, reoviruses are capable of establishing persistent infections in many types of cells in culture [41]. These cultures are maintained by horizontal transmission of virus from cell to cell and can be cured of persistent infection by passage in the presence of anti-reovirus serum. Cured (LX) cells and the viruses isolated from persistently infected L-cell cultures (PI viruses) harbor mutations that affect viral disassembly [41].

Parental L cells support growth of reovirus after infection by virions or in vitro generated ISVPs. In contrast, LX cells do not support growth of reovirus after infection by virions of wild-type virus but do so after infection by PI virus virions or wild-type ISVPs [4, 44] (Fig. 5A). Since LX cells allow growth of wild-type reovirus only when infection is initiated by ISVPs, these cells are altered in the capacity to support steps in viral replication leading to ISVP formation. L cells and LX cells do not differ in the capacity to bind or internalize virions or distribute them to a perinuclear compartment [4]. Intravesicular pH is equivalent in both cell types, and virions colocalize with an acid-sensitive fluorophore in both L cells and LX cells. However, LX cells

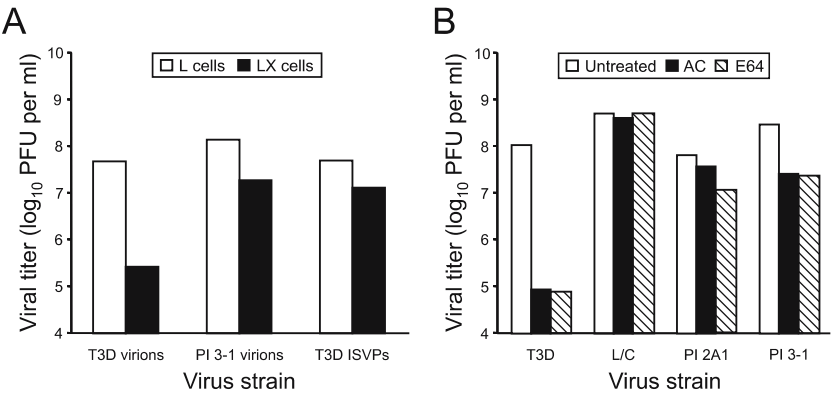

Fig. 5A, B Growth of wild-type and PI viruses in parental L cells and mutant LX cells in the presence and absence of inhibitors of reovirus disassembly. **A** Growth of T3D virions, PI 3–1 virions, and T3D ISVPs in L cells and LX cells. Monolayers of cells (5×10^5) were adsorbed with the viral particles shown at an MOI of 2 PFU per cell. After 1 h, the inoculum was removed, fresh medium was added, and cells were incubated at 37 °C for 24 h. Cells were frozen and thawed twice, and viral titers in cell lysates were determined by plaque assay. The results are presented as the mean viral titers for two independent experiments. (Figure adapted from Wilson et al. [160] and Dermody et al. [44]) **B** Growth of wild-type and PI viruses in the presence and absence of AC and E64. Monolayers of L cells (5×10^5) were adsorbed with T3D or the PI viruses shown at an MOI of 2 PFU per cell. After 1 h, the inoculum was removed, fresh medium was added (with or without 10 mM AC or 100 μM E64), and cells were incubated at 37 °C for either 0 or 24 h. Cells were frozen and thawed twice, and viral titers in cell lysates were determined by plaque assay. The results are presented as the mean viral yields (viral titer at 24 h divided by that at 0 h) for two independent experiments. (Figure adapted from Wetzel et al. [157] and Baer and Dermody [3])

do not support the proteolytic disassembly of the viral outer-capsid following internalization into the endocytic pathway [4, 51], suggesting a defect in proteolytic activity in LX cells.

The major cysteine proteases in the endocytic compartment of fibroblasts like L cells are cathepsins B, H, and L, with cathepsin L being the most abundant in several cell types [6, 16, 62, 69, 78]. These enzymes are first produced as inactive proenzyme precursors that are processed to yield single-chain intermediates that are subsequently cleaved in lysosomes to form two-chain mature forms consisting of heavy and light chains [63, 88, 93, 121, 125, 128]. In LX cells, only the precursor form of cathepsin L is found [4]. The mature, double-chain form of cathepsin B is found in these cells; however, the enzyme is inactive [51]. Neither cathepsin B nor cathepsin L is genetically altered in LX cells, indicating an extrinsic block to the function of these enzymes. Mixed

lysates of L cells and LX cells lack activity of both cathepsin B and cathepsin L [51], suggesting the presence of an inhibitor of cathepsin function in LX cells. These findings suggest that a mutation in LX cells selected during persistent reovirus infection alters the activity of cathepsin B and cathepsin L, suggesting a critical function for these enzymes in reovirus disassembly in fibroblasts. Consistent with a role for cysteine proteases in reovirus uncoating, treatment of virions with either cathepsin B or cathepsin L in vitro results in the formation of particles that have biochemical and growth properties similar to ISVPs generated by treatment of virions with chymotrypsin or trypsin [4, 50].

7.3 Proteases That Mediate Disassembly Vary Depending on Cell Type

The involvement of cathepsin B and cathepsin L in the disassembly of reovirus virions in fibroblasts was confirmed in studies using pharmacologic inhibitors (Fig. 6) and genetically deficient cell lines [50]. Infection of either L cells treated with the cathepsin L inhibitor A-Phe-Tyr(*t*-Bu)-diazomethyl ketone or cathepsin L-deficient mouse embryo fibroblasts results in inefficient proteolytic disassembly and decreased viral yields. In contrast, both L cells treated with the cathepsin B inhibitor CA-074Me and cathepsin B-deficient mouse embryo fibroblasts support reovirus disassembly and growth. However, removal of both cathepsin B and cathepsin L activity completely abrogates disassembly and growth of reovirus. Concordantly, cathepsin L mediates reovirus disassembly more efficiently than cathepsin B in vitro [50]. These results demonstrate that either cathepsin L or cathepsin B is required for reovirus entry into murine fibroblasts and indicate that cathepsin L is the primary mediator of reovirus disassembly in these cells.

Proteases other than cathepsin B and cathepsin L also are capable of ISVP formation. In P388D cells, a macrophage-like cell line, cathepsin S mediates uncoating of some strains of reovirus [68]. Like cathepsins B and L, cathepsin S is a cysteine protease required for processing internalized antigens by antigen-presenting cells [98, 101, 118]. The role of cathepsin S in reovirus disassembly is important because during enteric infection, primary replication is thought to occur in mononuclear cells of Peyer's patches [58, 99].

8 Outer-Capsid Protein σ3 Regulates Reovirus Disassembly

The fist step in the disassembly of reovirus virions is the proteolytic removal of outer-capsid protein σ3. The σ3 protein is a major outer-capsid component

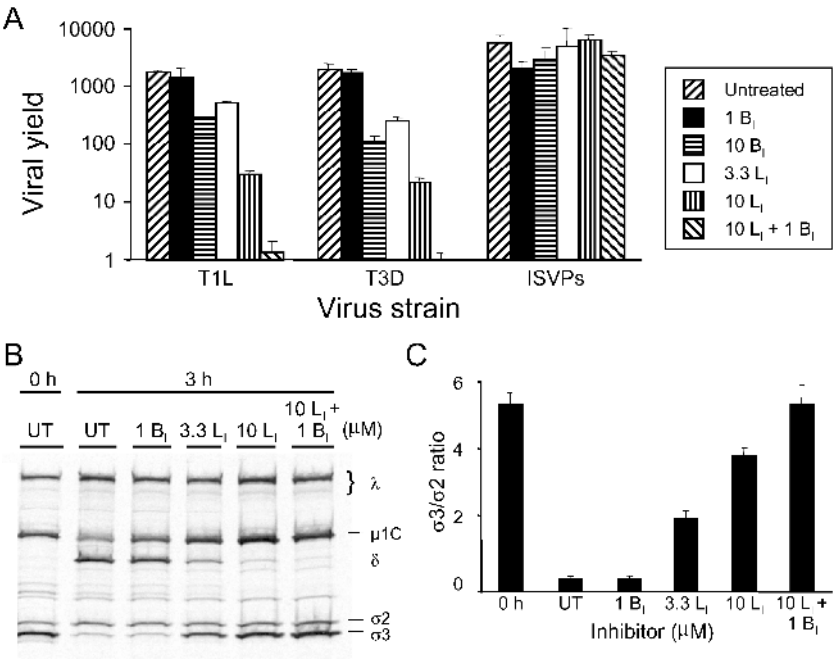

Fig. 6A–C Effect of cathepsin B inhibitor CA-074Me (B_I) and cathepsin L inhibitor Z-Phe-Tyr(*t*-Bu)-diazomethyl ketone (L_I) on growth and disassembly of reovirus strains T1L and T3D in L cells. **A** Monolayers of L cells (4×10^5) were preincubated for 1 h in medium supplemented with B_I, L_I, or both B_I and L_I at the concentrations shown in μM. The medium was removed, and cells were adsorbed with each virus strain at an MOI of 2 PFU per cell. After 1 h, the inoculum was removed, fresh medium with or without B_I and L_I was added, and cells were incubated for 24 h. Viral titers in cell lysates were determined by plaque assay. The results are presented as the mean viral yield, calculated by dividing titer at 24 h by that at 0 h, for three independent experiments. Error bars indicate standard deviations. *UT*, untreated. **B** Monolayers of L cells (1×10^7) were preincubated for 1 h in medium supplemented to contain 0–10 μM B_I or L_I. The medium was removed, and cells were adsorbed with purified ^{35}S-labeled T1L virions at 10,000 particles per cell. After incubation at 4°C for 1 h, the inoculum was removed, fresh medium with or without B_I or L_I was added, and cells were incubated at 37°C for either 0 or 3 h. Viral particles in cell lysates were subjected to SDS-PAGE. Concentrations of B_I and L_I (μM) are shown at the top. *UT*, untreated. Viral proteins are labeled on the right. **C** Quantitation of σ2 and σ3 band intensities. The densities of bands corresponding to the σ2 and σ3 proteins were determined, and the results are expressed as the mean σ3/σ2 ratios for three independent experiments. Error bars indicate standard deviations. (Figure and legend modified from Ebert et al. [50])

that protects the virion from degradation in the environment [105] and forms a protective cap for the μ1 protein [46]. The latter function is especially important during entry as μ1 is thought to be responsible for penetration of ISVPs into the cytoplasm. By capping the μ1 protein, σ3 controls the timing of penetration: if too early, the resulting particle may not be primed to initiate transcription; if too late, the particle may be proteolytically degraded in the lysosome before it gains access to the cytoplasm where transcription occurs.

The σ3 protein contains two large domains separated by a flexible hinge [46, 112] (Fig. 7). The N-terminus of σ3 is in the smaller, virion-proximal lobe, and the C-terminus is in the larger, virion-distal lobe. These domains are not discrete in primary sequence as the peptide chain passes back and forth between the two lobes. A σ3-specific monoclonal antibody that inhibits the σ1-mediated property of sialic acid binding engages the very tip of the virion-distal lobe [102].

Studies of PI viruses have shed light on mechanisms of σ3 cleavage during reovirus disassembly. In contrast to wild-type reoviruses, PI viruses can infect cells treated with either AC [4, 44, 157] or E64 [3] (Fig. 5B). In most cases, growth of PI viruses in the presence of AC or E64 segregates with the S4 gene segment [3, 157], which encodes σ3 [96, 100]. Moreover, passage of wild-type reovirus in the presence of E64 selects E64-resistant viruses (D-EA viruses) that contain mutations in the σ3-encoding S4 gene [52]. Therefore, mutations in σ3 protein confer the capacity of variant reoviruses to grow in the presence of pharmacologic inhibitors of reovirus disassembly.

All PI viruses analyzed to date have a mutation of Tyr354 to His near the C-terminus of σ3 [3, 157]. This mutation is also selected in D-EA viruses [52]. PI and D-EA viruses exhibit altered kinetics of disassembly with degradation of σ3 and cleavage of μ1 occurring much more rapidly both in vitro and in cells [52, 157]. Image reconstructions of cryo-EM images of virions of PI viruses indicate that the Tyr354 to His mutation confers an alteration in σ3 structure at the hinge region between the two lobes [160]. These findings suggest that the C-terminus of σ3 regulates susceptibility of the protein to cleavage.

The σ3 C-terminus also has been shown to dictate strain-specific differences in the susceptibility of σ3 to proteolytic attack [73, 74]. The σ3 protein of strain T1L is cleaved more rapidly than that of T3D. Analysis of ISVPs recoated with chimeric σ3 proteins generated from T1L and T3D revealed that the C-terminus is primarily responsible for the rate of σ3 proteolysis. Moreover, sequence polymorphisms at residues 344, 347, and 353 in σ3 contribute to this effect [74].

Treatment of reovirus virions in vitro with either cathepsin B or cathepsin L leads to an initial cleavage of σ3 at a terminus [50]. Given that sequence

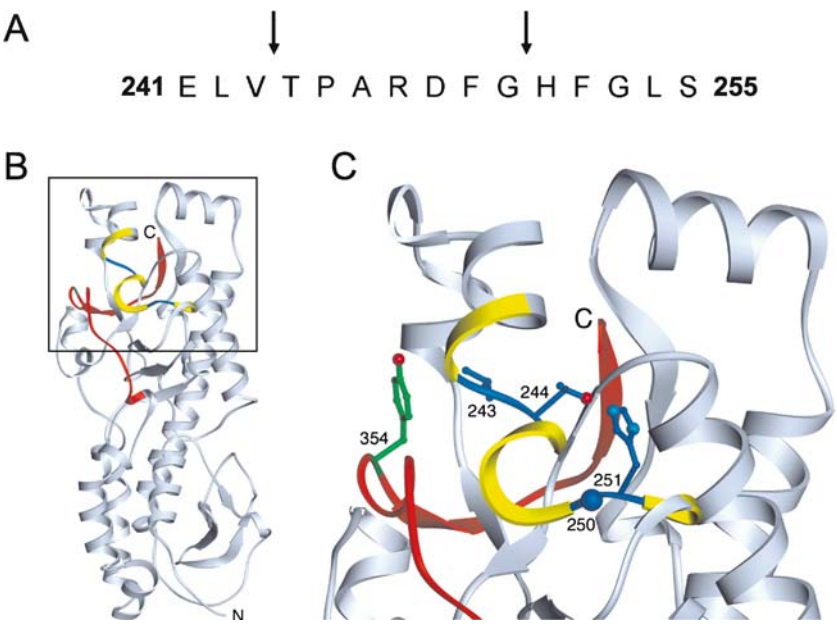

Fig. 7A–C Cathepsin L cleavage sites in T1L σ3. **A** The primary amino acid sequence of σ3 from amino acids 241 to 255 is shown. The *arrows* highlight cathepsin L cleavage sites identified by N-terminal sequencing of σ3 cleavage products following treatment of reovirus T1L with cathepsin L in vitro. **B** Cathepsin L cleavage sites are highlighted in the crystal structure of σ3. A ribbon diagram of the crystal structure of T3D σ3 [112] is displayed. The cathepsin L cleavage sites in T1L are depicted in *blue* between amino acids 243 and 244 and between 250 and 251. Surrounding residues, from amino acids 241 to 253, are shown in *yellow*. The C-terminal residues of σ3, from amino acids 340 to 365, are colored *red*. Amino acid 354, which is a site altered in PI and D-EA viruses, is colored *green*. The virion-distal end of σ3 is at the *top* of the figure, and the virion-proximal end and N-terminus are at the *bottom*. **C** An enlarged view of the boxed region of σ3 indicated in *panel B* is shown using the same color scheme. Amino acids 243, 244, 250, 251, and 354 are depicted in ball-and-stick representation. (Figure and legend modified from Ebert et al. [50])

polymorphisms in the C-terminus determine susceptibility to proteolysis, the initial cleavage of σ3 probably occurs in this region. During proteolysis by cathepsin L, subsequent cleavages occur between residues 243–244 and 250–251 [50] (Fig. 7A). These cleavage sites are physically located near the C-terminus in the σ3 crystal structure [112] (Fig. 7C). Because of this proximity, the small end fragment released following initial cathepsin L cleavage likely exposes the other two sites, rendering them sensitive to subsequent cleavage

events. The C-terminus therefore appears to act as a safety latch that controls access to internal, proteolytically sensitive sites in σ3. Because reovirus disassembly in some cell types is an acid-dependent process, the safety latch might be primed for movement at acidic pH. In viruses with mutations near the C-terminus, such as PI and D-EA viruses, the safety latch may be altered by structural rearrangements.

9 Conformational Changes in σ1

The disassembly of reovirus virions to ISVPs is accompanied by a dramatic conformational change in σ1. EM images of negatively stained reovirus virions and ISVPs reveal filamentous projections extending up to 400 Å from the surface of ISVPs but not virions [61]. These images suggest that σ1 adopts a compact form in the virion and a more extended one in the ISVP. Cryo-EM image reconstructions of virions of reovirus prototype strains and cores of T1L each lack a discernible density corresponding to σ1 at the icosahedral vertices [46, 97]. However, in cryo-EM image reconstructions of T1L ISVPs, discontinuous density is observed for σ1 extending approximately 100 Å from each vertex (Fig. 4B). Presumably, the full length of σ1 is not visible in reovirus particles because icosahedral averaging was employed for the cryo-EM image reconstructions. The trimeric σ1 protein is positioned at an icosahedral fivefold axis; therefore, it does not obey icosahedral symmetry. Moreover, σ1 possesses structural flexibility, which also may preclude its visualization by this technique.

The flexibility of σ1 has been observed in EM images of negatively stained σ1 isolated from virions, which show bending in individual fibers at specific regions within the molecule [60] (Fig. 1) and in the crystal structure of the C-terminal half of T3D σ1 [31] (Fig. 2). In addition, a highly unusual cluster of conserved aspartic acid residues is found at the trimer interface at the base of the σ1 head [31] (Fig. 8). These residues may be important for triggering conformational changes in the low pH environment of the endocytic pathway. Acid-dependent conformational changes in the attachment proteins of enveloped viruses, such as influenza virus and tick-borne encephalitis virus, are well-documented [20, 137]. A four-residue linker that connects β-spiral repeats 2 and 3 of the crystallized fragment of σ1, which are just N-terminal to the σ1 head, confers flexibility between the head and tail regions [31] (Fig. 2). Despite the importance of σ1 in mediating attachment to host cells, the conformational changes that occur in σ1 during the viral entry and uncoating steps and their significance at present are poorly understood.

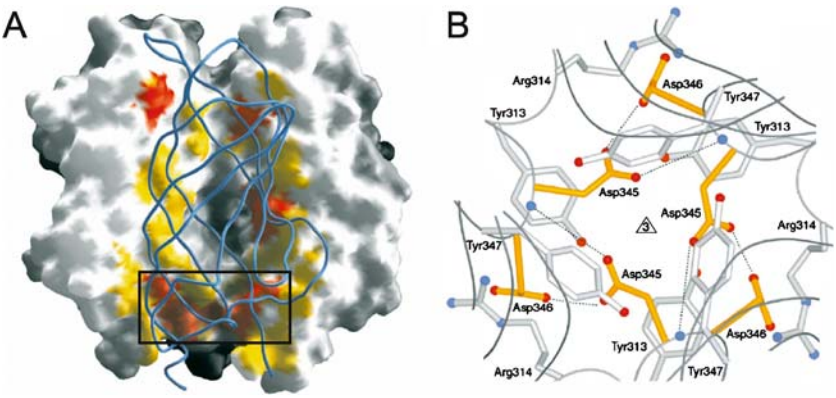

Fig. 8A, B The σ1 head trimer interface. **A** View into the head trimer interface. Two monomers are shown as surface representations and the third monomer is shown as a *blue ribbon*. Surface residues that are within 4 Å of residues in the third monomer are shown in *red* (residues conserved in T1L, T2J, and T3D σ1) and *yellow* (residues unique to T3D σ1). The contact area involving conserved residues Val344, Asp345, and Asp346 is boxed, and this region is shown in more detail in **B**. **B** View along the trimer axis, centered at conserved residues Asp345 and Asp346 (*yellow*) located at the base of the σ1 head. Residues Tyr313, Arg314, and Tyr347 engage in contacts with the two aspartic acids. The side chains of Asp345 are likely to be protonated to avoid an accumulation of negative charge at the interface. Hydrogen bonds involving protonated Asp345 are indicated. Oxygen and nitrogen atoms of side chains are shown as *red and blue spheres*, respectively. The Asp346 main chain amides also are shown as *blue spheres*. (Image from Chappell et al. [31])

Mutations found in PI viruses provide additional evidence of a role for σ1 in viral entry independent of its function in receptor binding. All mutations identified to date in PI virus σ1 protein are found in the tail region of σ1 and alter the stability of σ1 oligomers [159]. Several mutations also are found in the region of σ1 responsible for anchoring the protein into the virion surface. Thus, mutations selected during persistent infection suggest that oligomerization and σ1-capsid interactions are important for viral disassembly and growth.

10 Outer-Capsid Protein μ1 Mediates Membrane Penetration

Insight into mechanisms employed by reovirus to penetrate into the cytoplasm first came from studies of ISVPs generated in vitro. ISVPs, but not intact virions, release ^{51}Cr from preloaded L cells [17], lyse red blood cells in the

presence of cesium ions [25, 27, 73], and form ion-permeant channels in planar phospholipid bilayers [143]. ISVPs also facilitate entry into cells of the toxin alpha-sarcin in the presence of inhibitors of reovirus uncoating [26, 91, 110]. These observations suggest that ISVPs are the immediate precursor to the disassembly intermediate that facilitates delivery of the core particle into the cytoplasm.

Following formation of ISVPs in endosomes, transcriptionally active core particles, which lack both σ1 and μ1, are released into the cytoplasm. The mechanism of penetration and the shedding of these outer-capsid proteins has been the focus of recent work, which has led to the identification of an additional intermediate particle formed subsequent to the ISVP, the ISVP* [24, 26, 110] (Fig. 4A).

Most of the μ1 protein on mature virions is autocatalytically cleaved near the N-terminus to generate two fragments, μ1N and μ1C [106, 130] (Fig. 9). This cleavage is not required for virion assembly [110] and may occur physiologically during the transition from the ISVP to the ISVP* [108]. In ISVPs, μ1C is further cleaved by either endocytic [50, 139] or intestinal [15] proteases to form fragments δ and φ, which remain particle-associated [103]. However, the role of this cleavage in viral penetration is not understood, as core particles recoated with mutant forms of μ1 incapable of δ/φ cleavage can establish productive infection [27]. In addition, μ1 is not cleaved at the δ/φ junction in ISVPs generated in the presence of alkyl sulfate detergents (dpSVPs), yet dpSVPs are infectious [25].

Transformation from the ISVP to the ISVP* in vitro is triggered by differential cationic concentration or interactions with membranes [24, 26]. In contrast to ISVPs, ISVP*s lack σ1 and have an altered conformer of μ1 in which internal hydrophobic residues are exposed. ISVP*s are capable of membrane penetration and transcription initiation [24, 26]. The conformational change in μ1 may be the driving force for both the loss of σ1 and the initiation of transcription [86]. Mechanisms underlying these events are unknown, but it is possible that μ1 rearrangement induces a conformational change in λ2, the pentameric turret that anchors σ1, causing σ1 release. A μ1-induced conformational change in λ2 may also activate the transcriptional machinery through interactions with either or both of the core proteins λ1 and σ2.

Cleavage of intact μ1 to form μ1N and μ1C is required for the generation of the ISVP* [108, 110]. Particles recoated with mutant forms of μ1 incapable of μ1N/μ1C cleavage can facilitate each of the entry steps, including μ1 conformational changes and transcription initiation but are deficient in membrane penetration [110]. In addition to σ1, the N-terminal μ1 fragment μ1N is released from the ISVP* [26]. The function of the released μ1 fragment in membrane penetration is not understood. However, the presence of a myris-

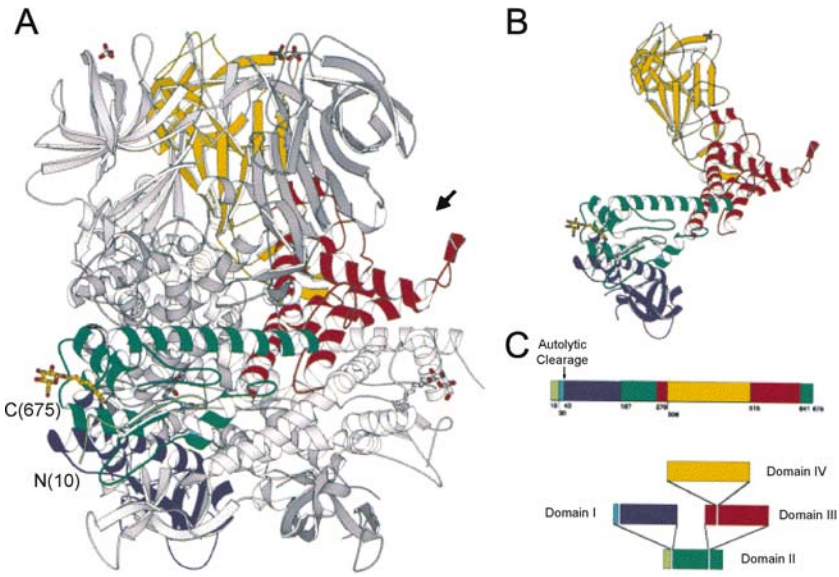

Fig. 9A–C The μ1 protein. **A** The μ1 trimer shown without bound σ3. One μ1 subunit is colored by domain (domain I, *light and dark blue* [μ1N, μ1C]; domain II, *light and dark green* [μ1N, μ1C]; domain III, *red*; domain IV, *yellow*); the other two μ1 subunits are shown in *gray*. The β-octyl glucoside in the colored subunit is in *yellow*; the sulfate ion is shown in *green* and *red*. The σ3 binding site is indicated by an *arrow*. **B** Ribbon diagram of an isolated μ1 subunit. Colors are as in **A**. **C** Domain segmentation of the amino acid sequence as determined from the three-dimensional structure. Domain color code as in **A**. The central domain II contains domains I and III as inserts, and domain III similarly contains domain IV. (Figure and legend modified from Liemann et al. [86])

toyl group at the N-terminus of μ1N suggests that this fragment interacts with membranes and that the released μ1N may form a membrane-penetration complex.

High-resolution structural analysis of μ1 has led to the development of a model for its role in membrane penetration (Figs. 9, 10). The protein consists of four domains: domains 1–3 are primarily α-helical while domain 4, which sits atop the molecule, is a jelly-roll β-barrel [86] (Fig. 9). Three μ1 subunits assemble into an oblong homotrimer, which is bound by the lower lobes of three σ3 subunits. This arrangement gives rise to a heterohexameric complex in which each σ3 subunit interacts intimately with two different μ1 subunits (Fig. 10). The μ1 proteins serve as the principal means of capsid association by mediating contacts between different heterohexamers [86]. The σ3 proteins

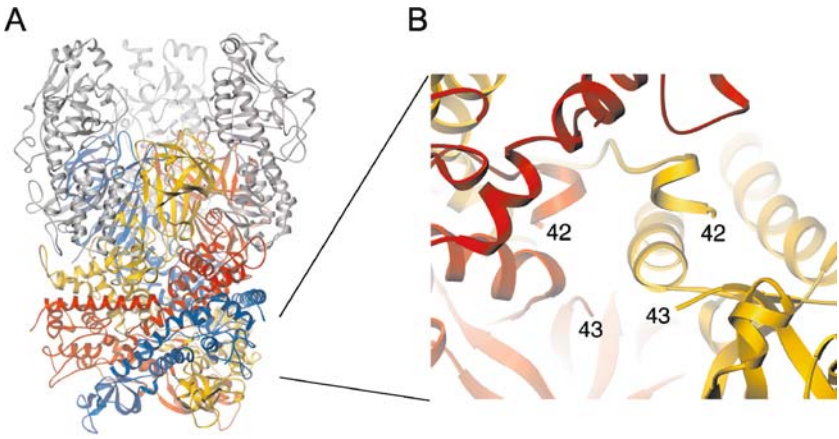

Fig. 10 Structure of the $\mu1_3\sigma3_3$ heterohexamer. **A** A $\mu1_3\sigma3_3$ complex, viewed from the side. The bottom of the complex would contact σ2 proteins on the surface of the reovirus core. Three σ3 proteins (shown in *gray*) bind to the upper part of the underlying trimer of μ1 (shown in *yellow*, *red*, and *blue*). The three μ1 chains are wound tightly around each other. Each σ3 contacts two μ1 proteins. **B** Enlarged view of the lower portion of the trimer, with the blue monomer removed for clarity. In this view, it is evident that the protein has undergone autocatalytic cleavage between residues 42 and 43. (Figure and legend modified from Liemann et al. [86])

do not contribute to the formation of this network but project outward, away from the virion surface. The C-terminal lobe of each σ3 protein is therefore easily accessible to proteases. The autocatalytic cleavage site that yields μ1N and μ1C is located between residues 42 and 43, at the center of the trimer near the base of the protein (Fig. 10). This site is buried in μ1 and distant from residues that interact with σ3. The crystallized protein has undergone cleavage at this position, resulting in separation of residues 42 and 43. The δ/φ cleavage site is located in domain 3.

There are amphipathic helices and other hydrophobic residues in the center of μ1, including the myristoylated Gly2 at the N-terminus [86]. Cleavage of μ1 to μ1N and μ1C does not appear to result in conformational rearrangements, but this cleavage, along with the loss of σ3, may render the μ1 trimer metastable. Since the μ1N/μ1C cleavage sites in the three monomers lie next to each other, cleavage may soften this area of the molecule by altering protein–protein contacts and allow an influx of solvent into an area at the center of the trimer structure. When the steric hindrance imposed by σ3 is released, μ1 may then undergo the conformational alterations necessary to allow membrane penetration.

The conformational changes in μ1 that accompany viral disassembly are thought to expose internal hydrophobic residues and release μ1N from the particle [24, 26, 110]. Massive rearrangements are necessary to expose the hydrophobic residues and myristoylated N-terminus [86]. The cleavage of μ1 to form μ1N and μ1C is necessary for productive infection [110]. However, it is not clear whether membrane penetration is accomplished by soluble or particle-associated μ1N, perhaps acting in concert with other regions of the molecule. For example, an anion-binding site in domain 4 lies on the outermost, solvent-exposed surface of the ISVP [86]. This site may bind to phospholipid head groups bringing the virus particle into proximity with the endosomal membrane. This association also might trigger rearrangements in μ1, revealing the myristoylated μ1N and the internal hydrophobic residues.

11 Conclusions and Future Directions

Despite the accumulated knowledge about reovirus attachment to cell-surface receptors and internalization into host cells, a precise understanding of the mechanisms underlying the serotype-dependent differences in tropism exhibited by reovirus in the murine CNS remains elusive. Since prototype and field-isolate strains of all three serotypes of reovirus utilize JAM-A as a receptor [8, 165], more work is required to determine the basis for serotype-dependent differences in reovirus disease. We envision four possibilities. First, JAM-A may serve as a serotype-independent reovirus receptor at some sites within the host, and other as yet unidentified receptors may confer serotype-dependent tropism in the CNS. Studies using JAM-A-null mice [23] should permit assessment of the role of JAM-A in reovirus pathogenesis and may serve to highlight the existence of additional receptors. Second, it is possible that the carbohydrate specificity of a particular strain of reovirus directs infection to specific cells or tissues. In support of this idea, reovirus strains that vary in sialic acid utilization have also been shown to vary in disease pathogenesis in the hepatobiliary system [9]. A third possibility is that reovirus requires independent receptors for attachment and internalization. It has not been definitively demonstrated that JAM-A alone can mediate internalization into host cells. Therefore, it is possible that virus is tethered to the cell surface through interactions with carbohydrate and JAM-A, but only the strains or serotypes that are capable of interactions with an internalization receptor, which may be expressed in a cell- or tissue-specific manner, achieve entry. Finally, differences in receptor utilization and internalization pathways might influence disease pathogenesis by virtue of activating different types

of signaling networks. Reovirus strains T1L and T3D differ in the capacity to induce apoptosis [36, 119, 148], a property that has been linked to receptor binding and disassembly [8, 34, 35]. Studies of reovirus-induced myocarditis provide support for the hypothesis that postattachment signaling plays a role in disease production. Treatment of reovirus-infected mice with a calpain inhibitor dramatically reduces myocardial injury and apoptotic myocardial cell death [38]. Additional studies are required to confirm an association of apoptosis with reovirus-induced disease. However, it appears that the role of reovirus receptors in disease pathogenesis is more complex than simply mediating the virus-docking event.

Tropism of reovirus in the host may also be influenced by postattachment entry steps. All available evidence suggests that reovirus virions are internalized by clathrin-mediated endocytosis. However, inhibition of clathrin-mediated uptake by treatment of cells with hypertonic sucrose or dominant-negative Eps15 has only a modest effect on virus entry [56]. This observation suggests that reovirus is capable of using more than a single entry pathway, a situation observed for other viruses. Influenza virus utilizes both clathrin-mediated and clathrin- and caveolin-independent uptake pathways [94, 124, 129], and human papillomaviruses use different pathways of entry depending on the viral type [19]. Additional studies of reovirus entry pathways are required to dissect the functional mechanisms used by reovirus to internalize into cells. If cell-specific entry pathways are elucidated, then the type of uptake mechanism may influence target cell selection in the host.

Tissue-specific expression of endocytic proteases might serve as an additional determinant of reovirus tropism. Cathepsin B and cathepsin L are required for reovirus uncoating in fibroblasts [50], whereas cathepsin S is required in macrophage-like P388D cells [68]. Interestingly, not all reovirus strains infect P388D cells [68], suggesting that different strains use different enzymes for uncoating in different cell types. While cathepsins B and L are ubiquitously expressed, cathepsin S displays a more restricted and regulated expression pattern with increased levels in tissues and cells of the immune system (reviewed in [28]). It is noteworthy that influenza virus [76, 77] and rotavirus [40, 57] display tropism partly on the basis of expression of proteases required for viral entry. Studies of reovirus pathogenesis using mice deficient in various proteases should clarify the role of these enzymes in viral tropism and disease.

The role of acidic pH in reovirus disassembly is unclear. Viruses with a His at residue 354 in σ3 can grow in the presence of AC [157]. This finding suggests that the altered conformation of σ3-His354 imparts an increased susceptibility to cleavage, allowing proteases enhanced access to internal cleavage sites. Thus, σ3-His354 may mimic a pH-dependent conformational intermediate

in the uncoating pathway. However, cathepsin B and cathepsin L require acidic pH for activity. Therefore, it is possible that the requirement for acidic pH during viral entry and disassembly serves to provide the appropriate conditions for the action of these enzymes. AC does not alter reovirus growth in P388D cells in which disassembly is catalyzed by cathepsin S [68], an enzyme that does not require acidic pH [79]. However, yields of reovirus in P388D cells are substantially less after infection by virions than by ISVPs [68], suggesting that entry into these cells is not optimally efficient. The role of acidic pH in internalization and disassembly may be better understood through studies of AC-resistant viral variants currently ongoing in our laboratory [166].

The massive rearrangements of μ1 during disassembly and membrane penetration are of considerable interest. The trigger for these conformational changes is not known, nor is it understood whether the process is simply dependent on the removal of σ3 or on other factors as yet unidentified. In addition, it is not apparent whether the N-terminal myristoylated fragment of μ1 must be released from the virion to mediate membrane penetration or whether the entire particle in some way contributes to membrane rupture. Ongoing studies in this area will likely contribute general insights into nonenveloped virus penetration and establish how viral assembly is precisely coordinated to prime the particle for the stepwise disassembly process.

Acknowledgements We thank Annie Antar, Jackie Campbell, Kartik Chandran, and Denise Wetzel for review of the manuscript and members of our laboratories for helpful discussions. We acknowledge support from Public Health Service awards T32 GM08554 (K.M.G.), T32 AI07611 (E.M.J.), R01 AI45716 (T.S.), R01 AI38296 (T.S.D.), R01 AI32539 (T.S.D.), and R01 GM67853 (T.S. and T.S.D.) and the Elizabeth B. Lamb Center for Pediatric Research.

References

1. Amerongen HM, Wilson GAR, Fields BN, Neutra MR (1994) Proteolytic processing of reovirus is required for adherence to intestinal M cells. J Virol 68:8428–8432
2. Arrate MP, Rodriguez JM, Tran TM, Brock TA, Cunningham SA (2001) Cloning of human junctional adhesion molecule 3 (JAM3) and its identification as the JAM2 counter-receptor. J Biol Chem 276:45826–45832
3. Baer GS, Dermody TS (1997) Mutations in reovirus outer-capsid protein σ3 selected during persistent infections of L cells confer resistance to protease inhibitor E64. J Virol 71:4921–4928
4. Baer GS, Ebert DH, Chung CJ, Erickson AH, Dermody TS (1999) Mutant cells selected during persistent reovirus infection do not express mature cathepsin L and do not support reovirus disassembly. J Virol 73:9532–9543
5. Balda MS, Matter K (2000) Transmembrane proteins of tight junctions. Semin Cell Dev Biol 11:281–289

6. Barrett AJ, Kembhavi AA, Brown MA, Kirschke H, Knight CG, Tamai M, Hanada K (1982) L-*trans*-Epoxysuccinyl-leucylamido(4-guanidino)butane (E-64) and its analogues as inhibitors of cysteine proteinases including cathepsins B, H and L. Biochem J 201:189–198
7. Barton ES, Connolly JL, Forrest JC, Chappell JD, Dermody TS (2001) Utilization of sialic acid as a coreceptor enhances reovirus attachment by multistep adhesion strengthening. J Biol Chem 276:2200–2211
8. Barton ES, Forrest JC, Connolly JL, Chappell JD, Liu Y, Schnell F, Nusrat A, Parkos CA, Dermody TS (2001) Junction adhesion molecule is a receptor for reovirus. Cell 104:441–451
9. Barton ES, Youree BE, Ebert DH, Forrest JC, Connolly JL, Valyi-Nagy T, Washington K, Wetzel JD, Dermody TS (2003) Utilization of sialic acid as a coreceptor is required for reovirus-induced biliary disease. J Clin Invest 111:1823–1833
10. Bass DM, Bodkin D, Dambrauskas R, Trier JS, Fields BN, Wolf JL (1990) Intraluminal proteolytic activation plays an important role in replication of type 1 reovirus in the intestines of neonatal mice. J Virol 64:1830–1833
11. Bassel-Duby R, Spriggs DR, Tyler KL, Fields BN (1986) Identification of attenuating mutations on the reovirus type 3 S1 double-stranded RNA segment with a rapid sequencing technique. J Virol 60:64–67
12. Bazzoni G, Martinez-Estrada OM, Mueller F, Nelboeck P, Schmid G, Bartfai T, Dejana E, Brockhaus M (2000) Homophilic interaction of junctional adhesion molecule. J Biol Chem 275:30970–30976
13. Bazzoni G, Martinez-Estrada OM, Orsenigo F, Cordenonsi M, Citi S, Dejana E (2000) Interaction of junctional adhesion molecule with the tight junction components ZO-1, cingulin, and occludin. J Biol Chem 275:20520–20526
14. Bergelson JM, Cunningham JA, Droguett G, Kurt-Jones EA, Krithivas A, Hong JS, Horwitz MS, Crowell RL, Finberg RW (1997) Isolation of a common receptor for Coxsackie B viruses and adenoviruses 2 and 5. Science 275:1320–1323
15. Bodkin DK, Nibert ML, Fields BN (1989) Proteolytic digestion of reovirus in the intestinal lumens of neonatal mice. J Virol 63:4676–4681
16. Bond JS, Butler PE (1987) Intracellular proteases. Ann Rev Biochem 56:333–364
17. Borsa J, Morash BD, Sargent MD, Copps TP, Lievaart PA, Szekely JG (1979) Two modes of entry of reovirus particles into L cells. J Gen Virol 45:161–170
18. Borsa J, Sargent MD, Lievaart PA, Copps TP (1981) Reovirus: evidence for a second step in the intracellular uncoating and transcriptase activation process. Virology 111:191–200
19. Bousarghin L, Touze A, Sizaret PY, Coursaget P (2003) Human papillomavirus types 16, 31, and 58 use different endocytosis pathways to enter cells. J Virol 77:3846–3850
20. Bullough PA, Hughson FM, Skehel JJ, Wiley DC (1994) Structure of influenza haemagglutinin at the pH of membrane fusion. Nature 371:37–43
21. Canning WM, Fields BN (1983) Ammonium chloride prevents lytic growth of reovirus and helps to establish persistent infection in mouse L cells. Science 219:987–988
22. Carson M (1987) Ribbon models of macromolecules. J Mol Graph 5:103–106

23. Cera MR, Del Prete A, Vecchi A, Corada M, Martin-Padura I, Motoike T, Tonetti P, Bazzoni G, Vermi W, Gentili F, Bernasconi S, Sato TN, Mantovani A, Dejana E (2004) Increased DC trafficking to lymph nodes and contact hypersensitivity in junctional adhesion molecule-A-deficient mice. J Clin Invest 114:729–738
24. Chandran K, Farsetta DL, Nibert ML (2002) Strategy for nonenveloped virus entry: a hydrophobic conformer of the reovirus membrane penetration protein μ1 mediates membrane disruption. J Virol 76:9920–9933
25. Chandran K, Nibert ML (1998) Protease cleavage of reovirus capsid protein μ1/μ1C is blocked by alkyl sulfate detergents, yielding a new type of infectious subvirion particle. J Virol 762:467–475
26. Chandran K, Parker JS, Ehrlich M, Kirchhausen T, Nibert ML (2003) The delta region of outer-capsid protein μ1 undergoes conformational change and release from reovirus particles during cell entry. J Virol 77:13361–13375
27. Chandran K, Walker SB, Chen Y, Contreras CM, Schiff LA, Baker TS, Nibert ML (1999) In vitro recoating of reovirus cores with baculovirus-expressed outer-capsid proteins μ1 and σ3. J Virol 73:3941–3950
28. Chapman HA, Riese RJ, Shi GP (1997) Emerging roles for cysteine proteases in human biology. Annu Rev Physiol 59:63–88
29. Chappell JD, Duong JL, Wright BW, Dermody TS (2000) Identification of carbohydrate-binding domains in the attachment proteins of type 1 and type 3 reoviruses. J Virol 74:8472–8479
30. Chappell JD, Gunn VL, Wetzel JD, Baer GS, Dermody TS (1997) Mutations in type 3 reovirus that determine binding to sialic acid are contained in the fibrous tail domain of viral attachment protein σ1. J Virol 71:1834–1841
31. Chappell JD, Prota A, Dermody TS, Stehle T (2002) Crystal structure of reovirus attachment protein σ1 reveals evolutionary relationship to adenovirus fiber. EMBO J 21:1–11
32. Clarke P, Meintzer SM, Gibson S, Widmann C, Garrington TP, Johnson GL, Tyler KL (2000) Reovirus-induced apoptosis is mediated by TRAIL. J Virol 74:8135–8139
33. Cohen CJ, Shieh JT, Pickles RJ, Okegawa T, Hsieh JT, Bergelson JM (2001) The coxsackievirus and adenovirus receptor is a transmembrane component of the tight junction. Proc Natl Acad Sci U S A 98:15191–15196
34. Connolly JL, Barton ES, Dermody TS (2001) Reovirus binding to cell surface sialic acid potentiates virus-induced apoptosis. J Virol 75:4029–4039
35. Connolly JL, Dermody TS (2002) Virion disassembly is required for apoptosis induced by reovirus. J Virol 76:1632–1641
36. Connolly JL, Rodgers SE, Clarke P, Ballard DW, Kerr LD, Tyler KL, Dermody TS (2000) Reovirus-induced apoptosis requires activation of transcription factor NF-κB. J Virol 74:2981–2989
37. Cunningham SA, Arrate MP, Rodriguez JM, Bjercke RJ, Vanderslice P, Morris AP, Brock TA (2000) A novel protein with homology to the junctional adhesion molecule. Characterization of leukocyte interactions. J Biol Chem 275:34750–34756
38. DeBiasi R, Edelstein C, Sherry B, Tyler K (2001) Calpain inhibition protects against virus-induced apoptotic myocardial injury. J Virol 75:351–361

39. Del Maschio A, De Luigi A, Martin-Padura I, Brockhaus M, Bartfai T, Fruscella P, Adorini L, Martino G, Furlan R, De Simoni MG, Dejana E (1999) Leukocyte recruitment in the cerebrospinal fluid of mice with experimental meningitis is inhibited by an antibody to junctional adhesion molecule (JAM). J Exp Med 190:1351–1356
40. Denisova E, Dowling W, LaMonica R, Shaw R, Scarlata S, Ruggeri F, Mackow ER (1999) Rotavirus capsid protein VP5* permeabilizes membranes. J Virol 73:3147–3153
41. Dermody TS (1998) Molecular mechanisms of persistent infection by reovirus.In: Tyler KL, Oldstone MBA (eds), Curr Topics Micro Immunol, vol. 233. Reoviruses, II Cytopathogenicity and pathogenesis. Springer-Verlag, Berlin Heidelberg, New York, pp 1–22
42. Dermody TS, Nibert ML, Bassel-Duby R, Fields BN (1990) A σ1 region important for hemagglutination by serotype 3 reovirus strains. J Virol 64:5173–5176
43. Dermody TS, Nibert ML, Bassel-Duby R, Fields BN (1990) Sequence diversity in S1 genes and S1 translation products of 11 serotype 3 reovirus strains. J Virol 64:4842–4850
44. Dermody TS, Nibert ML, Wetzel JD, Tong X, Fields BN (1993) Cells and viruses with mutations affecting viral entry are selected during persistent infections of L cells with mammalian reoviruses. J Virol 67:2055–2063
45. Dichter MA, Weiner HL (1984) Infection of neuronal cell cultures with reovirus mimics in vitro patterns of neurotropism. Ann Neurol 16:603–610
46. Dryden KA, Wang G, Yeager M, Nibert ML, Coombs KM, Furlong DB, Fields BN, Baker TS (1993) Early steps in reovirus infection are associated with dramatic changes in supramolecular structure and protein conformation: analysis of virions and subviral particles by cryoelectron microscopy and image reconstruction. J Cell Biol 122:1023–1041
47. Dryden KA, Farsetta DL, Wang G, Keegan JM, Fields BN, Baker TS, Nibert ML (1998) Internal structures containing transcriptase-related proteins in top component particles of mammalian orthoreovirus. Virology 245:33–46
48. Duncan R, Lee PWK (1994) Localization of two protease-sensitive regions separating distinct domains in the reovirus cell-attachment protein sigma 1. Virology 203:149–152
49. Duncan R, Horne D, Strong JE, Leone G, Pon RT, Yeung MC, Lee PWK (1991) Conformational and functional analysis of the C-terminal globular head of the reovirus cell attachment protein. Virology 182:810–819
50. Ebert DH, Deussing J, Peters C, Dermody TS (2002) Cathepsin L and cathepsin B mediate reovirus disassembly in murine fibroblast cells. J Biol Chem 277:24609–24617
51. Ebert DH, Kopecky-Bromberg SA, Dermody TS (2004) Cathepsin B is inhibited in mutant cells selected during persistent reovirus infection. J Biol Chem 279:3837–3851
52. Ebert DH, Wetzel JD, Brumbaugh DE, Chance SR, Stobie LE, Baer GS, Dermody TS (2001) Adaptation of reovirus to growth in the presence of protease inhibitor E64 segregates with a mutation in the carboxy terminus of viral outer-capsid protein σ3. J Virol 75:3197–3206

53. Ebnet K, Schulz CU, Meyer Zu Brickwedde MK, Pendl GG, Vestweber D (2000) Junctional adhesion molecule interacts with the PDZ domain-containing proteins AF-6 and ZO-1. J Biol Chem 275:27979–27988
54. Ebnet K, Suzuki A, Horikoshi Y, Hirose T, Meyer Zu Brickwedde MK, Ohno S, Vestweber D (2001) The cell polarity protein ASIP/PAR-3 directly associates with junctional adhesion molecule (JAM). EMBO J 20:3738–3748
55. Ebnet K, Suzuki A, Ohno S, Vestweber D (2004) Junctional adhesion molecules (JAMs): more molecules with dual functions? J Cell Sci 117:19–29
56. Ehrlich M, Boll W, Van Oijen A, Hariharan R, Chandran K, Nibert ML, Kirchhausen T (2004) Endocytosis by random initiation and stabilization of clathrin-coated pits. Cell 118:591–605
57. Estes MK, Graham DY, Mason BB (1981) Proteolytic enhancement of rotavirus infectivity: molecular mechanisms. J Virol 39:879–888
58. Fleeton M, Contractor N, Leon F, Wetzel JD, Dermody TS, Kelsall B (2004) Peyer's patch dendritic cells process viral antigen from apoptotic epithelial cells in the intestine of reovirus-infected mice. J Exp Med 200:235–245
59. Forrest JC, Campbell JA, Schelling P, Stehle T, Dermody TS (2003) Structure-function analysis of reovirus binding to junctional adhesion molecule 1. Implications for the mechanism of reovirus attachment. J Biol Chem 278:48434–48444
60. Fraser RDB, Furlong DB, Trus BL, Nibert ML, Fields BN, Steven AC (1990) Molecular structure of the cell-attachment protein of reovirus: correlation of computer-processed electron micrographs with sequence-based predictions. J Virol 64:2990–3000
61. Furlong DB, Nibert ML, Fields BN (1988) Sigma 1 protein of mammalian reoviruses extends from the surfaces of viral particles. J Virol 62:246–256
62. Gal S, Gottesman MM (1986) The major excreted protein (MEP) of transformed mouse cells and cathepsin L have similar protease specificity. Biochem Biophys Res Commun 139:156–162
63. Gal S, Willingham MC, Gottesman MM (1985) Processing and lysosomal localization of a glycoprotein whose secretion is transformation stimulated. J Cell Biol 100:535–544
64. Gentsch JR, Pacitti AF (1985) Effect of neuraminidase treatment of cells and effect of soluble glycoproteins on type 3 reovirus attachment to murine L cells. J Virol 56:356–364
65. Gentsch JR, Pacitti AF (1987) Differential interaction of reovirus type 3 with sialylated receptor components on animal cells. Virology 161:245–248
66. Georgi A, Mottola-Hartshorn C, Warner A, Fields B, Chen LB (1990) Detection of individual fluorescently labeled reovirions in living cells. Proc Natl Acad Sci U S A 87:6579–6583
67. Geraghty RJ, Krummenacher C, Cohen GH, Eisenberg RJ, Spear PG (1998) Entry of alphaherpesviruses mediated by poliovirus receptor-related protein 1 and poliovirus receptor. Science 280:1618–1620
68. Golden JW, Bahe JA, Lucas WT, Nibert ML, Schiff LA (2004) Cathepsin S supports acid-independent infection by some reoviruses. J Biol Chem 279:8547–8557
69. Gottesman MM, Sobel ME (1980) Tumor promoters and Kirsten sarcoma virus increase synthesis of a secreted glycoprotein by regulating levels of translatable mRNA. Cell 19:449–455

70. Hamazaki Y, Itoh M, Sasaki H, Furuse M, Tsukita S (2002) Multi-PDZ domain protein 1 (MUPP1) is concentrated at tight junctions through its possible interaction with claudin-1 and junctional adhesion molecule. J Biol Chem 277:455–461
71. Helander A, Silvey KJ, Mantis NJ, Hutchings AB, Chandran K, Lucas WT, Nibert ML, Neutra MR (2003) The viral sigma1 protein and glycoconjugates containing alpha2–3-linked sialic acid are involved in type 1 reovirus adherence to M cell apical surfaces. J Virol 77:7964–7977
72. Itoh M, Sasaki H, Furuse M, Ozaki H, Kita T, Tsukita S (2001) Junctional adhesion molecule (JAM) binds to PAR-3: a possible mechanism for the recruitment of PAR-3 to tight junctions. J Cell Biol 154:491–497
73. Jané-Valbuena J, Nibert ML, Spencer SM, Walker SB, Baker TS, Chen Y, Centonze VE, Schiff LA (1999) Reovirus virion-like particles obtained by recoating infectious subvirion particles with baculovirus-expressed σ3 protein: an approach for analyzing σ3 functions during virus entry. J Virol 73:2963–2973
74. Jané-Valbuena J, Breun LA, Schiff LA, Nibert ML (2002) Sites and determinants of early cleavages in the proteolytic processing pathway of reovirus surface protein sigma3. J Virol 76:5184–5197
75. Kaye KM, Spriggs DR, Bassel-Duby R, Fields BN, Tyler KL (1986) Genetic basis for altered pathogenesis of an immune-selected antigenic variant of reovirus type 3 Dearing. J Virol 59:90–97
76. Kido H, Towatari T, Niwa Y, Okumura Y, Beppu Y (1996) Cellular proteases involved in the pathogenicity of human immunodeficiency and influenza viruses. Adv Exp Med Biol 389:233–240
77. Kido H, Murakami M, Oba K, Chen Y, Towatari T (1999) Cellular proteinases trigger the infectivity of the influenza A and Sendai viruses. Mol Cells 9:235–244
78. Kirschke H, Langner J, Wiederanders B, Ansorge S, Bohley P (1977) Cathepsin L. A new proteinase from rat-liver lysosomes. Eur J Biochem 74:293–301
79. Kirschke H, Wiederanders B, Bromme D, Rinne A (1989) Cathepsin S from bovine spleen. Purification, distribution, intracellular localization and action on proteins. Biochem J 264:467–473
80. Kostrewa D, Brockhaus M, D'Arcy A, Dale GE, Nelboeck P, Schmid G, Mueller F, Bazzoni G, Dejana E, Bartfai T, Winkler FK, Hennig M (2001) X-ray structure of junctional adhesion molecule: structural basis for homophilic adhesion via a novel dimerization motif. EMBO J 20:4391–4398
81. Kothandaraman S, Hebert MC, Raines RT, Nibert ML (1998) No role for pepstatin-A-sensitive acidic proteinases in reovirus infections of L or MDCK cells. Virology 251:264–272
82. Lechner F, Sahrbacher U, Suter T, Frei K, Brockhaus M, Koedel U, Fontana A (2000) Antibodies to the junctional adhesion molecule cause disruption of endothelial cells and do not prevent leukocyte influx into the meninges after viral or bacterial infection. J Infect Dis 182:978–982
83. Lee PW, Hayes EC, Joklik WK (1981) Protein σ1 is the reovirus cell attachment protein. Virology 108:156–163
84. Leone G, Duncan R, Lee PWK (1991) Trimerization of the reovirus cell attachment protein (σ1) induces conformational changes in σ1 necessary for its cell-binding function. Virology 184:758–761

85. Lerner AM, Cherry JD, Finland M (1963) Haemagglutination with reoviruses. Virology 19:58–65
86. Liemann S, Chandran K, Baker TS, Nibert ML, Harrison SC (2002) Structure of the reovirus membrane-penetration protein, μ1, in a complex with is protector protein, σ3. Cell 108:283–295
87. Liu Y, Nusrat A, Schnell FJ, Reaves TA, Walsh S, Ponchet M, Parkos CA (2000) Human junction adhesion molecule regulates tight junction resealing in epithelia. J Cell Sci 113:2363–2374
88. Mach L, Stuwe K, Hagen A, Ballaun C, Glossl J (1992) Proteolytic processing and glycosylation of cathepsin B. The role of the primary structure of the latent precursor and of the carbohydrate moiety for cell-type-specific molecular forms of the enzyme. Biochem J 282:577–582
89. Mann MA, Knipe DM, Fischbach GD, Fields BN (2002) Type 3 reovirus neuroinvasion after intramuscular inoculation: direct invasion of nerve terminals and age-dependent pathogenesis. Virology 303:222–231
90. Maratos-Flier E, Goodman MJ, Murray AH, Kahn CR (1986) Ammonium inhibits processing and cytotoxicity of reovirus, a nonenveloped virus. J Clin Invest 78:617–625
91. Martinez CG, Guinea R, Benavente J, Carrasco L (1996) The entry of reovirus into L cells is dependent on vacuolar proton-ATPase activity. J Virol 70:576–579
92. Martin-Padura I, Lostaglio S, Schneemann M, Williams L, Romano M, Fruscella P, Panzeri C, Stoppacciaro A, Ruco L, Villa A, Simmons D, Dejana E (1998) Junctional adhesion molecule, a novel member of the immunoglobulin superfamily that distributes at intercellular junctions and modulates monocyte transmigration. J Cell Biol 142:117–127
93. Mason RW (1989) Interaction of lysosomal cysteine proteinases with alpha-2-macroglobulin: conclusive evidence for the endopeptidase activities of cathepsins B and H. Arch Biochem Biophys 273:367–374
94. Matlin KS, Reggio HV, Helenius A, Simons K (1982) Infectious entry pathway of influenza virus in a canine kidney cell line. J Cell Biol 91:601–613
95. Maxfield FR (1982) Weak bases and ionophores rapidly and reversibly raise the pH in endocytic vesicles in cultured mouse fibroblasts. J Cell Biol 95:676–681
96. McCrae MA, Joklik WK (1978) The nature of the polypeptide encoded by each of the ten double-stranded RNA segments of reovirus type 3. Virology 89:578–593
97. Metcalf P, Cyrklaff M, Adrian M (1991) The 3-dimensional structure of reovirus obtained by cryoelectron microscopy. EMBO J 10:3129–3136
98. Mizuochi T, Yee ST, Kasai M, Kakiuchi T, Muno D, Kominami E (1994) Both cathepsin B and cathepsin D are necessary for processing of ovalbumin as well as for degradation of class II MHC invariant chain. Immunol Let 43:189–193
99. Morrison LA, Sidman RL, Fields BN (1991) Direct spread of reovirus from the intestinal lumen to the central nervous system through vagal autonomic nerve fibers. Proc Natl Acad Sci U S A 88:3852–3856
100. Mustoe TA, Ramig RF, Sharpe AH, Fields BN (1978) Genetics of reovirus: identification of the dsRNA segments encoding the polypeptides of the μ and σ size classes. Virology 89:594–604
101. Nakagawa T, Roth W, Wong P, Nelson A, Farr A, Deussing J, Villadangos JA, Ploegh H, Peters C, Rudensky AY (1998) Cathespin L: critical role in Ii degradation and CD4 T cell selection in the thymus. Science 280:450–453

102. Nason E, Wetzel J, Mukherjee S, Barton E, Prasad B, Dermody T (2001) A monoclonal antibody specific for reovirus outer-capsid protein σ3 inhibits σ1-mediated hemagglutination by steric hindrance. J Virol 75:6625–6634
103. Nibert ML, Fields BN (1992) A carboxy-terminal fragment of protein μ1/μ1C is present in infectious subvirion particles of mammalian reoviruses and is proposed to have a role in penetration. J Virol 66:6408–6418
104. Nibert ML, Schiff LA (2001) Reoviruses and their replication. In: Knipe DM, Howley PM (eds) Fields virology, 4th edn. Lippincott Williams Wilkins, Philadelphia, pp 1679–1728
105. Nibert ML, Furlong DB, Fields BN (1991) Mechanisms of viral pathogenesis: distinct forms of reoviruses and their roles during replication in cells and host. J Clin Invest 88:727–734
106. Nibert ML, Schiff LA, Fields BN (1991) Mammalian reoviruses contain a myristoylated structural protein. J Virol 65:1960–1967
107. Nibert ML, Chappell JD, Dermody TS (1995) Infectious subvirion particles of reovirus type 3 Dearing exhibit a loss in infectivity and contain a cleaved σ1 protein. J Virol 69:5057–5067
108. Nibert ML, Odegard AL, Agosto MA, Chandran K, Schiff LA (2005) Putative autocleavage of reovirus mu1 protein in concert with outer-capsid disassembly and activation for membrane permeabilization. J Mol Biol 345:461–474
109. Oberhaus SM, Smith RL, Clayton GH, Dermody TS, Tyler KL (1997) Reovirus infection and tissue injury in the mouse central nervous system are associated with apoptosis. J Virol 71:2100–2106
110. Odegard AL, Chandran K, Zhang X, Parker JS, Baker TS, Nibert ML (2004) Putative autocleavage of outer capsid protein μ1, allowing release of myristoylated peptide μ1N during particle uncoating, is critical for cell entry by reovirus. J Virol 78:8732–8745
111. Ohkuma S, Poole B (1978) Fluorescence probe measurement of the intralysosomal pH in living cells and the perturbation of pH by various agents. Proc Natl Acad Sci U S A 75:3327–3331
112. Olland AM, Jané-Valbuena J, Schiff LA, Nibert ML, Harrison SC (2001) Structure of the reovirus outer capsid and dsRNA-binding protein σ3 at 1.8 Å resolution. EMBO J 20:979–989
113. Ostermann G, Weber KS, Zernecke A, Schroder A, Weber C (2002) JAM-1 is a ligand of the beta(2) integrin LFA-1 involved in transendothelial migration of leukocytes. Nat Immunol 3:151–158
114. Ozaki H, Ishii K, Horiuchi H, Arai H, Kawamoto T, Okawa K, Iwamatsu A, Kita T (1999) Cutting edge: combined treatment of TNF-alpha and IFN-gamma causes redistribution of junctional adhesion molecule in human endothelial cells. J Immunol 163:553–557
115. Paul RW, Lee PWK (1987) Glycophorin is the reovirus receptor on human erythrocytes. Virology 159:94–101
116. Paul RW, Choi AH, Lee PWK (1989) The α-anomeric form of sialic acid is the minimal receptor determinant recognized by reovirus. Virology 172:382–385
117. Prota AE, Campbell JA, Schelling P, Forrest JC, Peters TR, Watson MJ, Aurrand-Lions M, Imhof B, Dermody TS, Stehle T (2003) Crystal structure of human junctional adhesion molecule 1: implications for reovirus binding. Proc Natl Acad Sci U S A 100:5366–5371

118. Riese RJ, Wolf PR, Bromme D, Natkin LR, Villadangos JA, Ploegh HL, Chapman HA (1996) Essential role for cathepsin S in MHC class II-associated invariant chain processing and peptide loading. Immunity 4:357–366
119. Rodgers SE, Barton ES, Oberhaus SM, Pike B, Gibson CA, Tyler KL, Dermody TS (1997) Reovirus-induced apoptosis of MDCK cells is not linked to viral yield and is blocked by Bcl-2. J Virol 71:2540–2546
120. Rosen L (1960) Serologic grouping of reovirus by hemagglutination-inhibition. Am J Hyg 71:242–249
121. Rowan AD, Mason P, Mach L, Mort JS (1992) Rat procathepsin B. Proteolytic processing to the mature form in vitro. J Biol Chem 267:15993–15999
122. Rubin DH, Weiner DB, Dworkin C, Greene MI, Maul GG, Williams WV (1992) Receptor utilization by reovirus type 3: distinct binding sites on thymoma and fibroblast cell lines result in differential compartmentalization of virions. Microb Pathog 12:351–365
123. Rubin DH, Wetzel JD, Williams WV, Cohen JA, Dworkin C, Dermody TS (1992) Binding of type 3 reovirus by a domain of the σ1 protein important for hemagglutination leads to infection of murine erythroleukemia cells. J Clin Invest 90:2536–2542
124. Rust MJ, Lakadamyali M, Zhang F, Zhuang X (2004) Assembly of endocytic machinery around individual influenza viruses during viral entry. Nat Struct Mol Biol 11:567–573
125. Ryan RE, Sloane BF, Sameni M, Wood PL (1995) Microglial cathepsin B: an immunological examination of cellular and secreted species. J Neurochem 65:1035–1045
126. Sabin AB (1959) Reoviruses: a new group of respiratory and enteric viruses formerly classified as ECHO type 10 is described. Science 130:1387–1389
127. Sagik B, Puck T, Levine S (1954) Quantitative aspects of the spontaneous elution of influenza virus from red cells. J Exp Med 99:251–260
128. Salminen A, Gottesman MM (1990) Inhibitor studies indicate that active cathepsin L is probably essential to its own processing in cultured fibroblasts. Biochem J 272:39–44
129. Sieczkarski SB, Whittaker GR (2002) Influenza virus can enter and infect cells in the absence of clathrin-mediated endocytosis. J Virol 76:10455–10464
130. Smith RE, Zweerink HJ, Joklik WK (1969) Polypeptide components of virions, top component and cores of reovirus type 3. Virology 39:791–810
131. Songyang Z, Fanning AS, Fu C, Xu J, Marfatia SM, Chishti AH, Crompton A, Chan AC, Anderson JM, Cantley LC (1997) Recognition of unique carboxyl-terminal motifs by distinct PDZ domains. Science 275:73–77
132. Spear PG (2002) Viral interactions with receptors in cell junctions and effects on junctional stability. Dev Cell 3:462–464
133. Spriggs DR, Fields BN (1982) Attenuated reovirus type 3 strains generated by selection of haemagglutinin antigenic variants. Nature 297:68–70
134. Spriggs DR, Bronson RT, Fields BN (1983) Hemagglutinin variants of reovirus type 3 have altered central nervous system tropism. Science 220:505–507
135. Stehle T, Dermody TS (2003) Structural evidence for common functions and ancestry of the reovirus and adenovirus attachment proteins. Rev Med Virol 13:123–132

136. Stehle T, Dermody TS (2004) Structural similarities in the cellular receptors used by adenovirus and reovirus. Viral Immunol 17:129–143
137. Stiasny K, Allison SL, Marchler-Bauer A, Kunz C, Heinz FX (1996) Structural requirements for low-pH-induced rearrangements in the envelope glycoprotein of tick-borne encephalitis virus. J Virol 70:8142–8147
138. Strong JE, Leone G, Duncan R, Sharma RK, Lee PW (1991) Biochemical and biophysical characterization of the reovirus cell attachment protein sigma 1: evidence that it is a homotrimer. Virology 184:23–32
139. Sturzenbecker LJ, Nibert ML, Furlong DB, Fields BN (1987) Intracellular digestion of reovirus particles requires a low pH and is an essential step in the viral infectious cycle. J Virol 61:2351–2361
140. Takahashi K, Nakanishi H, Miyahara M, Mandai K, Satoh K, Satoh A, Nishioka H, Aoki J, Nomoto A, Mizoguchi A, Takai Y (1999) Nectin/PRR: an immunoglobulin-like cell adhesion molecule recruited to cadherin-based adherens junctions through interaction with Afadin, a PDZ domain-containing protein. J Cell Biol 145:539–549
141. Tardieu M, Weiner HL (1982) Viral receptors on isolated murine and human ependymal cells. Science 215:419–421
142. Tardieu M, Powers ML, Weiner HL (1983) Age-dependent susceptibility to reovirus type 3 encephalitis: role of viral and host factors. Ann Neurol 13:602–607
143. Tosteson MT, Nibert ML, Fields BN (1993) Ion channels induced in lipid bilayers by subvirion particles of the nonenveloped mammalian reoviruses. Proc Natl Acad Sci U S A 90:10549–10552
144. Tsukita S, Furuse M, Itoh M (1999) Structural and signalling molecules come together at tight junctions. Curr Opin Cell Biol 11:628–633
145. Turner DL, Duncan R, Lee PW (1992) Site-directed mutagenesis of the C-terminal portion of reovirus protein σ1: evidence for a conformation-dependent receptor binding domain. Virology 186:219–227
146. Tyler KL (2001) Mammalian reoviruses. In: Knipe DM, Howley PM (eds) Fields virology, 4th edn. Lippincott Williams Wilkins, Philadelphia, pp 1729–1945
147. Tyler KL, McPhee DA, Fields BN (1986) Distinct pathways of viral spread in the host determined by reovirus S1 gene segment. Science 233:770–774
148. Tyler KL, Squier MK, Rodgers SE, Schneider SE, Oberhaus SM, Grdina TA, Cohen JJ, Dermody TS (1995) Differences in the capacity of reovirus strains to induce apoptosis are determined by the viral attachment protein σ1. J Virol 69:6972–6979
149. Ullmer C, Schmuck K, Figge A, Lubbert H (1998) Cloning and characterization of MUPP1, a novel PDZ domain protein. FEBS Lett 424:63–68
150. Van Raaij MJ, Mitraki A, Lavigne G, Cusack S (1999) A triple β-spiral in the adenovirus fibre shaft reveals a new structural motif for a fibrous protein. Nature 401:935–938
151. Virgin HW, Tyler KL, Dermody TS (1997) Reovirus. In: Nathanson N (ed) Viral pathogenesis. Lippincott-Raven, New York, pp 669–699
152. Warner MS, Geraghty RJ, Martinez WM, Montgomery RI, Whitbeck JC, Xu R, Eisenberg RJ, Cohen GH, Spear PG (1998) A cell surface protein with herpesvirus entry activity (HveB) confers susceptibility to infection by mutants of herpes simplex virus type 1, herpes simplex virus type 2, and pseudorabies virus. Virology 246:179–189

153. Weiner HL, Drayna D, Averill DR Jr, Fields BN (1977) Molecular basis of reovirus virulence: role of the S1 gene. Proc Natl Acad Sci U S A 74:5744–5748
154. Weiner HL, Ault KA, Fields BN (1980) Interaction of reovirus with cell surface receptors. I. Murine and human lymphocytes have a receptor for the hemagglutinin of reovirus type 3. J Immunol 124:2143–2148
155. Weiner HL, Powers ML, Fields BN (1980) Absolute linkage of virulence and central nervous system tropism of reoviruses to viral hemagglutinin. J Infect Dis 141:609–616
156. Weis W, Brown JH, Cusack S, Paulson JC, Skehel JJ, Wiley DC (1988) Structure of the influenza virus haemagglutinin complexed with its receptor, sialic acid. Nature 333:426–431
157. Wetzel JD, Wilson GJ, Baer GS, Dunnigan LR, Wright JP, Tang DSH, Dermody TS (1997) Reovirus variants selected during persistent infections of L cells contain mutations in the viral S1 and S4 genes and are altered in viral disassembly. J Virol 71:1362–1369
158. Williams LA, Martin-Padura I, Dejana E, Hogg N, Simmons DL (1999) Identification and characterisation of human junctional adhesion molecule (JAM). Mol Immunol 36:1175–1188
159. Wilson GJ, Wetzel JD, Puryear W, Bassel-Duby R, Dermody TS (1996) Persistent reovirus infections of L cells select mutations in viral attachment protein σ1 that alter oligomer stability. J Virol 70:6598–6606
160. Wilson GJ, Nason EL, Hardy CS, Ebert DH, Wetzel JD, Prasad BVV, Dermody TS (2002) A single mutation in the carboxy terminus of reovirus outer-capsid protein σ3 confers enhanced kinetics of σ3 proteolysis, resistance to inhibitors of viral disassembly, and alterations in σ3 structure. J Virol 76:9832–9843
161. Wilson JH, Luftig RB, Wood WB (1970) Interaction of bacteriophage T4 tail fiber components with a lipopolysaccharide fraction from Escherichia coli. J Mol Biol 51:423–434
162. Wolf JL, Rubin DH, Finberg R, Kaufman RS, Sharpe AH, Trier JS, Fields BN (1981) Intestinal M cells: a pathway of entry of reovirus into the host. Science 212:471–472
163. Yoon M, Spear PG (2002) Disruption of adherens junctions liberates nectin-1 to serve as receptor for herpes simplex virus and pseudorabies virus entry. J Virol 76:7203–7208
164. Zahraoui A, Louvard D, Galli T (2000) Tight junction, a platform for trafficking and signaling protein complexes. J Cell Biol 151:F31–F36
165. Campbell JA, Schelling P, Wetzel JD, Johnson EM, Forrest JC, Wilson GA, Aurrand-Lions M, Imhof BA, Stehle T, Dermody TS (2005) Junctional adhesion molecule a serves as a receptor for prototype and field-isolate strains of mammalian reovirus. J Virol 79:7967–778
166. Clark KM, Wetzel JD, Gu Y, Ebert DH, McAbee SA, Stoneman EK, Baer GS, Zhu Y, Wilson GJ, Prasad BVV, Dermody TS (2006) Reovirus variants selected for resistance to ammonium chloride have mutations in viral outer capsid protein σ3. J Virol 80:671–681

CTMI (2006) 309:39–66

Early Steps in Rotavirus Cell Entry

S. Lopez (✉) · C. F. Arias

Departamento de Genética del Desarrollo y Fisiología Molecular,
Instituto de Biotecnología, Universidad Nacional Autónoma de México,
62210 Cuernavaca, Mexico
susana@ibt.unam.mx

Abstract Rotaviruses, the leading cause of severe dehydrating diarrhea in infants and young children worldwide, are non-enveloped viruses formed by three concentric layers of protein that enclose a genome of double-stranded RNA. These viruses have a specific cell tropism in vivo, infecting primarily the mature enterocytes of the villi of the small intestine. It has been found that rotavirus cell entry is a complex multistep process, in which different domains of the rotavirus surface proteins interact sequentially with different cell surface molecules, which act as attachment and entry receptors. These recently described molecules include integrins (α2β1, αvβ3, and αxβ2) and a heat shock protein (hsc70), and have been found to be associated with cell membrane lipid microdomains. The requirement for several cell molecules, which might need to be present and organized in a precise fashion, could explain the cell and tissue tropism of these viruses. This review focuses on recent data describing the interactions between the virus and its receptors, the role of lipid microdomains in rotavirus infection, and the possible mechanism of rotavirus cell entry.

This chapter is dedicated to the memory of Jean Cohen, an excellent scientist and an even better friend.

1 Introduction

Acute, infectious diarrhea is the most common cause of morbidity and mortality among young children living in developing countries, accounting for as many as one billion illnesses and between 2.5 and 3.2 million deaths annually [75]. Rotaviruses are the leading etiologic agent of severe diarrheal disease in infants and young children, a frequent cause of hospitalization both in developed and developing countries. The frequency of rotavirus infection is remarkably similar in both settings [52]; however, while the mortality from rotavirus disease in developed countries is low, rotavirus causes an estimated 500,000–600,000 deaths each year, worldwide [75]. Since rotaviruses play such an important role in severe dehydrating gastroenteritis, and because even advanced levels of hygiene seem unable to control the spread of rotavirus infections, there is an urgent need to develop effective vaccination and therapeutic strategies. Two live attenuated vaccines are likely to be licensed shortly [34]; however, previous experience with the first licensed rotavirus vaccine, which after being released in 1998 was withdrawn from the market 1 year later due to a possible correlation between vaccine application and occurrence of intussusception [74], has reinforced the idea of the need to develop alternative prophylactic approaches to protect against rotaviral disease. Fundamental to these developments is a basic understanding of the molecular mechanisms by which rotaviruses interact with their host cell.

2
Virus Tropism

Rotavirus infection in children is primarily restricted to enterocytes located at the tip of intestinal villi. Although rotavirus can infect older children and adults, severe diarrheal disease is primarily observed in children under 2 years of age [26, 52]. This virus is also an important veterinary pathogen, causing disease in the young of calves, sheep, swine, and poultry. Under field conditions, rotavirus infections show a remarkable host specificity. Cross-species infections are rare events, although the species barrier is not absolute, and there are serological, epidemiological, and molecular data that document these events [49].

The marked cell tropism observed in vivo for the mature enterocytes of the small intestine has suggested that these cells bear specific receptors for the virus. Recent reports suggest, however, an additional extraintestinal spread of rotavirus during infection of animals, indicating a wider host tissue range than previously appreciated [68, 79]. In vitro, rotaviruses bind to a wide variety of cell lines, although only a subset of these—including cells of renal or intestinal origin and transformed cell lines derived from breast, stomach, bone, and lung—are productively infected [10]. This suggests that the binding of rotavirus to cells is promiscuous, while the interaction with cell receptors responsible for virus entry probably occurs at a postbinding step. The initial stages of rotavirus interactions with the host cell are complex and are the focus of intense current research. Most of these investigations have been conducted using model cell culture lines. The most characterized cells are the monkey kidney epithelial cell line, MA104, and the human colon carcinoma cell line, Caco-2 cells, both of which are highly permissive to rotavirus infection.

3
Rotavirus Structure and Classification

The rotavirus genus is divided into five serological groups (A–E). Groups A–C infect humans, whereas all groups have been found to infect animals. The most relevant for human disease are group A rotaviruses, which are also the best characterized [52].

Group A rotaviruses are nonenveloped viruses formed by three concentric layers of protein that enclose a genome composed of 11 segments of double-stranded RNA (dsRNA), ranging in size from approximately 660 to 3,300 base pairs. The core of the virion is formed by 120 molecules of protein VP2, which surrounds the viral genome, and 12 copies each of VP1, the RNA-dependent

RNA polymerase, and VP3, a guanylyl transferase and methylase. The middle layer is formed by 260 trimers of VP6, which assemble on top of the VP2 layer to form double-layered particles (DLPs). The outermost layer, characteristic of triple-layered particles (TLPs), is composed of two proteins, VP4 and VP7. The smooth external surface of the virus is made up of 780 copies of glycoprotein VP7, organized as trimers, while 60 spike-like structures, formed by dimers of VP4, extend about 12 nm from the VP7 surface [77]. The mature virus particle is approximately 100 nm in diameter (including the VP4 extensions) and contains 132 porous channels, which allow the influx of compounds in aqueous solution to the inside of the capsid and the efflux of newly formed mRNAs [26, 76]. Both outer-layer proteins, VP4 and VP7, are involved in the initial interactions of the virus with the host cell [55]; accordingly, they are targets of neutralizing and protective antibodies against the virus [52]. Rotavirus serotype designations are based on neutralization determinants, on both VP4 (serotype P, for protease-sensitive protein) and VP7 (serotype G, for glycoprotein) [49, 52]. Alternatively, sequence analysis of the VP4 and VP7 genes is also used to classify these genes into different genotypes that correlate well with serologically determined serotypes (as far as available). Given the important role of VP4 and VP7 during the early interactions of the virus with the cell surface, they have been the topic of many studies.

4 Rotavirus Surface Proteins

4.1 VP7

VP7, the most abundant protein of the outer layer, is a calcium-binding glycoprotein 326 amino acids (aa) in length that forms a thin layer on the surface of the viral particle. Reconstructions from cryoelectron microscopy images have shown that this protein forms trimers on the surface of the virion [78, 96]. Recent biochemical characterization of this protein has confirmed these observations, and has suggested that the VP7 layer of the virion assembles from calcium-dependent VP7 trimers; the dissociation of these trimers might be the biochemical basis for the EDTA-induced rotavirus uncoating [20]. Until recently, the role of VP7 during the early interactions of the virus with the cell was not recognized. However, it has now been demonstrated that this protein interacts directly with cell surface molecules at a step subsequent to the initial cell attachment of the virus through the spike protein VP4 [36, 100]. The VP7 proteins of different rotavirus strains contain the LDV (at aa positions 237–239) and GPR (at aa positions 253–255) tripeptide sequence binding motifs for

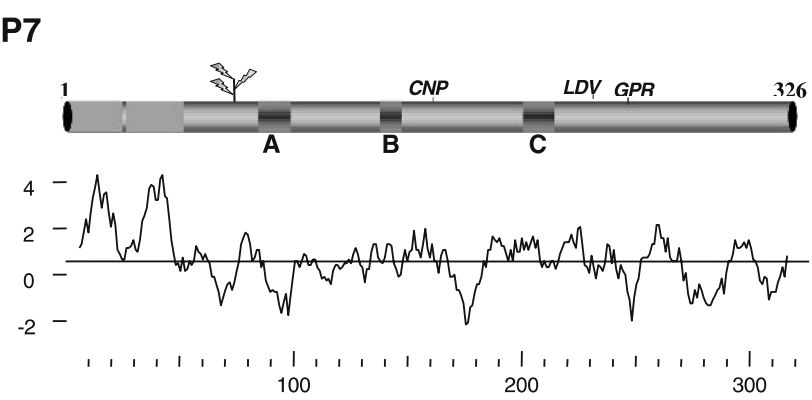

Fig. 1 Diagram of the surface layer glycoprotein VP7. The immature form of this protein contains two hydrophobic regions that are removed cotranslationally during the translocation of VP7 into the lumen of the ER. The mature protein starts at Gln-51. *A* (aa 86–101), *B* (aa 142–152), and *C* (aa 208–221) denote the major antigenic sites of the protein. *CNP* (aa 161–169), *LDV* (aa 237–239), and *GPR* (aa 253–255) indicate the regions that have been proposed to interact with integrins αvβ3, α4β1, and αxβ2, respectively (see text). The glycosylation site at aa 69 is marked. The hydropathic profile of the protein is shown at the *bottom*

integrins α4β1 and αxβ2, respectively (Fig. 1) [15, 44]. VP7 also contains a CNP domain (at aa positions 161–169) responsible for the interaction with integrin αvβ3 [100]. The neutralizing antibodies that interact with VP7 have been mapped to three major antigenic domains named A, B, and C, which are located at amino acid positions 86–101, 142–152, and 208–221, respectively [52].

4.2 VP4

VP4, the spike protein of the virus, formed by 776 aa residues (in most rotavirus strains), has essential functions in the virus life cycle, including receptor binding and cell penetration.

4.2.1 Trypsin Cleavage

The penetration of rotaviruses into the cell's cytoplasm is activated by trypsin treatment of the virus, which results in the specific cleavage of VP4 at three closely spaced arginines located at amino acid positions 231, 241, and 247, to yield polypeptides VP8 (aa 1–231) and VP5 (aa 248–776) (Fig. 2), both of which remain associated to the virion (VP5 and VP8 have been termed VP5*

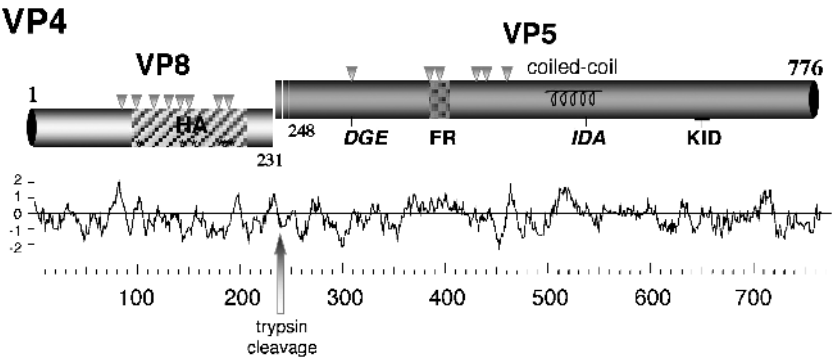

Fig. 2 Diagram of the spike protein VP4. VP4 is cleaved in three closely spaced arginine residues located at aa positions 231, 241, and 247, to yield VP8 and VP5. The hemagglutination domain is located in VP8 and labeled HA; within this domain, the aa residues known to participate in SA binding are labeled with *asterisks*. *Arrowheads* indicate the regions where the interaction sites of neutralizing monoclonal antibodies have been mapped. The neutralizing epitopes in VP8 and the neutralizing epitope that maps to the FR have been described for NA-sensitive rotavirus strains, while the two neutralizing epitopes in VP5 have been described for NA-resistant strains. The location of the fusogenic region (*FR*, aa 385–404) in VP5 is shown. *DGE* (aa 308–310) shows the tripeptide-binding motif known to interact with integrin α2β1 and *IDA* (aa 538–540) represents a potential interaction site for integrin α4β1. *KID* (aa 642–658) indicates the region that has been shown to interact with the ligand-binding site of the heat shock cognate protein, hsc70. A predicted heptad repeat that forms part of a coiled-coil structure (aa 494–554) is shown. The hydropathic profile of the protein is shown at the *bottom*

and VP8*, respectively, by other authors) [1, 13, 25, 27, 57]. Trypsin cleavage of VP4 does not affect the binding of the virus to the cell surface, but rather is required for the entry of the virus into the cell's cytoplasm, and probably for the uncoating of the virus particle. It has been shown that the ability of rotaviruses to induce fusion from without in MA104 cells supplemented with cholesterol depends on the cleavage of VP4 at arginine 247 [33], and it has also been found that trypsin cleavage of VP4 activates membrane-destabilizing properties of the viral outer capsid proteins [7, 18, 28, 82]. Recent studies have shown that while the VP4 spikes of nontrypsinized particles of the simian rotavirus strain SA11 4F could not be visualized by cryoelectron microscopy, these spikes became visible upon treatment of the virions with trypsin, indicating that the cleavage of VP4 yields icosahedrally ordered spikes, and demonstrating that the spikes are structurally different in trypsin-cleaved and uncleaved virions. It has been suggested that the trypsin cleavage of VP4 primes the virus for entry, by triggering a conformational change that rigidifies the spikes [16].

4.2.2 VP8 Domain

Some rotavirus strains bind to N-acetylneuraminic acid (sialic acid, SA) on the surface of cells, and it has been shown that the VP8 trypsin cleavage fragment of VP4 (the viral hemagglutinin) is responsible for this activity. Baculovirus expressed chimeric VP4 proteins (and fragments thereof), derived from hemagglutinating and nonhemagglutinating virus strains, localized this domain of VP8 to a region between aa 93 and 208 [29, 30]. Alanine-scanning mutagenesis of this region later showed that Y155, and the tripeptide YYS at aa positions 188–190 were essential for sialic acid binding [47] (Fig. 2). More recently, the atomic structure of a protease-resistant VP8 core bound to sialic acid was determined by X-ray crystallography. This study showed that the sialoside binding site of VP8 is an open-ended, shallow groove in which the side chains of Y188 and S190 form one rim of the groove, Y155 forms the opposite rim, and the floor of the groove is formed by the side chains of R101, V144, K187, and Y189 [23].

4.2.3 VP5 Domain

The VP5 subunit of VP4 also contains several regions that have been shown to be important for the initial interactions of the virus with the cell surface (Fig. 2). It has a hydrophobic region between amino acids 385 and 404 that shares sequence similarity with an internal fusogenic domain of the E1 glycoprotein of some alphaviruses [61], and which has been involved in the permeabilization of model and cellular membranes [18, 24]. VP5 fragments expressed in bacteria and containing the putative fusogenic domain permeabilize those membranes, apparently through the formation of pores, and residues 265–404 of VP5 have been shown to be required for this activity [24]. The mechanism by which VP5 interacts with cellular membranes and forms pores remains to be defined. However, it has recently been shown that at least two domains are necessary for the interactions between VP5 and the membrane: one domain that directs the peripheral membrane association of VP5 (aa 265–279), and a second, hydrophobic domain required for the formation of the pore [35]. It has been suggested that this permeabilization activity of VP5 might be important for rotavirus penetration into cells to permeabilize early endosomes and for facilitating virion uncoating and viral entry [24, 35]. Although this is a reasonable suggestion, direct evidence of the involvement of the fusogenic domain on virus entry in vivo is thus far lacking.

VP5 also contains a DGE (aa 308–310) tripeptide sequence-binding motif that interacts with integrin α2β1 [36, 98] and an IDA tripeptide sequence (aa 538–540) that has been proposed to interact with integrin α4β1 [15]. A predicted heptad repeat (aa 494–554) [58] that forms part of a coiled-coil structure is apparently needed for the trimerization of the protein [21] (see below); the region between aa 642–658 contains a peptide KID sequence that is known to interact with the heat shock protein hsc70 [97] (see below).

4.2.4 Spike Structure

Cryoelectron microscopy image reconstructions of trypsinized rotavirus particles have shown that the spikes formed by VP4 are structured as dimers, with lobed heads connected to a square-shaped body, which in turn is connected to a "stalk" and "foot" regions [21] (Fig. 3). The VP4 foot penetrates the thin layer formed by VP7, and interacts with the intermediate layer formed by VP6 [21, 77, 84, 90, 95]. Image reconstructions of rotavirus particles bound by Fab fragments from monoclonal antibodies directed to VP8 or VP5 have shown that VP8 is located at the heads of the spikes, while an epitope that maps to a hydrophobic region of VP5 (described below) is located just proximal to the heads [90].

Recently, the atomic structure of the protease-resistant cores of both VP8 and VP5 have been determined [21, 23]. The structure of the VP8 core, which comprises aa 46–231, was found to consist of a monomeric, compactly folded 12-stranded antiparallel β-sandwich, which fits into the lobed heads of the spikes seen by cryoelectron microscopy. The VP8 core, which contains all mapped antigenic sites in this domain, was found to have the same basic fold as the carbohydrate-binding domains in members of the galectin family of lectins [22, 23] (Fig. 3). The crystal structure of the VP5 core (VP5CT) containing aa residues 248–528, which includes the DGE integrin-binding domain, the fusogenic peptide, the predicted coiled-coil, and all mapped antigenic sites in VP5, was determined at 3.2-Å resolution. Surprisingly, this structure revealed that contrary to the two-fold character of the globular head of the spike, the VP5CT crystal structure appeared as a coiled-coil stabilized trimer, in which each of the monomers is formed by an N-terminal globular domain made up of a eight-stranded antiparallel β-sandwich that fits into the spike body, as seen in a 12-Å resolution cryomicroscopy image reconstruction of the trypsin-cleaved viral particle [21] (Fig. 3). These findings prompted Dormitzer et al. [21] to propose a model in which each spike in the viral particle is formed by three VP4 molecules. In this model, trypsin cleavage of VP4 rigidifies the spikes formed by two of the three VP4 molecules, while

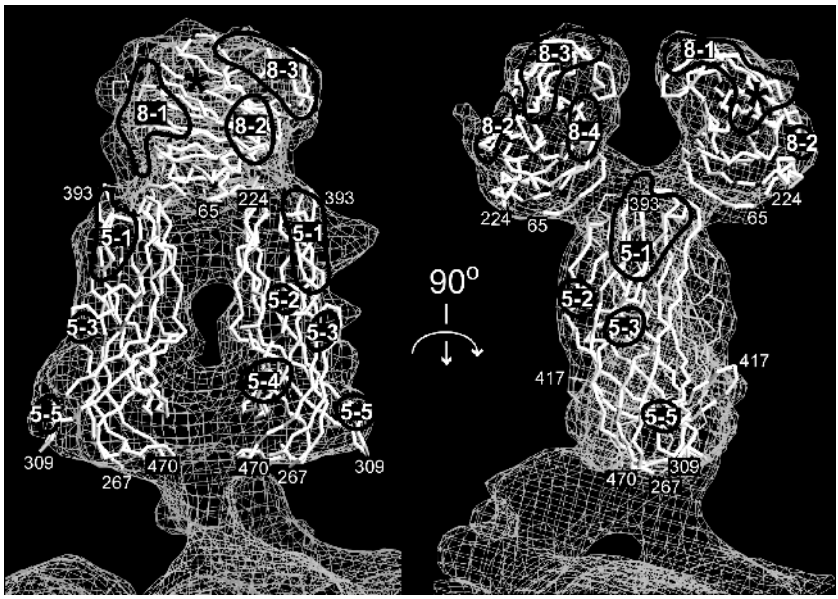

Fig. 3 Carbon αtraces (*white lines*) of the VP8 protease-resistant core and VP5 antigen domain fit to a virus spike electron cryoelectron microscopy image reconstruction of trypsinized virions at 12-Å resolution. The *right* side model is rotated 90° around a vertical axis relative to the model at *left*. Labeled aa residues *65* and *224* indicate the amino and carboxy termini of the VP8 core; aa residues *267* and *470* indicate the amino and carboxy termini of the VP5 antigen domain; *309* is the glycine in the DGE integrin α2β1 binding motif; *393*, aa residue within the putative fusion region of VP5. The *black asterisk* in the VP8 core indicates the sialoside binding site, defined by the sialoside binding aa residues 101, 105, 188, 189, and 190. Neutralization epitopes are outlined in *black*: Epitope 5–1 is defined by neutralization escape mutations (at aa residues 384, 386, 388, 393, 394, 398, 440, and 441) mapped selected with different neutralizing antibodies in several different rotavirus strains; epitope 5–1 is defined by a escape mutation in aa residue 434; epitope 5–3 is defined by aa residue 459; epitope 5–4 is defined by a escape mutation at aa residue 429; epitope 5–5 is defined by aa residue 306. The neutralization epitopes in VP8 are defined by the following neutralization escape mutations: epitope 8–1, aa residues 100, 146, 148, 150, 188, and 190; epitope 8–2, aa residues 180 and 183; epitope 8–3, aa residues 114, 116, 132, 133, 135, and 136; epitope 8–4, aa residues 87, 88, and 89. Courtesy of Philip Dormitzer (Harvard Medical School). The nomenclature of the VP5 and VP8 neutralization epitopes are described in references [21] and [23], respectively

the third molecule remains flexible. It is proposed that VP4-trypsin primed virions undergo a second rearrangement, triggered by an as yet unidentified entry event, in which the spike reorganizes and each VP4 subunit folds back into itself, forming the trimer seen in the crystal structure and exposing new

sites of VP5. It is also proposed that during this conformational change, the VP8 domain is lost. The hypothesis proposed in this work is challenging and inspiring, and future experiments aimed to validate it will help to elucidate the mechanisms by which the viral particle interacts with the cell surface and traverses the membrane to reach the interior of the cell.

5 Viral Receptors

The interaction of viruses with specific receptors on the cell surface determines the tissue tropism and part of the pathogenesis of viruses. The common idea that viruses recognize a single cell receptor to infect a cell is becoming more the exception than the rule, and the occurrence of multiple receptor-binding events during cell entry has been a frequent observation in virus–cell interactions. A number of viruses utilize at least two different receptors to interact with their host cells: the attachment or binding receptors, which allow the virus to rapidly bind to the cell surface, and the entry receptors, also known as co-receptors, postattachment, postbinding, fusion, entry, or internalization receptors, which in general promote the entry process of the virus. In the case of HIV-1, coxsackievirus A9, human cytomegalovirus, herpes simplex virus, and adenovirus [12, 14, 87, 92, 94], the various interactions that take place between the virus and cell surface molecules have been proposed to occur in a sequential manner. These interactions frequently induce conformational changes in the viral surface proteins, which expose hidden domains in the proteins that are essential for the penetration of the virus into the cell [3, 4, 43], and which could represent sensitive, potential targets for novel antiviral agents designed to interrupt virus entry [19].

6 Rotavirus Receptors

The interaction of rotavirus with the cell surface is a complex process in which several different contacts between cell receptors and different domains of the virus outer layer proteins, VP4 and VP7, take place. In addition to sialic acid, which has long been known to function as an attachment receptor for some rotavirus strains, five additional cell molecules have been recently reported to be implicated in rotavirus cell infection, namely, integrins $\alpha 2\beta 1$, $\alpha x\beta 2$, $\alpha v\beta 3$, and $\alpha 4\beta 1$, and the heat shock cognate protein hsc70. In the following sections, we summarize what is known about the interaction of rotavirus with each of these cell molecules.

6.1 Sialic Acid

Carbohydrate–protein interactions are known to play an important role during viral invasion. The carbohydrate moiety of host cell glycoproteins, proteoglycans, and/ or glycosphingolipids has emerged as a widely used virus receptor, with sialic acid (SA) and heparan sulphate among the most used. Viruses in different families use SA-containing molecules as attachment receptors, including influenza virus [93], adenovirus [5], polyomavirus [88], Sendai virus [63], and reovirus [6]. In many cases, the cell molecule containing the sialyloligosaccharide carbohydrate receptor remains unknown, and in some cases, such as influenza virus, different cell surface molecules may play this role.

Different rotavirus strains display different requirements to initially bind, and thus infect, susceptible cells. The cell attachment of some strains isolated from animals is greatly diminished by treatment of cells with neuraminidase (NA), indicating the need for SA on the cell surface [11, 31, 53, 65]. However, the interaction with a SA-containing receptor does not seem to be essential, since variants that do not need SA to infect the cells can be isolated from SA-dependent strains [59, 65]. Furthermore, the infectivity of many animal rotavirus strains and most, if not all, strains isolated from humans is not affected by treatment of cells with neuraminidase [11, 31, 66]. This does not mean, however, that these strains do not use SA for cell attachment, since SA moieties that are internal in oligosaccharide structures are less or not sensitive at all to NA treatment [17]. Furthermore, the fact that many rotavirus strains apparently do not need to bind to SA to infect cells in culture conditions, does not imply that binding to these acid sugars is not important for enterocyte infection in the gut, in a more dynamic environment. Under these conditions, a rapid binding to the abundant SA present in the lumen of the intestine might slow down the passage of the virus, which would allow it to then search locally for less abundant, specific receptors.

A number of glycoconjugates have been shown to bind and to block the infectivity of NA-sensitive animal rotavirus strains, and some of them have been suggested to play a role as possible receptors, such as ganglioside GM1 in LLC-MK2 cells [89], 300- to 330-kDa glycoproteins in murine enterocytes [2], and ganglioside GM3 containing N-glycolyl neuraminic acid as the sialic acid moiety (NeuGc-GM3), in newborn piglet intestine [80]. Ganglioside GM1, which is resistant to NA treatment, has been proposed as a receptor for human rotavirus strains KUN and MO in MA104 cells [40]. In addition, galactose has also been suggested to be an important component of glycoprotein receptors in MA104 cells for rotaviruses of human, simian, and porcine origin [50].

The glycosphingolipid-binding specificities of both NA-sensitive and NA-resistant animal rotavirus strains have recently been determined using a thin-layer chromatography binding assay. It was found that the simian rotavirus strain SA11 and the bovine rotavirus strain NCVD, both of which require SA to infect the cells, bound to external SA residues in gangliosides, while the bovine strain UK, which is NA-resistant, recognized gangliosides containing internal SA residues, which are resistant to NA treatment [17]. Although the effect of these gangliosides on the infectivity of rotaviruses was not determined, it was concluded that the widespread concept that the NA-resistant strains bind in a SA-independent manner is probably misleading. Instead, it was proposed that the NA-resistant strains bind to gangliosides with internal sialic acids that are not cleaved off by NA [17]. Altogether, these results suggest that the initial interaction of most, if not all rotavirus strains with the cell (independently to their sensitivity to the NA treatment) is most probably through glycosphingolipids or other SA-containing compounds present in the plasma membrane. This first interaction might allow the viral particle to dock on the cell surface and then to search for more specific receptors that would facilitate their entry into the cell.

As previously mentioned, the initial contact of NA-sensitive rotavirus strains with the cell surface is through the VP8 domain of VP4. Using NMR spectroscopy, it was found that the VP8 core binds alfa-anomeric *N*-acetylneuraminic acid with a *Kd* of 1.2 mM and does not require additional carbohydrate moieties for binding [22]. In addition, it was shown that VP8 does not distinguish 3′ from 6′ sialyllactose, and has approximately ten-fold lower affinity for *N*-glycolylneuraminic than for *N*-acetylneuraminic acid [22]. The broad specificity and low affinity of this protein for SA is consistent with the idea that after binding to this acid sugar, the virus surface proteins interact more specifically, and probably with higher affinity, with other cell receptors that may contribute to the cell type and host specificity of rotaviruses [22, 38, 66]. A number of mutations that allow NA-sensitive viruses to escape neutralizing antibodies have been mapped within or close to the SA-binding site on VP8, and, as expected, antibodies to this region inhibit virus infectivity by blocking the binding of the virus to the cell surface [81].

6.2 Integrins

Integrins are a family of cell surface receptors that mediate interactions between the cell surface and the extracellular matrix, and also mediate important cell–cell adhesion events. These interactions play a crucial role in the regulation of cell proliferation, migration, differentiation, and survival.

Integrins are transmembrane heterodimers composed of noncovalently associated α and β subunits. Human integrins are assembled from a repertoire of at least 18 different α, and 8 different β subunits, to form 24 different heterodimers. Each integrin heterodimer has distinct ligand binding specificity and signaling properties. The integrin recognition motifs on several integrin ligands have been described and often they have been found to consist of short peptide sequences [45, 46]. Several viruses and bacteria that contain canonical integrin-binding motifs on their surface proteins take advantage of this family of proteins to gain access into the cell [91]. In addition, some viruses have been found to interact with integrins through untypical sequence motifs [72].

In the case of rotaviruses, several integrins have been proposed to facilitate the initial steps of virus infection. VP4 contains tripeptide sequence-binding motifs for integrins α2β1 and α4β1, while VP7 has potential ligand sites for integrins αxβ2 and α4β1 [15, 44]. Also, it has been reported that VP7 interacts with integrin αvβ3 through a nonclassical sequence motif [100]. Integrin α2β1 has been suggested to function as both binding and postbinding receptor, depending on the virus strain, while integrins αxβ2 and αvβ3 are thought to interact with the virus at a postattachment step. The participation of integrin α4β1 in rotavirus infection is less clear and therefore is not described in detail below. Integrins have been shown to be used by both NA-resistant and NA-sensitive rotavirus strains [15, 38]. However, it has recently been observed that some rotavirus strains do not depend on integrins to infect cells, and the integrin usage was reported to correlate with the VP4 serotype and was independent of the VP7 serotype, as well as independent of the NA-sensitivity of the virus [36].

6.2.1 Integrin α2β1

Most of the known physiological ligands of integrin α2β1 interact with this protein through the tripeptide motif DGE. In the case of rotavirus VP4, it was reported that 97% of the available sequences contain a DGE motif located at aa residues 308–310, in the VP5 domain of the protein [15, 36], and it was shown that peptides containing the DGE sequence, and antibodies to the integrin subunit α2 inhibit viral infection [15]. The role of α2β1 as a rotavirus receptor was later reinforced by the characterization of the cell-binding properties of rotavirus strain nar3, a NA-resistant mutant isolated from the NA-sensitive simian rotavirus strain RRV. It was shown that this virus attaches to the cell surface by interacting with integrin α2β1, whereas the parental strain RRV interacts with this integrin at a postattachment step, subsequent to its initial

binding to a SA-containing molecule [65, 99]. It cannot be discarded, however, that nar3 and other NA-resistant strains might initially bind to the cell by interacting with NA-resistant containing molecules. This initial interaction could have been obscured in the binding assays reported [98, 99], by the higher affinity of these viruses for integrin α2β1, as compared to NA-sensitive strains. The interaction of both RRV and nar3 viruses with integrin α2β1 has been shown to be indeed mediated by the VP5 DGE integrin-recognition motif [98, 99] and by a solid-phase assay; the DGE motif in a recombinant VP5 protein was shown to bind to the I domain of the α2 integrin subunit, and it was concluded that this integrin domain is both necessary and sufficient for binding the viral protein [54].

Different studies have reached different conclusions regarding the role of integrin α2β1 as an attachment or postattachment receptor. Expression of the integrin α2 and β1 subunits in Chinese hamster ovary (CHO) cells, which are poorly susceptible to rotavirus infection, caused these cells to become three- to tenfold more susceptible to infection by rotavirus strains RRV and WC3. However, the binding of these viruses to α2β1-expressing CHO cells was not augmented, leading the authors to conclude that although rotaviruses might bind α2β1, this integrin alone is not solely responsible for the initial binding, nor for the entry of rotaviruses, and that other postattachment interactions must be necessary for rotavirus infection [10]. On the other hand, it has been reported that the binding of both NA-resistant (strains NCDV and Wa) and NA-sensitive (strains RRV and SA11) rotavirus strains to MA104 cells is partially blocked by a monoclonal antibody to integrin α2β1 [36] and that transfection with integrin α2 and β1subunits of human erythroleukemic K562 cells, which are also poorly infected by rotavirus, leads to an enhanced binding and infectivity of the NA-sensitive strain SA11 [44]. The apparently opposite results obtained in the various studies may result from differences in the assays used to measure virus binding. In any case, it is clear that this integrin plays an important role during the initial steps of rotavirus attachment to the cell surface but that it is not the only receptor needed for virus entry.

6.2.2 Integrin αxβ2

Using reassortant viruses having one of the surface proteins derived from an integrin-dependent strain and the second surface protein from an integrin-independent virus, it has been recently shown that the interaction of the virus with integrin αxβ2 correlates with the presence of the VP7 protein derived from the integrin-using virus [36]. This is consistent with the observation that VP7 contains the αxβ2 ligand sequence GPR at aa positions 253–255.

The characterization of the αxβ2–VP7 interaction showed that the synthetic peptide GPRP blocked the infectivity of RRV and Wa viruses [36], but not their cell binding, confirming that, as previously suggested [98], the interaction of the virus with αxβ2 occurs at a postattachment step. In support of these findings, it has been described that antibodies to VP7 neutralize rotavirus infectivity by blocking a postbinding step [60].

6.2.3 Integrin αvβ3

Even though neither one of the two outer surface proteins of rotavirus contains the RGD motif, typical of the proteins that interact with αvβ3, the relevance of this integrin for rotavirus infection was demonstrated by the fact that antibodies to the β3 subunit reduced the infectivity of rotavirus strains RRV, nar3, and Wa and that preincubation of the cells with vitronectin, a β3 integrin ligand, specifically and efficiently blocked rotavirus infectivity [38]. In addition, it was shown that CHO cells transfected with the αv and β3 integrin subunit genes, became three to four times more susceptible to rotavirus infection than the parental CHO cell line, and this increase in infectivity was blocked by incubation of the cells with either MAbs to β3, or vitronectin [38]. Furthermore, antibodies to αvβ3, as well as ligands to this integrin, reduced the infectivity of rotaviruses, but did not block their attachment to cells, indicating that rotaviruses interact with this integrin at a postbinding step. As expected from the fact that neither VP4 nor VP7 contain the RGD tripeptide binding motif for integrin αvβ3, the interaction of rotavirus with this integrin was shown to be RGD-independent. Amino acid sequence comparison of the surface proteins of rotavirus and hantavirus, both of which interact with integrin αvβ3 in an RGD-independent manner [32, 38], identified a region shared by rotavirus VP7 and hantavirus G1G2 proteins, which has six out of nine identical aa. The sequence of this region in VP7 (NEWLCNPMD), named CNP, is highly conserved among different rotavirus strains, since 586 out of 621 reported VP7 sequences in the GenBank are identical in this region, while the remaining 35 have 1 (30 sequences), or 2 (5 sequences) amino acid differences. A synthetic peptide containing this conserved region was shown to block the infectivity of RRV and nar3 strains, but not their cell binding, indicating that rotaviruses interact with αvβ3 through the CNP region located at amino acids 161–169 of VP7, at a step subsequent to their initial binding to the cell surface [100], as shown for integrin αxβ2 [36]. Of interest, peptide CNP was found to bind to αvβ3 through a site different from the RGD-binding site; thus, the CNP peptide sequence could represent a new integrin αvβ3 binding motif. These findings confirmed and extended those by Graham et al. [36], who reported

that similarly to integrin αxβ2, the interaction of the virus with αvβ3 occurred at a postattachment step and correlated with the presence of a VP7 derived from the integrin-using virus.

Since integrins α2β1, α4β1, αvβ3, and αxβ2 have been suggested to play a role during rotavirus infection [15, 98], blocking experiments using mixtures of antibodies directed to these integrins have been conducted. An additive blocking effect was found when mixtures of antibodies to integrins α2β1 and αvβ3 were used, suggesting that these two integrins are involved in different stages of rotavirus infection [38].

6.3 Heat Shock Protein hsc70

Hsc70 is a constitutive member of the heat shock-induced hsp70 protein family. The proteins of this family are highly conserved nucleocytoplasmic ATPases that have been associated with a number of functions in cellular physiology, including protein folding, translocation across biological membranes, and assembly and disassembly of oligomeric complexes. In response to different stress conditions, these proteins prevent the formation of protein aggregates by stabilizing unfolded intermediates that are subsequently refolded to the native state or degraded [42, 64, 67]. In particular, hsc70 has been shown to favor protein transport across organella membranes, bind nascent polypeptides, and dissociate clathrin from clathrin coats [73]. Despite their typical nucleocytoplasmic residence, members of this family of chaperones have been reported to be present on the surface of several cells [69]. Hsc70 was reported to be present on the surface of MA104 and Caco-2 cells by immunofluorescence and flow cytometry analysis, and antibodies to this protein were shown to specifically block the infectivity of NA-sensitive and NA-resistant rotaviruses by about 80% [37]. The interaction of rotaviruses with hsc70 was found to occur at a postattachment step, since despite their efficient blocking activity, the antibodies to this chaperone did not prevent the binding of the viruses to the surface of cells. These findings suggest that rotaviruses interact with hsc70 late during the virus entry process, and that this interaction represents a common step for both neuraminidase-sensitive and -resistant strains [37].

The interaction of rotavirus RRV strain with hsc70 is mediated by a domain in VP5 located between amino acids 642 and 659 of the protein. A synthetic peptide that mimics this VP5 region (peptide KID) blocks the infectivity of rotavirus but not its cell binding, confirming that the interaction of VP5 with hsc70 occurs at a postattachment step during the virus entry process [97]. Using a different approach, Jolly et al. [51] found a similar region (between aa 650 and 657) in the VP5 protein of rotavirus strain CRW8, which was able to

bind to the surface of MA104 cells, and may also represent the hsc70-binding region of this rotavirus strain. The region contained in the peptide KID is not conserved among many of the different strains of rotavirus that have been sequenced so far, suggesting that its interaction with hsc70 is not strictly sequence-specific, as has also been observed for the hsc70 cellular targets. It is not known if the chaperone activity of hsc70 plays a role during rotavirus entry by triggering, for instance, conformational changes in the viral particle that allow the virus to reach the cytoplasm of the cell, or by promoting the uncoating of the viral particle. Nevertheless, it has recently been found that hsc70 binds to the virus through its ligand-binding site, and known ligands of this protein efficiently block the infectivity of rotavirus at a postattachment step (Pérez-Vargas et al., unpublished results).

7 Lipid Rafts

Lipid rafts are detergent-insoluble, glycosphingolipid- and cholesterol-enriched cell membrane microdomains that form lateral assemblies in the plasma membrane. These lipid microdomains are thought to function as specialized platforms for apical cell sorting of proteins and signal transduction, and as such are also enriched in glycophosphatidylinositol (GPI) -linked proteins, as well as in other signaling proteins and receptors [85]. Lipid rafts are also increasingly being reported to serve as the entry portal for several enveloped and nonenveloped viruses [8, 62].

As mentioned above, the cell attachment of rotaviruses seems to depend on gangliosides; accordingly, it has been shown that the infectivity of both NA-resistant and NA-sensitive rotavirus strains is partially blocked by metabolic inhibitors of glycolipid synthesis (PDMP), while it is not affected by the inhibition of the cellular O-glycosylation [39]. In addition, sequestration of cholesterol from the cell membrane with methyl-β-cyclodextrin reduced the infectivity of rotaviruses by more than 90%, while not affecting their binding to the cell [39]. Based on these findings it was suggested that lipid rafts might be involved in rotavirus cell entry [39, 56]. More recently, it was reported that ganglioside GM1, integrin subunits α2 and β3, and hsc70, associate with lipid rafts in MA104 cells, and it was also found that infectious viral particles associate with these microdomains early during cell infection [48]. Altogether, these observations suggest that rafts may play an important role in the cell entry of rotaviruses, where they could serve as organizing platforms to facilitate the efficient interaction of the viral particle with the cellular receptors.

8
Rotavirus Entry into Cells Is a Multistep Process

Different experimental approaches suggest that rotavirus entry into cells is a multistep process in which several interactions between the virus and the cell surface receptors occur. The available data indicates that at least three of these interactions occur in a sequential manner (reviewed in [55]): (a) in a competition infection assay that detects virus competition at both binding and postbinding steps, it was found that at least three cellular structures were involved in rotavirus cell infection, and the results suggest that these three virus–cell interactions occurred in an orderly fashion [66]; (b) the characterization of the binding properties of the rhesus rotavirus RRV and its mutant virus nar3, which binds to the cell surface with a modified specificity, showed that while nar3 interacts directly, or with higher affinity, with integrin α2β1, the wild-type parental strain RRV initially interacts with a SA-containing molecule, previous to its interaction with α2β1 [65, 99]; and (c) the use of receptor ligands and antibodies (to both cell receptors and viral proteins) that block virus infection by preventing either binding or postbinding events has established the order of some of the interactions. Thus, RRV and nar3 viruses were described to interact with integrins αxβ2 and αvβ3 after binding to α2β1, indicating that the contact with these two integrins occurs downstream of their interaction with α2β1. In a recent work by Graham et al. [36], it was shown that rotavirus strains SA11, RRV, and Wa bound to cells by interacting with integrin α2β1, and blockage of the interaction of the viruses with either integrin αxβ2 or integrin αvβ3 antibodies prevented cell infection by these viruses but not their binding to the cell surface, indicating that after binding to α2β1, the reported viruses interact (thus, in a sequential manner) with either αxβ2 or αvβ3, or both. Similarly, in a paper by Guerrero et al. [38], it was described that antibodies to integrin αvβ3, as well as ligands to this integrin, blocked the infectivity of rotaviruses Wa, nar3, and RRV, but did not prevent their binding to the cell surface. Since, as described above, these three viruses have been shown to interact with α2β1 (Wa and nar 3 during cell binding, while RRV has been reported to interact with this integrin either during cell binding [36] or after interaction with SA [99]), the interaction with αvβ3 must be at a later step, and therefore sequential. Finally, similar results were reported for the interaction of rotavirus RRV, nar3, and Wa with Hsc70 [37, 97], since the infection, but not the cell binding of these viruses was blocked when the virus hsc70-interaction was prevented.

In summary, there is much evidence for the sequential usage of SA and α2β1 as receptors. After the interaction with α2β1 (either at a postattachment level for some viruses or at the binding step for others), there is also clear

evidence for the downstream interaction of rotaviruses with hsc70, and integrins αxβ2 and αvβ3. Whether the three latter molecules are used by the viruses alternatively, such that interaction with only one of them is required for cell infection, or sequentially, i.e., that interaction with two or all three molecules is required, is not known at this stage. However, the fact that the five molecules described (SA, α2β1, αvβ3, αxβ2, and hsc70) have been shown to interact with different domains on the two virus surface proteins suggests that more than the three proven sequential interactions [SA→α2β1→X (where X could be either αvβ3, hsc70, or αxβ2)] could occur.

Based on these data, a working model for the early interactions of rotavirus with the host cell is presented in Fig. 4. In this model, the initial contact of a NA-sensitive virus strain with the cell surface occurs through a SA-containing cell receptor, most probably a ganglioside, using the VP8 domain of VP4. This initial interaction of the virus with SA probably induces a subtle conformational change in VP4, which allows the virus to interact subsequently with a second, NA-resistant cell receptor (here proposed to be the α2β1 integrin) through the DGE-binding motif of VP5. After the second interaction, at least one and up to three additional contacts involving VP5 and hsc70, and VP7 and integrins αvβ3 and αxβ2, take place. Whether these three late interactions occur sequentially or alternatively has not been established. These interactions probably mediate the penetration of the viruses into the cell by a mechanism that is not completely understood, but which finally leads to uncoating of the virus and initiation of the virus genome transcription in the cell's cytoplasm. In this model, most, if not all, of the molecules involved in rotavirus binding and entry are proposed to form a complex, embedded in lipid rafts on the cell surface.

The surface proteins of several enveloped and nonenveloped viruses have been shown to undergo major conformational changes during cell entry [86], and it seems that rotaviruses will not be the exception, since the analysis of the crystal structure of VP5 has suggested that the spike protein VP4 might undergo a severe conformational change during this process [21]. In fact, the sequential pathway of some of the interactions of the viral proteins with the cell surface, and the observation that VP5 contacts hsc70 through a domain that is most likely hidden below, or very close to, the VP7 layer, support the idea that the spike must change its conformation to allow these interactions to take place. Thus, it is reasonable to hypothesize that the proposed conformational rearrangements of VP4 could occur during one or more of the multiple contacts that take place between the virus particle and cellular surface molecules. In this scenario, it is tempting to speculate that a protein with chaperone activity, such as hsc70, could have a pivotal role to help in these processes.

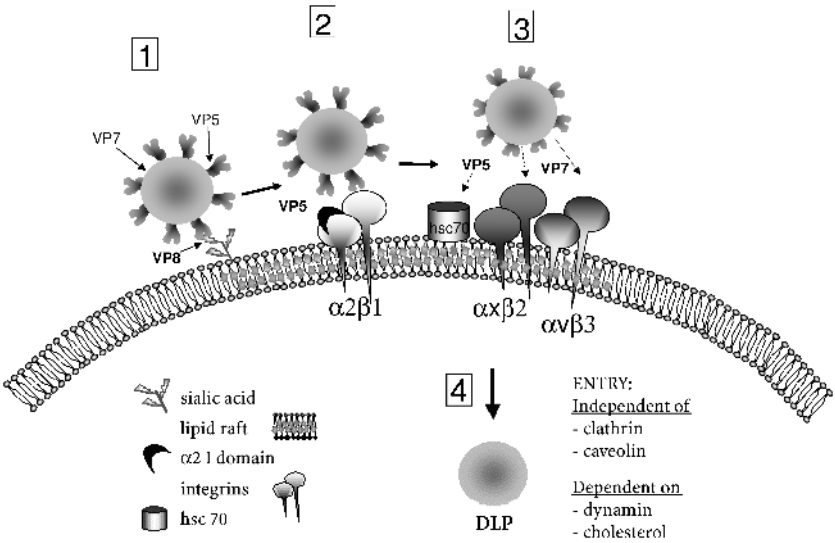

Fig. 4 Model for the early interactions of rotavirus with its host cell. This model illustrates the multistep interaction of a NA-sensitive strain with the cell surface. (*1*) The SA-dependent virus binds initially to a SA-containing molecule (most likely a ganglioside) present in the cell surface, through the VP8 domain of VP4. (*2*) After this initial interaction, the virus interacts with the I domain of the α subunit of integrin α2β1, using the DGE tripeptide sequence motif present in the VP5 fragment of VP4. (*3*) After the second interaction, the virus interacts with integrins αxβ2 and αvβ3, through VP7, and with hsc70 through VP5. These three interactions occur at a postattachment step, and they may represent alternative or subsequent interactions (see text). (*4*) Finally, the virus enters the cell by a still poorly defined mechanism which is clathrin- and caveolae-independent, but depends on the presence of cholesterol on the cell membrane and also needs a functional dynamin. During or shortly after the entry, the virus uncoats losing the outer layer proteins and yielding a transcriptionally active double-layered particle. Integrin α4β1 is not included in the model, since its role in rotavirus infections has not been clearly demonstrated

9 Mechanism of Virus Entry

The specific interactions of a virus with its receptors on the cell surface finally lead to the entry of the viral particle into the cell's interior. In general, enveloped viruses enter cells by fusion of the viral and cellular membranes at the plasma membrane or in endocytic vesicles. Much less is known, however, about the mechanism of cell entry for nonenveloped viruses. Early electron microscopy studies of rotavirus-infected cells suggested endocytosis as the viral internalization pathway. However, since rotavirus infectivity is not in-

hibited either by preventing the acidification of endosomes or by drugs that block the intracellular traffic of endocytic vesicles, the classical endocytotic pathway seems not to be important for cell entry of rotaviruses. A direct cell membrane penetration has also been proposed as the mechanism of virus entry based on electron microscopy data and on the observation that rotavirus infection induces a rapid permeabilization of the cell membrane [26]. More recently, it was found that drugs and dominant-negative mutants known to impair clathrin- as well as caveolae-mediated endocytosis did not affect rotavirus cell infection, while cells expressing a dominant-negative mutant of dynamin, a GTPase known to function in several membrane scission events, were not infected by the virus [83]. These results, together with the observation that depletion of cholesterol inhibits rotavirus infection, suggest that, to enter cells, rotaviruses might use a recently defined cell internalization pathway described as raft-dependent endocytosis, defined by its clathrin- and caveolin-independence, its dependence on dynamin, and its sensitivity to cholesterol depletion [70]. Also, it was recently reported that bafilomycin A, an inhibitor of the vacuolar proton-ATPase pump, blocks rotavirus infectivity. Based on this observation, it was suggested that an endocytotic mechanism could be involved in the entry of rotaviruses [9]; it would be of interest to determine if there is a proton-ATPase pump in the vesicles internalized by the non-clathrin, non-caveolin pathway.

10
Virus Infection of Polarized Epithelial Cells

It seems a paradox that integrins have been identified as receptors for rotaviruses in cultured epithelial cells, since in polarized epithelia, such as those of the enteric tract, these molecules have a polarized distribution and localize primarily at the basolateral plasma membrane [41, 46]. Rotaviruses reaching the intestinal epithelium would find the integrin receptors hidden beneath the tight junctions (TJs). The question then is how rotaviruses can reach their basolateral receptor to infect polarized epithelia? An indication of how the virus might open the TJs to expose the basolateral receptors has been recently suggested by the finding that VP8 is capable of opening the TJs. A recombinant VP8 protein diminished the transepithelial electrical resistance of MDCK polarized cell monolayers in a dose-dependent and reversible manner. This VP8 protein also increased the paracellular passage of nonionic tracers, and allowed the diffusion of the basolateral proteins Na^+/K^+-ATPase, $\alpha v\beta 3$ integrin, and a $\beta 1$ integrin subunit, to the apical side of the cells. These changes correlated with an altered subcellular distribution of the TJ proteins ZO-1,

claudin-3, and occludin [71]. The observations suggest that the virus could generate leaky TJs that would expose integrins to the apical surface, allowing the virus to bind and infect from the apical side. However, the ability of viruses to disrupt TJs during the early interaction with polarized epithelia remains to be shown. When the TJs of polarized MDCK cells in culture are opened artificially, the infectivity of rotaviruses is markedly increased (M. Realpe et al., unpublished data), suggesting that under those conditions, a basolateral molecule required for the efficient infection of cells probably diffuses to the apical side of the cells, facilitating its encounter with the virus and thus favoring its cell entry. Interestingly, it was shown that the recombinant VP8 was also able to disrupt the TJs in vivo, since this protein, when given orally to diabetic rats allowed the efficient oral administration of insulin, indicating that it is able to modulate the epithelial permeability [71].

11 Concluding Remarks

The entry of rotavirus into the host cell is a complex process that involves several cell surface receptors and several domains on both outer layer viral proteins. At least some of the interactions between the cellular receptors and viral proteins occur in a sequential manner, and they seem to take place in glycosphingolipid-enriched lipid microdomains. The requirement of several cell molecules, which need to be present and probably organized in a precise fashion in lipid rafts, might explain the cell and tissue tropism of these viruses. Even though many of the cell molecules involved in the early interactions of the virus with the cell surface have been identified, it remains to be defined which role each individual receptor plays in virus entry, the conformational changes experienced by the viral proteins upon interaction with these receptors, and the mechanism of virus internalization. Work to determine the receptors and the entry pathway used by rotaviruses to infect mature enterocytes in a natural infection will be of particular importance.

Acknowledgements We appreciate the support of Phil Dormitzer for providing the crystal images of the spike protein. Work on rotavirus cell entry in our laboratories is supported by grants 55003662 and 55000613 from the Howard Hughes Medical Institute, and G37621 N from the National Council for Science and Technology Mexico.

References

1. Arias CF, Romero P, Alvarez V, López S (1996) Trypsin activation pathway of rotavirus infectivity. J Virol 70:5832–5839

2. Bass DM, Mackow ER, Greenberg HB (1991) Identification and partial characterization of a rhesus rotavirus binding glycoprotein on murine enterocytes. Virology 183:602–610
3. Bergelson JM (2003) Virus interactions with mucosal surfaces: alternative receptors, alternative pathways. Curr Opin Microbiol 6:386–391
4. Bomsel M, Alfsen A (2003) Entry of viruses through the epithelial barrier: pathogenic trickery. Nat Rev Mol Cell Biol 4:57–68
5. Burmeister WP, Guilligay D, Cusack S, Wadell G, Arnberg N (2004) Crystal structure of species D adenovirus fiber knobs and their sialic acid binding sites. J Virol 78:7727–7736
6. Chappell JD, Prota AE, Dermody TS, Stehle T (2002) Crystal structure of reovirus attachment protein sigma1 reveals evolutionary relationship to adenovirus fiber. EMBO J 21:1–11
7. Charpilienne A, Abad MJ, Michelangeli F, Alvarado F, Vasseur M, Cohen J, Ruiz MC (1997) Solubilized and cleaved VP7, the outer glycoprotein of rotavirus, induces permeabilization of cell membrane vesicles. J Gen Virol 78:1367–1371
8. Chazal N, Gerlier D (2003) Virus entry, assembly, budding, and membrane rafts. Microbiol Mol Biol Rev 67:226–237, table of contents
9. Chemello ME, Aristimuno OC, Michelangeli F, Ruiz MC (2002) Requirement for vacuolar H+ -ATPase activity and Ca2+ gradient during entry of rotavirus into MA104 cells. J Virol 76:13083–13087
10. Ciarlet M, Crawford SE, Cheng E, Blutt SE, Rice DA, Bergelson JM, Estes MK (2002) VLA-2 (alpha2beta1) integrin promotes rotavirus entry into cells but is not necessary for rotavirus attachment. J Virol 76:1109–1123
11. Ciarlet M, Estes MK (1999) Human and most animal rotavirus strains do not require the presence of sialic acid on the cell surface for efficient infectivity. J Gen Virol 80:943–948
12. Clapham PR, McKnight A (2002) Cell surface receptors, virus entry and tropism of primate lentiviruses. J Gen Virol 83:1809–1829
13. Clark SM, Roth JR, Clark ML, Barnett BB, Spendlove RS (1981) Trypsin enhancement of rotavirus infectivity: mechanism of enhancement. J Virol 39:816–822
14. Compton T (2004) Receptors and immune sensors: the complex entry path of human cytomegalovirus. Trends Cell Biol 14:5–8
15. Coulson BS, Londrigan SL, Lee DJ (1997) Rotavirus contains integrin ligand sequences and a disintegrin-like domain that are implicated in virus entry into cells. Proc Natl Acad Sci U S A 94:5389–5394
16. Crawford SE, Mukherjee SK, Estes MK, Lawton JA, Shaw AL, Ramig RF, Prasad BV (2001) Trypsin cleavage stabilizes the rotavirus VP4 spike. J Virol 75:6052–6061
17. Delorme C, Brussow H, Sidoti J, Roche N, Karlsson KA, Neeser JR, Teneberg S (2001) Glycosphingolipid binding specificities of rotavirus: identification of a sialic acid-binding epitope. J Virol 75:2276–2287
18. Denisova E, Dowling W, LaMonica R, Shaw R, Scarlata S, Ruggeri F, Mackow ER (1999) Rotavirus capsid protein VP5* permeabilizes membranes. J Virol 73:3147–3153
19. Dimiter S (2004) Virus entry: molecular mechanisms and biomedical applications. Nat Rev Microbiol 2:109–122

20. Dormitzer PR, Greenberg HB, Harrison SC (2000) Purified recombinant rotavirus VP7 forms soluble, calcium-dependent trimers. Virology 277:420–428
21. Dormitzer PR, Nason EB, Prasad BV, Harrison SC (2004) Structural rearrangements in the membrane penetration protein of a non-enveloped virus. Nature 430:1053–1058
22. Dormitzer PR, Sun ZY, Blixt O, Paulson JC, Wagner G, Harrison SC (2002) Specificity and affinity of sialic acid binding by the rhesus rotavirus VP8* core. J Virol 76:10512–10517
23. Dormitzer PR, Sun ZYJ, Wagner G, Harrison SC (2002) The rhesus rotavirus VP4 sialic acid binding domain has a galectin fold with a novel carbohydrate binding site. EMBO J 21:885–897
24. Dowling W, Denisova E, LaMonica R, Mackow ER (2000) Selective membrane permeabilization by the rotavirus VP5* protein is abrogated by mutations in an internal hydrophobic domain. J Virol 74:6368–6376
25. Espejo RT, Lopez S, Arias C (1981) Structural polypeptides of simian rotavirus SA11 and the effect of trypsin. J Virol 37:156–160
26. Estes MK (2001) Rotaviruses and their replication. In: Knipe DM, Howley PM et al. (eds) Fields virology 4th edn. Lippincott Williams and Wilkins, Philadelphia, pp 1747–1785
27. Estes MK, Graham DY, Mason BB (1981) Proteolytic enhancement of rotavirus infectivity: molecular mechanisms. J Virol 39:879–888
28. Falconer MM, Gilbert JM, Roper AM, Greenberg HB, Gavora JS (1995) Rotavirus-induced fusion from without in tissue culture cells. J Virol 69:5582–5591
29. Fiore L, Greenberg HB, Mackow ER (1991) The VP8 fragment of VP4 is the rhesus rotavirus hemagglutinin. Virology 181:553–563
30. Fuentes Panana EM, López S, Gorziglia M, Arias CF (1995) Mapping the hemagglutination domain of rotaviruses. J Virol 69:2629–2632
31. Fukudome K, Yoshie O, Konno T (1989) Comparison of human, simian, and bovine rotaviruses for requirement of sialic acid in hemagglutination and cell adsorption. Virology 172:196–205
32. Gavrilovskaya IN, Shepley M, Shaw R, Ginsberg MH, Mackow EM (1998) β3 integrins mediate the cellular entry of hantaviruses that cause respiratory failure. Proc Natl Acad Sci U S A 95:7074–7079
33. Gilbert JM, Greenberg HB (1998) Cleavage of rhesus rotavirus VP4 after arginine 247 is essential for rotavirus-like particle-induced fusion from without. J Virol 72:5323–5327
34. Glass RI, Bresee JS, Parashar UD, Jiang B, Gentsch J (2004) The future of rotavirus vaccines: a major setback leads to new opportunities. Lancet 363:1547–1550
35. Golantsova NE, Gorbunova EE, Mackow ER (2004) Discrete domains within the rotavirus VP5* direct peripheral membrane association and membrane permeability. J Virol 78:2037–2044
36. Graham KL, Halasz P, Tan Y, Hewish MJ, Takada Y, Mackow ER, Robinson MK, Coulson BS (2003) Integrin-using rotaviruses bind alpha2beta1 integrin alpha2 I domain via VP4 DGE sequence and recognize alphaXbeta2 and alphaVbeta3 by using VP7 during cell entry. J Virol 77:9969–9978

37. Guerrero CA, Bouyssounade D, Zárate S, Isa P, López T, Espinosa R, Romero P, Méndez E, López S, Arias CF (2002) Heat shock cognate protein 70 is involved in rotavirus cell entry. J Virol 76:4096–4102
38. Guerrero CA, Méndez E, Zárate S, Isa P, López S, Arias CF (2000) Integrin alpha(v)beta(3) mediates rotavirus cell entry. Proc Natl Acad Sci U S A 97:14644–14649
39. Guerrero CA, Zárate S, Corkidi G, López S, Arias CF (2000) Biochemical characterization of rotavirus receptors in MA104 cells. J Virol 74:9362–9371
40. Guo C, Nakagomi O, Mochizuki M, Ishida H, Kiso M, Ohta Y, Suzuki T, Miyamoto D, Jwa Hidari KI, Suzuki Y (1999) Ganglioside GM1a on the cell surface is involved in the infection by human rotavirus KUN and MO strains1. J Biochem (Tokyo) 126:683–688
41. Gut A, Balda MS, Matter K (1998) The cytoplasmic domains of a beta1 integrin mediate polarization in Madin-Darby canine kidney cells by selective basolateral stabilization. J Biol Chem 273:29381–29388
42. Hartl FU (1996) Molecular chaperones in cellular protein folding. Nature 381:571–579
43. Haywood AM (1994) Virus receptors: binding, adhesion strengthening, and changes in viral structure. J Virol 68:1–5
44. Hewish MJ, Takada Y, Coulson BS (2000) Integrins a2b1 and a4b1 can mediate SA11 rotavirus attachment and entry into cells. J. Virol 74:228–236
45. Hynes RO (1992) Integrins: versatility, modulation, and signaling in cell adhesion. Cell 69:11–25
46. Hynes RO (2002) Integrins: bidirectional, allosteric signaling machines. Cell 110:673–687
47. Isa P, López S, Segovia L, Arias CF (1997) Functional and structural analysis of the sialic acid-binding domain of rotaviruses. J Virol 71:6749–6756
48. Isa P, Realpe M, Romero P, Lopez S, Arias CF (2004) Rotavirus RRV associates with lipid membrane microdomains during cell entry. Virology 322:370–381
49. Iturriza-Gomara M, Desselberger U, Gray J (2003) Molecular epidemiology of rotaviruses: Genetic mechanisms associated with diversity. In: Desselberger U and Gray J (eds) Viral gastroenteritis, Elsevier, Amsterdam, pp 317–344
50. Jolly CL, Beisner BM, Holmes IH (2000) Rotavirus infection of MA104 cells is inhibited by Ricinus lectin and separately expressed single binding domains. Virology 275:89–97
51. Jolly CL, Huang JA, Holmes IH (2001) Selection of rotavirus VP4 cell receptor binding domains for MA104 cells using a phage display library. J Virol Methods 98:41–51
52. Kapikian AZ, Hoshino Y, Chanock RM (2001) Rotaviruses. In: Knipe DM, Howley PM et al. (eds) Fields virology, 4th edn. Lippincott Williams and Wilkins, Philadelphia, pp 1787–1833
53. Keljo DJ, Smith AK (1988) Characterization of binding of simian rotavirus SA-11 to cultured epithelial cells. J Pediatr Gastroenterol Nutr 7:249–256
54. Londrigan SL, Graham KL, Takada Y, Halasz P, Coulson BS (2003) Monkey rotavirus binding to alpha2beta1 integrin requires the alpha2 I domain and is facilitated by the homologous beta1 subunit. J Virol 77:9486–9501

55. Lopez S, Arias CF (2004) Multistep entry of rotavirus into cells: a Versaillesque dance. Trends Microbiol 12:271–278
56. López S, Arias CF (2003) Attachment and post-attachment receptors for rotavirus. In: Desselberger U and Gray J (eds) Viral gastroenteritis, Elsevier, Amsterdam, pp 143–163
57. Lopez S, Arias CF, Bell JR, Strauss JH, Espejo RT (1985) Primary structure of the cleavage site associated with trypsin enhancement of rotavirus SA11 infectivity. Virology 144:11–19
58. Lopez S, Lopez I, Romero P, Mendez E, Soberon X, Arias CF (1991) Rotavirus YM gene 4: analysis of its deduced amino acid sequence and prediction of the secondary structure of the VP4 protein. J Virol 65:3738–3745
59. Ludert JE, Feng NG, Yu JH, Broome RL, Hoshino Y, Greenberg HB (1996) Genetic mapping indicates that VP4 is the rotavirus cell attachment protein in vitro and in vivo. J Virol 70:487–493
60. Ludert JE, Ruiz MC, Hidalgo C, Liprandi F (2002) Antibodies to rotavirus outer capsid glycoprotein VP7 neutralize infectivity by inhibiting virion decapsidation. J Virol 76:6643–6651
61. Mackow ER, Shaw RD, Matsui SM, Vo PT, Dang MN, Greenberg HB (1988) The rhesus rotavirus gene encoding protein VP3: location of amino acids involved in homologous and heterologous rotavirus neutralization and identification of a putative fusion region. Proc Natl Acad Sci U S A 85:645–649
62. Manes S, del Real G, Martinez AC (2003) Pathogens: raft hijackers. Nat Rev Immunol 3:557–568
63. Markwell MA, Paulson JC (1980) Sendai virus utilizes specific sialyloligosaccharides as host cell receptor determinants. Proc Natl Acad Sci U S A 77:5693–5697
64. Mayer MP, Bukau B (1998) Hsp70 chaperone systems: diversity of cellular functions and mechanism of action. Biol Chem 379:261–268
65. Méndez E, Arias CF, López S (1993) Binding to sialic acids is not an essential step for the entry of animal rotaviruses to epithelial cells in culture. J Virol 67:5253–5259
66. Méndez E, López S, Cuadras MA, Romero P, Arias CF (1999) Entry of rotaviruses is a multistep process. Virology 263:450–459
67. Morimoto RI, Kline MP, Bimston DN, Cotto JJ (1997) The heat-shock response: regulation and function of heat-shock proteins and molecular chaperones. Essays Biochem 32:17–29
68. Mossel EC, Ramig RF (2003) A lymphatic mechanism of rotavirus extraintestinal spread in the neonatal mouse. J Virol 77:12352–12356
69. Multhoff G, Hightower LE (1996) Cell surface expression of heat shock proteins and the immune response. Cell Stress Chaperones 1:167–176
70. Nabi IR, Le PU (2003) Caveolae/raft-dependent endocytosis. J Cell Biol 161:673–677
71. Nava P, Lopez S, Arias CF, Islas S, Gonzalez-Mariscal L (2004) The rotavirus surface protein VP8 modulates the gate and fence function of tight junctions in epithelial cells. J Cell Sci 117:5509–5519
72. Nemerow GR, Stewart PL (2001) Antibody neutralization epitopes and integrin binding sites on nonenveloped viruses. Virology 288:189–191

73. Newmyer SL, Schmid SL (2001) Dominant-interfering Hsc70 mutants disrupt multiple stages of the clathrin-coated vesicle cycle in vivo. J Cell Biol 152:607–620
74. Offit PA, Clark FH, Ward RL (2003) Current state of development of human rotavirus vaccines. In: Desselberger U, Gray J (eds) Viral gastroenteritis. Elsevier, Amsterdam, pp 345–368
75. Parashar UD, Hummelman EG, Bresee JS, Miller MA, Glass RI (2003) Global illness and deaths caused by rotavirus disease in children. Emerg Infect Dis 9:565–572
76. Pesavento JB, Estes MK, Prasad BVV (2003) Structural organization of the genome in rotavirus. In: Viral Gastroenteritis. Desselberger U, Gray J (eds) Viral gastroenteritis. Elsevier, Amsterdam, pp 115–128
77. Prasad BV, Burns JW, Marietta E, Estes MK, Chiu W (1990) Localization of VP4 neutralization sites in rotavirus by three-dimensional cryo-electron microscopy. Nature 343:476–479
78. Prasad BV, Wang GJ, Clerx JP, Chiu W (1988) Three-dimensional structure of rotavirus. J Mol Biol 199:269–275
79. Ramig RF (2004) Pathogenesis of intestinal and systemic rotavirus infection. J Virol 78:10213–10220
80. Rolsma MD, Kuhlenschmidt TB, Gelberg HB, Kuhlenschmidt MS (1998) Structure and function of a ganglioside receptor for porcine rotavirus. J Virol 72:9079–9091
81. Ruggeri FM, Greenberg HB (1991) Antibodies to the trypsin cleavage peptide VP8 neutralize rotavirus by inhibiting binding of virions to target cells in culture. J Virol 65:2211–19
82. Ruiz MC, Alonso-Torre SR, Charpilienne A, Vasseur M, Michelangeli F, Cohen J, Alvarado F (1994) Rotavirus interaction with isolated membrane vesicles. J Virol 68:4009–4016
83. Sanchez-San Martin C, Lopez T, Arias CF, Lopez S (2004) Characterization of rotavirus cell entry. J Virol 78:2310–2318
84. Shaw AL, Rothnagel R, Chen D, Ramig RF, Chiu W, Prasad BV (1993) Three-dimensional visualization of the rotavirus hemagglutinin structure. Cell 74:693–701
85. Simons K, Ikonen E (1997) Functional rafts in cell membranes. Nature 387:569–72
86. Smith AE, Helenius A (2004) How viruses enter animal cells. Science 304:237–242
87. Spear PG (2004) Herpes simplex virus: receptors and ligands for cell entry. Cell Microbiol 6:401–410
88. Stehle T, Harrison SC (1997) High-resolution structure of a polyomavirus VP1-oligosaccharide complex: implications for assembly and receptor binding. EMBO J 16:5139–5148
89. Superti F, Donelli G (1991) Gangliosides as binding sites in SA-11 rotavirus infection of LLC-MK2 cells. J Gen Virol 72:2467–2474
90. Tihova M, Dryden KA, Bellamy AR, Greenberg HB, Yeager M (2001) Localization of membrane permeabilization and receptor binding sites on the VP4 hemagglutinin of rotavirus: implications for cell entry. J Mol Biol 314:985–992
91. Triantafilou K, Takada Y, Triantafilou M (2001) Mechanisms of integrin-mediated virus attachment and internalization process. Crit Rev Immunol 21:311–322
92. Triantafilou K, Triantafilou M (2003) Lipid raft microdomains: key sites for Coxsackievirus A9 infectious cycle. Virology 317:128–135

93. Weis W, Brown JH, Cusack S, Paulson JC, Skehel JJ, Wiley DC (1988) Structure of the influenza virus haemagglutinin complexed with its receptor, sialic acid. Nature 333:426–431
94. Wu E, Nemerow GR (2004) Virus Yoga: the role of flexibility in virus host cell recognition. Trends Microbiol 12:162–169
95. Yeager M, Berriman JA, Baker TS, Bellamy AR (1994) Three-dimensional structure of the rotavirus haemagglutinin VP4 by cryo-electron microscopy and difference map analysis. EMBO J 13:1011–1018
96. Yeager M, Dryden KA, Olson NH, Greenberg HB, Baker TS (1990) Three-dimensional structure of rhesus rotavirus by cryoelectron microscopy and image reconstruction. J Cell Biol 110:2133–2144
97. Zárate S, Cuadras MA, Espinosa R, Romero P, Juárez KO, Camacho-Nuez M, Arias CF, López S (2003) Interaction of rotaviruses with Hsc70 during cell entry is mediated by VP5. J Virol 77:7254–260
98. Zárate S, Espinosa R, Romero P, Guerrero CA, Arias CF, López S (2000) Integrin alpha2beta1 mediates the cell attachment of the rotavirus neuraminidase-resistant variant nar3. Virology 278:50–54
99. Zárate S, Espinosa R, Romero P, Méndez E, Arias CF, López S (2000) The VP5 domain of VP4 can mediate attachment of rotaviruses to cells. J. Virol 74:593–599
100. Zárate S, Romero P, Espinosa R, Arias CF, López S (2004) VP7 mediates the interaction of rotaviruses with integrin alphavbeta3 through a novel integrin-binding site. J Virol 78:10839–10847

CTMI (2006) 309:67–85

Early Steps in Avian Reovirus Morphogenesis

J. Benavente · J. Martínez-Costas (✉)

Departamento de Bioquímica y Biología Molecular, Universidad de Santiago de Compostela, 15782 Santiago de Compostela,Spain
bnjmm@usc.es

Abstract Avian reoviruses are important pathogens that may cause considerable economic losses in poultry farming. Their genome expresses at least eight structural and four nonstructural proteins, three of them encoded by the S1 gene. These viruses enter cells by receptor-mediated endocytosis, and acidification of virus-containing endosomes is necessary for the virus to uncoat and release transcriptionally active cores into the cytosol. Avian reoviruses replicate within cytoplasmic inclusions of globular morphology, termed viral factories, which are not microtubule-associated, and which are formed by the nonstructural protein μNS. This protein also mediates the association of some viral proteins (but not of others) with inclusions, suggesting that the recruitment of viral proteins into avian reovirus factories has specificity. Avian reovirus morphogenesis is a complex and temporally controlled process that takes place exclusively within viral factories of infected cells. Core assembly takes place within the first 30 min after the synthesis of their protein components, and fully formed cores are then coated by outer-capsid polypeptides over the next 30 min to generate mature infectious reovirions. Based on data from avian reovirus studies and on results reported for other members of the *Reoviridae* family, we present a model for avian reovirus gene expression and morphogenesis.

1 Introduction

Avian and mammalian reoviruses constitute the two main groups of the genus *Orthoreovirus*, one of the 12 genera of the *Reoviridae* family (Mertens 2004). Although their reovirions are very similar in structure and molecular composition (Martínez-Costas et al. 1997; Spandidos and Graham 1976), members of the two groups differ in host range, degree of pathogenicity, and genome coding capacity, as well as in various biological properties (Nibert and Shiff 2001). Only avian reoviruses induce the formation of large syncytia in infected cells, and only mammalian reoviruses induce erythrocyte agglutination (Duncan 1999; Glass et al. 1973).

Avian reoviruses are ubiquitous in poultry flocks, but infection is usually asymptomatic, and most reoviruses isolated from birds are nonpathogenic. A direct link between the presence of the virus and disease has only been conclusively demonstrated for the viral arthritis syndrome or tenosynovitis, which is characterized by swelling of the hock joints and lesions in the gastrocnemius tendons (reviewed in Jones 2000; van der Heide 2000). A phylogenetic analysis, based on the sequences of the cell-attachment protein σC, grouped avian reoviruses into five different genotypic clusters. However, no correlation could be established between a particular genotype and the disease condition the virus was isolated from (Kant et al. 2003). Furthermore, to date all attempts to classify avian reoviruses according to their serological properties have been unsuccessful, because these viruses display a high degree of antigenic heterogeneity, while showing considerable cross-reactivity in neutralization tests.

The avian reovirion possesses a genome consisting of ten segments of double-stranded RNA (dsRNA) encased within a nonenveloped double protein capsid of icosahedral symmetry (Spandidos and Graham 1973). At least ten different structural polypeptides are present in the avian reovirion, and their distribution within the virus particle is diagramatically shown in Fig. 1 (Martínez-Costas et al. 1997; Schnitzer et al. 1982; Varela and Benavente 1994). The avian reovirus structural proteins have been assigned alphabetical subscripts (λA, λB, etc.) in reverse order of electrophoretic mobility, to distinguish them from the mammalian reovirus proteins that have been assigned numerical subscripts (λ1, λ2, etc.).

The initial extracellular attachment of the virus to the host cell is mediated by specific interactions of the minor outer-capsid protein σC with as yet unknown host receptors (Grande et al. 2002; Martínez-Costas et al. 1997; Shapouri et al. 1996). Avian reoviruses enter host cells by receptor-mediated endocytosis (Fig. 2), and acidification of the virus-containing endosomes is

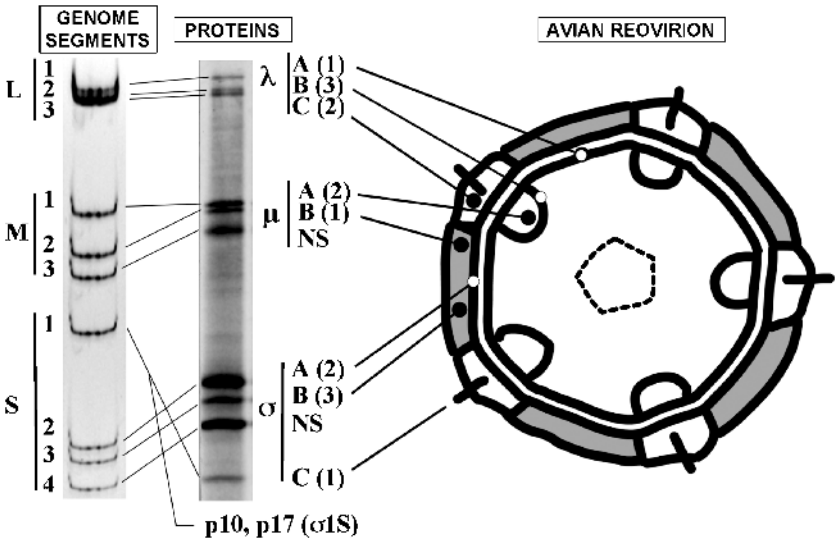

Fig. 1A–C Electrophoretic analysis of avian reovirus S1133 genome segments (**A**) and primary translation products (**B**). The numerical nomenclature of the homologous mammalian reovirus polypeptides is indicated within *brackets*. **C** Diagrammatic representation of the avian reovirion, indicating the location of the structural polypeptides

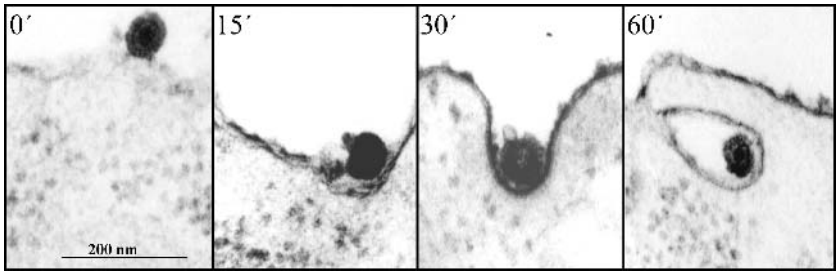

Fig. 2 Electron micrographs showing the process of avian reovirus penetration into avian cells. Purified avian reovirions were added to chicken embryo fibroblast monolayers and incubated for 1 h at 4°C. Cells were then incubated at 37°C for the times indicated on *top*, fixed and subjected to electron microscopy analysis

necessary for the avian reovirus to uncoat and replicate within the infected cell (Duncan 1996; Labrada et al. 2002). Virus uncoating is thought to facilitate the membrane interactions necessary for releasing transcription-competent avian reovirus cores into the cytoplasm.

Intracellular viral transcription, which is catalyzed by a core-associated dsRNA-dependent RNA polymerase, generates viral mRNAs that are identical to the positive strands of their encoding genes, possessing a type-1 cap at their 5′ ends and lacking a polyadenylated 3′ tail (Martínez-Costas et al. 1995). Reoviral mRNAs exert a dual function in the infected cell, since they program viral protein synthesis at the ribosomes and serve as templates for the production of minus strands with which they associate, thereby generating the progeny dsRNA genome segments (Nibert and Schiff 2001). The identity of the gene that codes for each of the avian reovirus polypeptides has been determined by in vitro translation of denatured individual genome segments (Fig. 1; Varela and Benavente 1994). Although most avian reovirus genome segments appear to be monocistronic, the S1 segment is a functional tricistronic gene that expresses two nonstructural proteins (p10 and p17) and one structural protein (σC) in infected cells (Fig. 1; Bodelon et al. 2001). Two other nonstructural proteins, μNS and σNS, are encoded by the M3 and S4 genome segments, respectively (Varela and Benavente 1994), and an amino-truncated μNS isoform, termed μNSC, has recently been shown to be produced in avian reovirus-infected cells (Tourís-Otero et al. 2004a).

The primary translation product of the avian reovirus M2 gene, the μB protein, is intracellularly modified by myristoylation and proteolysis. Site-specific cleavage of μB yields a myristoylated N-terminal peptide, μBN, and a large C-terminal protein, μBC; both precursor and cleaved products are structural components of the reovirion (Varela et al. 1996). It has recently been shown that the nonstructural p10 protein is palmitoylated at a conserved membrane-proximal dicysteine motif, and this covalent modification appears to be essential for the fusogenic activity of this protein (Shmulevitz et al. 2003). All avian reovirus proteins of infected cells, with the exception of σA and possibly λB, appear to be glycosylated, although the extent of glycosylation appears to be very low.

2 Viral Factories

The results of a number of early studies with different members of the *Reoviridae* family revealed that these agents replicate and assemble within cytoplasmic phase-dense inclusions, which have been variously termed viral inclusions, viral factories, or viroplasms. These specialized structures contain structural and nonstructural proteins, as well as viral double-stranded RNA and partially and fully assembled viral particles, but lack membranes and cellular organelles, including ribosomes. They first appear as numerous

small granules dispersed throughout the cytoplasm and, as infection progresses, they become larger, less numerous, and perinuclear in distribution (Fields et al. 1971; Rhim et al. 1962; Silverstein and Schur 1970). The genesis and composition of reoviral factories, as well as their roles in the virus life cycle, are only just beginning to be elucidated.

Cells infected with avian reoviruses have also been found to contain large cytoplasmic phase-dense inclusions believed to be the sites of viral replication and assembly (Tourís-Otero et al. 2004a, 2004b; Xu et al. 2004). Paracrystalline arrays of large perinuclear inclusions, containing mainly complete virions and empty viral particles, have been observed by electron microscopy of thin sections of avian reovirus-infected cells (Xu et al. 2004). Immunofluorescence microscopy analysis of infected cells has further revealed that the avian reovirus factories are discrete structures with globular morphology, not microtubule-associated (Tourís-Otero et al. 2004a). Globular factories are also generated during infection with the type-3 mammalian reovirus strains $T3D^N$ and T3C12 (Parker et al. 2002). In contrast, most mammalian reovirus strains form microtubule-associated factories, whose filamentous disposition appears to be determined by the capacity of the core protein μ2 to interact with microtubules and to anchor viral factories to them (Broering et al. 2002; Parker et al. 2002). These results suggest that, like its mammalian reovirus $T3D^N$ and T3C12 μ2 counterparts, avian reovirus μA does not associate with filamentous microtubules, although this hypothesis and the putative μA–μNS association await experimental confirmation.

A comparative analysis of the intracellular distributions of several avian reovirus proteins within infected vs transfected cells has revealed that, while all these proteins are present within viral factories of infected cells, only the M3-encoded nonstructural protein μNS is located within cytoplasmic globular inclusions when expressed individually in transfected cells (Fig. 3, panel 1A). This result suggests that μNS is the minimal viral factor required for factory formation in infected cells, and that the matrix of the factories is composed mainly of μNS. Like the avian reovirus protein μNS, several nonstructural proteins of other members of the *Reoviridae* family have also been reported to induce the formation of viroplasm-like structures in the absence of other viral components. For example, viral inclusions were formed in cells infected with a recombinant baculovirus expressing nonstructural bluetongue virus protein NS2, and in cells co-transfected with rotavirus nonstructural proteins NSP5 and NSP2 or transfected with mammalian reovirus protein μNS (Broering et al. 2002; Fabbretti et al. 1999; Thomas et al. 1990).

The inclusion-forming capacity of avian reovirus μNS suggests that this protein plays important roles in the early stages of the avian reovirus life cycle, by initiating sites of viral replication. The μNS protein is also a strong candi-

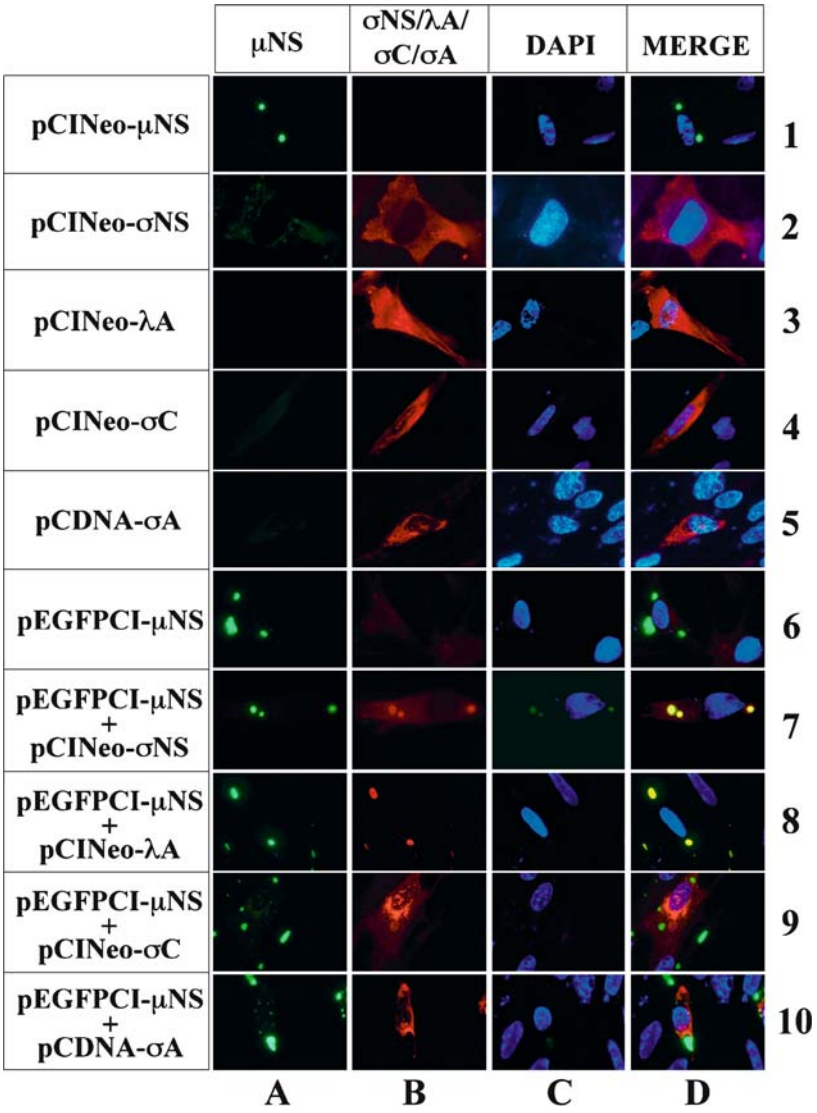

Fig. 3 Immunofluorescence microscopy analysis of the intracellular distribution of μNS/GFP-μNS and of other avian reovirus proteins in transfected cells. Chicken embryo fibroblast monolayers were transfected with the recombinant plasmids indicated on the left. At 18 h after transfection, the cells were stained with DAPI (*column C*), or immunostained (*column B*) with antibodies against σNS (*rows 2 and 7*), avian reovirus cores (*rows 3 and 8*), σC (r*ows 4 and 9*), and σA (*rows 5 and 10*). As with μNS, GFP-μNS forms globular inclusions and mediates the recruitment of σNS into factories (*column A*). See text for details. (With permission from Tourís-Otero et al. 2004a)

date for recruiting structural proteins to viral factories for subsequent assembly into viral particles. Examination of transfected cells expressing μNS and various other viral proteins reveals that only λA and σNS were redistributed to globular inclusions when expressed in combination with μNS (Fig. 3). These results and the observation that λA and σNS are present in viral factories within infected cells suggest that μNS mediates a selective recruitment of these two proteins into factories in avian reovirus-infected cells. Furthermore, experiments in triply transfected cells have shown that the capacity of μNS to recruit λA into inclusions is not inhibited by expression of σNS (Tourís-Otero et al. 2004a). This finding, together with the observations that σNS and λA are both present in single μNS inclusions, and that the two proteins bind to distinct μNS sites, suggests that σNS and λA can be simultaneously recruited to a viral factory through noncompetitive interactions with the same μNS molecule. In contrast to σNS and λA, the intracellular distribution of core protein σA and outer-capsid protein σC was not affected by coexpression of μNS (Fig. 3), suggesting that they are both shuttled into factories by a μNS-independent mechanism and that they are not required for the initial steps of factory formation. Collectively, these data suggest that the recruitment of viral proteins into avian reovirus factories is a selective and temporally controlled process, in which certain viral proteins are initially shuttled to factories via μNS association, whereas others are recruited later through interactions with as yet unknown factors. In contrast with the avian reovirus situation, each of the mammalian reovirus core proteins λ1, λ2, and σ2 has been reported to be independently recruited to μNS inclusions in transfected cells, suggesting that the three core proteins are shuttled to mammalian reovirus factories through specific associations with μNS (Broering et al. 2004). Thus, it appears that avian and mammalian reoviruses use different mechanisms for recruiting their homologous core proteins σA and σ2 to their respective viral factories. Hopefully, cloning and expression of all avian reovirus genes will allow the identification of all viral proteins whose factory recruitment is μNS-dependent, and of viral factors involved in the μNS-independent recruitment of other structural viral proteins. This information should be useful to understand the time course of protein incorporation into factories and viral particles.

3
Core Assembly

Avian reovirus core assembly requires that its protein components associate together in a coordinated fashion, that one copy of each of the ten viral mRNAs is selected and encapsidated, and that these mRNAs subsequently are used as

templates for complementary-strand synthesis in order to regenerate all ten dsRNA genome segments.

Although immunofluorescence microscopy has been successfully used to monitor the association of reoviral proteins with μNS inclusions in transfected cells, the recruitment of individual proteins into viral factories and viral particles within infected cells cannot be directly assayed by immunochemical techniques, since antibodies do not distinguish between free and inclusion-associated proteins. To overcome this problem, Tourís-Otero et al. (2004a) have devised an experimental approach that combines metabolic pulse-chase radiolabeling with cell fractionation and antibody immunoprecipitation. The discriminatory capacity of this approach is based on the ability of a Triton X-100-containing lysis buffer, previously used to discriminate between soluble and cytoskeleton-associated reoviral proteins (Mora et al. 1987), to solubilize the free proteins distributed diffusely throughout the cytoplasm, whereas the inclusion-associated proteins remain resistant to buffer extraction (Fig. 4A). The results of this combined approach reveal that μNS is the only newly synthesized viral polypeptide exclusively associated with the insoluble fraction (Fig. 4B), suggesting that μNS forms globular inclusions as soon as it is synthesized and that all other viral proteins are synthesized in the cytosol before becoming associated with μNS inclusions.

Core assembly was addressed by immunoprecipitating soluble and insoluble extracts from ^{35}S-amino acid pulse-chased cells with monoclonal antibodies against core protein σA (Fig. 4D). The results show that core assembly is a complex and temporally controlled process that takes place exclusively within viral factories. The data further suggest that cores are fully formed within the first 30 min after the synthesis of their protein components, and that only when they are fully assembled are the outer-capsid proteins incorporated onto them to produce mature reovirions. Although it has not been directly tested, the fact that cores assemble exclusively within viral factories

Fig. 4A–F Electrophoretic analysis of the recruitment of avian reovirus polypeptides into viral factories and viral particles. Chicken embryo fibroblast monolayers were mock-infected (*M*) or infected with avian reovirus (*AR*) for 14 h. The cells were then incubated with [^{35}S]amino acids for 15 min and then chased in medium containing an excess of nonradioactive methionine and cysteine for the time periods indicated on top. The cells were subsequently lysed with a Triton X-100-containing buffer, and the resulting soluble and insoluble fractions were analyzed by SDS-PAGE and autoradiography either before (**A**) or after immunoprecipitation with the antibodies indicated on the *upper-left corners* of **B–F**. See text for details. (With permission from Tourís-Otero et al. 2004a)

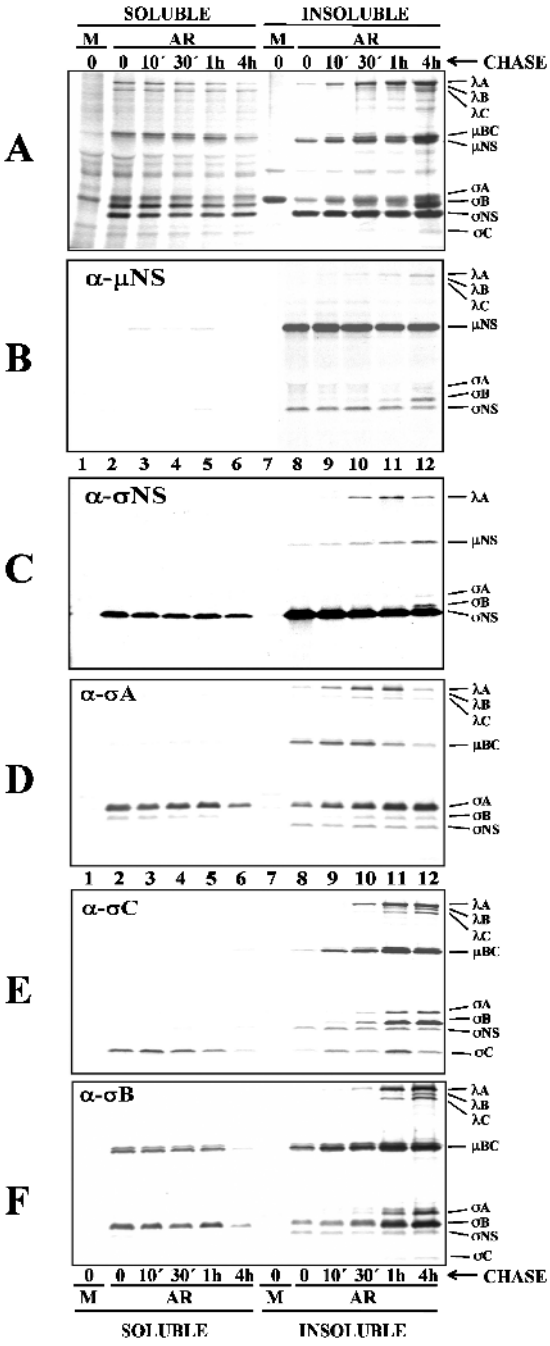
SOLUBLE
INSOLUBLE
M
AR
0 0 10′ 30′ 1h 4h 0 0 10′ 30′ 1h 4h
CHASE
A
λA
λB
λC
μBC
μNS
σA
σB
σNS
σC
B
α-μNS
1 2 3 4 5 6 7 8 9 10 11 12
C
α-σNS
D
α-σA
E
α-σC
F
α-σB
SOLUBLE
INSOLUBLE

suggests that these structures are the sites of mRNA-dependent minus-strand synthesis as well. This hypothesis is supported by the observation that large amounts of newly transcribed viral mRNAs localize to factories in mammalian reovirus-infected cells (Broering et al. 2004), as well as by the data of a recent study conducted by Silvestri et al. (2004). The results of this study suggest that there are two functionally distinct classes of plus-strand viral RNAs in rotavirus-infected cells: those that never leave viroplasms, which are the primary source of templates for the synthesis of minus-strand RNAs; and those that, by exceeding the RNA-binding capacity of viroplasms, are released into the cytosol for programming viral protein synthesis at the ribosomes. Their results further suggest that the rotaviral mRNAs released into the cytosol cannot be transported back into viroplasms, and therefore cannot be used as templates for minus-strand synthesis.

The first step in avian reovirus morphogenesis appears to be the formation of a λA core shell, since this major core protein is the first structural protein to become incorporated into viral factories (Fig. 4A), and its recruitment is mediated by μNS (Fig. 3, panel 8). By contrast, σA appears to associate at a later stage of core morphogenesis, via a μNS-independent mechanism. A recent study using avian reovirus 138-derived temperature-sensitive mutants that carry lesions in the major core protein σA has shed some light on the role of this protein in avian reovirus morphogenesis (Xu et al. 2004). Cells infected with the mutant *tsA12*, which contains a proline-to-leucine substitution at residue158 in the σA protein, accumulate a higher proportion of core-like particles at a nonpermissive temperature than at permissive temperatures, suggesting that σA plays an important role in core coating by outer-shell proteins. On the other hand, when the strain 138-derived mutant *tsA12* was crossed with the avian reovirus strain 176, all of the resulting reassortants carrying a *tsA12* σA-encoding S2 gene also contained the λB- and σNS-encoding genes derived from *tsA12*. This result suggests that there is a strain-specific interaction between the three proteins, raising the possibility that σNS and/or λB can mediate the recruitment of σA into avian reovirus factories. Finally, studies with the temperature-sensitive mutant *tsA146*, which carries a proline-to-serine substitution at residue 55 and a threonine-to-isoleucine substitution at position 290, have revealed a significant increase in the proportion of complete virions and a significant decrease in the proportion of empty viral particles when cells were infected with the mutant at a restrictive temperature vs infection at a permissive temperature (Xu et al. 2004). This result is consistent with a role of σA in the stabilization of the λA shell, since a reduced affinity of the mutated σA for the shell would cause more RNA to enter nascent progeny particles before the λA shell becomes rigid and refractory to RNA penetration. This hypothesis is supported by results obtained with other members of the

Reoviridae family. Thus, analysis of the mammalian reovirus core by X-ray crystallography revealed that σ2, the avian reovirus σA counterpart, lies on top of the λ1 shell and stabilizes it (Reinisch et al. 2000). Furthermore, while the expression of mammalian reovirus core shell protein λ1 is not sufficient to yield core-like particles that can withstand purification, coexpression of λ1 and the core nodule protein σ2 generates purification-resistant particles, suggesting that σ2 stabilizes the λ1 core shell (Kim et al. 2002; Xu et al. 1993). On the other hand, analysis of the bluetongue virus core structure by X-ray crystallography showed that a fragile inner core shell is initially formed by the VP3 protein, and that this structure is then made rigid by the incorporation of VP7 on top of the VP3 shell (Grimes et al. 1998). Collectively, these results suggest that the homologous proteins σ2, σA, and VP7 act as clamps for stabilization of the shell formed by the major core protein of their respective viruses. In contrast with the reovirus/orbivirus situation, individual expression of the most abundant rotavirus core protein VP2 produces stable core-like particles (Labbé et al. 1991), suggesting that a VP2-stabilizing activity is not required for the formation of the innermost protein shell of the rotavirus particle.

Although specific antibodies and cloned genes are obviously needed to evaluate the μNS dependence and temporal order of incorporation of all other avian reovirus core proteins into viral factories and viral cores, examination of the protein distribution between the soluble and insoluble fractions suggests that protein λB becomes associated with viral factories before σA (Fig. 4A). On the other hand, by analogy with the mammalian reovirus situation, if μNS mediates the recruitment of core protein μA into avian reovirus factories and if λC is the protein that completes core morphogenesis, primary avian reovirus core intermediates might be formed by the addition of λB and μA onto the λA core shell, and core assembly might be subsequently completed by the incorporation of proteins σA and λC. This model is consistent with the positions that the mammalian counterparts of the avian reovirus proteins occupy within the core structure. Thus, the mammalian counterparts of λB and μA are located beneath the core shell, whereas the counterparts of σA and λC lay on top of the shell (Dryden et al. 1998; Reinisch et al. 2000).

The precise role that viral factories play in reovirus morphogenesis is not yet clear. On the one hand, all members of the *Reoviridae* family investigated so far have been shown to assemble within intracellular viral factories, suggesting that these specialized structures are necessary for viral replication and assembly within infected cells. On the other hand, viral factories appear to be dispensable for the assembly of viral proteins into particles in the *Reoviridae* family, since core-like particles can be formed by expression of reovirus, rotavirus, and bluetongue virus core proteins from recombinant baculoviruses or vaccinia viruses (Labbé et al. 1991; Loudon and Roy 1992; Xu

et al. 1993), indicating that core proteins can assemble into particles outside the factories. This apparent contradiction regarding the absolute requirement of viral factories for core morphogenesis can, however, be reconciled by considering: (a) that the core-like particles generated in baculovirus- or vaccinia virus-infected cells are empty particles that lack viral RNA; and (b) that the efficiency of particle formation from recombinant proteins diminishes as the number of proteins to be assembled increases. This latter observation seems to suggest that viral factories may be important for the selective recruitment of viral proteins in a temporal order and proper arrangement required for maximal core assembly efficiency. Consistent with this hypothesis, a selective recruitment of viral proteins into factories has been shown to occur in avian reovirus-infected cells (Tourís-Otero et al. 2004a). On the other hand, a recent study revealed that many of the parental mammalian reovirus core particles released into the cytoplasm after intraendosomal uncoating become bound to preformed μNS inclusions, because of the core-binding activity of the mammalian reovirus protein μNS (Broering et al. 2004). Thus, it appears that following μNS synthesis and factory formation, viral mRNAs are exclusively synthesized within the viral factories, which in turn suggests that factories might also be required for retaining and concentrating the newly synthesized viral mRNAs that are necessary for packaging and replication. Furthermore, this activity is presumably necessary during the early stages of core morphogenesis, since viral mRNAs are thought to enter the core shell before the shell becomes rigid as a result of the clamping activity of protein σ. In this scenario, the nonstructural protein σNS appears to be the most likely candidate for retaining viral mRNAs within avian reovirus factories, since this protein possesses RNA-binding activity and since it is recruited early into factories through a specific association with μNS (Tourís-Otero et al. 2004b; Yin and Lee 1998). Recent results from our laboratory (unpublished data) have revealed that the RNA-binding activity of avian reovirus σNS is dispensable for μNS binding, suggesting that RNA does not contribute to the σNS–μNS association. In contrast, RNA has been reported to contribute to, although not to be strictly required for, the association of mammalian reovirus nonstructural proteins σNS and μNS (Miller et al. 2003). This discrepancy could be related to the different structural RNA-binding requirements of the two σNS proteins. Thus, while the N-terminal 118 residues of mammalian reovirus σNS are sufficient for binding RNA (Gillian and Nibert 1998), basic residues spread widely along the entire avian reovirus σNS sequence are necessary for RNA binding (Tourís-Otero et al. 2005).

Although σNS has been shown to lack specificity for binding viral sequences in vitro, a viral cofactor could provide σNS with RNA-binding specificity within infected cells. In the absence of experimental evidence, a likely

cofactor candidate is μNS, which associates with σNS in infected cells and mediates its recruitment into viral factories (Tourís-Otero et al. 2004b). Another possibility is that cellular mRNAs are excluded from and not allowed to penetrate into the factories, obviating the need for inclusion-associated σNS to have a preference for viral sequences. In this scenario, σNS would only retain viral mRNAs within the factories, and only when the amount of viral mRNA within factories exceeds the RNA-binding capacity of σNS would excess transcripts be released into the cytoplasm for programming viral protein synthesis at the ribosomes, since viral factories do not contain ribosomes. Furthermore, if by analogy with the rotavirus situation reported by Silvestri et al. (2004) there is no trafficking pathway allowing transport of cytosolic viral mRNAs back into factories, the reoviral mRNAs released from factories into the cytoplasm would only be used for translation, not for minus-strand synthesis.

4
Core Coating

Coating of cores by outer-capsid polypeptides is necessary to complete the intracellular production of infectious mature reovirions. This process was investigated by Tourís-Otero et al. (2004a) by immunoprecipitating soluble and insoluble extracts from ^{35}S-amino acid pulse-chased cells with antibodies against the outer-capsid proteins σB and σC (Fig. 4E, F). The data revealed that core coating by outer-capsid proteins occurs exclusively within viral factories, and that core assembly and coating are nonconcurrent successive events. They further showed that σB associates spontaneously and very rapidly with μB and μBC in the cytosol to form a ternary hetero-oligomeric complex that contains stoichiometrically equal amounts of the three viral proteins, and that the three viral proteins incorporate onto core particles forming part of this complex. On the other hand, even though σB and σC are detected within viral inclusions just after their synthesis (Fig. 4E, F), they do not associate with core proteins until 30 min later. This, and the fact that coimmunoprecipitation of the full spectrum of viral structural proteins is not detected until 60 min after their synthesis, confirm that cores are assembled within the first 30 min after the synthesis of their protein components, and suggest that cores are coated by outer-capsid proteins during the next 30 min to complete reovirion morphogenesis. A study conducted with mammalian reoviruses revealed that highly infectious mammalian reovirions can be generated by recoating purified core particles with recombinant forms of the outer-capsid proteins (Chandran et al. 2001). Similarly, the infectivity of rotavirus cores and single-shelled particles could be rescued by adding soluble proteins iso-

lated from the intermediate and/or outer capsid shells of purified rotavirions (Chen and Ramig 1993a, 1993b). These results suggest that core coating can be dissociated from core assembly and that the incorporation of outer-capsid polypeptides onto cores does not require the presence of viral factories.

5 Conclusions and a Model for Avian Reovirus Gene Expression and Morphogenesis

Although some progress has been made in recent years in gaining an understanding of the molecular mechanisms governing avian reovirus replication and morphogenesis, several major questions remain unresolved. We have recently learned that progeny avian reovirus particles assemble exclusively within globular cytoplasmic viral factories, and that these structures are initially formed by the nonstructural protein μNS. We have also discovered that μNS mediates the factory recruitment of the nonstructural protein σNS and of the major core-shell protein λA, suggesting that these three proteins play key roles in the early stages of core morphogenesis. Conversely, the fact that core protein σA is not shuttled into factories via a μNS-dependent mechanism suggests that σA is not involved in the first stage of core assembly. Further progress in understanding when and how other avian reovirus proteins are recruited into factories and into viral particles has been hindered to date by the lack of availability of viral cloned genes and specific antibodies, although these tools are expected to be available soon. The phenotypic characterization of other temperature-sensitive avian reovirus mutants, the coexpression of structural avian reovirus proteins in the baculovirus system and the use of viral-specific small interfering RNAs appear to be promising alternative approaches for further investigation of avian reovirus morphogenesis. Efforts should also be directed at identifying the signals and mechanisms involved in viral mRNA selection and encapsidation, as well as in mRNA-dependent minus-strand synthesis. Better knowledge of the events involved in avian reovirus gene expression and morphogenesis would be very useful for designing efficient reverse genetic systems allowing manipulation of the reoviral genome, and may also be important for the development of antiviral agents that could interfere with these viral processes, and hence with viral replication.

By combining the results obtained with avian reoviruses with the data reported by different laboratories on the replication of other members of the *Reoviridae* family, here we propose a model for avian reovirus replication and assembly (Fig. 5). According to this model, transcriptionally active parental reoviral cores released into the cytoplasm after intraendosomal uncoating

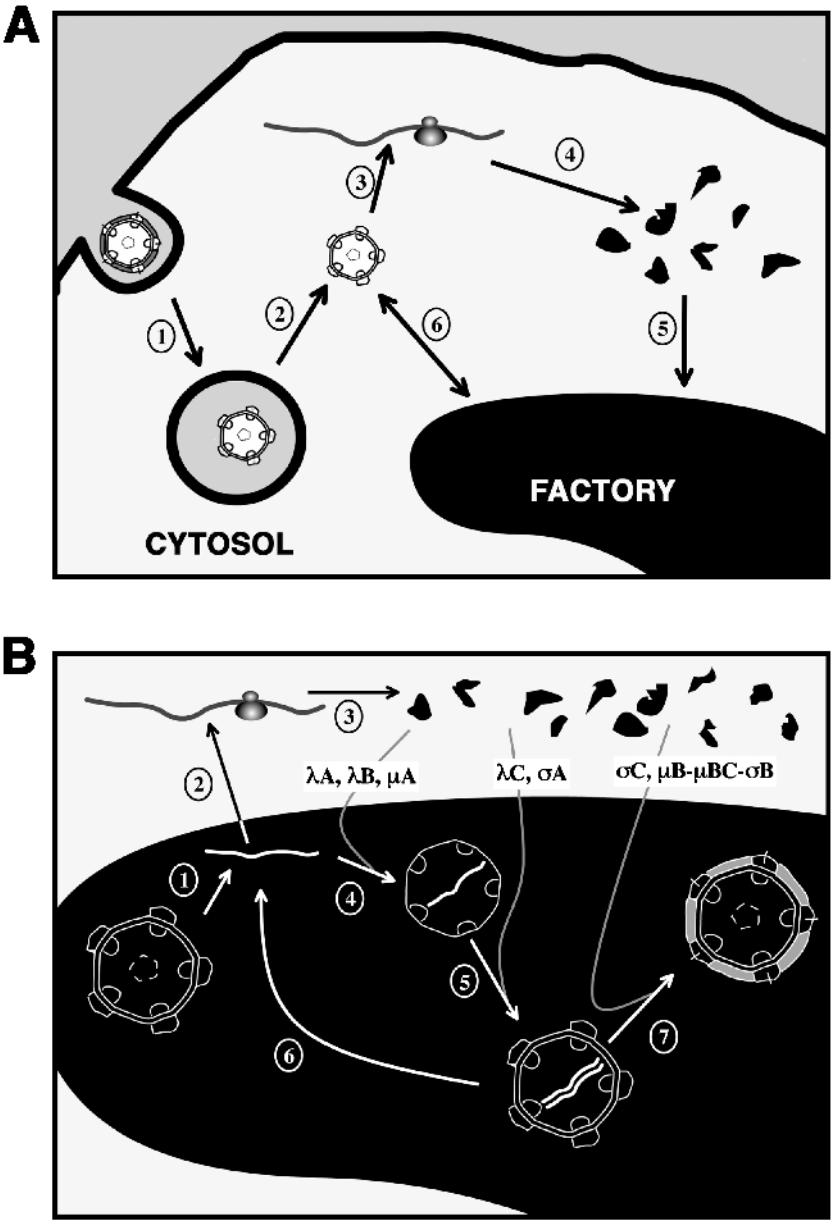

Fig. 5A, B Proposed model of avian reovirus replication. **A** Virus internalization and factory formation. **B** Viral morphogenesis within the viral factories. The pathways are explained in the last section of the text

(Fig. 5A, step 2) produce viral mRNAs (Fig. 5A, step 3). Viral polypeptides are subsequently synthesized by ribosomal translation of the viral transcripts (Fig. 5A, step 4). The nonstructural protein μNS and σNS would rapidly form viral factories and would recruit parental cores into the factories, by virtue of the core-binding activity of μNS (Fig. 5A, steps 5 and 6). Inclusion-associated parental cores would then catalyze the synthesis of viral transcripts (Fig. 5B, step 1), most of which would be retained within the factory by the RNA-binding activity of σNS, and these mRNAs would serve as templates for minus-strand RNA synthesis and progeny genome formation; only transcripts exceeding the retention capacity of σNS would be released into the cytoplasm (Fig. 5B, step 2), allowing viral protein synthesis to continue (Fig. 5B, step 3). Proteins μA, λA, and λB would then be recruited into the factories by association with μNS, and a fragile inner core shell would then be formed by the association of λA molecules, into which proteins μA and λB, as well as one copy of each of the ten viral mRNAs, would penetrate to form an unstable primary core intermediate (Fig. 5B, step 4). Protein σA would then be recruited into the factories and would bind the outside of the shell, causing its stabilization and precluding further RNA/protein penetration. Core morphogenesis would be subsequently completed by the incorporation of the guanylyltransferase protein λC and by synthesis of the RNA minus strands, which by associating with the plus strands would form the progeny genomes (Fig. 5B, step 5). The newly formed cores would perform a dual function in the infected cell: they would transcribe their genome into plus-strand RNAs for amplifying virus replication (Fig. 5B, step 6), and they would be subsequently coated by outer-capsid polypeptides to generate mature progeny reovirions (Fig. 5B, step 7).

References

Bodelon G, Labrada L, Martínez-Costas J, Benavente J (2001) The avian reovirus genome segment S1 is a functionally tricistronic gene that expresses one structural and two nonstructural proteins in infected cells. Virology 290:181–191

Broering TJ, Parker JSL, Joyce PL, Kim J, Nibert ML (2002) Mammalian reovirus nonstructural protein μNS forms large inclusions and colocalizes with reovirus microtubule-associated protein μ2 in transfected cells. J Virol 76:8285–8297

Broering TJ, Kim J, Miller CL, Piggot CDS, Dinoso JB, Nibert ML, Parker JSL (2004) Reovirus nonstructural protein μNS recruits viral core surface proteins and entering core particles to factory-like inclusions. J Virol 78:1882–1892

Chandran K, Zhang X, Olson NH, Walker SB, Chappell JD, Dermody TS, Baker TS, Nibert ML (2001) Complete in vitro assembly of the reovirus outer capsid produces highly infectious particles suitable for genetic studies of the receptor-binding protein. J Virol 75:5335–5342

Chen D, Ramig RF (1993a) Rescue of infectivity by in vitro transcapsidation of rotavirus single-shelled particles. Virology 192:422–429

Chen D, Ramig RF (1993b) Rescue of infectivity by sequential in vitro transcapsidation of rotavirus core particles with inner capsid and outer capsid proteins. Virology 194:743–751

Dryden KA, Farsetta DL, Wang GJ, Keegan JM, Fields BN, Baker TS, Nibert ML (1998) Internal structures containing transcriptase-related proteins in top component particles of mammalian orthorevirus. Virology 225:33–46

Duncan R (1996) The low pH-dependent entry of avian reovirus is accompanied by two specific cleavages of the major outer capsid protein μ2C. Virology 219:179–189

Duncan R (1999) Extensive sequence divergence and phylogenetic relationships between the fusogenic and nonfusogenic orthoreoviruses: a species proposal. Virology 260:316–328

Fabbretti E, Afrikanova I, Vascotto F, Burrone OR (1999) Two non-structural rotavirus proteins, NSP2 and NSP5, form viroplasm-like structures in vivo. J Gen Virol 80:333–339

Fields BN, Raine CS, Baum SG (1971) Temperature-sensitive mutants of reovirus type 3: defects in viral maturation as studied by immunofluorescence and electron microscopy. Virology 43:569–578

Gillian AL, Nibert ML (1998) Amino terminus of reovirus nonstructural protein σNS is important for ssRNA binding and nucleoprotein complex formation. Virology 240:1–11

Glass SE, Naqi SA, Hall CF, Kerr KM (1973) Isolation and characterization of a virus associated with arthritis of chickens. Avian Dis 17:415–424

Grande A, Costas C, Benavente J (2002) Subunit composition and conformational stability of the oligomeric form of the avian reovirus cell-attachment protein σC. J Gen Virol 83:131–139

Grimes JM, Burroughs JN, Gouet P, Diprose JM, Malby R, Zientara S, Mertens PPC, Stuart DI (1998) The atomic structure of the bluetongue virus core. Nature 395:470–478

Jones RC (2000) Avian reovirus infections. Rev Sci Tech 19:614–625

Kant A, Balk F, Born L, van Roozelaar D, Heijmans J, Gielkins A, ter Huurne A (2003) Classification of Dutch and German avian reoviruses by sequencing the σC protein. Vet Res 34:203–212

Kim J, Zhang X, Centonze VE, Bowman VD, Noble S, Baker TS, Nibert ML (2002) The hydrophilic amino-terminal arm of reovirus core shell protein λ1 is dispensable for particle assembly. J Virol 76:12211–12222

Labbé M, Charpilienne A, Crawford SE, Estes MK, Cohen J (1991) Expression of rotavirus VP2 produces empty corelike particles. J Virol 65:2946–2952

Labrada L, Bodelon G, Vinuela J, Benavente J (2002) Avian reoviruses cause apoptosis in cultured cells: viral uncoating but not viral gene expression is required for apoptosis induction. J Virol 76:7932–7941

Loudon PT, Roy P (1992) Interaction of nucleic acids with core-like and subcore-like particles of bluetongue virus. Virology 191:231–236

Martínez-Costas J, Varela R, Benavente J (1995) Endogenous enzymatic activities of the avian reovirus S1133: identification of the viral capping enzyme. Virology 206:1017–1026

Martínez-Costas J, Grande A, Varela R, García-Martínez C, Benavente J (1997) Protein architecture of avian reovirus S1133 and identification of the cell attachment protein. J Virol 71:59–64

Mertens, P (2004) The dsRNA viruses. Virus Res 101:3–13

Miller CL, Broering TJ, Parker JSL, Arnold MM, Nibert ML (2003) Reovirus σNS protein localizes to inclusions through an association requiring the μNS amino terminus. J Virol 77:4566–4576

Mora M, Partin K, Bhatia M, Partin J, Carter C (1987) Association of avian reovirus proteins with the structural matrix of infected cells. Virology 159:265–277

Nibert ML, Schiff LA (2001) Reoviruses and their replication. In: Knipe DM, Hooley PM (eds) Fields virology. Lippincott Willams & Wilkins, Philadelphia, pp. 1679–1728

Parker JSL, Broering TJ, Kim J, Higgins DE, Nibert ML (2002) Reovirus core protein μ2 determines the filamentous morphology of viral inclusion bodies by interacting with and stabilizing microtubules. J Virol 76:4483–4496

Reinisch KM, Nibert ML, Harrison SC (2000) Structure of the reovirus core at 3.6 Å resolution. Nature 404:960–967

Rhim JS, Jordan LE, Mayor HD (1962) Cytochemical, fluorescent-antibody and electron microscopic studies on the growth of reovirus (ECHO 10) in tissue culture. Virology 17:342–355

Schnitzer TJ, Ramos T, Gouvea V (1982) Avian reovirus polypeptides: analysis of intracellular virus-specified products, virions, top component, and cores. J Virol 43:1006–1014

Shapouri MR, Arella M, Silim A (1996) Evidence for the multimeric nature and cell binding ability of avian reovirus sigma 3 protein. J Gen Virol 77:1203–1210

Shmulevitz M, Salsman J, Duncan R (2003) Palmytoylation, membrane-proximal basic residues, and transmembrane glycine residues in the reovirus p10 protein are essential for syncytium formation. J Virol 77:9769–9779

Silverstein SC, Schur PH (1970) Immunofluorescent localization of double-stranded RNA in reovirus-infected cells. Virology 41:564–566

Silvestri LS, Taraporewala ZF, Patton JT (2004) Rotavirus replication: plus-sense templates for double-stranded RNA synthesis are made in viroplasms. J Virol 78:7763–7774

Spandidos DA, Graham AF (1976) Physical and chemical characterization of an avian reovirus. J Virol 19:968–976

Thomas CP, Booth TF, Roy P (1990) Synthesis of bluetongue virus-encoded phosphoprotein and formation of inclusion bodies by recombinant baculovirus in insect cells: it binds the single-stranded RNA species. J Gen Virol 71:2073–2083

Tourís-Otero F, Cortez-San Martín M, Martínez-Costas J, Benavente J (2004a) Avian reovirus morphogenesis occurs within viral factories and begins with the selective recruitment of σNS and λA to μNS inclusions. J Mol Biol 341:361–374

Tourís-Otero F, Martínez-Costas J, Vakharia VN, Benavente J (2004b) Avian reovirus nonstructural protein μNS forms viroplasm-like inclusions and recruits σNS to these structures. Virology 319:94–106

Tourís-Otero F, Martínez-Costas J, Vakharia VN, Benavente J (2005) Characterization of the nucleic acid-binding activity of the avian reovirus nonstructural protein σNS. J Gen Virol 86:1159–1169

Van der Heide L (2000) The history of avian reovirus. Avian Dis 44:638–641

Varela R, Benavente J (1994) Protein coding assignment of avian reovirus strain S1133. J Virol 68:6775–6777

Varela R, Martínez-Costas J, Mallo M, Benavente J (1996) Intracellular posttranslational modifications of S1133 avian reovirus proteins. J Virol 70:2974–2981

Xu P, Miller SE, Joklik WK (1993) Generation of reovirus core-like particles in cells infected with hybrid vaccinia viruses that express genome segments L1, L2, L3, and S2. Virology 197:726–731

Xu W, Patrick MK, Hazelton PR, Coombs KM (2004) Avian reovirus temperature-sensitive mutant *tsA12* has a lesion in major core protein σA and is defective in assembly. J Virol 78:11142–11151

Yin HS, Lee LH (1998) Identification and characterization of RNA-binding activities of avian reovirus non-structural protein σNS. J Gen Virol 79:1411–1413

CTMI (2006) 309:87–116

Bluetongue Virus Assembly and Morphogenesis

P. Roy (✉) · R. Noad

Department of Infectious and Tropical Diseases, London School
of Hygiene and Tropical Medicine, Keppel Street, London WC1E 7HT, UK
polly.roy@lshtm.ac.uk

Abstract Like other members of the *Reoviridae*, bluetongue virus faces the same constraints on structure and assembly that are imposed by a large dsRNA genome. However, since it is arthropod-transmitted, BTV must have assembly pathways that are sufficiently flexible to allow it to replicate in evolutionarily distant hosts. With this background, it is hardly surprising that BTV interacts with highly conserved cellular pathways during morphogenesis and trafficking. Indeed, recent studies have revealed striking parallels between the pathways involved in the entry and egress of nonenveloped BTV and those used by enveloped viruses. In addition, recent studies with the protein that is the major component of the BTV viroplasm have revealed how the assembly and, as importantly, the disassembly of this structure may be achieved. This is a first step towards resolving the interactions that occur in these virus 'assembly factories'. Overall, this review demonstrates that the integration of structural, biochemical and molecular data is necessary to fully understand the assembly and replication of this complex RNA virus.

1 Introduction

Bluetongue virus (BTV) is the type species of the genus *Orbivirus* within the family *Reoviridae*. Orbiviruses are distinct from reoviruses and rotaviruses, both in the organisation of structural proteins and in the nonstructural proteins expressed in virus-infected cells. Despite many functional similarities, there is no primary sequence similarity between orbivirus proteins and the corresponding proteins of other genera within the family. In addition, orbiviruses express proteins that apparently have no functional equivalent in either reoviruses or rotaviruses. These differences between orbiviruses and the other two genera within the *Reoviridae* family may be a reflection of the difference in the mode of transmission of these three virus genera. Whereas reoviruses and rotaviruses are transmitted by the faecal-oral route, orbiviruses are arthropod-transmitted and also replicate in the arthropod host. Thus, in addition to facing the structural and enzymatic constraints imposed by the dsRNA genome common to all the members of *Reoviridae*, orbiviruses must be sufficiently flexible to replicate in two very different hosts. This difference in virus transmission is also reflected in very different physical characteristics. For example, orbivirus virions are more fragile than reovirus and rotavirus virions, with infectivity being lost in mildly acidic conditions and on treatment with detergents (Gorman et al. 1983).

BTV is transmitted by *Culicoides* spp., causing diseases in ruminants of economic importance in many parts of the world. Bluetongue disease in sheep, goats, cattle and other domestic animals as well as in wild ruminants (e.g. blesbuck, white-tailed deer, elk, pronghorn antelope, etc.) was first described in the late eighteenth century. In sheep, the disease is acute, and the mortality can be very high. To date, BTV has been isolated in tropical, subtropical and temperate zones of the world, and 24 different serotypes have been identified. Other orbiviruses infect a wide variety of vertebrates, including man (sometimes causing severe infection). Vector–virus interactions play a crucial role in vector-borne disease epidemiology. The spread of *Culicoides* species from endemic to non-BTV (and also related African horse sickness virus, AHSV, and Epizootic haemorrhagic disease virus, EHDV, of deer) regions of the world in the past raises the concern that these viruses represent an emerging threat for regions that are presently free from viral infection. As a result of its economic significance, BTV has been the subject of extensive molecular, genetic and structural studies.

Although BTV is well characterised at structural and molecular levels, to fully understand the BTV infection cycle it is important to understand the dynamic protein–protein and protein–RNA interactions between viral

components and proteins of the host cell. A complete understanding of virus infection of a cell, replication, synthesis and release of new virions can only be achieved through an approach that integrates structural, molecular and cell biology data. In this chapter, we present the current understanding of how the complex interplay between BTV and cellular proteins contributes to the assembly and morphogenesis of new virus particles within the host cell. *In vitro* studies using individual virus proteins and complexes of virus proteins will also be reviewed.

2
BTV Morphology, Cell Entry and Transcription

Like the other members of the *Reoviridae* described within this volume, BTV virions (550S) are architecturally complex structures composed of multiple layers of proteins that undergo incomplete disassembly upon entry into host cells. In the case of BTV, there are seven structural proteins (VP1-VP7) that are organised into an outer capsid and an inner capsid (commonly known as "core") and containing the ten double-stranded (ds) RNA segments of the viral genome (Fig. 1). The outer capsid is composed of two proteins, VP2 and VP5, and is necessary for cell attachment and virus penetration of the mammalian host cell during the initial stages of infection. Although a great deal is known about the structure of the viral core from atomic resolution structural data (Grimes et al. 1998), there is not yet an equivalent structure for the BTV outer capsid, or for any of the outer capsid proteins. However, recent biochemical analyses together with high-resolution cryoelectron microscopy (EM) structural studies of the BTV outer capsid have given some insights towards the role of each of these proteins in cell entry.

2.1
BTV Outer Capsid and Virus Entry into Cells

In mammalian cells, BTV entry proceeds via virus attachment to the cell, followed by endocytosis and release of a transcriptionally active core particle into the cytoplasm. (Grubman et al. 1983; Huismans et al. 1983, 1987; Eaton and Hyatt 1989; Hassan and Roy 1999; Hassan et al. 2001; Forzan et al. 2004). From our recent studies, it appears that unlike rotavirus, BTV does not use an alternate direct penetration process to enter mammalian cells (M. Forzan and P. Roy, unpublished data). The structural features of VP2 and VP5 correlate with their biological roles in the virus attachment and penetration of the endosomal vesicle, as discussed below.

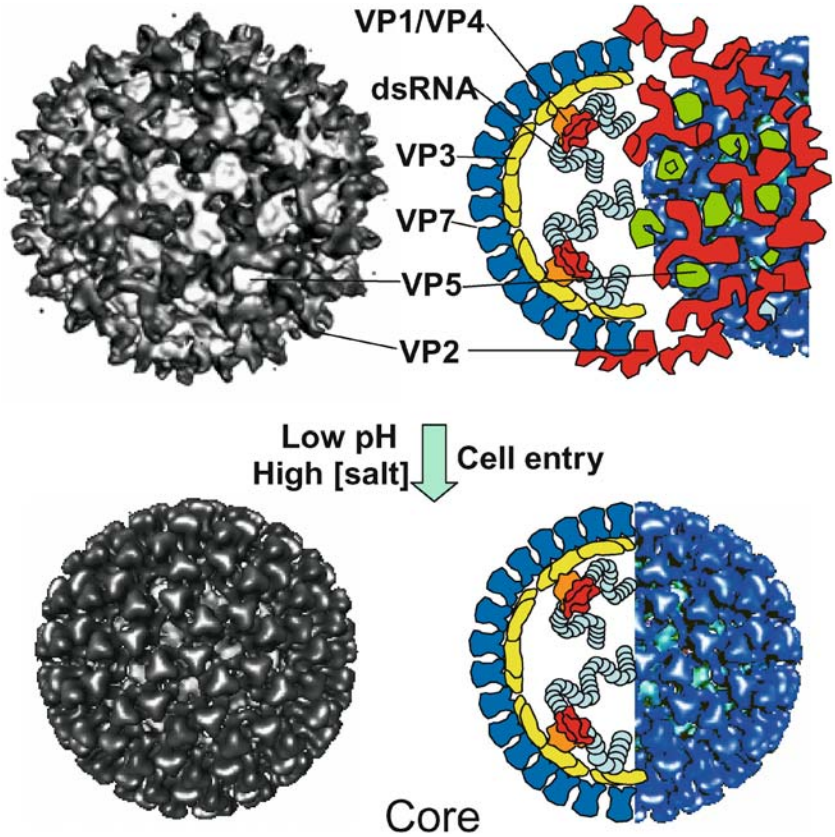

Fig. 1 The arrangement of proteins and nucleic acid in BTV virion (*top*) and core (*bottom*) particles: for each particle a cryo-EM reconstruction (*left*) and a diagramme (*right*) is shown. VP1 (polymerase) and VP4 (capping enzyme) co-localise to the five-fold axes of symmetry on the inner face of the VP3 layer in contact with the viral dsRNA. The transition from virus to core particle occurs during cell entry and can be mimicked *in vitro* by lowering pH or increasing salt concentration. (Adapted from Forzan et al. 2004; Nason et al. 2004)

The BTV outer capsid has an icosahedral configuration with a diameter of approximately 880 Å (Fig. 1). Cryo-EM analyses have revealed that the outer capsid is composed of a total of sixty triskelion spike-like structures formed by VP2 (110 kDa) trimers and 120 globular VP5 (60 kDa) trimers (Hewat et al. 1992b, 1994; Nason et al. 2004). The VP2 spikes extend up to 3 nm from the main body of the particle and have bent tips. The globular VP5 trimers, although also entirely exposed in the virion, are located more internally than

VP2. Both proteins make extensive contacts with the underlying outer layer of the core (VP7). Nevertheless both proteins, in particular VP2, are easily removed by high salt concentrations and/or in acidic pH (Verwoerd et al. 1972; Huismans et al. 1987).

The propeller-like VP2 spike contains the cell attachment sites of the virion. VP2 is responsible for eliciting neutralising antibodies, possesses haemagglutination activity and is the major serotype determinant of the virus. When VP2 is added to susceptible cell lines, it is rapidly internalised by endocytosis (Hassan and Roy 1999). Following internalisation, the clathrin coats of endocytic vesicles are rapidly lost, larger vesicles form, the membranes of which become rapidly destabilised allowing the penetration of the now uncoated core particle into the cytoplasm. This pathway of virus entry relies on specific conformational changes that occur to the BTV outer capsid in response to the changing environment of the virion as it enters the endocytic pathway. Additions of compounds that raise the endosomal pH and block the normal endosomal acidification process prevent virus particles from entering the cytoplasm (Hyatt et al. 1989; Forzan et al. 2004).

The globular outer capsid protein VP5 shares certain structural features with the fusion proteins of enveloped viruses. In its monomeric form, VP5 can be divided into an amino terminal coiled-coil domain and a carboxyl terminal globular domain with a flexible hinge region in between. In addition, the amino terminus of VP5 has the potential to form two amphipathic helices with the capacity for membrane destabilisation (Hassan et al. 2001; Forzan et al. 2004). Indeed, when VP5 is presented appropriately on the cell surface it induces cell-to-cell fusion, confirming that it has the capability to destabilise the cellular membranes. Critically, VP5 only exhibits its membrane-destabilising properties after it has undergone a low pH-triggered activation step, which mimics the endosomal environment encountered during cell entry and results in a change in the VP5 conformation. VP5 lacks the autocatalytic cleavage and N-terminal myristoyl group present in the entry proteins of reoviruses and rotaviruses and does not require proteolytic activation in contrast to some other viral fusion proteins (Colman and Lawrence 2003).

In summary, current data suggest a model in which VP2 makes initial contact with the host cell and triggers receptor-mediated endocytosis of the virus particle and then VP5 undergoes a low pH-triggered conformational change that results in the destabilisation of the endosomal membrane. It is likely that the change in conformation of VP5 that promotes membrane destabilisation, forming a protein layer with intrinsic outside-in curvature, weakens the contacts between VP5 and VP7, the surface layer of the core. This then allows core particles (470S), from which both outer-capsid proteins have been lost, to be released into the cytoplasm (Fig. 2).

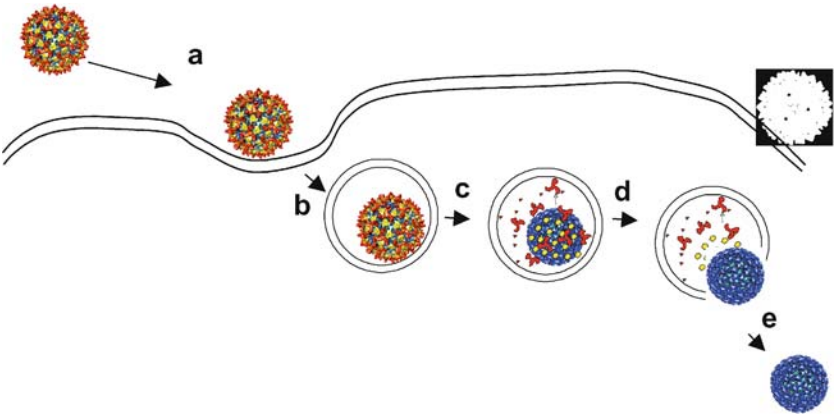

Fig. 2 Summary of structural changes which occur to the virus particle during BTV entry. (*a*) Virus particle binds to cellular receptor(s). (*b*) Receptor-mediated endocytosis of the virus particle. (*c*) Acidification of the endosome triggers the release of VP2 (*red*) from the particle and the activation of VP5, the viral fusion-like protein. (*d*) VP5 molecules (*yellow*) penetrate the endosomal membrane and are released from the particle. (*e*) The transcriptionally active core particle is released into the cytoplasm

2.2 BTV Core Particles and mRNA Synthesis

Upon release into the cytoplasm, BTV core particles become transcriptionally active and synthesise capped but not polyadenylated viral messenger-sense RNA (vmRNA) (Van Dijk and Huismans 1980, 1982; Mertens et al. 1987; Van Dijk and Huismans 1988). The transcriptionally active core is composed of 10 dsRNA genome segments, two major capsid proteins, VP3 and VP7, and three minor enzymatic proteins, VP1, VP4 and VP6. In this structure, the major proteins account for the overall morphology of the core and the minor proteins are responsible for the transcription of vmRNA. The fact that the enzymatic proteins necessary for transcribing vmRNAs from dsRNA template are contained within the core particle avoids any requirement for the viral core to disassemble completely. Thus, the viral dsRNA is sequestered away from cellular dsRNA surveillance systems which are linked to innate antiviral defences (Jacobs and Langland 1996; Samuel 1998). The newly synthesised, capped mRNA species are extruded from core particles into the cytoplasm and program the translation of virus proteins. A detailed review of the atomic structure of the BTV core is provided by in the chapter by Stuart and Grimes in this volume. Although the structural integrity of the core particle appears to be essential for maintaining efficient transcriptional activity, it has been

possible to use *in vitro* assays with each enzymatic protein of the core to delineate specific protein functions within the transcription complex.

Since transcription of the dsRNA genome of members of the *Reoviridae* occurs by a fully conservative process (Bannerjee and Shatkin 1970), it is logical that this process would involve a helicase protein either to unwind the dsRNA ahead of the transcriptase protein or to separate the parental and newly synthesised RNAs following transcription. For BTV, the 38-kDa minor core protein VP6 possesses helicase activity *in vitro* and exhibits physical properties characteristic of other helicases, including an oligomeric nature and an ability to form ring-like structures in the presence of BTV RNA (Stauber et al. 1997; Kar and Roy 2003).

The replication of viral dsRNA occurs in two distinct steps. First, plus-strand RNA (vmRNA) is transcribed, using the dsRNA genome segments as template, and extruded from the core particle (Bannerjee and Shatkin 1970; Cohen 1977; Van Dijk and Huismans 1980). Second, the plus-strand RNAs serve as templates for the synthesis of new minus-strand RNA at an undefined stage during the assembly of a new virus core particle. The largest minor core protein VP1 (150 kDa) has the ability to both initiate and elongate minus-strand synthesis de novo (Boyce et al. 2004). This does not require a specific secondary structure present at the 3′ end of the plus strand template. This polymerase activity was lost when a GDD motif (amino acids 287–289), characteristic of other RNA polymerases, was deleted (M. Boyce and P. Roy, unpublished observation). Studies of replicase activity in other members of the *Reoviridae* have used very short templates (Tao et al. 2002) or have required a particulate replicase in which the catalytic subunit is proposed to possess replicase activity only in the context of a subviral particle (Kohli et al. 1993; Chen et al. 1994; Patton 1996, 1997; Charpilienne et al. 2002). Such apparent discrepancy with the BTV polymerase may be attributable to the varied experimental systems used to assay replicase activity. Since the replicase activity associated with recombinant BTV VP1 is low, it is possible that the activity of VP1 is enhanced by other viral proteins present in the assembling core particle, although to date our studies have revealed little evidence for this hypothesis.

Although VP1 has been shown to be active as the viral RNA-dependent RNA polymerase it is not sufficient for the synthesis of the methylated cap structure found at the 5′ end of BTV vmRNA. Within the assembled core particle, VP1 is closely associated with VP4 (Nason et al. 2004). Recombinant, purified VP4 (76.4 kDa) is an enzyme that can synthesise type 1-like ‘cap’ structures *in vitro* that are identical to those found on authentic BTV vmRNA. The protein represents a model enzyme, which has methyltransferase, guanylyltransferase and RNA triphosphatase activities in a single protein. VP4 is unusual in

that it is capable of completing several distinct enzymatic reactions in the absence of any other viral protein (Martinez Costas et al. 1998; Ramadevi et al. 1998; Ramadevi and Roy 1998). This is notably different to other viral capping enzymes, e.g. those of vaccinia virus, where capping is dependent on a complex of 3 proteins (Venkatesan et al. 1980).

3 Synthesis of Viral Proteins and Assembly of Particles

Following virus entry, uncoating of the core and initiation of transcription, vmRNA are released into the cytosol and serve as both templates for viral dsRNA genome synthesis and messengers for the synthesis of viral proteins. The first virus-specific proteins are detectable at 2–4 h after infection, and the rate of protein synthesis increases rapidly until 11–13 h after infection, after which it slows down but continues until cell death (Huismans 1979). Most viral proteins are synthesised throughout the infection cycle and accumulate during infection until cell lysis. Infection of mammalian cells with BTV leads to a rapid inhibition of cellular macromolecular synthesis and the induction of an apoptotic response. The latter response appears to be triggered by the combination of two signals involving attachment of the virus to the cell and the activity of the membrane permeabilising protein, VP5 (Mortola et al. 2004).

In addition to the seven structural proteins of the virion, four nonstructural proteins, NS1, NS2, and NS3/NS3A are synthesised in BTV infected cells. In common with the corresponding proteins of many other viruses, the nonstructural proteins of BTV are key components of the infection machinery, modulating host–virus interplay as well as virus morphology. The two larger BTV NS proteins, NS1 and NS2, are produced at high levels in the cytoplasm and multimerise into discrete structures. While NS2 is clearly involved in virus replication and assembly processes (discussed below), a defined role for NS1 that multimerises into tubules is yet to emerge. However, in the absence of NS1 and NS2, all structural proteins except VP6 readily assemble when co-expressed using a heterologous expression system. Therefore, the viral structural proteins possess inherent properties to assemble, and neither NS1 or NS2 nor genomic RNAs are essential for capsid assembly. Nevertheless, it is clear that the assembly process is sequential and highly precise (see below).

In contrast to NS1 and NS2, the steady-state level of the small viral nonstructural proteins, NS3/NS3A, is highly variable (from being barely detectable to being highly expressed) and is dependent on the host cell species. The level of NS3/NS3A in different cell types appears to correlate with the efficiency of virus release with those cells producing the most NS3 releasing the

most virus. In this context, it is noteworthy that orbiviruses such as BTV and African horse sickness virus establish persistent infections in susceptible insect cells with little apparent cytopathic effect (CPE). In contrast, both viruses cause dramatic CPE in mammalian cells. While the majority of the progeny particles remain cell-associated in mammalian cell infection, as is commonly observed with reoviruses, there is clear evidence that virus particles can, in contrast to reoviruses, also leave host cells by budding at the cell membrane.

3.1 Virus Inclusion Bodies and NS2

For a number of animal and plant viruses, replication complexes, transcription complexes, replication and assembly intermediates, as well as nucleocapsids and virions accumulate in specific locations within the host cell in structures described as virus assembly factories or virus inclusion bodies (VIBs). During BTV infection, core particles become very rapidly associated with a matrix that gradually surrounds the particles to form virus inclusion bodies. As the infection progresses, these VIBs increase both in size and numbers. In addition to being the site of transcription, vmRNA and proteins can be identified within these VIBs; thus, they appear to be the site of BTV replication and of early viral assembly (Eaton et al. 1988; Hyatt and Eaton 1988; Brookes et al. 1993). This has largely been inferred from data on the localisation of incomplete virus particles within VIBs.

Expression of BTV NS2 without other viral proteins in both insect and mammalian cells results in the formation of inclusion bodies that are indistinguishable from the VIBs found in virus-infected cells (Thomas et al. 1990). Furthermore, purified recombinant NS2 possesses ssRNA binding activity *in vitro*, and BTV RNAs are preferentially bound over nonspecific RNAs (Theron and Nel 1997; Lymperopoulos et al. 2003; Markotter et al. 2004). These observations support the suggestion that NS2 may have a role in the recruitment of RNA for replication (Thomas et al. 1990). While the amino terminus, but not the carboxy terminus, of NS2 is essential for ssRNA binding, neither the amino (up to 92 residues) nor carboxy terminus (including the last 130 amino acids) of the protein is required for oligomerisation (Zhao et al. 1994). These observations are important because how the ten dsRNA segments that make up the viral genome are selectively recruited and packaged into newly assembling virus particles is one of the most enduring questions in the field. It is commonly believed that each of the viral segments must possess some specific sequence or RNA structure, which is recognised by one or more virally encoded proteins to facilitate these processes. In particular, one recent study using recombinant purified NS2 in combination with BTV RNA species and a range of specific and

nonspecific ssRNA competitors has demonstrated that NS2 has high affinity for specific BTV RNA structures that are unique in each RNA segment (Lymperopoulos et al. 2003). Intriguingly, the sequences that represent the putative binding partners for NS2 are neither the octanucleotides and hexanucleotides conserved at the 5′ and 3′ termini of all BTV RNA segments nor the potential panhandle structures (formed by the partial complimentary sequences of the 5′ and 3′ termini). Instead the sequences that are predicted to be bound by NS2 on the basis of this initial study are distributed throughout the coding and noncoding regions of the different genome segments (Lymperopoulos et al. 2003). Chemical and enzymatic structure probing of regions bound preferentially by NS2 revealed that the NS2 bound regions of the BTV RNA transcripts folds into unique hairpin-loop secondary structures. The NS2–hairpin interaction was further confirmed by using hairpin mutants that had a decreased affinity for NS2. No other RNA binding protein of any other member of *Reoviridae* has been shown to have RNA structural specificity so far. However, rotavirus NSP3 appears to bind a linear sequence found at the 3′ end of all rotavirus RNA segments (Poncet et al. 1993) and rotavirus VP1 also binds to the 3′ end of rotavirus RNA (Patton 1996). The significance of these interactions for genome packaging is at this stage unclear, and it is worth pointing out that, other than BTV, there are several systems where viral proteins recognise packaging signals that are contained in hairpin structures with no apparent sequence homology (Bae et al. 2001; Beasley and Hu 2002). Although the RNA binding activity of NS2 explains how BTV vmRNA are selected from the pool of cellular messages for incorporation into assembling virus particles, how only a single copy of each genome segment is included in newly formed core particles remains to be elucidated. The two most likely scenarios at this stage are either that NS2 brings the viral RNAs into close proximity, and intersegment RNA interactions allow the formation of an RNA complex that is the basis of core assembly, or that different RNA subsets that already interact are bound by the same NS2/NS2 complex. The latter hypothesis is consistent with the observations that NS2 may form decameric complexes (Butan et al. 2004) and that each NS2 protein subunit may have several RNA binding domains (Fillmore et al. 2002). Establishing the precise order of events and the molecular mechanisms of virus assembly will be an exciting area of future research.

In addition to a role in RNA selection, NS2 VIBs also act as the nucleation site for a number of the viral structural proteins that form the core structure. Since the VIB structure could alternately act both as a virus assembly factory and as a trap that prevents egress of newly assembled core particles from exiting infected cells, it is necessary that their formation is a dynamic, reversible process. Recent data on the nature of different phosphorylation variants of NS2 have begun to reveal how the reversible assembly/disassembly

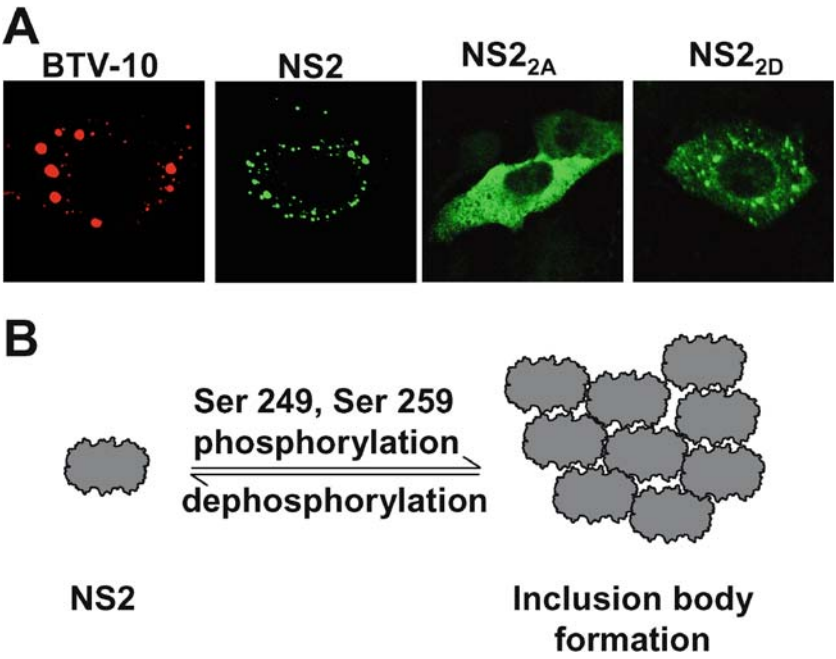

Fig. 3A, B Phosphorylation of BTV NS2 controls the assembly of virus inclusion bodies. **A** Confocal data showing the effect of mutating the phosphorylated serine residues of NS2 to alanine ($NS2_{2A}$) or aspartic acid ($NS2_{2D}$). **B** Cartoon showing how phosphorylation/ dephosphorylation of NS2 may control inclusion body integrity, and core release. (Modrof et al. 2005)

of bluetongue VIBs is achieved. NS2 is the only BTV encoded phosphoprotein and this phosphorylation is reproduced when NS2 is expressed in insect cells (Devaney et al. 1988; Thomas et al. 1990). Consistent with the role of phosphorylation to effect changes in protein–protein interactions of many other proteins, phosphorylation plays a key role in the formation of BTV VIBs. Mutagenesis of two normally phosphorylated serine residues in NS2 to alanine abrogates formation of distinct VIBs, while mutation of the same residues to aspartic acid, mimicking a constitutively phosphorylated state, results in the formation of normal inclusion body structures (Fig. 3; Modrof et al. 2005). Furthermore the expression of the nonphosphorylated mutant of NS2 was sufficient to disrupt the formation of VIBs in virus-infected cells, thus demonstrating the potential of the mutant to act in a dominant negative fashion and of the potential that phosphorylation could control BTV VIB stability (Modrof et al. 2005).

Recent data suggest that a first candidate cellular protein that interacts with NS2 is the protein kinase casein kinase II (CKII), which is able to phosphorylate NS2 *in vitro*. (Modrof et al. 2005). Additionally, both proteins co-localise intracellularly upon recombinant expression of NS2. Zetina et al. have reported that phosphorylation of the conserved motif (LS/SL)(D/E)(D/E)(D/E)X(D/E) could stabilise helix unfolding (Zetina 2001; Meggio and Pinna 2003). The sequence context of phosphorylated serine residue 249 ($_{248}$L**S**DDDDQ$_{254}$) in NS2 conforms to this conserved sequence except for the last residue. This indicates that phosphorylation of NS2 could be involved in stabilising its folding.

Intriguingly, it has recently been shown that rotavirus NSP5, which along with NSP2 is involved in the formation of inclusion bodies, is also phosphorylated at a CKII recognition site within its C-terminus (Eichwald et al. 2002). Phosphorylation and hyperphosphorylation of NSP5 result in widely variable migration patterns in SDS-PAGE (Afrikanova et al. 1996), but this is not the case for BTV NS2. Using NS2 expressed from different sources (mammalian cells, insect cells or bacteria) or NS2 alanine mutants which are not phosphorylated, the migration velocity of the proteins remained the same in denaturing PAGE. The question of whether rotavirus NSP5 phosphorylation is similar to BTV NS2 phosphorylation in affecting intracellular localisation is still unclear. A possible influence of NSP5 phosphorylation on localisation to VIBs had been suggested but is contradicted by recent investigations which showed that the deletion of the phosphorylated sites within the protein did not prevent NSP5 from localising with VIBs in infected cells (Poncet et al. 1997; Eichwald et al. 2002). For reoviruses, μNS and σNS have been suggested to be responsible for the formation of VIBs (Broering et al. 2002; Becker et al. 2003). However, these proteins are not known to be post-translationally modified.

As the formation of BTV VIBs, the centres for viral replication and early assembly, requires phosphorylated NS2, it is reasonable to assume that newly synthesised, unphosphorylated, NS2 might take on other functions prior to its association to VIBs. In this scenario, NS2 could bind the viral polymerase VP1 and other BTV core proteins in the cytoplasm and recruit these components to the VIBs on phosphorylation. In support of this hypothesis, we have recently obtained evidence that the phosphorylation of NS2 is important for VIB formation but not for the interaction with other viral proteins (Modrof et al. 2005). Following core assembly dephosphorylation of NS2 would allow disassembly of NS2 inclusions and the release of immature virus particles into the cytoplasm.

3.2 Assembly of the Viral Core Particle

While NS2 is intimately involved in the synthesis of infectious core particles, particularly at the level of RNA packaging, BTV structural proteins, with the possible exception of VP6, also have the inherent capacity to self-assemble into virus-like particles (VLPs) that lack the viral genome (French et al. 1990; French and Roy 1990). This has been exploited to explore atomic structures of the core for understanding of the protein–protein interactions that drive viral capsid assembly. The assembly of BTV capsids is especially intriguing as it requires a complex highly ordered series of protein–protein interactions and recent studies have focussed on the use of VLPs and core-like particles (CLPs), formed by expression of viral structural proteins in insect cells. Some of the key findings from a number of recent studies are summarised below.

3.2.1 VP3 Assembly and Minor Proteins

In the virion particle, 120 VP3 molecules are arranged as 60 dimers, each consisting of two different conformations of VP3 (A & B) on a T=2 icosahedral lattice (Grimes et al. 1998). A set of five VP3 AB dimers are arranged as decamers and 12 of these decamers are interconnected via the dimerisation domain in each molecule to form the final VP3 shell (Grimes et al. 1998). Such icosahedral organisation of the inner shell is shared by all members of *Reoviridae* and other viruses with segmented dsRNA genomes (Hewat et al. 1992a; Prasad et al. 1992, 1996; Grimes et al. 1998; Reinisch et al. 2000), emphasising the importance of their essential roles in the assembly process of these viruses. Moreover, the primary amino acid sequences of VP3 (100 kDa) across 24 BTV serotypes as well as other related orbiviruses (EHDV and AHSV) are highly conserved, highlighting the structural constraints that may govern virus assembly (Iwata et al. 1992, 1995; Roy 1996).

A key question in VP3 assembly is whether the decamer present in the final assembled particle is an identifiable intermediate in the assembly process or only arises upon assembly. To gauge this, a recent study deleted the dimerisation domain of VP3 and showed that subcore formation was abolished (Kar et al. 2004). The deletion of this domain, however, did not perturb decamer or dimer formation. Decamers were highly stable and due to their hydrophobic nature a higher order of decamers were particularly evident from the cryo-EM and dynamic light scattering experiments (Kar et al. 2004). These data suggest that decamers are probably the first stable assembly intermediates of the VP3 layer and subsequent core assembly and those decamer–decamer interactions via the dimerisation domain drive the assembly of the viral subcore.

The atomic structure of the BTV core shows that VP3 is associated with genomic dsRNA and indicates the possible locations of the internal proteins that form the transcription complex of the virion at the vertices of the five-fold axes of the decamers (Grimes et al. 1998; Gouet et al. 1999). However, the exact contribution of each of the internal proteins to the densities of the transcription complex was not resolved in the X-ray diffraction studies. High-resolution cryo-EM analysis has been used successfully to reveal the shape of the complex formed by two of these proteins, the polymerase VP1 and the capping enzyme VP4. This has been possible because of the use of CLPs consisting of VP1, VP3, VP4 and VP7 but not the genomic RNAs (Nason et al. 2004). Co-expression studies indicated that both VP1 and VP4 proteins are independently associated with the VP3 layer, although recent data suggest that VP4 protein has more direct contact with VP3 (Le Blois et al. 1991; Loudon and Roy 1992; Nason et al. 2004). In addition, VP1 and VP4 are very tightly associated with each other and form a stable complex that can be visualised by cryo-EM analysis. This complex directly interacts with the VP3 decamer in solution, supporting the cryo-EM analyses (Kar et al. 2004). However, BTV RNA was not able to bind VP3 decamers under conditions where the intact VP3 bound RNA very efficiently. The interaction of VP1 and VP4 in the absence of the BTV genome or VP3 and the association of VP1 and VP4 with VP3 decamers suggests that assembly of the BTV core initiates with the complex formed by these two enzymes which simultaneously associate with the VP3 decamers. VP3 decamers as assembly intermediates are most likely involved in the recruitment of the polymerase complex prior to completion of the assembly of the VP3 subcore. The viral genome, by contrast, wraps around the VP1–VP4 complex while the subcores are assembling.

Unlike VP1 and VP4, it has not been possible to confirm the location of VP6 in the core, although it is likely that VP6 is also located within the five-fold axes of the VP3 layer directly beneath the decamer together with VP1 and VP4. However, VP6 forms defined hexamers in the presence of BTV transcripts and assembles into distinct ring-like structures that could be isolated by glycerol gradient centrifugation. At present, it is not known if such structures are indeed present within the core and incorporated either together with VP1 and VP4 into the VP3 decamer intermediate stage or independently during the assembly of the 12 VP3 decamers.

3.2.2 VP7 Assembly

The mismatch between the number of subunits in the VP3 and VP7 layers poses an interesting problem as to how these layers reconcile to form an

intact icosahedral structure. In the absence of VP3, VP7 forms trimers but these trimers do not assemble as icosahedral particles. The construction of the T=13 icosahedral shell requires polymorphism in the association of the VP7 subunits, each of which has two domains that contribute to trimer formation. The lower helical domain controls both the formation of the VP7 lattice and its interaction with the scaffolding layer of VP3. Structural and comparative sequence information have guided investigation of how such a complex structure is achieved during virus assembly and what residues are required to form a stable capsid. Extensive site-directed mutagenesis in combination of various assembly assay systems have given insight into the order of the assembly pathway of VP7 and stable core formation that subsequently serve as a foundation for the deposition of the outer capsid.

Since the lower domains are in direct contact with the VP3 layer, and the interactions between the lower domains within the trimers are intensive, a series of VP7 mutations were generated focusing on the lower domain residues that appeared to be involved in intramolecular (within the VP7 subunit) and intermolecular (between the VP7 subunits) interactions. Another set of mutations was created to perturb the trimer–trimer interactions. The rationale behind these experiments was that since VP7 molecules oligomerise into trimers even when expressed in the absence of VP3, it is possible that attachment of preformed trimers onto the VP3 subcore and subsequent formation of the VP7 layer would be directed by side-to-side interaction of adjacent trimers. Interactions between neighbouring trimers at the two-fold axis appear to be through a thin band around the lower domains. A series of single and multiple substitution mutants of VP7 were created targeting these regions to examine their involvement in assembly (Limn et al. 2000). Another series of single or multiple site-specific substitution mutations have been introduced into the regions of the flat under-surface of the VP7 trimers that adhere closely to the VP3 surface in order to examine the VP7 and VP3 assembly (Limn and Roy 2003). The effects of these mutations on VP7 solubility, ability to trimerise and formation of CLPs in the presence of the VP3 scaffold were investigated.

In brief, the detailed analysis of an extensive range of targeted VP7 mutations not only precisely identified the critical residues responsible for formation of the VP7 layer, but also revealed that core assembly depends on trimer formation. Furthermore, the precise shape of the trimers drives the formation of the tight lattice of 260 VP7 trimers on the core surface. In terms of the overall assembly pathway of the BTV core, combination of cryo-EM and X-ray structures have revealed that of the 13 unique contacts made between the VP3 and VP7 shells in the atomic structure, the contact that aligns the VP7 trimer axis with the icosahedral three-fold axis of the VP3 layer is the strongest. This suggests that these trimers may nucleate the assembly of the

VP7 lattice on the VP3 subcore once the first trimer is anchored. It has been postulated that preformed hexamers of VP7 may propagate around the initial VP7 trimer forming a sheet that loosely wraps the VP3 layer (Grimes et al. 1998). However, the data obtained from mutagenesis studies did not support a gradient of trimer association from a single nucleation site, as mutations that destabilise the CLP particle still allow assembly of some VP7 lattice on the VP3 shell. More likely is an alternate model for assembly where multiple sheets of VP7 form around different nucleation sites. A likely pathway of core assembly is therefore that a number of strong VP7 trimer-VP3 contacts act as multiple preferred initiation sites and a second set of weaker interactions then fill the gaps to complete the outer layer of the core. There is a clear sequential order of trimer attachment on VP3 scaffold. The T trimers (of the P, Q, R, S, T trimers) which are at the three-fold axis of the icosahedron act as nucleation, while P trimers that are furthest from the three-fold axis and closer to the five-fold axis, are the last to attach (Nason et al. 2004). The distinction between those VP7 trimers that first occupy the subcore and those that follow is necessarily subtle as it must be sufficient to allow variation in packing yet not prevent the overall biological purpose of virus assembly.

3.3 Assembly of Outer Capsid

Following the assembly of the core particle, the next logical step in virus assembly is the addition of the viral outer capsid, consisting of the proteins VP2 and VP5. While at a structural level, recent cryo-EM experiments have aided our understanding of how the outer capsid proteins interact with the outer VP7 layer of the core, our understanding of where in the cell these proteins are added to the core is limited. Since the addition of VP2 and VP5 abolishes the transcription activity of the particle, addition of the outer capsid is likely to be a highly regulated process to prevent premature shut-off of virus transcription. Within BTV-infected cells, virus particles are found associated with the vimentin intermediate filaments (Eaton et al. 1987). Furthermore, the presence of both VP2 and VP5 was found to be necessary to direct VLP to the cytoskeleton of insect cells (Hyatt et al. 1993). However, our own recent studies have suggested that VP2 alone associates with vimentin intermediate filaments and disruption of these structures prevents the normal release of virus particles from cells. Given the importance of these structures for the assembly and egress of other viruses (Garcia-Barreno et al. 1988; Murti et al. 1988; Ferreira et al. 1994; Karczewski and Strebel 1996; Arcangeletti et al. 1997; Nedellec et al. 1998; Cordo and Candurra 2003), it may be that intermediate filaments are used to control the addition of the VP2 layer to the assembled core.

The assembly of VP2 and/or VP5 with core is easily mimicked using the baculovirus expression system (French et al. 1990; Le Blois et al. 1991; Loudon et al. 1991; Liu et al. 1992). Both proteins can be added to the core and assemble onto that structure independently of each other, implying that the two proteins are directly attached to the core. This has recently been confirmed by high-resolution cryo-EM studies that have revealed the separate regions of the VP7 trimers that are involved in attachment of VP2 and VP5 (Nason et al. 2004). The structural organisation of the outer layer represents a drastic mismatch with the underlying VP7 layer. The VP7 trimers with a triangular top portion serve as the platform for the deposition of the VP2 and VP5. Each triskelion motif (VP2 trimers) essentially interacts with four VP7 trimers by its underside in four places. The base of the triskelion interacts with the Q type VP7, whereas the propeller-like arms make three other connections with the P, R, and S VP7 trimers. By docking the X-ray structure of the VP7 trimer into the virion reconstruction it was possible to identify the VP7 residues that are in contact with VP2. The base of the VP2 trimer interacts exclusively with the upper flattish surface of the VP7 trimer, which includes amino acid residues 141–143, 164–166, 195–205, and 238–241 of the VP7(Nason et al. 2004). All the VP7 molecules of the core are covered by the connections that are made with the tips of the propeller except the VP7 at the icosahedral three-fold axis (T type). The top of the VP7 trimer at this position is thus clearly exposed to the exterior.

The globular densities (VP5 trimers) on the other hand, sit right above the type II and type III channels, between the VP7 trimers, making contacts with the sides of VP7 trimer which face these channels. Thus, the channels are filled with triangle-shaped densities that are connected to the VP5 trimers. The inner triangle-shaped density interacts mainly with the lower portion of the β-barrel domain of VP7 and includes residues 168–173, 210–215, and 226–234 (Nason et al. 2004).

Overall, the principal protein–protein contacts of the two outer capsid proteins of the BTV appear to be with the outer layer of the core rather than with each other. This may be related to the sequential attachment and endosomal penetration steps mediated by each protein respectively during virus entry into uninfected cells.

4
Egress of Progeny Virions

Once virions are newly assembled, they must be trafficked to the plasma membrane for release. The efficiency of BTV release varies between host cell types, with insect cells allowing a nonlytic release of virus while the

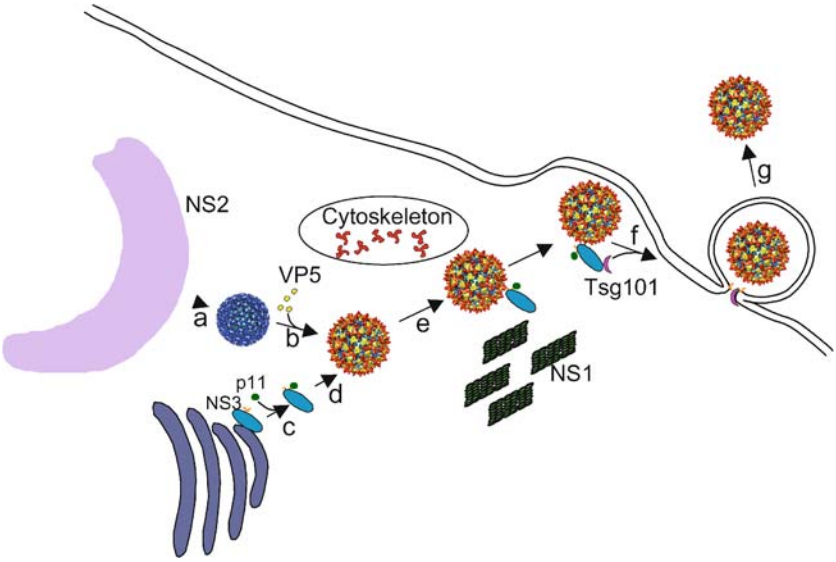

Fig. 4 Diagram summarising key interactions in the assembly and release of BTV: cores are released from NS2 inclusion bodies (*a*) and associate with outer-capsid proteins VP5 and VP2 (*b*). BTV NS3 associates with the intracellular trafficking protein p11 (*c*) and forms a bridge between this protein and newly assembled virus particles by a secondary interaction with VP2 (*d*). This leads to trafficking of the virus particle to the cell membrane (*e*) where interaction between the PSAP motif in NS3 and the cellular release factor Tsg101 results in the pinching off of vesicles containing virus particles (*f*) followed by release of mature virion particles from these vesicles (*g*)

majority of virus in mammalian cells remain cell-associated (Hyatt et al. 1989). However, even in mammalian cells that show substantial cytopathic effect as a result of BTV infection, the titre of virus in the culture supernatant increases significantly before the onset of dramatic CPE. Thus it is clear that there are defined mechanisms that traffic newly formed virus particles out of infected cells. Recent evidence has implicated the viral nonstructural proteins NS1 and NS3 in this process and has revealed intriguing parallels between the egress of nonenveloped BTV and enveloped viruses (Fig. 4) (Beaton et al. 2002; Owens and Roy 2004).

4.1 The Role of NS3 in the Intracellular Trafficking of Virus Particles

The only membrane proteins that are encoded by BTV are NS3 (229 aa) and its shorter form NS3A (216 aa), which lacks the N-terminal 13 amino acids of

NS3 (Van Dijk and Huismans 1988). Both proteins have been found associated with smooth-surfaced, intracellular vesicles (Hyatt et al. 1993) but do not form part of the stable structure of the mature virus. NS3/NS3A proteins comprise a long N-terminal and a shorter C-terminal cytoplasmic domain, which are connected by two transmembrane domains and a short extracellular domain (Wu et al. 1992; Bansal et al. 1998; Beaton et al. 2002). A single glycosylation site is present in the extracellular domain of BTV NS3 but is missing in NS3 of African horse sickness virus (AHSV), a closely related orbivirus, and therefore does not seem to be essential for the function of the protein (van Staden and Huismans 1991; Bansal et al. 1998). The NS3/NS3A proteins accumulate to only very low levels in BTV-infected mammalian cells, but in invertebrate cells the expression level of these proteins is high (French et al. 1989; Guirakhoo et al. 1995). The correlation between high level of NS3/NS3A expression and nonlytic virus release suggests a significant functional role for NS3 in virus egress from invertebrate cells. When NS3/NS3A is expressed using recombinant baculoviruses, it facilitates the release of baculovirus-expressed virus-like particles, VLPs (acting as surrogates for authentic virions) from host cells and NS3 protein is localised at the site of the membrane from which VLPs are released (Hyatt et al. 1993). This suggests that the integration of NS3/NS3A into the plasma membrane may release mature virions, a function that is similar to that described for NSP4, a nonstructural glycoprotein of rotaviruses, which interacts with viral double-layered particles to facilitate their transport across the rough endoplasmic reticulum of infected cells (Meyer 1989). NS3 of BTV and AHSV exhibit cytoxicity when expressed singly in mammalian or insect cells (French et al. 1989; van Staden et al. 1995). The cytoxicity of NS3 requires membrane association of the protein and depends on the presence of the first transmembrane domain, leading to the suggestion that NS3 might function as a viroporin, facilitating virus release by inducing membrane permeabilisation (Han and Harty 2004). Recent study showed that NS3 can indeed act as viroporin, causing permeabilisation of host cell membranes (Han and Harty 2004). It is possible that this permeabilisation activity facilitates local disruption of the plasma membrane allowing virus particles to be extruded through a membrane pore without acquiring a lipid envelope. Whether this process requires any of the cellular proteins that participate in the formation of an enveloped viral particle merits further investigation.

The first 13 amino acids of NS3 that are absent in NS3A have the potential to form an amphipathic helix. This cytoplasmic region of NS3 also specifically interacts with the calpactin light chain (p11) of cellular annexin II complex (Beaton et al. 2002). The complex has been implicated in membrane-related events along the endocytic and regulated secretory pathways including the trafficking of vesicles (for reviews see Creutz 1992; Raynal and Pollard 1994).

The interaction between NS3 with p11 is highly specific. Moreover, an NS3 peptide (a mimic of the sequences of the p11 binding domain) has inhibitory effects on virus release of progeny virions from BTV-infected insect vector cells (Beaton et al. 2002). Even though the exact physiological role of this interaction is still unknown, it is likely that interaction of p11 with NS3 may help direct NS3 to sites of active cellular exocytosis, or it could be part of an active extrusion process. Furthermore, there are some indications that cytoskeletal material was seen at sites of BTV egress (Hyatt et al. 1991), which may be annexin II being drawn through the membrane during the extrusion process, as it is still associated with NS3. The significance of this interaction to BTV egress becomes more apparent in the light of the observation that the other cytoplasmic domain of the protein, situated at the C-terminal end, interacts specifically with the BTV outer-capsid protein VP2.

In addition to its interaction with the p11 component of the annexin II complex, NS3 is also capable of interaction with Tsg101 (Wirblich et al. 2005), a cellular protein implicated in the intracellular trafficking and release of a number of enveloped viruses (Garrus et al. 2001; Freed 2004; Morita and Sundquist 2004). Tsg101 specifically interacts with a PTAP motif that is present in the late domain of the retroviral Gag protein. Other motifs present include the YPDL motif that interacts with the protein Alix, which functions downstream of Tsg101, and the PPxY motif, which plays a role in recruiting host ubiquitin ligases. The PTAP and PPxY motif have also been identified in proteins of other enveloped viruses, such as VP40 of Ebola virus, the matrix protein of VSV and the Z protein of Lassa virus, where they exhibit an equivalent function as the late domain motifs of retroviruses (Craven et al. 1999; Harty et al. 1999, 2000, 2001; Licata et al. 2003; Perez et al. 2003; Timmins et al. 2003; Yasuda et al. 2003). Interestingly, similar motifs are also present within the NS3 of BTV and certain other orbiviruses (Wirblich et al. 2005). Recent findings showed that both NS3 and NS3A of BTV and AHSV bind with similar affinity *in vitro* to human Tsg101 and also its orthologue from *Drosophila melanogaster*. This interaction is mediated by the conserved PSAP motif in NS3 of BTV and ASAP in the NS3 of AHSV. Mutation of the PSAP motif abolished binding of NS3 to Tsg101, but had little effect on binding to p11. The interaction of NS3 and Tsg101 also plays a role in orbivirus release, as knockdown of Tsg101 with siRNA inhibits release of BTV and AHSV from mammalian cells (Wirblich et al. 2005).

Like most other viral proteins which recruit Tsg101, NS3 also binds NEDD4-like ubiquitin ligases *in vitro* via a resident PPXY late domain motif (Yasuda et al. 2003; Blot et al. 2004; Heidecker et al. 2004; Sakurai et al. 2004). However, the late domain motifs in NS3 do not function as effectively as the late domains of other enveloped viruses. This appears to be mainly due to the presence of

a unique arginine at position 3 of the PPXY motif in NS3. The low activity of the NS3 late domain motifs can be reversed by converting the PPRY motif of NS3 into a more universal PPPY, rendering NS3 as effective as Gag in facilitating retroviral VLP release as the late domains of enveloped viruses. It was also apparent that PSAP motif of NS3 is as efficient as the PTAP motif in retrovirus VLP release (Wirblich et al. 2005).

Of all the viruses utilising conventional late domains that have been examined, BTV is the only one that encodes arginine at position three of the PPxY motif (Wirblich et al.y 2005). The reason for this may be that orbiviruses replicate in insects, whereas the other viruses do not. Hence, the arginine could be an adaptation to growth in insect cells. NS3 is also unusual among viral proteins containing a late domain since it also functions as a viroporin. While both activities seem to facilitate virus release, the relative contribution of the two activities could differ between different orbiviruses. This conclusion is consistent with our observation that cells infected with AHSV displayed a much stronger cytopathic effect at early times after infection than cells infected with BTV, which could reflect a higher intrinsic cytotoxic activity of AHSV NS3 or a higher expression level of NS3 in cells infected with AHSV (van Staden et al. 1995). In any case, particle release due to cell lysis caused by viroporin activity of NS3 presumably does not require the function of Tsg101.

Thus, orbivirus NS3 recruits the cellular protein Tsg101 to facilitate virus release from mammalian cells and presumably insect cells as well. The ability to usurp the vacuolar protein sorting pathway is likely to be more important in insect hosts as orbiviruses establish persistent infections in insect cells without causing significant cytopathic effect. While full clarification of this issue will have to await the availability of a reverse genetics system for BTV, it should be possible to identify insect proteins that interact with NS3 and to shed more light on the question of whether NS3 is better adapted to engage insect proteins so facilitating improved virus release.

4.2
The BTV Tubules in Infected Cells and NS1 Protein

One of the most striking intracellular morphologic features during BTV and other orbivirus infection is the formation of abundant tubular structures within the cytoplasm. Orbivirus tubules are biochemically and morphologically distinct from the microtubules and neurofilaments of normal cells. BTV tubules are formed by the 64-kDa protein NS1 (Huismans and Els 1979; Urakawa and Roy 1988), which is synthesised in large amounts, up to 25% of the virus-specified proteins, in infected cells. Following synthesis, the protein rapidly oligomerises into a high-molecular-weight tubular structure formed

by helically coiled ribbons of NS1 dimers with a diameter of 52 nm and lengths of up to 1,000 nm that sediment as 300–500S structures (Urakawa and Roy 1988). Early and abundant synthesis of NS1 and tubules suggests their involvement in virus replication and/or virus translocation.

Indeed our recent data suggests the role of this protein in virus replication. Intracellular expression of a single-chain antibody to the viral NS1 protein (scFv-αNS1) has demonstrated that high levels of NS1 in BTV-infected cells are critical to the morphology and trafficking of virus particles (Owens and Roy 2004). Four major changes were apparent: first, there was a tremendous reduction in virus-induced cytopathic effect (CPE); second, there was a more than tenfold increase in the amount of virus released into the culture medium; third, there was a shift from lytic release of virus to budding from the plasma membrane (Fig. 5); and forth, NS1 tubule formation was completely inhibited by scFv-αNS1 expression. Each of these changes, except for the lack of tubule formation, is reminiscent of what occurs during BTV infection of insect cells in culture. Based on these findings, we propose that the NS1 protein is a major determinant of pathogenesis in the vertebrate host, and that its mechanism of action is the augmentation of virus–cell association (but not transport of virus to the cell surface), which ultimately leads to lysis of the infected cell. It is possible that NS1 is somehow involved in virus trafficking. Differential virus release in different cells suggests the involvement of host proteins. Indeed a yeast two-hybrid analysis has identified NS1 interaction with the cellular protein SUMO-1 (R. Noad and P. Roy, unpublished data). This protein is conjugated to cellular targets as a post-translational modification involved in the intracellular trafficking. In addition, it appears that sumoylation of cellular

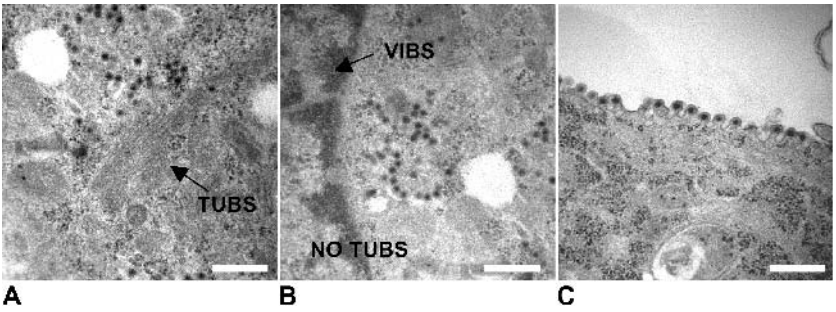

Fig. 5A–C Ultrastructural analysis of BTV Infected cells. **A** Normal BTV infection in BSR cells showing the presence of Tubules (*TUBS*). **B, C** Negatively stained cell section infected by BTV in the presence of anti-NS1 antibody. Note in **C**, virus particles are exiting cells by budding from the plasma membrane. *Bar*, 500 nm. (Owens and Roy 2004)

proteins is highly enhanced in BTV-infected cells. Upregulation of SUMO-1 has recently been shown to regulate dynamin-dependent protein trafficking within the cell (Mishra et al. 2004). Thus, it could be speculated that the role of NS1 is to control the trafficking of immature or mature virus particles in infected cells through the interaction with cellular proteins such as SUMO-1.

5 Concluding Remarks

Our understanding of the assembly of BTV within virus-infected cells continues to advance rapidly. The roles of the VP2 and VP5 proteins in virus entry have been elucidated and, surprisingly, reveal striking similarity to the entry mechanisms of enveloped viruses. Based on structure-informed mutagenesis of the major proteins of the core, we now have a clearer picture of the order in which VP7 trimers are assembled onto the underlying VP3 layer, which enhances the static model provided by the core structure. In addition, there remain a number of significant unanswered questions regarding the assembly of mature virus particles and the egress of virus from infected cells. In particular, the mechanism by which the virus manages to efficiently package its genome into the assembling particle and the route taken by newly assembled particles as they exit infected cells remain poorly understood. Recent studies have provided tantalising glimpses of the solution to these problems and have indicated that, as with virus disassembly during entry into the cell, interactions involved in these mechanisms are dynamic and complex.

References

Afrikanova I, Miozzo MC, Giambiagi S, Burrone O (1996) Phosphorylation generates different forms of rotavirus NSP5. J Gen Virol 77:2059–2265

Arcangeletti MC, Pinardi F, Missorini S, De Conto F, Conti G, Portincasa P, Scherrer K, Chezzi C (1997) Modification of cytoskeleton and prosome networks in relation to protein synthesis in influenza A virus-infected LLC-MK2 cells. Virus Res 51:19–34

Bae SH, Cheong HK, Lee JH, Cheong C, Kainosho M, Choi BS (2001) Structural features of an influenza virus promoter and their implications for viral RNA synthesis. Proc Natl Acad Sci U S A 98:10602–10607

Bannerjee AK, Shatkin AJ (1970) Transcription in vitro by reovirus associated ribonucleic acid-dependent polymerase. J Virol 6:1–11

Bansal OB, Stokes A, Bansal A, Bishop DHL, Roy P (1998) Membrane organization of bluetongue virus non-structural glycoprotein NS3. J Virol 72:3362–3369

Beasley BE, Hu WS (2002) cis-Acting elements important for retroviral RNA packaging specificity. J Virol 76:4950–4960

Beaton AR, Rodriguez J, Reddy YK, Roy P (2002) The membrane trafficking protein calpactin forms a complex with bluetongue virus protein NS3 and mediates virus release. Proc Natl Acad Sci U S A 99:13154–13159

Becker MM, Peters TR, Dermody TS (2003) Reovirus sigma NS and mu NS proteins form cytoplasmic inclusion structures in the absence of viral infection. J Virol 77:5948–5963

Blot V, Perugi F, Gay B, Prevost MC, Briant L, Tangy F, Abriel H, Staub O, Dokhelar MC, Pique C (2004) Nedd4.1-mediated ubiquitination and subsequent recruitment of Tsg101 ensure HTLV-1 Gag trafficking towards the multivesicular body pathway prior to virus budding. J Cell Sci 117:2357–2367

Boyce M, Wehrfritz J, Noad R, Roy P (2004) Purified recombinant bluetongue virus VP1 exhibits RNA replicase activity. J Virol 78:3994–4002

Broering TJ, Parker JS, Joyce PL, Kim J, Nibert ML (2002) Mammalian reovirus nonstructural protein muNS forms large inclusions and colocalizes with reovirus microtubule-associated protein mu2 in transfected cells. J Virol 76:8285–8297

Brookes SM, Hyatt AD, Eaton BT (1993) Characterization of virus inclusion bodies in bluetongue virus infected cells. J Gen Virol 74:525–530

Butan C, Van Der Zandt H, Tucker PA (2004) Structure and assembly of the RNA binding domain of bluetongue virus non-structural protein 2. J Biol Chem 279:37613–37621

Charpilienne A, Lepault J, Rey F, Cohen J (2002) Identification of rotavirus VP6 residues located at the interface with VP2 that are essential for capsid assembly and transcriptase activity. J Virol 76:7822–7831

Chen D, Zeng CQ, Wentz MJ, Gorziglia M, Estes MK, Ramig RF (1994) Template-dependent, in vitro replication of rotavirus RNA. J Virol 68:7030–7039

Cohen J (1977) Ribonucleic acid polymerase activity associated with purified calf rotavirus. J Gen Virol 36:395–402

Colman PM, Lawrence MC (2003) The structural biology of type I viral membrane fusion Nat Rev Mol Cell Biol 4:309–319

Cordo SM, Candurra NA (2003) Intermediate filament integrity is required for Junin virus replication. Virus Res 97:47–55

Craven RC, Harty RN, Paragas J, Palese P, Wills JW (1999) Late domain function identified in the vesicular stomatitis virus M protein by use of rhabdovirus-retrovirus chimeras. J Virol 73:3359–3365

Creutz CE (1992) The annexins and exocytosis. Science 258:924–931

Devaney MA, Kendall J, Grubman MJ (1988) Characterization of a non-structural phosphoprotein of two orbiviruses. Virus Res 11:151–164

Eaton BT, Hyatt AD (1989) Association of bluetongue virus with the cytoskeleton. Subcell Biochem 15:233–273

Eaton BT, Hyatt AD, White JR (1987) Association of bluetongue virus with the cytoskeleton. Virology 157:107–116

Eaton BT, Hyatt AD, White JR (1988) Localization of the nonstructural protein NS1 in bluetongue virus-infected cells and its presence in virus particles. Virology 163:527–537

Eichwald C, Vascotto F, Fabbretti E, Burrone O (2002) Rotavirus NSP5: mapping phosphorylation sites and kinase activation and viroplasm localization domains. J Virol 76:3461–3470

Ferreira LR, Moussatche N, Moura Neto V (1994) Rearrangement of intermediate filament network of BHK-21 cells infected with vaccinia virus. Arch Virol 138:273–285

Fillmore GC, Lin H, Li JK-K (2002) Localization of the single-stranded RNA-binding domains of bluetongue virus nonstructural protein NS2. J Virol 76:499–506

Forzan M, Wirblich C, Roy P (2004) A capsid protein of nonenveloped Bluetongue virus exhibits membrane fusion activity. Proc Natl Acad Sci U S A 101:2100–2105

Freed EO (2004) Mechanisms of enveloped virus release. Virus Res 106:85–86

French TJ, Roy P (1990) Synthesis of bluetongue virus (BTV) corelike particles by a recombinant baculovirus expressing the two major structural core proteins of BTV. J Virol 64:1530–1536

French TJ, Inumaru S, Roy P (1989) Expression of two related nonstructural proteins of bluetongue virus (BTV) type 10 in insect cells by a recombinant baculovirus: production of polyclonal ascitic fluid and characterization of the gene product in BTV-infected BHK cells. J Virol 63:3270–3278

French TJ, Marshall JJ, Roy P (1990) Assembly of double-shelled, virus-like particles of bluetongue virus by the simultaneous expression of four structural proteins. J Virol 64:5695–5700

Garcia-Barreno B, Jorcano JL, Aukenbauer T, Lopez-Galindez C, Melero JA (1988) Participation of cytoskeletal intermediate filaments in the infectious cycle of human respiratory syncytial virus (RSV). Virus Res 9:307–321

Garrus JE, von Schwedler UK, Pornillos OW, Morham SG, Zavitz KH, Wang HE, Wettstein DA, Stray KM, Cote M, Rich RL, Myszka DG, Sundquist WI (2001) Tsg101 and the vacuolar protein sorting pathway are essential for HIV-1 budding. Cell 107:55–65

Gorman BM, Taylor J, Walker PJ (1983) Orbiviruses. In: Joklik WK (ed) The Reoviridae. Plenum, New York, pp 287–357

Gouet P, Diprose JM, Grimes JM, Malby R, Burroughs JN, Zientara S, Stuart DI, Mertens PP (1999) The highly ordered double-stranded RNA genome of bluetongue virus revealed by crystallography. Cell 97:481–490

Grimes JM, Burroughs JN, Gouet P, Diprose JM, Malby R, Zientara S, Mertens PPC, Stuart DI (1998) The atomic structure of the bluetongue virus core. Nature 395:470–478

Grubman MJ, Appleton JA, Letchworth GJ (1983) Identification of bluetongue virus type 17 genome segments coding for polypeptides associated with virus neutralization and intergroup reactivity. Virology 131:355–366

Guirakhoo F, Catalan JA, Monath TP (1995) Adaptation of bluetongue virus in mosquito cells results in overexpression of NS3 proteins and release of virus particles. Arch Virol 140:967–974

Han Z, Harty RN (2004) The NS3 protein of bluetongue virus exhibits viroporin-like properties. J Biol Chem 279:43092–43097

Harty RN, Paragas J, Sudol M, Palese P (1999) A proline-rich motif within the matrix protein of vesicular stomatitis virus and rabies virus interacts with WW domains of cellular proteins: implications for viral budding. J Virol 73:2921–2929

Harty RN, Brown ME, Wang G, Huibregtse J, Hayes FP (2000) A PPxY motif within the VP40 protein of Ebola virus interacts physically and functionally with a ubiquitin ligase: implications for filovirus budding. Proc Natl Acad Sci U S A 97:13871–13876

Harty RN, Brown ME, McGettigan JP, Wang G, Jayakar HR, Huibregtse JM, Whitt MA, Schnell MJ (2001) Rhabdoviruses and the cellular ubiquitin-proteasome system: a budding interaction. J Virol 75:10623–10629

Hassan SH, Roy P (1999) Expression and functional characterization of bluetongue virus VP2 protein: role in cell entry. J Virol 73:9832–9842

Hassan SH, Wirblich C, Forzan M, Roy P (2001) Expression and functional characterization of bluetongue virus VP5 protein: role in cellular permeabilization. J Virol 75:8356–8367

Heidecker G, Lloyd PA, Fox K, Nagashima K, Derse D (2004) Late assembly motifs of human T-cell leukemia virus type 1 and their relative roles in particle release. J Virol 78:6636–6648

Hewat EA, Booth TF, Loudon PT, Roy P (1992a) Three-dimensional reconstruction of baculovirus expressed bluetongue virus core-like particles by cryo-electron microscopy. Virology 189:10–20

Hewat EA, Booth TF, Roy P (1992b) Structure of bluetongue virus particles by cryo-electron microscopy. J Struct Biol 109:61–69

Hewat EA, Booth TF, Roy P (1994) Structure of correctly self-assembled bluetongue virus-like particles. J Struct Biol 112:183–191

Huismans H (1979) Protein synthesis in bluetongue virus-infected cells. Virology 92:385–396

Huismans H, Els HJ (1979) Characterization of the tubules associated with the replication of three different orbiviruses. Virology 92:397–406

Huismans H, Van der Walt NT, Cloete M, Erasmus BJ (1983) The biochemical and immunological characterization of bluetongue virus outer capsid polypeptides In: Compans RW, Bishop DHL (eds) Double-stranded RNA viruses. Elsevier, New York, pp 165–172

Huismans H, Van Dijk AA, Els HJ (1987) Uncoating of parental bluetongue virus to core and subcore particles in infected L cells. Virology 157:180–188

Hyatt AD, Eaton BT (1988) Ultrastructural distribution of the major capsid proteins within bluetongue virus and infected cells. J Gen Virol 69:805–815

Hyatt AD, Eaton BT, Brookes SM (1989) The release of bluetongue virus from infected cells and their superinfection by progeny virus. Virology 173:21–34

Hyatt AD, Gould AR, Coupar B, Eaton BT (1991) Localization of the non-structural protein NS3 in bluetongue virus-infected cells. J Gen Virol 72:2263–2267

Hyatt AD, Zhao Y, Roy P (1993) Release of bluetongue virus-like particles from insect cells is mediated by BTV nonstructural protein NS3/NS3A. Virology 193:592–603

Iwata H, Yamagawa M, Roy P (1992) Evolutionary relationships among the gnat-transmitted orbiviruses that cause African horse sickness, bluetongue, and epizootic hemorrhagic disease as evidenced by their capsid protein sequences. Virology 191:251–261

Iwata H, Yamakawa M, Roy P (1995) Nucleotide sequences of African horsesickness virus serotype 4 RNA segments for encoding major capsid proteins and its evolutionary relationships among Orbiviruses. In: Proceedings of the International Workshop for the Development of Diagnostic and Preventative Methods by Genetic Engineering for African Horsesickness and Related Orbiviruses, NIAH, Tokyo, Japan, pp 109–127

Jacobs BL, Langland JO (1996) When two strands are better than one: the mediators and modulators of the cellular responses to double-stranded RNA. Virology 219:339–349

Kar AK, Roy P (2003) Defining the structure-function relationships of bluetongue virus helicase protein VP6. J Virol 77:11347–11356

Kar AK, Ghosh M, Roy P (2004) Mapping the assembly of Bluetongue virus scaffolding protein VP3. Virology 324:387–399

Karczewski MK, Strebel K (1996) Cytoskeleton association and virion incorporation of the human immunodeficiency virus type 1 Vif protein. J Virol 70:494–507

Kohli E, Pothier P, Tosser G, Cohen J, Sandino AM, Spencer E (1993) In vitro reconstitution of rotavirus transcriptional activity using viral cores and recombinant baculovirus expressed VP6. Arch Virol 133:451–458

Le Blois H, Fayard B, Urakawa T, Roy P (1991) Synthesis and characterization of chimaeric particles between epizootic haemorrhagic disease virus and bluetongue virus: functional domains are conserved on the VP3 protein. J Virol 65:4821–4831

Licata JM, Simpson-Holley M, Wright NT, Han Z, Paragas J, Harty RN (2003) Overlapping motifs (PTAP, PPEY) within the Ebola virus VP40 protein function independently as late budding domains: involvement of host proteins TSG101 and VPS-4. J Virol 77:1812–1819

Limn CK, Roy P (2003) Intermolecular interactions in a two-layered viral capsid that requires a complex symmetry mismatch. J Virol 77:11114–11124

Limn C-H, Staeuber N, Monastyrskaya K, Gouet P, Roy P (2000) Functional dissection of the major structural protein of bluetongue virus: identification of key residues within VP7 essential for capsid assembly. J Virol 74:8658–8669

Liu HM, Booth TF, Roy P (1992) Interactions between bluetongue virus core and capsid proteins translated in vitro. J Gen Virol 73:2577–2584

Loudon PT, Roy P (1992) Interaction of nucleic acids with core-like and subcore-like particles of bluetongue virus. Virology 191:231–236

Loudon PT, Hirasawa T, Oldfield S, Murphy M, Roy P (1991) Expression of the outer capsid protein VP5 of two bluetongue viruses, and synthesis of chimeric double-shelled virus-like particles using combinations of recombinant baculoviruses. Virology 182:793–801

Lymperopoulos K, Wirblich C, Brierley I, Roy P (2003) Sequence specificity in the interaction of Bluetongue virus non-structural protein 2 (NS2) with viral RNA. J Biol Chem 278:31722–31730

Markotter W, Theron J, Nel LH (2004) Segment specific inverted repeat sequences in bluetongue virus mRNA are required for interaction with the virus nonstructural protein NS2. Virus Res 105:1–9

Martinez Costas J, Sutton G, Ramadevi N, Roy P (1998) Guanylyltransferase and RNA 5'-triphosphatase activities of the purified expressed VP4 protein of bluetongue virus. J Mol Biol 280:859–866

Meggio F, Pinna L (2003) One-thousand-and-one substrates of protein kinase CK2? FASEB J 17:349–368

Mertens PP, Burroughs JN, Anderson J (1987) Purification and properties of virus particles, infectious subviral particles, and cores of bluetongue virus serotypes 1 and 4. Virology 157:375–386

Meyer JC, Bergmann CC, Bellamy AR (1989) Interaction of rotavirus cores with the non-structural glycoprotein NS28. Virology 171:98–107

Mishra RK, Jatiani SS, Kumar A, Simhadri VR, Hosur RV, Mittal R (2004) Dynamin interacts with members of the sumoylation machinery. J Biol Chem 279:31445–31454

Modrof J, Lymperopoulos K, Roy P (2005) Phosphorylation of Bluetongue virus non-structural protein 2 is essential for formation of viral inclusion bodies. J Virol 79:10023–10031

Morita E, Sundquist WI (2004) Retrovirus budding. Annu Rev Cell Dev Biol 20:395–425

Mortola E, Noad R, Roy P (2004) Bluetongue virus outer capsid proteins are sufficient to trigger apoptosis in mammalian cells. J Virol 78:2875–2883

Murti KG, Goorha R, Klymkowsky MW (1988) A functional role for intermediate filaments in the formation of frog virus 3 assembly sites. Virology 162:264–269

Nason E, Rothnagel R, Muknerge SK, Kar AK, Forzan M, Prasad BVV, Roy P (2004) Interactions between the inner and outer capsids of Bluetongue virus. J Virol 78:8059–8067

Nedellec P, Vicart P, Laurent-Winter C, Martinat C, Prevost MC, Brahic M (1998) Interaction of Theiler's virus with intermediate filaments of infected cells. J Virol 72:9553–9560

Owens R, Roy P (2004) Role of an arbovirus nonstructural protein in cellular pathogenesis and virus release. J Virol 78:6649–6656

Patton JT (1996) Rotavirus VP1 alone specifically binds to the 3′ end of viral mRNA, but the interaction is not sufficient to initiate minus-strand synthesis. J Virol 70:7940–7947

Patton JT, Jones MT, Kalbach AN, He YW, Xiaobo J (1997) Rotavirus RNA polymerase requires the core shell protein to synthesize the double-stranded RNA genome. J Virol 71:9618–9626

Perez M, Craven RC, de la Torre JC (2003) The small RING finger protein Z drives arenavirus budding: implications for antiviral strategies. Proc Natl Acad Sci U S A 100:12978–12983

Poncet D, Aponte C, Cohen J (1993) Rotavirus protein NSP3 (NS34) is bound to the 3′ end consensus sequence of viral mRNAs in infected cells. J Virol 67:3159–3165

Poncet D, Lindenbaum P, L'Haridon R, Cohen J (1997) In vivo and in vitro phosphorylation of rotavirus NSP5 correlates with its localization in viroplasms J Virol 71:34–41

Prasad BVV, Yamaguchi S, Roy P (1992) Three-dimensional structure of single-shelled bluetongue virus. J Virol 66:2135–2142

Prasad BVV, Rothnagel R, Zeng CQ, Jakana J, Lawton JA, Chiu W, Estes MK (1996) Visualization of ordered genomic RNA and localization of transcriptional complexes in rotavirus. Nature 382:471–473

Ramadevi N, Roy P (1998) Bluetongue virus core protein VP4 has nucleoside triphosphate phosphohydrolase activity. J Gen Virol 79:2475–2480

Ramadevi N, Burroughs JN, Mertens PPC, Jones IM, Roy P (1998) Capping and methylation of mRNA by purified recombinant VP4 protein of Bluetongue virus. Proc Natl Acad Sci U S A 95:13537–13542

Raynal P, Pollard HB (1994) Annexins: the problem of assessing the biological role for a gene family of multifunctional calcium- and phospholipid-binding proteins. Biochem Biophys Res Acta 1197:63–93

Reinisch KM, Nibert ML, Harrison SC (2000) Structure of the reovirus core at 3.6 Å resolution. Nature 404:960–967

Roy P (1996) Orbivirus structure and assembly. Virology 216:1–11

Sakurai A, Yasuda J, Takano H, Tanaka Y, Hatakeyama M, Shida H (2004) Regulation of human T-cell leukemia virus type 1 (HTLV-1) budding by ubiquitin ligase Nedd4. Microbes Infect 6:150–156

Samuel CE (1998) Reoviruses and the interferon system. Curr Top Microbiol Immunol 233:125–145

Stauber N, Martinez-Costas J, Sutton G, Monastyrskaya K, Roy P (1997) Bluetongue virus VP6 protein binds ATP and exhibits an RNA-dependent ATPase function and a helicase activity that catalyze the unwinding of double-stranded RNA substrates. J Virol 71:7220–7226

Tao Y, Farsetta DL, Nibert ML, Harrison SC (2002) RNA Synthesis in a cage-structural studies of reovirus polymerase lambda3. Cell 111:733–745

Theron J, Nel LH (1997) Stable protein-RNA interaction involves the terminal domains of bluetongue virus mRNA, but not the terminally conserved sequences. Virology 229:134–142

Thomas CP, Booth TF, Roy P (1990) Synthesis of bluetongue virus-encoded phosphoprotein and formation of inclusion bodies by recombinant baculovirus in insect cells: it binds the single-stranded RNA species. J Gen Virol 71:2073–2083

Timmins J, Schoehn G, Ricard-Blum S, Scianimanico S, Vernet T, Ruigrok RW, Weissenhorn W (2003) Ebola virus matrix protein VP40 interaction with human cellular factors Tsg101 and Nedd4. J Mol Biol 326:493–502

Urakawa T, Roy P (1988) Bluetongue virus tubules made in insect cells by recombinant baculoviruses: expression of the NS1 gene of bluetongue virus serotype 10. J Virol 62:3919–3927

Van Dijk AA, Huismans H (1980) The in vitro activation and further characterization of the bluetongue virus-associated transcriptase. Virology 104:347–356

Van Dijk AA, Huismans H (1982) The effect of temperature on the in vitro transcriptase reaction of bluetongue virus, epizootic haemorrhagic disease virus and African horsesickness virus. Onderstepoort J Vet Res 49:227–232

Van Dijk AA, Huismans H (1988) In vitro transcription and translation of bluetongue virus mRNA. J Gen Virol 69:573–581

Van Staden V, Huismans H (1991) A comparison of the genes which encode nonstructural protein NS3 of different orbiviruses. J Gen Virol 72:1073–1079

Van Staden V, Stoltz MA, Huismans H (1995) Expression of nonstructural protein NS3 of African horsesickness virus (AHSV): evidence for a cytotoxic effect of NS3 in insect cells, and characterization of the gene products in AHSV infected Vero cells. Arch Virol 140:289–306

Venkatesan S, Gershowitz A, Moss B (1980) Modification of the 5′ end of mRNA. Association of RNA triphosphatase with the RNA guanylyltransferase-RNA (guanine-7-)methyltransferase complex from vaccinia virus. J Biol Chem 255:903–908

Verwoerd DW, Els HJ, De Villiers EM, Huismans H (1972) Structure of the bluetongue virus capsid. J Virol 10:783–794

Wirblich C, Bhattacharya P, Roy P (2005) Non-structural protein 3 of Bluetongue virus assists virus release by recruiting the ESCRT I protein Tsg101. J Virol 80:128–105

Wu X, Chen SY, Iwata H, Compans RW, Roy P (1992) Multiple glycoproteins synthesized by the smallest RNA segment (S10) of bluetongue virus J Virol 66:7104–7112

Yasuda J, Nakao M, Kawaoka Y, Shida H (2003) Nedd4 regulates egress of Ebola virus-like particles from host cells. J Virol 77:9987–9992

Zetina CR (2001) A conserved helix-unfolding motif in the naturally unfolded proteins. Proteins 44:479–483

Zhao Y, Thomas C, Bremer C, Roy P (1994) Deletion and mutational analyses of bluetongue virus NS2 protein indicate that the amino but not the carboxy terminus of the protein is critical for RNA-protein interactions. J Virol 68:2179–2185

CTMI (2006) 309:117–167

Reovirus Structure and Morphogenesis

K. M. Coombs (✉)

Department of Medical Microbiology and Infectious Diseases,
University of Manitoba, Winnipeg, Manitoba R3E 0W3, Canada
kcoombs@ms.umanitoba.ca

Abstract Assembly of a mature infectious virion from component parts is one of the last steps in the replicative cycle of most viruses. Recent advances in delineating aspects of this process for the mammalian orthoreoviruses (MRV), nonenveloped viruses composed of a genome of ten segments of double-stranded RNA enclosed in two concentric icosahedral protein capsids, are discussed. Analyses of temperature-sensitive (*ts*) assembly-defective reovirus mutants have been used to better understand requirements for viral inclusion formation and capsid morphogenesis. Newly determined high-resolution structures of virtually all MRV proteins, combined with complete MRV genomic sequence information and elucidation of sequence lesions in *ts* mutants, is now providing a context for molecularly understanding interactions that promote, or abrogate, reovirus capsid assembly. Additional advances in understanding required signals for whole genome construction from sets of the ten individual genes, and in transcapsidation of subviral particles with engineered outer capsid proteins, provide additional molecular genetic understanding of reovirus protein structure–function and morphogenesis.

1 Introduction

The normal process of virus infection and transmission from one host cell to another and from one host organism to another requires that the virus undergoes replication to make multiple progeny copies. Thus, for most viruses, which are constructed from at least one piece of nucleic acid, as well as multiple copies of one or more proteins, replication involves successfully completing all the following steps: entry into susceptible cells, uncoating of viral capsid(s) to expose virus genetic information to cellular enzymes, transcription to produce mRNA, which will be used to make viral-encoded proteins, replication to copy the viral genome, assembly of the progeny proteins and replicated genomes to produce functional infectious progeny virus, and release from host cell to allow infection of subsequent cells. The purpose of this review is to describe current knowledge related to how members of the mammalian orthoreoviruses are assembled.

The mammalian orthoreoviruses (MRVs) are the prototypic members of the *Orthoreovirus* genus of the family *Reoviridae*. The *Reoviridae* family currently contains 12 genera (Mertens et al. 2005). Members of this family are nonenveloped viruses of intermediate structural complexity. Their genomes consist of multiple segments (10–12) of double-stranded (ds) RNA surrounded by multiple (usually two or three) concentric protein capsids. In addition to the *Orthoreovirus* genus, this family includes rotaviruses, medically significant agents responsible for a significant amount of viral gastroenteritis in North America and millions of deaths annually worldwide (Offit 1994; Estes 2001; Kapikian et al. 2001), the economically important insect-

vectored orbiviruses (for review, see Roy 2001), and a variety of other viruses. Many of these viruses infect plants, vertebrates, and invertebrates, and many also can be classified as arboviruses because they are transmitted from plant to plant, or from vertebrate to vertebrate, by invertebrates. There also are a number of agents that possess reovirus characteristics (10–12 segments of double-stranded RNA contained within multiple concentric icosahedral nonenveloped capsids) that have not yet been formally classified, including agents pathogenic for snakes, baboons, and flying foxes.

2 Reovirus Structure

Understanding the interactions that allow multiple proteins and nucleic acids to recognize each other to participate in morphogenesis is aided by understanding the structures of individual proteins and nucleic acids, as well as structures of the entire completed particle. Initial comparative cryoelectron microscopic image reconstructions of the available naturally occurring subviral particles (Dryden et al. 1993, 1998) (see Fig. 1C) have now been supplemented with high-resolution X-ray crystallographic structure determinations for virtually all MRV structural proteins (Liemann et al. 2002; Chappell et al. 2002; Tao et al. 2002), as well as for one of the sub-viral particles (Reinisch et al. 2000) (Fig. 2). In addition, comparisons of sequence conservation between each of various MRV proteins and homologous proteins in other reoviruses, such as avian reoviruses (ARVs), aquareoviruses, rotaviruses, and orbiviruses (see, for example, Duncan 1999; Attoui et al. 2002; Kim et al. 2004; Taraporewala and Patton 2004; Noad et al. 2006) demonstrate regions of very high conservation. These comparisons, combined with apparent success in mapping sequences from one virus into medium- and high-resolution structures of other virus proteins (see, for example, Nason et al. 2000; Kim et al. 2004; Xu et al. 2004, 2005; Noad et al. 2006), have contributed to a better understanding of reovirus protein structure and function.

MRVs have a genome composed of ten segments of dsRNA that is encased by two concentric protein capsids built from multiple, nonequivalent copies of eight different proteins (Fig. 1B, D). (For reviews, see Nibert and Schiff 2001; Tyler 2001; Mertens et al. 2005). Three MRV serotypes (designated 1, 2, and 3) have been described. Prototype members of each serotype routinely used are type 1 Lang (T1L), type 2 Jones (T2J), and type 3 Dearing (T3D). For recent reviews, see Nibert and Schiff 2001; Tyler 2001. Some recent comparative sequence evidence supports establishment of a fourth serotype, represented by Ndelle virus (Attoui et al. 2001).

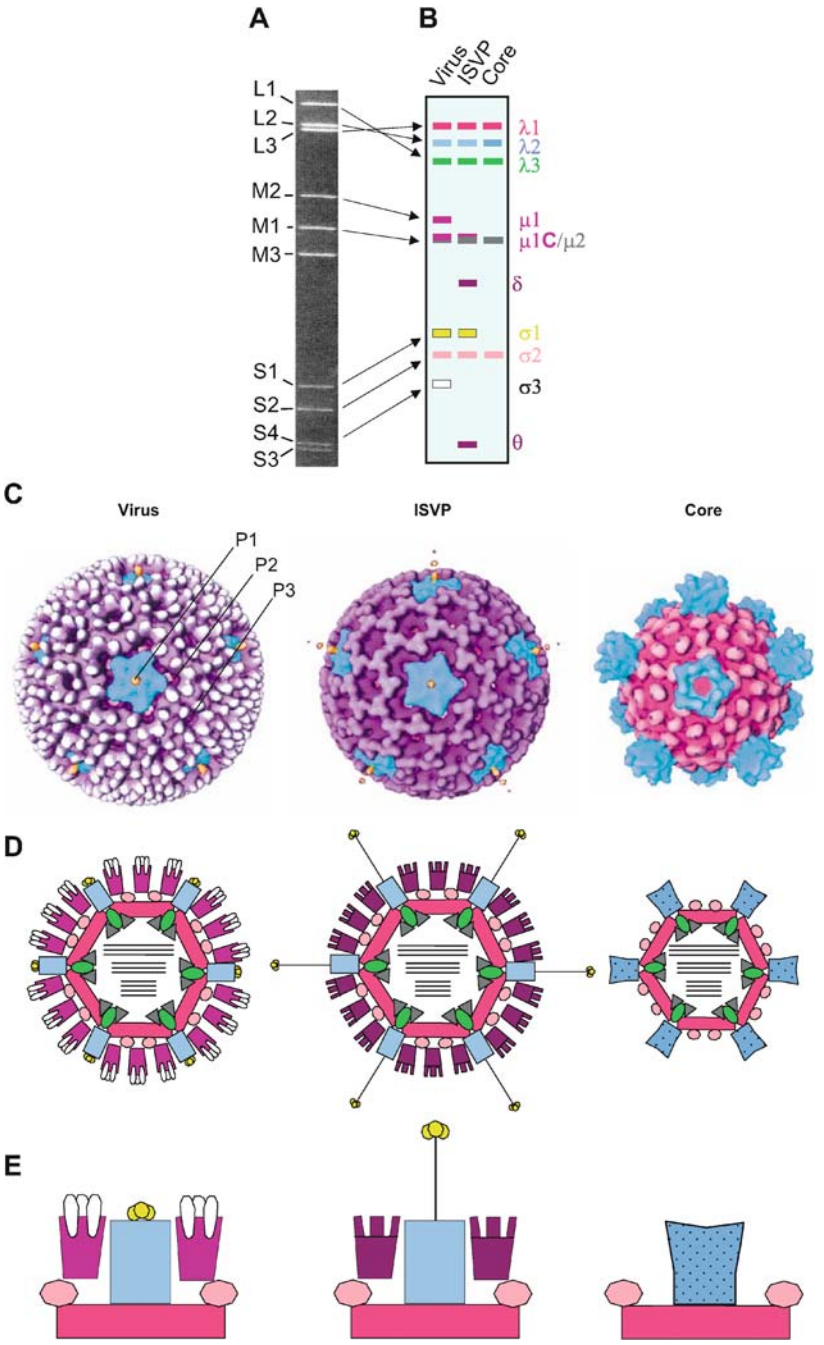
A
B
Virus
ISVP
Core
L1
L2
L3
M2
M1
M3
S1
S2
S4
S3
λ1
λ2
λ3
μ1
μ1C/μ2
δ
σ1
σ2
σ3
θ
C
Virus
ISVP
Core
P1
P2
P3
D
E

Fig. 1A–E Structure, gene coding, and protein locations within T1L reovirus particle. **A** T1L genomic RNA profile in 10% SDS-PAGE with gene segments (L1–S4) labeled on the *left*; note that the T1L M1 genome segment migrates faster than the M2 segment and the S3 segment migrates faster than the S4 segment. **B** Diagram of protein profiles of virus, ISVP and core in SDS-PAGE. Each protein is encoded by indicated gene segment in **A** (*arrows*). **C** Cryoelectron microscopy reconstructions of virus, ISVP, and core. (Reprinted from Spencer et al. 1997, with permission from M.L. Nibert and Elsevier). Images were recolorized with Adobe Photoshop software to facilitate comparison with colors in **B**, **D**, and **E** and examples of solvent channels P1, P2, and P3 are indicated. **D** Diagram of reovirus virion, ISVP and core, showing presumptive locations of various structural proteins and their conversion or removal from each type of particle. **E** Close-up views at viral vertices. Proteins in **B–E** are color-coded to facilitate comparisons. *Thick solid lines* inside particles in **D** represent genome segments. Changes in σ1 shape, and μ1 and δ coloration between virus and ISVP, as well as λ2 shape and coloration in core, in **D** and **E** correspond to known structural changes described in the text

2.1 Structure of the Genome

The complete genomic sequences of all ten genes of all three prototype MRVs have been determined (Wiener and Joklik 1989; Breun et al. 2001; Yin et al. 2004). The genome consists of three large segments (L1, L2, L3) ranging in size from 3,854 to 3,916 base pairs (bp), three medium segments (M1, M2, M3) ranging in size from 2,203 to 2,304 bp, and four small segments (S1, S2, S3, S4) ranging in size from 1,196 to 1,463 bp, for a total genomic size of 23,606 bp for T1L, 23,578 bp for T2J, and 23,560 bp for T3D. Every MRV gene sequenced to date consists of a short 5′ nontranslated region (NTR) of variable length (ranging from 12 bp in the S1 gene to 32 bp in the S4 gene), an open reading frame (ORF) of variable length, and a 3′ NTR ranging from 35 bp in the L1 gene to 83 bp in the M1 gene (Nibert and Schiff 2001; Wiener and Joklik 1989; Breun et al. 2001; Yin et al. 2004). Every gene contains a completely conserved consensus GCUA tetranucleotide at the extreme 5′ end of the gene and a completely conserved consensus UCAUC pentanucleotide (on the plus-sense strand) at the extreme 3′ end of the gene. Although still not known, the current belief is that signals that direct genomic assembly reside in one or both of the NTRs, although some signals may also reside in the ORF (discussed more fully below in Sect. 5).

2.2 Inner Capsid Structure

The reovirus inner capsid (called core) contains the viral genome and is constructed from five proteins, called λ1, λ2, λ3, μ2, and σ2. The core has

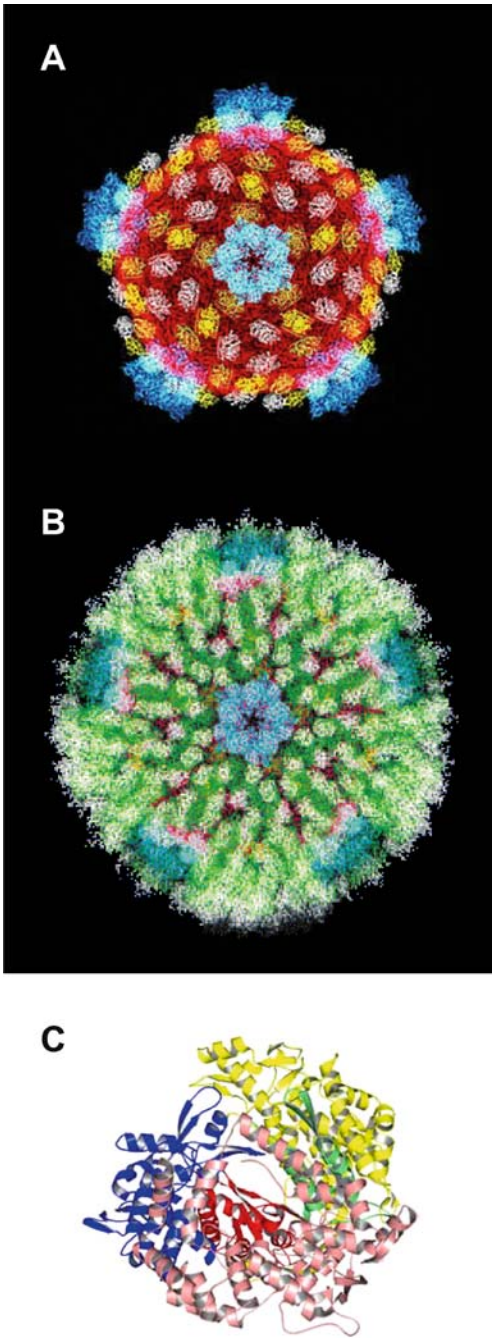
A
B
C

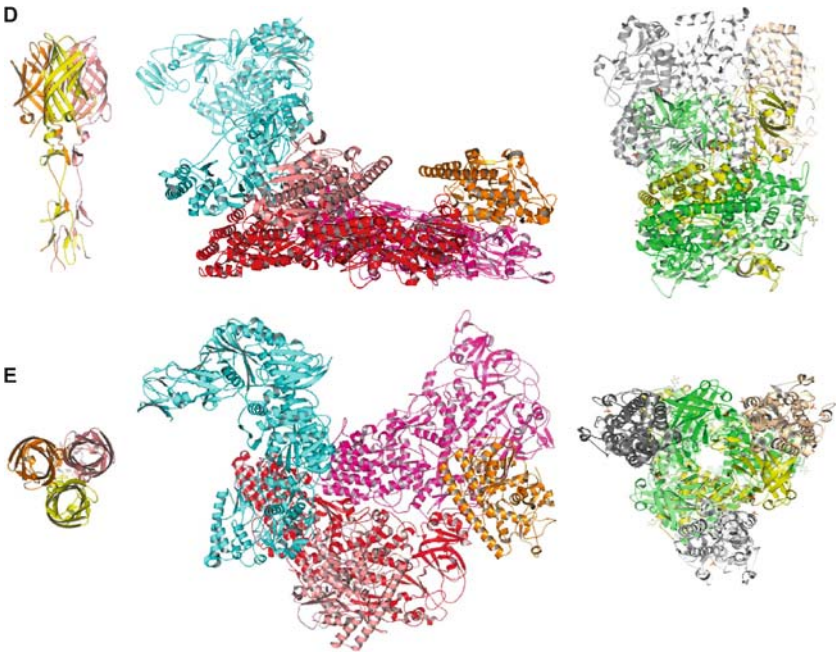

Fig. 2A–E Crystal structures of reovirus particles and proteins. **A** The reovirus core, determined by Reinisch et al. 2000 (Reprinted from Reinisch et al. 2000, with permission from S.C. Harrison and Nature Publishing Group), with λ1 proteins in *red*, λ2 proteins in *cyan*, and individual σ2 proteins in *pink* and *yellow*. **B** The reconstructed reovirus virion, determined by Liemann et al. 2002 (Reprinted from Liemann et al. 2002, with permission from S.C. Harrison and Elsevier), with μ1 in *green* and σ3 in *white*. Images in **A** and **B** are at the same scale. **C** Reovirus RdRp protein λ3, determined by Tao et al. 2002 (PDB 1MUK). The basic right-hand configuration seen in all crystallized DNA and RNA polymerases is shown in *blue* (fingers), *red* (palm), and *green* (thumb) and extra material not normally present in other polymerases is shown in *yellow* (N-terminal residues 1–380) and *salmon* (C-terminal bracelet residues 891–1267). **D** Side views and **E** top views of σ1 trimer (*left*), with individual σ1 molecules shown in *yellow*, *salmon*, and *orange*, determined by Chappell et al. 2002 (PDB 1KKE); core asymmetric unit (*middle*) determined by Reinisch et al. 2000 (PDB 1EJ6), with individual λ1 molecules in *red and hot pink*, λ2 in *cyan* (as in **A**), and σ2 in *orange and salmon*; and $(\mu1/\sigma3)_3$ heterohexamer (*right*) determined by Liemann et al. 2002 (PDB 1JMU), with μ1 in *green, olive, and lime*, and σ3 in *white, wheat, and gray*. Images in **C**–**E** were colorized and manipulated with PyMol (DeLano 2004). Images in **D**, **E** are at approximately the same scale and at about 1/2 scale of image in **C**

icosahedral symmetry and a diameter of approximately 52 nm (excluding the spike "turrets" which extend outward from each icosahedral five-fold axis [vertex] by an additional 5.5 nm) (Fig. 1C–E). The intact core serves as

the metabolically active macromolecular machine from which viral mRNA is transcribed (discussed more fully below in Sect. 3). Detailed structural information has been provided from X-ray crystallographic studies of the reovirus core particle (Reinisch et al. 2000), which greatly aid in understanding the structure–function relationships of each protein.

Full-length λ1 is a 1,275-amino-acid-long 142-kDa protein (Harrison et al. 1999) encoded by the L3 genome segment (McCrae and Joklik 1978) (Table 1).

Table 1 Characteristics of reovirus structural proteins[a]

Protein name	Gene segment	Copy number	Predicted[b] MW (kDa)	Pl	Location	Functions
λ1	L3	120	141.9	5.92	Core capsid	RNA binding; NTPase; helicase; RNA triphosphatase
λ2	L2	60	144	5.08	Core spike	Guanylyltransferase; methyltransferase
λ3	L1	12	142.4	8.1	Core internal	RNA-dependent RNA polymerase
μ1	M2	∼30[c]	76.2	4.92	Outer capsid	Cell penetration; transcriptase activation
μ1 C	M2	∼570[c]	72.1	4.95	Outer capsid	
μ2	M1	∼20[d]	83.3	6.75	Core internal	Binds RNA; NTPase?
σ1	S1	∼30[e]	49.4[f]	5.08[f]	Outer capsid	Attachment protein; hemmaglutinin; type-specific antigen
σ2	S2	150	47.1	8.3	Core nodule	Binds dsRNA
σ3	S4	600	41.2	6.56	Outer capsid	Binds ssRNA; role in assortment and replication

[a] Predicted molecular weights and isoelectric points deduced from genomic sequence information

[b] Estimated, based upon several observations that purified virions contain ∼95% of μ1 in cleaved μ1 C form

[c] Estimated, based upon several observations suggesting 18–24 copies per particle

[d] Estimated, based upon observations that σ1 exists as a trimer at each icosahedral vertex (3x12=36) but that not every vertex is occupied

[e] Values for reovirus, serotype 1, strain Lang (T1 L); values differ for T2J and T3D

[f] Gene protein coding assignments determined for T3D (McCrae and Joklik 1978) and assumed same for other serotypes; RNA segments M3 and S3 encode nonstructural proteins

Protein λ1 is present in 120 copies within each reovirus core particle. It is the major structural protein that forms the inner capsid. The 120 λ1 proteins are organized as 60 asymmetric dimers in a T=1 triangulation lattice (Reinisch et al. 2000) to form a thin capsid shell (Figs. 1D, E, 2A). The protein has a zinc finger motif (Bartlett and Joklik 1988), a separate region that binds dsRNA (Lemay and Danis 1994; Bisaillon and Lemay 1997b), and ATPase activity, which probably is involved in transcriptional events (Noble and Nibert 1997a; Bisaillon et al. 1997; Bisaillon and Lemay 1997a).

Full-length λ2 is a 1,289-amino-acid-long 144-kDa protein (1,288 aa for T2J) (Breun et al. 2001). Sixty copies of this protein are organized as distinctive pentameric turrets at each of the particle's 12 icosahedral vertices (Luftig et al. 1972; Metcalf et al. 1991; Dryden et al. 1993). Protein λ2 binds GMP (Fausnaugh and Shatkin 1990) and S-adenosyl-L-methionine (Luongo et al. 1998), possesses guanylyltransferase (Cleveland et al. 1986; Qiu and Luongo 2003) and methyltransferase activities, and serves to attach a type-1 ^{7}mG cap structure to nascent mRNA (Shatkin 1974; Furuichi et al. 1975; Luongo et al. 2002) as the mRNA is extruded from transcribing cores (Bartlett et al. 1974; Yeager et al. 1996). High-resolution structure determinations, coupled with mutagenesis studies, show λ2 to be a multi-domain protein (Reinisch et al. 2000; Luongo et al. 2000; Breun et al. 2001; Kim et al. 2004; Qiu and Luongo 2003).

Full-length λ3 is a 1,267-amino-acid-long 142-kDa protein (Wiener and Joklik 1989). Cores contain 12 copies of this minor protein (Smith et al. 1969; Coombs 1998a), which serves as the RNA-dependent RNA polymerase (RdRp) (Drayna and Fields 1982a; Koonin et al. 1989; Starnes and Joklik 1993). Current structural–functional data suggests that one copy of this protein is located inside the core shell at each of the icosahedral five-fold axes (Zhang et al. 2003). Recent X-ray crystallographic structure determinations indicate this protein follows the basic right-hand configuration of most nucleic acid polymerases, but also contains extra domains, including an approximately 380-amino-acid-long N-terminal domain and an approximately 380-amino-acid-long C-terminal "bracelet" domain (Tao et al. 2002) (Fig. 2C).

Full-length μ2 is a 736-amino-acid-long 83-kDa protein (Wiener et al. 1989a). This is the most enigmatic of the reovirus structural proteins. It is the only MRV structural protein for which there is currently no high-resolution structure determination, and the precise function(s) remain unknown (discussed more fully below in Sects. 3 and 7). The protein is thought to represent an RdRp co-factor (Yin et al. 1996; Noble and Nibert 1997b) and is present in 20–24 copies (Coombs 1998a), possibly also under each of the core shell icosahedral vertices (Zhang et al. 2003). Genetic mapping experiments suggest that μ2 plays a role in determining the severity of cytopathic effect in cultured cells (Moody and Joklik 1989) and the level of virus growth in various

cells (e.g., Matoba et al. 1993). The protein also is involved in the pathogenesis of myocarditis (Sherry and Fields 1989), in organ-specific virulence in SCID mice (Haller et al. 1995), in in vitro transcription of ssRNA (Yin et al. 1996), possesses nucleoside triphosphatase activity (Noble and Nibert 1997b), and plays important roles in virus inclusion formation and morphology (Parker et al. 2002; Yin et al. 2004) (discussed more fully below in Sect. 6), a process mediated, in part, by its level of ubiquitination (Miller et al. 2004).

Full-length σ2 is a 418-amino-acid-long 47-kDa protein (Wiener et al. 1989b). One hundred fifty copies of the σ2 protein decorate the thin λ1 shell (Reinisch et al. 2000) (Figures 1C–E, 2A) and may act as clamps to hold the shell together. Protein σ2 binds RNA (Schiff et al. 1988; Dermody et al. 1991) and is required for assembly of core capsids (Xu et al. 1993; Coombs et al. 1994; Kim et al. 2002) (discussed more fully below in Sects. 3 and 7.1.3).

2.3 Outer Capsid Structure

The outermost of the two viral protein shells (outer capsid) contains 600 copies each of two major proteins, μ1 and σ3 (Dryden et al. 1993), and up to 36 copies of σ1 (Strong et al. 1991), the cell attachment protein (Weiner et al. 1980; Lee et al. 1981b). Proteins in the outer capsid are organized in a fenestrated T=13(*l*) lattice (Metcalf et al. 1991; Dryden et al. 1993). The reovirus outer capsid serves as a gene delivery vehicle; proteins within this layer are responsible for recognizing host cells and in permitting entry of the viral core into the cellular cytosol. The structures of all outer capsid proteins have been determined by X-ray crystallography (Olland et al. 2001; Liemann et al. 2002; Chappell et al. 2002) (Fig. 2D, E).

Full-length μ1 is a 708-amino-acid-long, N-terminal myristoylated protein (Jayasuriya et al. 1988; Nibert et al. 1991). The protein folds into a four-domain structure; three lower predominantly α-helical domains (domains I, II, and III) plus a fourth jelly roll β-barrel head domain (domain IV) (Liemann et al. 2002). When resolved by standard SDS-PAGE, approximately 95% of virion μ1 appears as an approximately 4-kDa amino terminal myristoylated peptide (called μ1N and not resolved in standard SDS-PAGE) and a 72-kDa carboxyl-terminal portion (called μ1C). Much of this μ1N/μ1C cleavage in purified virions, which takes place between amino acids Asn_{42} and Pro_{43}, was recently shown to be an artifact of sample preparation prior to SDS-PAGE (Nibert et al. 2005). The Asn-Pro amino acid pair is found near the N-terminus in all MRVs, ARVs, and aquareovirus μ1 (and μ1 homolog) sequences determined to date (Noad et al. 2006), which suggests this μ1N/μ1C cleavage plays an important role in the replicative cycle (Odegard et al. 2004; Nibert et al. 2005).

This protein alone accounts for approximately half the total virion peptide mass, plays important roles in virion stability (Drayna and Fields 1982c; Middleton et al. 2002), and undergoes several specific cleavages during virus entry (Jayasuriya et al. 1988; Chandran and Nibert 1998; Chandran et al. 2002; Odegard et al. 2004) (discussed more fully below in Sect. 3).

Protein σ1 is the most variable of reovirus proteins. It is the cell attachment protein (Weiner et al. 1980; Lee et al. 1981b), the serotype determinant (Weiner et al. 1978), and has been associated with a very large number of viral functions (e.g., Weiner et al. 1977; Sharpe and Fields 1981; Tyler et al. 1986, 1995; Wilson et al. 1994). The protein length varies with particular virus type; full-length T1L σ1 is a 470-amino-acid-long (Dermody et al. 1990), N-terminally acetylated protein (Coombs et al. unpublished), whereas T2J σ1 is 462 and T3D σ1 is 455 amino acids long (Dermody et al. 1990). The σ1 molecules have an overall stalk/knob structure reminiscent of the adenovirus cell attachment fiber (Fraser et al. 1990; Chappell et al. 2002). The virion contains 36 copies of σ1, organized as trimers (Strong et al. 1991; Chappell et al. 2002) at each of the vertices, although evidence suggests that not all of the 12 icosahedral positions may be occupied in every virion (Larson et al. 1994). For fuller description of σ1 structure and function, see the chapter by Guglielmi et al. in this volume.

Full-length σ3 is a 365-amino acid long, 41-kDa N-terminally acetylated protein (Giantini et al. 1984; Kedl et al. 1995; Jané-Valbuena et al. 2002; Mendez et al. 2003). The protein folds into a two-lobed structure, with the small lobe in contact with the other major outer capsid protein μ1 and the large lobe exposed on the virion surface (Olland et al. 2001; Liemann et al. 2002). σ3 plays important roles in particle stability (Drayna and Fields 1982b, 1982c), in shutting down host macromolecular synthesis (Sharpe and Fields 1982), and in downregulation of interferon-induced dsRNA-activated protein kinase (PKR) (Imani and Jacobs 1988; Giantini and Shatkin 1989; Beattie et al. 1995), possibly by virtue of its intracellular distribution and capacity to interact with μ1C (Schmechel et al. 1997). σ3 contains a zinc finger motif (Giantini et al. 1984; Olland et al. 2001) and binds zinc (Schiff et al. 1988) in the protein's small lobe (Olland et al. 2001), which seems important both for correct folding (Danis et al. 1992) and stability (Mabrouk and Lemay 1994), as well as a separate motif that binds dsRNA (Huismans and Joklik 1976; Denzler and Jacobs 1994; Mabrouk et al. 1995; Bergeron et al. 1998). Structural analyses indicate three copies each of μ1 and σ3 form a heterohexameric $(\mu1/\sigma3)_3$ aggregate (Liemann et al. 2002) (see Fig. 2B, D, E). The three copies of μ1 are wound around each other to form a base upon which three σ3 monomers sit. Two hundred such heterohexameric aggregates decorate the viral outer capsid, with the $(\mu1)_3$ base contacting the core and the σ3 monomers most distally

located in the particle. This protein arrangement generates the approximately 85-nm diameter fenestrated T=13(*l*) lattice as well as three distinct types of solvent channels that span the inner and outer capsid layers (Dryden et al. 1993). The 12 P1 solvent channels are formed by the λ2 pentamers at the icosahedral five-fold vertices. This channel is blocked by presence of the σ1 trimers in virions and ISVPs, but opened when the particle is converted to a core and σ1 is lost. The 60 P2 channels, which span the outer capsid, are located at the centers of the peri-pentonal μ1/σ3 aggregates, between the aggregates and the λ2 turrets, and the 60 P3 channels are located at the centers of hexameric arrays of μ1/σ3 heterohexamers (Fig. 1C). Proteolytic processing of σ3, which initiates in a central specific hypersensitive region (HSR) (Jané-Valbuena et al. 2002; Ebert et al. 2002) and then proceeds bidirectionally towards the protein's termini (Mendez et al. 2003), plays critical roles in virus entry and uncoating (discussed more fully below in Sect. 3).

3 Overview of Reovirus Replication

Reoviruses infect a wide range of cells, both in vitro and in vivo (reviewed in Tyler 2001). Cells the virus usually infects in vivo are specialized intestinal epithelial cells (M cells) that overlie Peyer's patches. Virus then migrates between and/or through the M cells into mucosal mononuclear cells in the Peyer's patch, and subsequently into a large number of extraintestinal sites, including heart, liver, and central nervous system (reviewed in Tyler 2001). Delineation of intracellular steps in mammalian reovirus replication has been most studied in tissue-cultured mouse L929 fibroblast-like cells, the preferred cell type for in vitro studies, although numerous studies have also been conducted in a wide, and growing, range of other cells.

Reovirus replication is primarily cytoplasmic (Fig. 3). There appears to be no significant nuclear involvement, although nonstructural virus protein σ1s (which is translated from an alternate S1 reading frame) targets the nucleus (Rodgers et al. 1998). The first step in the replication cycle is binding of virion to susceptible host cells (Fig. 3, step 1), a process mediated by viral cell attachment protein σ1. Cellular proteins with which σ1 interact are not completely known, but sialic acid appears to be an important component of the receptors. Several proteins have been identified as possible receptors, including junction adhesion molecule (JAM) (Barton et al. 2001; see the chapter by Guglielmi and colleagues in this volume for a fuller description of σ1, JAM, and how they may interact). After initial σ1-mediated binding, virus enters cells by either of two mechanisms. The intact virion may be taken up by receptor-mediated

endocytosis (Fig. 3, step 2), and then seems to be converted into the intermediate (or infectious) subviral particle (ISVP) by both acid pH and proteolysis. A variety of agents that perturb either endosomal acidification [for example, lysosomotropic agents such as ammonium chloride and chloroquine (Canning and Fields 1983), or specific acidic protease inhibitors such as E-64 (Baer and Dermody 1997; Ebert et al. 2001)], can inhibit infection by intact virions. Accumulating evidence suggests that outer capsid protein σ3 must be proteolytically clipped, initially within the central HSR that is susceptible to a wide range of acidic, neutral, and basic proteases (Jané-Valbuena et al. 2002; Ebert et al. 2002; Mendez et al. 2003; Golden et al. 2004). Alternatively, the ISVP, which can be generated extracellularly by a variety of intestinal proteases (Bodkin et al. 1989; Bass et al. 1990), or in vitro, appears capable of directly penetrating the cell membrane (Fig. 3, step 3a) (Sturzenbecker et al. 1987; Lucia-Jandris et al. 1993; Tosteson et al. 1993). The acidification and protease inhibitors that block infection by intact virions do not block infection by ISVPs (Sturzenbecker et al. 1987; Baer and Dermody 1997; Chandran et al. 1999; Odegard et al. 2004; Nibert et al. 2005), making use of such inhibitors a convenient means for assessing outer capsid protein function. Cleavage, but not complete removal, of outer capsid protein σ3 appears to be a prerequisite for entry into the cell's cytosol (Chandran and Nibert 1998; Chandran et al. 2001; Nibert et al. 2005). Nibert's group described a method for preventing chymotrypsin-mediated digestion of T1L μ1C to δ and φ by including the detergent tetradecylsulfate during digestions (Chandran and Nibert 1998). This process has demonstrated that proteolytic processing of μ1C per se does not appear necessary for infectious entry (Chandran and Nibert 1998) and has allowed generation of a number of intermediate particles that have been used to delineate steps in reovirus uncoating. Two such particles, termed ISVP′ and ISVP*, proposed to lie between ISVPs and cores, have so far been described (Chandran et al. 2002, 2003). Compared to normal ISVPs, ISVP′ and ISVP* are characterized by possessing μ1 molecules that are more susceptible to protease digestion and in which more hydrophobic residues are exposed (Chandran et al. 2002, 2003; Odegard et al. 2004). The ISVP′, proposed to be an earlier intermediate, is defective in hemolysis, and was trapped at the μ1 → μ1N/μ1C cleavage step by introducing several mutations into the μ1 protein (A319E, P344L, and L359F) (Chandran et al. 2003). ISVP* has a greater propensity to lose σ1 and also has an activated transcriptase (Odegard et al. 2004). Final stages of membrane permeabilization and cell entry involve cleavage of μ1 to μ1N and μ1C and release of the myristoylated μ1N peptide from particles (Odegard et al. 2004). Upon entry into the cytosol, the remaining outer capsid proteins are removed, and the λ2 pentamers undergo a dramatic conformational change that opens the λ2 channels further (Dryden et al. 1993). Both

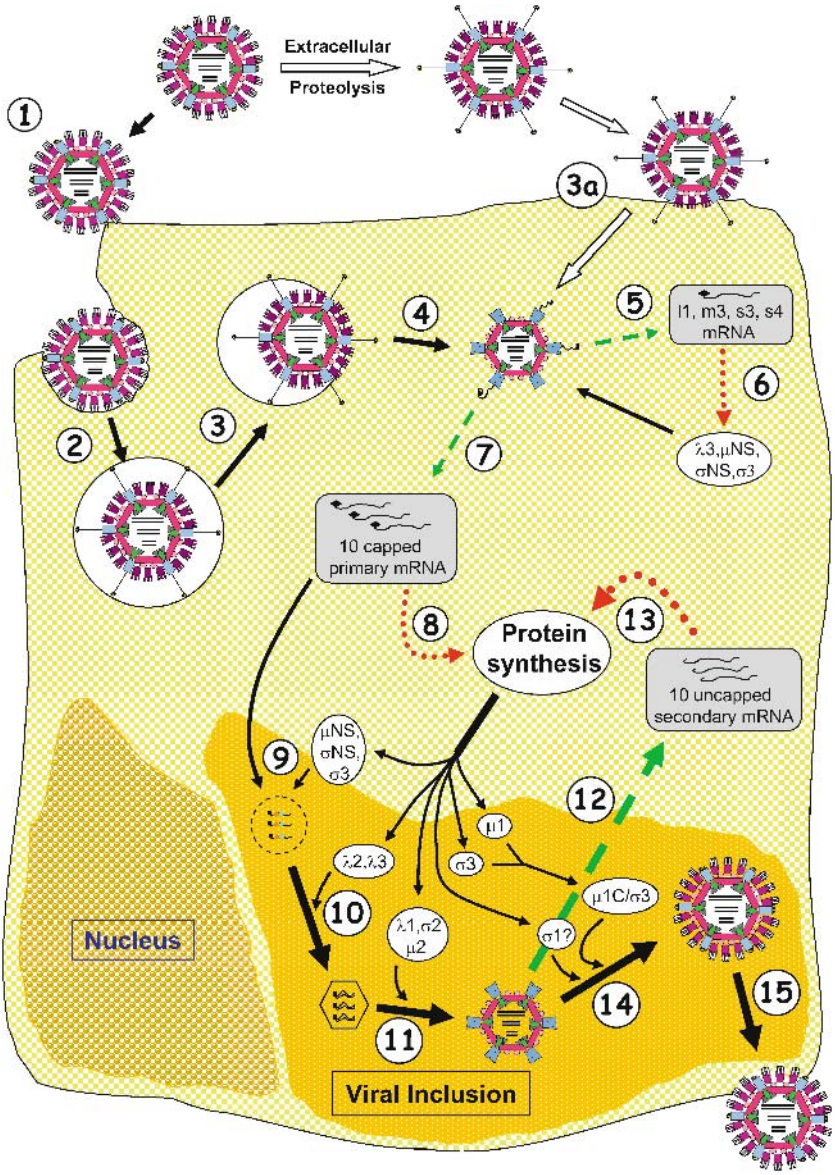
Extracellular
Proteolysis
1
2
3
3a
4
5
6
7
8
9
10
11
12
13
14
15
l1, m3, s3, s4
mRNA
λ3,μNS,
σNS,σ3
10 capped
primary mRNA
Protein
synthesis
10 uncapped
secondary mRNA
μNS,
σNS,
σ3
λ2,λ3
λ1,σ2
μ2
μ1
σ3
μ1C/σ3
σ1?
Nucleus
Viral Inclusion

Fig. 3 Diagrammatic representation of the reovirus replicative cycle. Details are provided in the text. The indicated steps are: (*1*) virus binding (*upper left*), (*2*) entry into endosomes where acid-mediated proteolysis occurs to remove outer capsid protein σ3, (*3*) membrane interaction to allow ISVP to escape endosome, (*4*) uncoating of ISVP to release transcriptionally active core particle, (*5*) initial pre-early capped transcription, (*6*) initial pre-early translation, (*7*) primary capped transcription, (*8*) primary translation, (*9*) assortment of mRNA segments into genome sets, probably mediated by σ3 and nonstructural proteins, (*10*) synthesis of negative RNA strands to generate progeny dsRNA (associated with accumulation of core proteins), (*11*) generation of transcriptase (replicase) complex, (*12*) secondary uncapped transcription, (*13*) secondary translation, (*14*) assembly of outer capsid, which halts transcription, and (*15*) virus release (*lower right*). *Dashed green arrows* indicate transcription events leading to production of mRNAs (indicated in *gray boxes*), *dotted red arrows* indicate translation events leading to production of proteins (indicated in *white ovals*), and *black arrows* indicate movement of proteins and viral complexes. *Arrow thicknesses* represent relative amounts of various components. An alternate entry mechanism for intermediate subviral particles (*ISVPs*), which may be generated in the intestinal lumen and that are capable of directly penetrating membranes, is shown with *white arrows* at the *top* and in *step 3a*. Recently proposed entry intermediates (known as ISVP′ and ISVP* (Chandran et al. 2002, 2003; Odegard et al. 2004) are suggested to be formed at *step 4*. Condensation of proteins and mRNAs into early aggregates (prior to detectable particle formation) is suggested by *dashed circle* at *step 9*, and further compositional and conformational alterations are implied by *hexagon* at *step 10*

alterations appear necessary for full activation of the viral transcriptase. The resulting core particle (Figs. 1C–E, 2A, 3, step 4) constitutes the final stage of uncoating, and such particles persist throughout the remainder of the viral replicative cycle (Silverstein et al. 1970; Chang and Zweerink 1971).

The released core particles serve as transcriptionally active RdRp machines that produce viral mRNA. Collectively, the λ2, λ3, and μ2 proteins manifest RdRp, helicase, RNA triphosphatase, methyltransferase, and guanylyltransferase activities (Table 1) to produce the viral mRNA, which is extruded through channels in the modified λ2 spikes. Early work suggested that initially only four (L1, M3, S3 and S4) of the ten dsRNA genes were transcribed to produce mRNA (Fig. 3, step 5) (Watanabe et al. 1968; Spandidos et al. 1976). The minus strands of the dsRNA serve as templates for conservative synthesis of these pre-early mRNA molecules. These four initial mRNA molecules (designated l1, m3, s3, and s4) are translated by host ribosomes to produce the λ3, μNS, σNS, and σ3 proteins, respectively. After these four proteins are initially produced, they act upon the core by unknown mechanisms to promote transcription of all ten genes (Fig. 3, step 7). These 10 early transcripts, like the (+) strands in the dsRNA parental genomes, contain methylated caps

and lack poly(A) tails. The cap structures are provided to nascent mRNAs by the λ2 proteins as the mRNAs are extruded through the λ2 spike turrets (Luongo et al. 2000, 2002; Luongo 2002). Viral transcripts are produced in quantities inversely proportional to transcript length. Viral early mRNAs are then translated to produce the full complement of viral proteins (Fig. 3, step 8). These proteins begin to coalesce and, along with the ten different mRNA molecules, are directed into non-membrane-containing inclusions in the cytoplasm by the σNS, μNS, and/or μ2 proteins (Broering et al. 2002, 2005) (Fig. 3, step 9). The ten different mRNA molecules are sorted by unknown mechanisms (a process called assortment) to ensure that nascent viral particles contain correct sets of genes. The assortment process probably uses nonstructural proteins σNS and μNS, both of which are translated in unusually large amounts and both of which bind single-stranded RNA (ssRNA) (Huismans and Joklik 1976; Gomatos et al. 1980, 1981; Stamatos and Gomatos 1982; Gillian and Nibert 1998). The σNS protein appears to perform its functions most efficiently as a multimer and binds nonspecifically most efficiently to ssRNA (Gillian et al. 2000). Outer capsid protein σ3 also participates in assortment. The ten mRNA molecules are then used as templates for progeny minus-strand synthesis (Fig. 3, step 10) (Ward et al. 1972; Ward and Shatkin 1972; Morgan and Zweerink 1975), a process most likely mediated by viral proteins. Immunoprecipitation studies have indicated that proteins λ2 and λ3 are added to these complexes at the same time mRNA is copied into dsRNA (Antczak and Joklik 1992). Once the mRNA is copied, the newly transcribed minus strand remains associated with it to generate progeny dsRNA. The plus-sense molecule is no longer available for translation. However, developing particles resemble cores that serve to transcribe additional mRNA, and so presumably also contain other core proteins (Fig. 3, step 11).

Progeny core-like particles (transcriptase complexes), like incoming uncoated cores, are capable of synthesizing viral mRNA (Fig. 3, step 12). These nascent particles (also called replicase particles) are responsible for the majority of transcription during the replicative cycle (Watanabe et al. 1967; Ito and Joklik 1972; Coombs 1996). Transcripts produced during this second wave of transcription are not capped. The switch in translation from cap-dependence to cap-independence remains poorly understood, but is currently believed to depend upon intracellular distribution of σ3, its capacity to interact with μ1C, and interactions with several cellular interferon-regulated gene products, including PKR and RNase-L (Schmechel et al. 1997; Smith et al. 2005). Assembly of progeny virions requires association of the correct numbers of eight different viral proteins with one copy of each of the ten progeny genes. In vitro recoating (transcapsidation) studies, as well as studies with assembly-defective, temperature-sensitive reovirus mutants, have shed some light on

pathways by which viral proteins may associate to generate the double capsid shell that will serve to protect the genome (discussed in more detail below in Sect. 7) (Fig. 3, steps 12–15). Assembly of the core capsid shell requires only major core proteins λ1 and σ2, as indicated by expression studies (Xu et al. 1993) and analyses of mutants defective in σ2 (Coombs et al. 1994). The λ2 proteins then associate with the core shell particles (Hazelton and Coombs 1999). However, it currently is not known whether λ2 proteins form pentamers before associating with the core shell or whether they associate as monomers and then pentamerize. Addition of σ1 may take place at about this same time because of its intimate association with the λ2 spikes in mature particles. The outer capsid proteins μ1 and σ3 associate with each other (Mabrouk and Lemay 1994; Shepard et al. 1996) to form heterohexamers ($(\mu1/\sigma3)_3$) (Dryden et al. 1993; Liemann et al. 2002). The μ1/σ3 association results in several conformational changes in both proteins (Shepard et al. 1995). These μ1/σ3 heterohexamers then associate with the nascent core particles to complete the double capsid (Fig. 2, step 14) (Morgan and Zweerink 1974; Shing and Coombs 1996; Chandran et al. 1999), a process that results in producing an intracellular infectious virion and in turning off the particle's transcriptase capability. Virus is released when infected cells lyse (Fig. 3, step 15).

4 Virus Assembly Considerations

Most viruses are aggregates of nucleic acid and protein, and many also contain cellularly derived lipids (some viruses, such as HIV and the papoviruses, also incorporate cellular proteins into their structure). Because viruses are macromolecular aggregates built from more than a single subunit, viruses have had to evolve processes to direct how individual building blocks may recognize each other, bind stably to each other, and form meta-stable structures, i.e., structures that are sufficiently stable to protect the genomic cargo during environmental passage, but sufficiently unstable to allow rapid uncoating once the virion enters a susceptible host cell.

Numerous methods have been used to study assembly of various viruses. These can be arbitrarily summarized as: direct observation, virion dissociation, virion re-association, use of assembly-defective mutants, and assembly from expressed components. The simplest method is to directly examine the process of virus morphogenesis within infected cells at various time points. Unfortunately, it usually is not possible to distinguish small virus-encoded complexes from nonviral complexes within stained thin-sections of infected cells. Furthermore, most normal virus infections are not synchronous, mak-

ing it difficult to precisely locate any given event along an assembly pathway. Although useful for delineating assembly of some plant viruses (see, for example, Butler 1999), the unusual stability of the reovirus particle precludes using virus dissociation and reassociation to analyze molecular forces that contribute to particle morphogenesis.

Genetic methods have been exploited to impose synchronicity on virus maturation. This strategy, which was used successfully to delineate assembly of coliphage T4 (see, for example, Black et al. 1994) was predicated upon the ability to generate and identify conditionally lethal T4 mutant viruses that had defects in each gene and that were arrested at various points along the morphogenetic pathway. Similar strategies have been exploited to delineate portions of the reovirus morphogenetic pathway (detailed below in Sect. 7).

With the advent of powerful molecular biologic approaches and capacity to express almost any protein, site-directed mutagenesis approaches are now being used to molecularly characterize the signals that promote or prevent virus assembly. Although it is still not possible to regenerate infectious reovirus particles completely from expressed components, it is possible to recoat reovirus subviral particles with expressed viral proteins to reconstitute intact virions (detailed below in Sect. 7.2). Thus, these strategies are being used to better understand molecular signals responsible for RNA–RNA, RNA–protein, and protein–protein interactions that lead to, or abrogate, reovirus morphogenesis (described in greater detail in Sects. 6 and 7).

5
Assembly of Reovirus Genome

Viruses that contain segmented genomes face additional challenges in assembly. There are two general strategies for such segmented genome viruses to successfully establish infection. Viruses such as alfalfa mosaic virus, which consist of four segments of ssRNA, package each of their segments in separate particles; the two largest segments are packaged in individual particles and the two smallest are packaged in another particle. Thus, all three particles must enter the same cell for a full infectious cycle to ensue. Another strategy, used by the *Orthomyxoviridae* (e.g., influenza virus), *Reoviridae*, and several other virus families, is to package a complete complement of all genome segments into individual particles. The packaging of at least one copy of each genome segment into an individual particle could occur by either of two general mechanisms. These are considered *random* or *specific*. The random model predicts, as the name implies, that there are no signals to direct particular gene segments into nascent virions; thus, progeny virions would

contain random numbers and random mixtures of gene segments (Bancroft and Parslow 2002). Mathematical modeling suggests that far more defective particles would be produced than infective particles because the chances of the correct set of all genes being placed into an individual particle are low. In the case of influenza A virus, which contains eight gene segments, such modeling suggests only 1 out of every 416 particles ($8!/8^8$) would be infectious. Even if individual influenza virions can contain more than the full complement of eight gene segments (Enami et al. 1991; Sekellick et al. 2000), such modeling suggests that only 2%–10% of virions would be infectious, a value in keeping with experimentally determined values (Lamb and Krug 2001). An alternate model, the specific model, predicts, as the name implies, that there are signals to direct particular gene segments into nascent virions (Fujii et al. 2003; McCown and Pekosz 2005); thus, the majority, or every progeny virion would contain the full complement of gene segments. In the case of reovirus, with ten genes, a random model would suggest that only 1 out of every 2,755 particles ($10!/10^{10}$) is infectious. Because the capsids are of a fixed size, it seems extremely unlikely that an individual particle could package more than the full complement of ten genes, although particle populations with 11 have been reported (Joklik 1983). Nevertheless, numerous investigators find particle-to-PFU ratios of viral preparations under 20:1, and, in some cases, the particle-to-PFU ratio has been reported to be 2:1 or less, for both MRV (Joklik 1998) and the related rotaviruses (Hundley et al. 1985). This strongly implies that assembly of the reovirus genome uses specific mechanisms.

The specific model implies that signals are present on individual genome segments that allow each of the virus's genomic segments to be recognized and recruited into a complex that will give rise to individual progeny virions. It is generally believed that these signals probably reside within each gene's NTR (Joklik 1998). However, signals may also be present within the ORF (Zou and Brown 1992), as also reported for influenza virus (Fujii et al. 2003; Watanabe et al. 2003) and rotavirus (Lymperopoulos et al. 2003). There is evidence that specific nucleotides or amino acids within the S4 gene (and/or σ3 protein) contain signals that direct assortment of reovirus gene segments (Roner et al. 1995). It had been assumed that genomic assortment would involve assembling appropriate sets of ssRNA rather than sets of dsRNA because ssRNA sequences are easier to read, whereas bases in dsRNA are occupied by complementary base-pairing and dsRNA is stiffer than ssRNA, making it more difficult to incorporate dsRNA segments into a nascent particle (reviewed in Joklik 1985; Joklik and Roner 1996), and this supposition has been supported by detailed studies that analyzed the genetic content of complexes immunoprecipitated by each of a variety of monoclonal antibodies (Antczak and Joklik 1992) (for detailed reviews, see Joklik and Roner 1995; Joklik

1998). An understanding of these signals, as well as success in generating a reverse genetics system (Roner et al. 1990) has allowed some manipulation of the reovirus genome (see for example Roner et al. 1997, 2004; Roner 1999; Roner and Joklik 2001). These important advances await confirmation and utilization for wider applications (discussed also below in Sect. 8).

6 Morphogenesis of Viral Inclusions

During the viral replicative cycle, viruses may induce the formation of phase-dense regions within the cell. These regions, generally observable by light microscopy, have been known for more than 100 years (Guarnieri 1893; Ewing 1905) and are called inclusions, factories, or viroplasm by various investigators. Electron microscopy and immuno-microscopic methods indicate these are localized regions within the cell cytoplasm or nucleus (depending upon virus) where virus proteins and nucleic acids coalesce during virion morphogenesis. Such structures have been observed in diverse systems, including cells infected with adenoviruses, alphaviruses, coxsackieviruses, herpesviruses, papillomaviruses, poxviruses, and reoviruses (reviewed in Rabin and Jenson 1967). It is generally believed that recruitment of viral components into such limited regions within the cell may make virus assembly more efficient by bringing various components into closer proximity to each other.

Such structures were initially identified within reovirus-infected cells by immunofluorescence microscopy and electron microscopy (Rhim et al. 1962; Dales 1965; Fields et al. 1971). Work with the reovirus temperature-sensitive mutant *tsE320*, which is defective in nonstructural protein σNS, showed that the mutant failed to generate inclusions at the nonpermissive temperature, that viral proteins that were produced were diffusely located within the cell, and that progeny virion production was severely impaired (Becker et al. 2001). These data strongly suggested that σNS plays an important role in inclusion formation. Other work, that has made use of strain-dependent phenotypic differences and reassortant mapping, as well as expression of individual proteins, has implicated minor core protein μ2 (Mbisa et al. 2000; Parker et al. 2002; Yin et al. 2004), as well as the other nonstructural protein μNS (Becker et al. 2003; Broering et al. 2002, 2004, 2005; Miller et al. 2003) as playing important roles in inclusion formation and morphology. Recent work has indicated that μNS plays a (or the) principal role in inclusion formation (Miller et al. 2003; Broering et al. 2004) and recent expression and mutagenesis work has determined important amino acid residues. The carboxyl-terminal 251 amino acids of the μNS protein, predicted to contain coiled-coil motifs,

is, by itself, capable of forming inclusion-like structures, removal of as few as eight amino acids from the μNS C-terminus abolishes inclusion formation, and His_{570} and $TCys_{572}$ are critically important residues (Broering et al. 2005).

7
Assembly of Reovirus Capsids

Most current understanding of reovirus capsid assembly and morphogenesis comes from analyses of assembly-defective temperature-sensitive mutants and by molecular expression of viral proteins and various site-directed mutants.

7.1
Studies Using Assembly-Defective Temperature-Sensitive Mutants

The success in using conditionally lethal virus mutants to elucidate coliphage T4 assembly (discussed above in Sect. 4) led several investigators to attempt similar strategies to delineate animal virus assembly. Mutant phage, that had premature termination codons in specific genes, could be grown in suppressor bacteria that complemented the phage defect (reviewed in Black et al. 1994). Unfortunately, there are few eukaryotic suppressor cell lines available to support similar eukaryotic virus studies. Thus, most animal virologists who apply conditionally lethal genetic strategies do so with temperature-sensitive (*ts*) mutants. *Ts* mutants have been used to examine a very wide range of virologic processes, including genomic integration, genomic replication, protein-folding pathways, viral pathogenesis, and virus morphogenesis and assembly (see, for example, Schwartzberg et al. 1993; Schildgen et al. 2005; Chiu et al. 2005).

Reovirus *ts* mutants were originally generated by chemical mutagenesis of wild-type reovirus stocks in two different laboratories (Ikegami and Gomatos 1968; Fields and Joklik 1969). Both groups treated stocks of reovirus serotype 3, strain Dearing (T3D) with various mutagens, including nitrous acid, nitrosoguanidine, proflavin, or 5-fluorouracil. The mutagen-treated (and nontreated) stocks then were diluted and plated at a low "permissive" temperature of 30–31°C. Potential *ts* clones were selected that showed impaired growth at higher "restrictive" temperatures, chosen as above 37°C. (For more detailed descriptions of *ts* mutant selections, see reviews by Ramig and Fields 1983; Coombs 1998b). The remainder of this section will focus on those reovirus *ts* mutants isolated by Fields and colleagues that have been used to understand reovirus morphogenesis; this includes members of temperature-sensitive groups A–E and G–I (Table 2).

Table 2 Characteristics of selected mammalian reovirus *ts* mutants

	Mutant			Nonpermissive characteristics[a]			
Group	Clone	Gene	Protein	EOP[b]	dsRNA	Protein	Phenotype
Wild-type T3 Dearing				0.2	+	+	Normal
A	*tsA201*	M2	μ1	0.009	+	+	Normal
	tsA279			0.0002	+	−	**Top component**[c]
		L2	λ2				**Spikeless cores**
B	*tsB35.2*	L2	λ2	0.00001	+	+	**Cores**
C	*tsC447*	S2	σ2	1×10^{-7}	−	−	**Empty outer shells**
D	*tsD357*	L1	λ3	0.00001	+	+	**Top component**[c]
E	*tsE320*	S3	σNS	0.002	−	−	No inclusions
G	*tsG453*	S4	σ3	1×10^{-7}	+	+	**Cores**
H	*tsH11.2*	M1	μ2	1×10^{-7}	−	−	No inclusions
I	*tsl138*	L3	λ1	0.0001	−	−	No inclusions

Bold indicates aberrant assembly structures
[a] At nonpermissive temperature of 39.5°C; (+) present, (−) absent
[b] EOP; (Titer at 39.5°C) / (Titer at 33.5°C)
[c] Top component: virion-like particles that lack genome

7.1.1 Temperature-Sensitive Group A

This is the largest group of reovirus mutants, containing almost 30 different clones. Initial electron microscopic observations of infected cells suggested that the prototype group A mutant (*tsA201*), subsequently mapped to the M2 gene (Mustoe et al. 1978), which encodes the major outer capsid protein μ1 (McCrae and Joklik 1978) as well as several other tested group A mutants (*tsA40* and *tsA270*), produced virus inclusions and intact particles indistinguishable from those produced by wild-type T3D under normal conditions (Fields et al. 1971). Subsequent studies indicated that *tsA201* synthesized normal amounts of protein (Fields et al. 1972) and RNA (Cross and Fields 1972) at the restrictive temperature (Table 2). Later work with another group A mutant (*tsA279*) showed that *tsA279* contained two *ts* lesions, one in the M2 gene and another in the L2 gene (Hazelton and Coombs 1995), which encodes core spike protein λ2 (McCrae and Joklik 1978). The defect in the *tsA279* M2 gene appeared responsible for temperature-sensitive defects in virus entry (Hazelton and Coombs 1995). The effects of the L2 gene defect will be discussed in the next section. In summary, to date, there have been no M2 *ts* mutants

identified that are defective in viral assembly. This is somewhat surprising, given that the M2 gene product, the μ1 protein, constitutes approximately half the total virion protein mass and the protein, in association with other major outer capsid protein σ3, must associate with nascent cores to generate progeny virions. It is likely that one, or more, of many other mutants within this group that have not yet been carefully examined will prove to have defects in morphogenesis. The importance of μ1 in particle morphogenesis has been demonstrated by expression studies (described more fully below in Sect. 7.2).

7.1.2 Temperature-Sensitive Group B

Mutations in group B (e.g., *tsB352*) were mapped to the λ2 protein (Mustoe et al. 1978). Virions contain 60 copies of this 145-kDa protein that forms the pentameric core spike turrets (White and Zweerink 1976) (Figs. 1C–E, 2A). There are six currently known *ts* mutants that have defective L2 genes, five of which were assigned to group B. Three of the five were originally isolated by Fields, one (*tsA279* ; see preceding section) belongs to group A, but also contains an L2 mutation (Hazelton and Coombs 1999), and the two newest members (*ts26/6* and *ts23.66*) were isolated as spontaneous mutants during analyses of reovirus *ts* revertants (Ahmed et al. 1980b; Coombs et al. 1994; Coombs 1996). The *ts23.66* clone appears to be a double mutant, with lesions in both the λ2 and λ3 (group D) proteins. Most clones have EOP values of approximately 10^{-3} or less at temperatures of 39°C or higher; thus, they represent "tight" lesions and are relatively easy to work with. Electron microscopic analyses, either of thin-sectioned cells infected with the three original group B mutants at the nonpermissive temperature (Fields et al. 1971) or of gradient purified particles recovered from infected cells (Morgan and Zweerink 1974) showed core-like particles. Thus, these group B mutants appear to have a defect in their λ2 proteins that prevents condensation of outer capsid proteins onto nascent cores. Additional studies of *tsB352*, the group B prototypic mutant, showed that it synthesized nearly normal amounts of protein (Fields et al. 1972) and RNA (Cross and Fields 1972) at the nonpermissive temperature. Studies with the L2 defect in the double mutant *tsA279* show different phenotypes. Because this clone contains two *ts* lesions, it was necessary to segregate the L2 lesion away from the dominant M2 lesion; this was accomplished by using selected *tsA279* × T1L reassortant clones that contained the *tsA279* L2 gene in combination with a T1L M2 gene. Examination of some of these reassortants indicated that clones with only the mutated *tsA279* L2 gene synthesized normal amounts of viral protein and RNA and assembled core capsid shells, but that neither

the mutant λ2 proteins nor outer capsid proteins were capable of condensing onto nascent cores (Hazelton and Coombs 1999; Hazelton and Coombs, unpublished data). Thus, the *tsA279* mutant λ2 protein appears to be defective in an earlier step of assembly, the attachment of λ2 to the core capsid. Temperature shift-down experiments indicated that defective λ2 (synthesized at restrictive temperature) would associate with core particles to generate infectious progeny at permissive temperatures (Hazelton and Coombs 1999). Thus, unlike core particles that have been made spikeless by dissociating cores (White and Zweerink 1976; Luongo et al. 2002), and which appear incapable of supporting λ2 re-association, spikeless core particles generated by *tsA279* may be useful substrates for studies to examine λ2 signals that promote its association with the core capsid shell. In summary, of the reovirus λ2 mutants characterized to date, many are assembly-defective and these defects are expressed at a minimum of two distinct steps in the assembly pathway (see Sect. 7.1.9 below).

7.1.3 Temperature-Sensitive Group C

A single group C mutant (*tsC447*) has been identified to date. This is the most temperature-sensitive of clones routinely used, having an EOP value of about 10^{-6} at 39°C and higher. The mutation was mapped to core protein σ2 (Ramig et al. 1978). Virions contain 150 copies of this 47-kDa protein that forms nodules on the core capsid shell (Figs. 1C–E, 2A). *TsC447* produces reduced amounts (approximately 5%) of ssRNA and protein (Fields et al. 1972; Cross and Fields 1972) and undetectable amounts (<0.1%) of progeny dsRNA (Cross

Fig. 4A–C Probable atomic locations of some known MRV and ARV mutations. **A** A portion of the MRV core asymmetric unit (PDB 1EJ6) is shown in diagram format (similar side view orientation and coloration as in Fig. 2D *middle*). The MRV *tsC447* σ2 Asn_{383} → Asp mutation is depicted by *red spheres* and the ARV *tsA12* σA Pro_{158} → Leu substitution is shown by *blue spheres*. **B** Same as **A**, but showing only σ proteins, and rotated by 90° to show top view. **C** A portion of the MRV $(\mu1/\sigma3)_3$ heterohexameric structure (PDB 1JMU) shown in diagram mode (similar to front *white* σ3 view in Fig. 2D right, but rotated approximately 60° clockwise around vertical axis to more clearly show locations of σ mutations and potential interacting μ residues). The *tsG453* mutations are indicated with *red spheres* and labeled. The probable location of the ARV *tsC37* σB mutation is indicated with *blue spheres*. The indicated μ1 residues Gln_{429} and Ala_{476} that lie very close to the *tsC37* and *tsG453* mutations are indicated with *gray spheres* and labeled. Images created with PyMol (DeLano 2004). *Larger arrows* indicate the residues into which labeled wild-type amino acids change in the respective mutants in either MRV σ2 or σ3, or ARV σA or σB

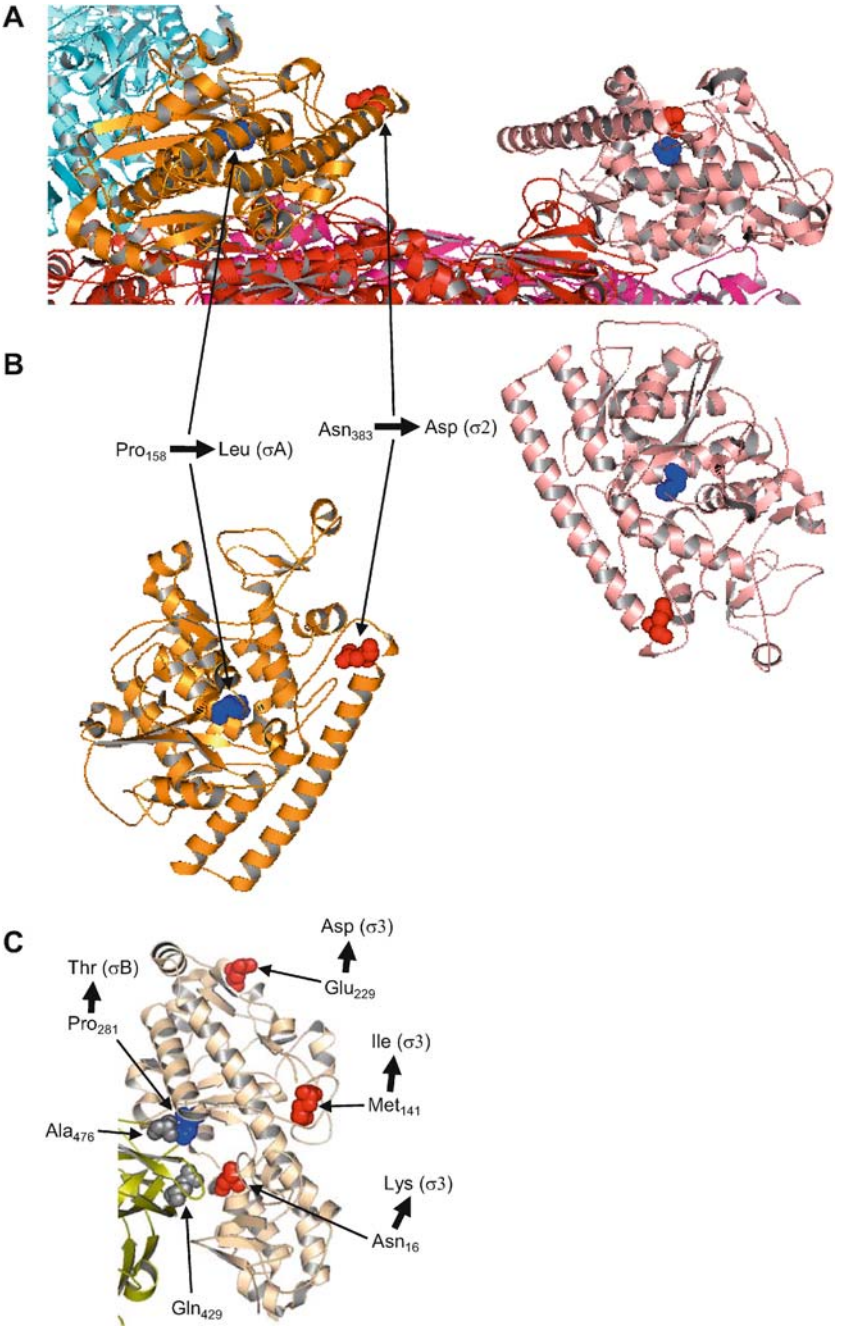
A
B
Pro158 → Leu (σA)
Asn383 → Asp (σ2)
C
Asp (σ3)
Thr (σB)
Glu229
Pro281
Ile (σ3)
Met141
Ala476
Lys (σ3)
Asn16
Gln429

and Fields 1972; Ito and Joklik 1972) at the nonpermissive temperature; thus, it is classified as an RNA^- mutant. However, the ability of mutant σ2 protein to bind RNA does not appear to be affected (Dermody et al. 1991). Protein σ2 is a major component of the core, and, along with the other major core capsid protein λ1, is required for core capsid assembly (Xu et al. 1993). The *tsC447* mutant appears incapable of generating a core shell but does assemble empty outer capsid structures at the nonpermissive temperature (Fields et al. 1971; Matsuhisa and Joklik 1974; Coombs et al. 1994), providing further evidence for the important role of this protein in core morphogenesis. The mutated *tsC447* σ2 protein contains three amino acid substitutions; $Ala_{188} \rightarrow$ Val, $Ala_{323} \rightarrow$ Val, and $Asn_{383} \rightarrow$ Asp (Wiener et al. 1989b). Analyses of *tsC447* revertants indicated that, in contrast to reversion occurring as a result of extragenic suppression, as happens for most reovirus reversion events (Ramig and Fields 1979; McPhillips and Ramig 1984; Ramig 1998), reversion of the *tsC447* lesion appeared to involve intragenic reversion (Coombs et al. 1994). These studies also indicated that $Asn_{383} \rightarrow$ Asp was solely responsible for the inability of mutant *tsC447* to assemble core particles at the nonpermissive temperature. The availability of high-resolution structures of many viral proteins (discussed above in Sect. 2) provides a molecular basis for understanding how the *tsC447* $Asn_{383} \rightarrow$ Asp alteration may prevent core formation. This alteration is located near the end of a long α-helix that spans residues $Thr_{350} \rightarrow Asn_{386}$ (Fig. 4A). The lesion's effects are not known, and although amino acid substitutions can have long-range effects upon a protein's tertiary structure (Creighton 1990), it is tempting to speculate that the $Asn_{383} \rightarrow$ Asp alteration may introduce a substantial change in the σ2 conformation, such that adjacent σ2 molecules cannot fit on the core capsid shell and clamp the λ1 capsid together. Comparative studies with homologous proteins from related orthoreoviruses may also shed light on how alterations in σ2 (or its σ-class core protein orthologs) affect virus morphogenesis. We recently generated ARV *ts* mutants (Patrick et al. 2001) for such studies and mapped one of these *ts* mutants (*tsA12*) to the homologous σA protein of avian orthoreovirus (Xu et al. 2004). The lesion in *tsA12* prevents attachment of outer capsid proteins to core structures (analogous to mammalian group B mutants), and this mutation involves a $Pro_{158} \rightarrow$ Leu substitution, which is predicted to reside in the middle of the σA protein, under the outer face of the protein (Xu et al. 2004) (Fig. 4A). This mutation might affect the outer surface (distal side) of the protein and prevent condensation of outer capsid proteins onto the core. Thus, *ts* lesions in available σ-class orthoreovirus core proteins can affect core morphogenesis (MRV *tsC447*) or outer capsid attachment (ARV *tsA12*).

7.1.4 Temperature-Sensitive Group D

The mutation in the prototype group D mutant (*tsD357*) was mapped to core protein λ3 (Ramig et al. 1978). Protein λ3 is the RNA-dependent RNA polymerase (Drayna and Fields 1982a; Morozov 1989; Starnes and Joklik 1993). Virions contain about 12 copies of this 142-kDa protein, with 1 copy located directly under each core vertex (Dryden et al. 1998). *TsD357* has an EOP value close to 10^{-3} at 39°C. Electron microscopy of restrictively infected cells revealed a heterogeneous mixture of empty particles (Fields et al. 1971). The mutant produces reduced amounts (approximately 10%) of ssRNA and protein (Cross and Fields 1972; Fields et al. 1972) and undetectable amounts (<0.1%) of progeny dsRNA (Cross and Fields 1972; Ito and Joklik 1972) at the nonpermissive temperature; thus, it is classified as an RNA^- mutant. Recent work with this mutant has not been reported, although preliminary studies suggest cores derived from *tsD357* are more heat stable than are cores derived from wild-type T3D (Mendez et al., unpublished data).

7.1.5 Temperature-Sensitive Group E

A single group E mutant (*tsE320*) has been identified to date. This is considered a "leaky" *ts* clone because its EOP value of about 0.2 at 39°C is indistinguishable from the EOP value of T3D at 39°C. The EOP value of this mutant can be reduced about 50-fold for each 0.5°C increase in nonpermissive temperature up to 40°C (Table 2) (Becker et al. 2001). The mutation in *tsE320* was mapped to nonstructural protein σNS (Ramig et al. 1978; Becker et al. 2001). Infected cells contain large amounts of this 41-kDa protein that may bind ssRNA (Huismans and Joklik 1976). *TsE320* produces reduced amounts (approximately 5%) of ssRNA and protein (Cross and Fields 1972; Fields et al. 1972), very low levels (approximately 1%) of progeny dsRNA (Cross and Fields 1972; Ito and Joklik 1972), and few, if any, viral inclusions (Cross and Fields 1972; Becker et al. 2001) at the restrictive temperature. Genetic and biochemical studies indicate that σNS helps form, and recruit other viral proteins to, viral inclusions (Becker et al. 2001, 2003; Miller et al. 2003); thus, the protein plays important roles in reovirus morphogenesis. The sequence of the mutated S3 gene was determined and the σNS protein contains a single amino acid substitution ($Met_{260} \rightarrow Thr$) (Wiener and Joklik 1987).

7.1.6 Temperature-Sensitive Group G

This is the second largest group of reovirus *ts* mutants. It is noteworthy that the two largest groups of mutants (group A, above, and this group) represent both major outer capsid proteins. The prototype group G mutant (*tsG453*) was initially identified as a group B mutant, but subsequently reclassified (Cross and Fields 1972). This is one of the most temperature-sensitive of known reovirus *ts* clones, with an EOP value less than 10^{-5} at temperatures of 39°C or greater. The *ts* lesion in this mutant was mapped to major outer capsid protein σ3 (Mustoe et al. 1978). Virions contain 600 copies of this 41-kDa protein. The protein plays numerous important roles (summarized above in Sect. 2.3), including its capacity to associate with μ1C during morphogenesis (Lee et al. 1981a; Shing and Coombs 1996; Liemann et al. 2002). *TsG453* synthesizes reduced amounts (approximately 20%) of protein (Fields et al. 1972; Danis et al. 1992; Shing and Coombs 1996) and RNA (Cross and Fields 1972) at the restrictive temperature. Paradoxically, the mutant σ3 molecule has a higher than normal affinity for dsRNA (Bergeron et al. 1998). Many electron microscopic analyses have shown that this mutant produces core-like particles, rather than ISVP-like particles, at the restrictive temperature (Fields et al. 1971; Morgan and Zweerink 1974; Danis et al. 1992). The apparently paradoxical observation that a mutation in σ3 caused the accumulation of core-like particles, rather than ISVP-like particles, was resolved by immunocoprecipitation experiments that indicated σ3–μ1 interactions are required for condensation of the outer capsid onto nascent cores and that restrictively grown mutant σ3 protein is misfolded in such a way that it cannot interact with μ1 to form these prerequisite complexes (Shing and Coombs 1996), a finding confirmed by various μ1 and σ3 expression studies (Chandran et al. 1999, 2001) (described in more detail below, Sect. 7.2). The sequence of the mutated *tsG453* σ3 protein has been determined and found to contain at least three alterations: $Asn_{16} \rightarrow$ Lys, $Met_{141} \rightarrow$ Ile, and $Glu_{229} \rightarrow$ Asp (Danis et al. 1992; Shing and Coombs 1996). These residues are scattered throughout the σ3 primary and tertiary structure, and each is predicted to reside at, or near, the σ3 surface (Fig. 4C). The identity of amino acids responsible for the *ts* phenotype have not yet been determined, but placement of these lesions into the known σ3 structure suggests $Asn_{16} \rightarrow$ Lys is most likely responsible for inability of mutated σ3 to interact with μ1 (Fig. 4C). Asn_{16} is the only altered σ3 residue that lies close to μ1 within the crystal structure, within very close proximity of μ1 Gln_{429}. Additional MRV group G mutants have been recovered from high-passage virus stocks (Ahmed et al. 1980a) and rescued during reversion analyses (Ahmed et al. 1980a; Coombs et al. 1994); however, little has been reported concerning

them. As indicated above (Sect. 7.1.3), we have initiated comparative analyses with ARV *ts* mutants. One of these new mutants (*tsC37*) was mapped to the homologous σB outer capsid protein (Xu et al. 2005). This mutant also makes core-like particles at restrictive temperature (Tran et al., unpublished data) and sequence determinations indicated *tsC37* contained a single amino acid substitution ($Pro_{281} \rightarrow$ Thr) (Xu et al. 2005). This mutation (if both ARV σB and μB are folded similarly to MRV σ3 and μ1, respectively) is predicted to lie within very close proximity to μB Ala_{476} (Fig. 4C). Thus, interestingly, both well-characterized σ-class outer capsid proteins from ARV and MRV appear to prevent σ-μ interactions and the mutants make core-like particles rather than ISVP-like particles, suggesting that the σ-class outer capsid protein must interact with the μ-class outer capsid protein before the μ-class outer capsid protein can attach to cores (discussed below in Sect. 7.1.9).

7.1.7
Temperature-Sensitive Group H

A number of reovirus mutant clones were recovered from high-passage stocks (Ahmed et al. 1980a) or during pseudorevertant rescue (Ramig and Fields 1979; Ahmed et al. 1980a; Coombs et al. 1994). These recovered clones were able to recombine (as determined by relative reassortment efficiencies) with all tested members of mutant recombination groups A–G, suggesting several of them belonged to new groups, subsequently designated H–J. Reassortant mapping of the original prototypic group H mutant (*tsH26/8*) indicated its defect resided in minor core protein μ2 (Ramig et al. 1983). Virions contain about 20 copies of this 83-kDa putative RdRp cofactor protein. Little additional work has been reported for the *tsH26/8* clone. While analyzing *tsC447* revertants (described above in Sect. 7.1.3) (Coombs et al. 1994), we isolated eight additional spontaneous mutants. These mutants represented T1L×*tsC447* reassortants, and studies of one of them (*tsH11.2*) indicated the clone's T1L-derived M1 gene contained a *ts* lesion (Coombs 1996). *TsH11.2* has an EOP value of about 10^{-4} at 39°C. When grown at nonpermissive temperature, the mutant fails to assemble identifiable particles, suggesting it is defective in morphogenesis. This mutant produces only about 0.1% the amount of dsRNA made at permissive temperature; thus it represents another RNA^- mutant. However, in contrast to RNA^- mutants in groups C–E, which also synthesize significantly reduced amounts of ssRNA at restrictive temperature, *tsH11.2* synthesizes normal levels of ssRNA at early time points. In addition, kinetic studies of viral protein synthesis show that protein synthesis from the primary RNA transcripts is normal under restrictive conditions; however, because of lack of progeny dsRNA, there are few secondary ssRNA transcripts, and thus

virtually no late protein synthesis (Coombs 1996). Sequence analysis of the mutated *tsH11.2* M1 gene showed two alterations; a $Met_{399} \rightarrow$ Thr and a $Pro_{414} \rightarrow$ His mutation in the encoded μ2 protein (Coombs 1996), both of which appear, by indirect analyses, to be responsible for expression of the *ts* phenotype (Zou et al., unpublished data). Additional work to better understand both *tsH26/8* and *tsH11.2* is clearly required, particularly in light of roles μ2 may play as an RdRp cofactor and in viral inclusion formation and morphology.

7.1.8 Temperature-Sensitive Group I

A single group I mutant (*tsI138*) has been described to date. This mutant was rescued from extragenically suppressed pseudorevertants (Ramig and Fields 1979) and was mapped to major core protein λ1 (Ramig et al. 1983). Virions contain 120 copies of this 142-kDa protein, which is the major component of the core capsid (Figs. 1C–E, 2A) and which is required for its assembly (Xu et al. 1993; Kim et al. 2002). The *tsI138* mutant has proven difficult to manipulate; although it has an EOP value of about 10^{-3} at 39°C, it generally grows to low titer, even at permissive temperature. The poor growth of this mutant also may explain the generally low reassortment values obtained when this clone is crossed with mutants in other groups (for examples, see Ahmed et al. 1980b; Coombs 1996). Although RNA and protein production under restrictive conditions have not yet been reported, preliminary experiments suggest *tsI138* may represent another RNA^- mutant (Hazelton and Coombs, unpublished data). Electron microscopic examination of restrictively infected cells does not reveal intact viral particles (Hazelton and Coombs, unpublished data; G. Lemay, personal communication). Additional work with this mutant is required.

7.1.9 Model for Reovirus Morphogenesis from Studying Temperature-Sensitive Mutants

As indicated earlier, conditionally lethal virus mutants were used to shed insight into assembly of bacteriophage T4 (Black et al. 1994), and similar strategies are being used by numerous animal virologists. Work with reovirus *ts* mutants, initiated more than 30 years ago, and continued during the past decade, has begun to shed light on the processes by which orthoreoviruses are assembled. When grown at nonpermissive temperature, numerous reovirus clones, mapped to several genome segments encoding various proteins, both structural and nonstructural, fail to produce identifiable viral inclusions (Fig. 5). This suggests that proteins λ1 (*tsI138*), μ2 (*tsH11.2*), and

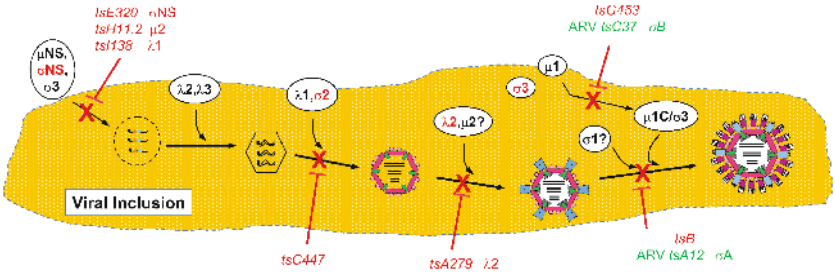

Fig. 5 Model of proposed reovirus assembly pathway, deduced from studies of *ts* mutants. Initial viral inclusion formation, mediated by viral nonstructural protein σNS, is blocked at nonpermissive temperature by mutations in *tsE320*. Similarly, other steps in assembly blocked by particular mutants, and their effected proteins, are shown in *red* and by ×. Some proteins have multiple effects; for example, lesions in the *tsA279* λ2 protein prevent attachment of λ2 onto spikeless core particles (*middle*), and λ2 mutations in all currently known group *B* mutants, as well as in the *tsG453* σ3 mutant, prevent attachment of outer capsid proteins onto core particles (*right*). Comparable avian reovirus *ts* mutants and their effects are shown in *green*

σNS (*tsE320*) are intimately involved in some of the earliest stages of reovirus morphogenesis. Indeed, other lines of evidence have implicated some of these, as well as additional proteins involved in viral inclusion formation. Reassortant mapping and site-directed mutagenesis studies have indicated the μ2 protein (Mbisa et al. 2000; Parker et al. 2002; Yin et al. 2004), μNS protein (Becker et al. 2003; Broering et al. 2002; Miller et al. 2003), as well as σNS protein (Becker et al. 2001, 2003; Miller et al. 2003) are involved in inclusion formation and morphology.

Reovirus normally produces large numbers of infectious particles from infected cells, a process that requires production of large amounts of precursor nucleic acids and proteins. Thus, defects in production of any of these precursors would be expected to dramatically impair production of infectious progeny. Numerous studies have suggested that reovirus protein production follows a cascade, with approximately 90% of total protein produced from secondary transcripts (Watanabe et al. 1968; Shatkin and Kozak 1983; Coombs 1996). Because transcription appears to take place in core, and core-like, subviral particles (Chang and Zweerink 1971; Shatkin and LaFiandra 1972; Silverstein et al. 1972; Drayna and Fields 1982a; Yeager et al. 1996; Yin et al. 1996; Luongo et al. 2002), defects in any core proteins, such as major structural ones (*tsC* - σ2, *tsI* - λ1) or enzymatic proteins (*tsD* - λ3, *tsH* - μ2) might seriously impair subsequent dsRNA synthesis, thereby accounting for the RNA^- phenotypes of each group of mutant. In addition, the σ3 protein appears to

play an important role in the switch from early cap-dependent translations to late cap-independent translation (Skup and Millward 1980; Lemieux et al. 1984, 1987), although the mechanism by which σ3 may induce this is under debate (Schmechel et al. 1997; Schiff 1998). Thus, such σ3-mediated roles could potentially explain why *tsG453* produces less ssRNA, dsRNA, and protein than do other RNA^+ mutants (Cross and Fields 1972; Shing and Coombs 1996).

Finally, analyses of mammalian reovirus *ts* mutants, combined with recent studies of newly generated avian reovirus assembly-defective *ts* mutants, have also made it possible to construct probable assembly pathways of the protein capsids by examining morphologies of particles produced by respective mutants at nonpermissive temperature (Fig. 5). For example, the observation that *tsC447* fails to assemble core particles at the nonpermissive temperature (Fields et al. 1971; Matsuhisa and Joklik 1974; Coombs et al. 1994) (Fig. 5, left) indicates the importance of σ2 in core capsid assembly, conclusions confirmed by various expression studies (Xu et al. 1993; Kim et al. 2002). It is generally assumed that most viruses constructed from multiple concentric protein capsids (the *Reoviridae* as well as the unrelated *Cystoviridae*) do so in an inside-out fashion; that is, the inner core capsid is believed to be built first and then outer capsid proteins are added (see Fig. 3; Poranen and Tuma 2004 and other reviews in this volume). Thus, assembly of the core capsid represents one of the earliest events in reovirus morphogenesis, although, as with other complex viruses, there are probably earlier steps that involve multimerization of a limited number of building blocks before observable structures (like the core) can be visualized. The ability of *tsC447* to assemble empty outer capsid structures at the restrictive temperature (Fields et al. 1971; Matsuhisa and Joklik 1974; Coombs et al. 1994) also indicates that prior assembly of the core is not necessarily required for condensation of the outer capsid and indicates that outer capsid proteins contain sufficient information for their own assembly. Association of core spike protein λ2 with these mutant outer capsids (Matsuhisa and Joklik 1974) also indicates extensive protein–protein interactions between core spikes and the outer capsid, as deduced from cryoelectron microscopic reconstructions (Dryden et al. 1993). Mutations in core spike protein λ2 appear to be responsible for the inability of most group B mutants to assemble past a core particle (Fields et al. 1971; Morgan and Zweerink 1974), supporting the conclusion of the importance of core spike–outer-capsid protein interactions. In addition, other mutations in λ2 (e.g., the *tsA279* L2 mutation) prevent attachment of the λ2 spike onto the core capsid shell (Hazelton and Coombs 1999). Finally, mutations in outer capsid protein σ3 appear to prevent association of this protein with the other outer capsid protein μ1 (Fig. 5, upper right), supporting the assumption that a σ3/μ1 association is a prerequisite for outer capsid condensation (Shing and Coombs

1996). This hypothesis is further supported by expression studies (Chandran et al. 1999; 2001) (and see next section) and by recent comparative analyses of ARV *ts* mutants (see Sect. 7.1.6). In conclusion, numerous mutants exist which affect multiple steps in the replicative and morphogenetic pathways, and continued study of them, in combination with molecular approaches (see next section) is hoped to shed further light on reovirus morphogenesis.

7.2 Recoating of Reovirus Subviral Particles

The reovirus core is a remarkable structure. It contains the viral RdRp, as well as other enzymes associated with guanylyltransferase, methyltransferase, and mRNA capping activities, and cores that have been disrupted lose RdRp activity. Likewise, when expressed alone, the RdRp molecule λ3 does not appear capable of faithfully transcribing reovirus dsRNA into mRNA. Thus, stably introducing selected mutations into the reovirus genome has been a challenge. A reverse genetics system has been developed for reovirus (Roner et al. 1990, 1995; Roner 1999) and has been used to construct a double-*ts* mutant virus (Roner et al. 1997) as well as incorporate the CAT marker into the virus (Roner and Joklik 2001). Unfortunately, this system is somewhat cumbersome; success requires co-transfection of a large number of components; ten dsRNA genomic segments, mRNA transcripts from each genomic segment, protein products from each transcript, plus a helper virus (see also Sect. 5).

An alternate strategy to molecularly examine reovirus protein structure–function was developed by Nibert's and Schiff's groups. This transcapsidation method involves recoating subviral particles with one or more expressed outer capsid proteins. For example, ISVPs may be recoated with expressed σ3 protein (Jané-Valbuena et al. 1999) and cores may be recoated with expressed μ1 and σ3 proteins (Chandran et al. 1999). Cores have also been recoated with μ1, σ1, and σ3 to regenerate fully infectious particles indistinguishable from intact native virions (Chandran et al. 2001). The basic method is to generate the ISVP or core substrate that will be recoated. This is accomplished by in vitro proteolysis of virions. The subviral particles may then be purified by equilibrium density ultracentrifugation in CsCl gradients (although the purification step has been omitted in some studies). Subviral particles are then mixed with recombinant baculovirus-infected cell extracts (usually at ratios of 10^{12} particles per 6–15×10^6 cells). Mixtures are then incubated at 37°C for 2 h and recoated particles separated from unreacted particles and proteins by density ultracentrifugation (Chandran et al. 1999, 2001). This powerful method is now being used to incorporate exogenous epitopes, such as hexahistidine tags, into virions (Rouault and Lemay 2003) and to insert selected mutations into any

or all outer-capsid proteins to determine their effects on early stages of virus replication. Similar studies are being conducted with the related rotaviruses (e.g., Chen and Ramig 1993a, 1993b; Charpilienne et al. 2001, 2002).

For example, Jané-Valbuena et al. (2002) used the recoating strategy to examine important amino acid residues in σ3 that are proteolytically processed during virus entry. Initial results indicated that the first cleavage site (the HSR), as well as the kinetics of σ3 digestion, differed between T1L and T3D. This difference was mapped by reassortant genetics to the S4 gene segment that encodes σ3. The T1L and T3D σ3 proteins differ in 11 amino acid positions, five of which are located within the C-terminal 100 amino acids, previously shown to contain signals that influenced endoproteinase lys-C digestion (Jané-Valbuena et al. 1999). Jané-Valbuena et al. (2002) recoated T1L ISVPs with each of various T1L/T3D chimera σ3 proteins. SDS-PAGE and densitometric analyses of peptides released from each recoated particle after brief chymotrypsin digestion indicated that the composition of the C-terminal 35 amino acids determined whether T1L-like digestion was favored. This region contains three amino acid differences; Ser_{344}, Thr_{347}, and Asp_{353} in T1L, as opposed to Pro_{344}, Ile_{347}, and Asn_{353} in T3D. When each of these substitutions, as well as some double substitutions, were expressed in reciprocal backgrounds, digestion of resulting recoated particles indicated that all three amino acid polymorphisms were primarily, but not exclusively, responsible for serotypic differences in σ3 cleavage rate and location (Jané-Valbuena et al. 2002). It is noteworthy that this region of σ3, located more than 100 amino acids away from the HSR in primary sequence, and which is not cleaved by proteases until late in σ3 digestion (Mendez et al. 2003), appears to be located approximately midway between the T1L and T3D HSR in the three-dimensional structure (Jané-Valbuena et al. 2002).

In another study, Odegard et al. (2003) used the recoating strategy to determine importance of the μ1 Cys_{679} residue in μ1 inter-trimeric disulfide binding. Preparation of virion samples for SDS-PAGE in the absence of reducing agents led to loss of the 7- kDa μ1C and 76-kDa μ1 bands and simultaneous appearance of an approximately 155-kDa band (Odegard et al. 2003). The 155-kDa band was shown to represent a μ1 and/or μ1C disulfide bonded multimer (most probably dimer) by subsequent reduction and re-electrophoresis, by α-chymotrypsin peptide mapping, and by ^{3}H-myristate labeling. Nonreducing gel analyses of ISVPs showed that the larger μ1 cleavage product μ1δ (as well as μ1C cleavage product δ) still migrated as monomers, but the smaller φ peptide migrated as a multimer, suggesting that Cys_{679} (the only Cys residue in the φ portion) was responsible for μ1 dimer formation (Odegard et al. 2003). The μ1 dimers appear to form late in the reovirus replication cycle as the cells die, most probably within the outer capsid P2 and P3 solvent channels (see

Fig. 1C). Core particles recoated with recombinant baculovirus-expressed μ1 that contained a serine instead of this cysteine (C679S), plus wt σ3, could be recovered in cesium chloride density gradients at a density corresponding to that of intact virions, indicating that disulfide-bonded μ1, which potentially increases particle stability in a manner analogous to *Polyomaviridae* VP1 "peptide arms" (Liddington et al. 1991), is not critical for reovirus outer capsid assembly (Odegard et al. 2003). C679S recoated particles also had particle-to-PFU ratios similar to those of native virions, further supporting the notion that disulphide bonds do not play a major role in particle infectivity (Odegard et al. 2003). It is noteworthy that the comparable μB proteins of ARV, which lack the Cys_{679} region (Noad et al. 2006), appear to lose infectivity during storage more rapidly than do MRV, suggesting that the μ1 Cys_{679} disulfide bonds do contribute somewhat to long-term survival, if no other intramolecular disulfide bonds are found in μB.

A study by Rouault and Lemay (2003) used this transcapsidation method to insert exogenous epitope tags into the σ3 protein to examine the capacity of modified σ3 to recoat particles and to explore the possibility of recoated reovirions serving as substrate for gene therapy strategies. Several σ3 constructs, that inserted a hexahistidine (6-His) tag at the N-terminus, the C-terminus, as well as a variety of locations throughout the σ3 sequence predicted to be exposed or in unstructured regions, were generated by PCR-mediated mutagenesis and transfected into COS-7 cells. Immunoblotting of transfected cells showed that all constructs were expressed; however, with the exception of the N-terminal insertion that accumulated to a relatively high level, other expressed proteins were relatively unstable and accumulated to lower levels. When ISVPs were mixed with extracts of COS-7 cells that had been transfected with the N-terminally-tagged 6-His construct, particles could be recovered that had incorporated the epitope-modified σ3 molecule into the outer capsid (Rouault and Lemay 2003). This indicates that outer capsid assembly can tolerate addition of supplementary material (including the 6-His, an influenza-derived HA dodecapeptide, or a 6-His-7Gly chimera), at least at the N-terminus (Rouault and Lemay 2003).

Another study by Odegard et al. (2004) used the recoating strategy to determine the importance of μ1N/μ1C cleavage in virus entry and assembly. As indicated earlier (Sect. 2.3), all mu-class major outer capsid proteins of mammalian and avian orthoreoviruses (and homologous proteins of aquareoviruses) sequenced to date contain an Asp_{42}–Pro_{43} dipeptide, and, where examined, this is the site of μ1 → μ1N/μ1C (or homologous protein) cleavage. The presence of Asn_{42} appears most critical as revealed by mutagenesis studies (Tillotson and Shatkin 1992). Cores were recoated with wt μ1 and σ3, or with a μ1 mutant that contained an Asn_{42} → Ala substitution ($\mu1^{N42A}$)

in combination with wt σ3; some experiments, to examine infectivity, also included adding wt σ1 during recoating (Odegard et al. 2004). Virion-like particles were recovered after density ultracentrifugation after cores were recoated with σ3 in the presence of either wt μ1 or $\mu1^{N42A}$. These virion-like particles contained normal amounts of σ3. By contrast, SDS-PAGE analyses showed that cores recoated with wt μ1 and σ3 contained normal amounts of μ1 and μ1C (approximately 5% and 95%, respectively), while cores recoated with $\mu1^{N42A}$ and wild-type σ3 contained mostly full-length μ1 and no detectable μ1C. This finding indicates that the μ1 → μ1N/μ1C cleavage is not necessary for outer-capsid assembly (Odegard et al. 2004). Proper outer-capsid assembly was confirmed (within resolution limits) by comparative cryoelectron microscopic analyses of particles recoated with both forms of μ1, as well as by protease-mediated ISVP generation, although the form of δ present (whether primarily μ1δ or δ) was consistent with the type of μ1 (whether $\mu1^{N42A}$ or wt) used to recoat cores. However, particles recoated with cleavage-defective $\mu1^{N42A}$ were much less infectious than cores recoated with wt μ1, σ1, and σ3, indicating that the μ1 → μ1N/μ1C cleavage is critical for infectivity (Odegard et al. 2004). Immunofluorescence microscopy showed $\mu1^{N42A}$-wt σ3-recoated cores could attach to, but not induce viral protein synthesis within CV1 and L929 cells, while flow cytometry and hemagglutination assays indicated wt μ1- and $\mu1^{N42A}$-recoated particles attached with the same efficiency. The $\mu1^{N42A}$-σ3-recoated cores were incapable of membrane permeabilization, as measured by hemolysis assays, α-sarcin-based transport assays, and rescue by membrane-permeabilizing genome-deficient particles, but were competent for a variety of ISVP* functions, including increased μ1 protease sensitivity, increased hydrophobicity, σ1 release, and transcriptase activation (Odegard et al. 2004).

It is noteworthy that, so far, it has not been possible to re-coat reovirus cores with only expressed μ1 to generate ISVP-like particles. This further supports the *ts* mutant studies described above (Sects. 7.1.6 and 7.1.9) that conclude that μ1 and σ3 must first associate with each other before the μ1/σ3 complex can coalesce onto cores (see also Fig. 5).

In summary, the newly developed recoating strategy provides a powerful means to explore molecular signals in outer-capsid proteins that play important roles in virus entry and virus morphogenesis. Such studies have, to date, indicated that intramolecular disulfide bond formation between μ1 molecules in adjacent $(\mu1/\sigma3)_3$ heterohexamers, which form late during MRV morphogenesis, as well as σ3-mediated μ1 → μ1N/μ1C cleavage, are not strictly required for particle assembly. These studies also suggest that some exogenous epitope tags can be added into some outer-capsid proteins without affecting assembly, and such studies provide supporting evidence that μ1 and

σ3 associate with each other before condensing onto core-like particles during assembly. It will prove interesting to exploit this system, as well as *ts* mutant systems, to continue to molecularly delineate reovirus morphogenetic signals in the future.

8 Future Directions

No rigorous and reproducible reverse genetics system currently exists for any members of the *Reoviridae*. Continued refinement of the infectious RNA system (Roner et al. 1990), combined with better understanding minimal requirements for inserting foreign or modified gene sequences into the virus (Zou and Brown 1992; Roner et al. 1995; 2004) should lead to a useable system that allows in vitro replication, transcription, assembly, and genetically stable passage, as exists for the dsRNA *Cystoviridae* (Poranen et al. 2001; Kainov et al. 2003; Poranen and Tuma 2004) and as is under development for the genus *Rotavirus* of the *Reoviridae* (e.g., Patton and Stacy-Phipps 1986; Patton et al. 2004; Jayaram et al. 2004).

Cell lines that constitutively express each of various reovirus proteins have been constructed. These cells specifically complement the *ts* mutants that are defective in the expressed protein when mutant-infected expressing cells are grown at the nonpermissive temperature. For example, Zou and Brown (1996) constructed μ2-expressing L929 cell lines that specifically complemented growth of *tsH11.2* (defective in μ2) at nonpermissive temperatures, but did not complement growth of other *ts* mutants with defects in other proteins (e.g., *tsC447*–σ2 protein). Likewise, Becker et al. (2001) constructed σNS-expressing cell lines that selectively complemented growth of the *tsE320* mutant at restrictive temperatures. Availability of such cell lines serves several important functions. In addition to examining effects of specific proteins outside the context of infection and other proteins, these cells can be used to rapidly screen for mutants defective in the protein expressed by the particular cell line. This could serve as a convenient means to rapidly map lesions in unknown mutants. In the case of reovirus *ts* mutants, such genetic characterization has been accomplished by the relatively rapid, but error-prone, recombination assay (analogous to classic complementation assays), or by the gold standard reassortant mapping method, which can be lengthy and tedious (reviewed in Ramig and Fields 1983; Coombs 1998b). Thus, development of additional cell lines that could complement each available *ts* mutant would provide an additional mapping tool, and would also shed light on the roles of the other reovirus proteins in various replicative stages, including morphogenesis.

Continued development and exploitation of the recoating strategy would provide additional information about molecular signals that direct each protein's functions. Unfortunately, it currently is not possible to assemble intact infectious reovirions from component parts (as has been done with the *Cystoviridae* that contain three segments of dsRNA as their genome [Poranen et al. 2001; Kainov et al. 2003]). The recoating strategy allows addition of any chosen mutation into only outer-capsid proteins μ1, σ1, and σ3. It is not yet possible to use this strategy to examine molecular signals in λ2 or other core proteins. It also is not currently feasible to use baculovirus-expressed proteins to examine reovirus *ts* mutations because recombinant baculovirus-infected insect cells must be grown at temperatures under 30°C and most mutants' phenotypes are only expressed at temperatures above 37°C. The strategy could be modified by generating *ts* mutant proteins at temperatures above 39°C. This might be accomplished by expressing the relevant mutated protein either in bacteria, yeast, or mammalian cells (see, for example, Rouault and Lemay 2003), or possibly by directly translating mutant proteins from expression plasmids in in vitro translation systems, and then attempting to recoat subviral particles with the resultant proteins.

Finally, ongoing sequence (Duncan 1999; Attoui et al. 2002; Noad et al. 2006) and structural (Nason et al. 2000; Zhang et al. 2005) analyses of other members of the *Orthoreovirus* genus, as well as of other closely related *Reoviridae* (such as aquareoviruses), when compared to similar analyses of MRV, are expected to shed further insight into molecular signals that contribute to each stage in reovirus replication. When combined with each of the other strategies outlined above, the next few years should prove an exciting time for delineating, in greater detail, aspects of reovirus morphogenesis.

Acknowledgements Research in my laboratory described in this review has been supported by awards from the Manitoba Health Research Council, the Dr. Paul H.T. Thorlakson Foundation Fund, the National Sciences and Engineering Research Council of Canada, and the Canadian Institutes of Health Research. I thank members of my research group for critical reviews of this manuscript and Dr. Max Nibert for formative discussions and for sharing avian and mammalian reovirus structural data prior to publication.

References

Ahmed R, Chakraborty PR, Fields BN (1980a) Genetic variation during lytic reovirus infection: high-passage stocks of wild-type reovirus contain temperature-sensitive mutants. J Virol 34:285–287

Ahmed R, Chakraborty PR, Graham AF, Ramig RF, Fields BN (1980b) Genetic variation during persistent reovirus infection: presence of extragenically suppressed temperature-sensitive lesions in wild-type virus isolated from persistently infected L cells. J Virol 34:383–389

Antczak JB, Joklik WK (1992) Reovirus genome segment assortment into progeny genomes studied by the use of monoclonal antibodies directed against reovirus proteins. Virology 187:760–776

Attoui H, Biagini P, Stirling J, Mertens PPC, Cantaloube JF, Meyer A, de Micco P, de Lamballerie X (2001) Sequence characterization of Ndelle virus genome segments 1, 5, 7, 8, and 10: evidence for reassignment to the genus Orthoreovirus, family Reoviridae. Biochem Biophys Res Commun 287:583–588

Attoui H, Fang Q, Jaafar FM, Cantaloube JF, Biagini P, de Micco P, deLamballerie X (2002) Common evolutionary origin of aquareoviruses and orthoreoviruses revealed by genome characterization of golden shiner reovirus, grass carp reovirus, striped bass reovirus and golden ide reovirus (genus Aquareovirus, family Reoviridae). J Gen Virol 83:1941–1951

Baer GS, Dermody TS (1997) Mutations in reovirus outer-capsid protein sigma3 selected during persistent infections of L cells confer resistance to protease inhibitor E64. J Virol 71:4921–4928

Bancroft CT, Parslow TG (2002) Evidence for segment-nonspecific packaging of the influenza A virus genome. J Virol 76:7133–7139

Bartlett JA, Joklik WK (1988) The sequence of the reovirus serotype 3 L3 genome segment which encodes the major core protein lambda 1. Virology 167:31–37

Bartlett NM, Gillies SC, Bullivant S, Bellamy AR (1974) Electron microscopy study of reovirus reaction cores. J Virol 14:315–326

Barton ES, Forrest JC, Connolly JL, Chappell JD, Liu Y, Schnell FJ, Nusrat A, Parkos CA, Dermody TS (2001) Junction adhesion molecule is a receptor for reovirus. Cell 104:441–451

Bass DM, Bodkin D, Dambrauskas R, Trier JS, Fields BN, Wolf JL (1990) Intraluminal proteolytic activation plays an important role in replication of type 1 reovirus in the intestines of neonatal mice. J Virol 64:1830–1833

Beattie E, Denzler KL, Tartaglia J, Perkus ME, Paoletti E, Jacobs BL (1995) Reversal of the interferon-sensitive phenotype of a vaccinia virus lacking E3L by expression of the reovirus S4 gene. J Virol 69:499–505

Becker MM, Goral MI, Hazelton PR, Baer GS, Rodgers SE, Brown EG, Coombs KM, Dermody TS (2001) Reovirus sigmaNS protein is required for nucleation of viral assembly complexes and formation of viral inclusions. J Virol 75:1459–1475

Becker MM, Peters TR, Dermody TS (2003) Reovirus sigma NS and mu NS proteins form cytoplasmic inclusion structures in the absence of viral infection. J Virol 77:5948–5963

Bergeron J, Mabrouk T, Garzon S, Lemay G (1998) Characterization of the thermosensitive ts453 reovirus mutant: increased dsRNA binding of sigma 3 protein correlates with interferon resistance. Virology 246:199–210

Bisaillon M, Lemay G (1997a) Characterization of the reovirus lambda1 protein RNA 5′-triphosphatase activity. J Biol Chem 272:29954–29957

Bisaillon M, Lemay G (1997b) Molecular dissection of the reovirus lambda1 protein nucleic acids binding site. Virus Res 51:231–237

Bisaillon M, Bergeron J, Lemay G (1997) Characterization of the nucleoside triphosphate phosphohydrolase and helicase activities of the reovirus lambda1 protein. J Biol Chem 272:18298–18303

Black LW, Showe MK, Steven AC (1994) Morphogenesis of the T4 head. In: Karam JD, Drake JW, Kreuzer KN, Mosig G, Hall D, Eiserling FA, Black LW, Kutter E, Spîcer E, Carlson K, Miller ES (eds) Molecular biology of bacteriophage T4. American Society for Microbiology, Washington, DC, pp 218–258

Bodkin DK, Nibert ML, Fields BN (1989) Proteolytic digestion of reovirus in the intestinal lumens of neonatal mice. J Virol 63:4676–4681

Breun LA, Broering TJ, McCutcheon AM, Harrison SJ, Luongo CL, Nibert ML (2001) Mammalian reovirus L2 gene and lambda2 core spike protein sequences and whole-genome comparisons of reoviruses type 1 Lang, type 2 Jones, and type 3 Dearing. Virology 287:333–348

Broering TJ, Parker JS, Joyce PL, Kim J, Nibert ML (2002) Mammalian reovirus nonstructural protein μNS forms large inclusions and colocalizes with reovirus microtubule-associated protein μ2 in transfected cells. J Virol 76:8285–8297

Broering TJ, Kim J, Miller CL, Piggott CDS, Dinoso JB, Nibert ML, Parker JSL (2004) Reovirus nonstructural protein mu NS recruits viral core surface proteins and entering core particles to factory-like inclusions. J Virol 78:1882–1892

Broering TJ, Arnold MM, Miller CL, Hurt JA, Joyce PL, Nibert ML (2005) Carboxyl-proximal regions of reovirus nonstructural protein mu NS necessary and sufficient for forming factory-like inclusions. J Virol 79:6194–6206

Butler PJ (1999) Self-assembly of tobacco mosaic virus: the role of an intermediate aggregate in generating both specificity and speed. Phil Trans R Soc Lond B Biol Sci 354:537–550

Canning WM, Fields BN (1983) Ammonium chloride prevents lytic growth of reovirus and helps to establish persistent infection in mouse L cells. Science 219:987–988

Chandran K, Nibert ML (1998) Protease cleavage of reovirus capsid protein mu1/mu1C is blocked by alkyl sulfate detergents, yielding a new type of infectious subvirion particle. J Virol 72:467–475

Chandran K, Walker SB, Chen Y, Contreras CM, Schiff LA, Baker TS, Nibert ML (1999) In vitro recoating of reovirus cores with baculovirus-expressed outer-capsid proteins mu1 and sigma3. J Virol 73:3941–3950

Chandran K, Zhang X, Olson NH, Walker SB, Chappell JD, Dermody TS, Baker TS, Nibert ML (2001) Complete in vitro assembly of the reovirus outer capsid produces highly infectious particles suitable for genetic studies of the receptor-binding protein. J Virol 75:5335–5342

Chandran K, Farsetta DL, Nibert ML (2002) Strategy for nonenveloped virus entry: a hydrophobic conformer of the reovirus membrane penetration protein mu 1 mediates membrane disruption. J Virol 76:9920–9933

Chandran K, Parker JSL, Ehrlich M, Kirchhausen T, Nibert ML (2003) The delta region of outer-capsid protein mu 1 undergoes conformational change and release from reovirus particles during cell entry. J Virol 77:13361–13375

Chang CT, Zweerink HJ (1971) Fate of parental reovirus in infected cell. Virology 46:544–555

Charpilienne A, Nejmeddine M, Berios M, Parez N, Neumann E, Hewat E, Trugnan G, Cohen J (2001) Individual rotavirus-like particles containing 120 molecules of fluorescent protein are visible in living cells. J Biol Chem 276:29361–29367

Charpilienne A, Lepault J, Rey F, Cohen J (2002) Identification of rotavirus VP6 residues located at the interface with VP2 that are essential for capsid assembly and transcriptase activity. J Virol 76:7822–7831

Chen D, Ramig RF (1993a) Rescue of infectivity by in vitro transcapsidation of rotavirus single-shelled particles. Virology 192:422–429

Chen D, Ramig RF (1993b) Rescue of infectivity by sequential in vitro transcapsidation of rotavirus core particles with inner capsid and outer capsid proteins. Virology 192:743–751

Chappell JD, Prota AE, Dermody TS, Stehle T (2002) Crystal structure of reovirus attachment protein sigma 1 reveals evolutionary relationship to adenovirus fiber. EMBO J 21:1–11

Chiu WL, Szajner P, Moss B, Chang W (2005) Effects of a temperature sensitivity mutation in the J1R protein component of a complex required for vaccinia virus assembly. J Virol 79:8046–8056

Cleveland DR, Zarbl H, Millward S (1986) Reovirus guanylyltransferase is L2 gene product lambda 2. J Virol 60:307–311

Coombs KM (1996) Identification and characterization of a double-stranded RNA^- reovirus temperature-sensitive mutant defective in minor core protein mu2. J Virol 70:4237–4245

Coombs KM (1998a) Stoichiometry of reovirus structural proteins in virus, ISVP, and core particles. Virology 243:218–228

Coombs KM (1998b) Temperature-sensitive mutants of reovirus. Curr Top Microbiol Immunol 233:69–107

Coombs KM, Mak SC, Petrycky-Cox LD (1994) Studies of the major reovirus core protein sigma 2: reversion of the assembly-defective mutant tsC447 is an intragenic process and involves back mutation of Asp-383 to Asn. J Virol 68:177–186

Creighton TE (1990) Protein folding. Biochem J 270:1–16

Cross RK, Fields BN (1972) Temperature-sensitive mutants of reovirus type 3: studies on the synthesis of viral RNA. Virology 50:799–809

Dales S (1965) Replication of animal viruses as studied by electron microscopy. Am J Med 38:699–715

Danis C, Garzon S, Lemay G (1992) Further characterization of the ts453 mutant of mammalian orthoreovirus serotype 3 and nucleotide sequence of the mutated S4 gene. Virology 190:494–498

DeLano WL (2004) The PyMOL molecular graphics system. (http://www.pymol.org)

Denzler KL, Jacobs BL (1994) Site-directed mutagenic analysis of reovirus sigma 3 protein binding to dsRNA. Virology 204:190–199

Dermody TS, Nibert ML, Bassel-Duby R, Fields BN (1990) Sequence diversity in S1 genes and S1 translation products of 11 serotype 3 reovirus strains. J Virol 64:4842–4850

Dermody TS, Schiff LA, Nibert ML, Coombs KM, Fields BN (1991) The S2 gene nucleotide sequences of prototype strains of the three reovirus serotypes: characterization of reovirus core protein sigma 2. J Virol 65:5721–5731

Drayna D, Fields BN (1982a) Activation and characterization of the reovirus transcriptase: genetic analysis. J Virol 41:110–118
Drayna D, Fields BN (1982b) Biochemical studies on the mechanism of chemical and physical inactivation of reovirus. J Gen Virol 63:161–170
Drayna D, Fields BN (1982c) Genetic studies on the mechanism of chemical and physical inactivation of reovirus. J Gen Virol 63:149–159
Dryden KA, Wang G, Yeager M, Nibert ML, Coombs KM, Furlong DB, Fields BN, Baker TS (1993) Early steps in reovirus infection are associated with dramatic changes in supramolecular structure and protein conformation: analysis of virions and subviral particles by cryoelectron microscopy and image reconstruction. J Cell Biol 122:1023–1041
Dryden KA, Farsetta DL, Wang G, Keegan JM, Fields BN, Baker TS, Nibert ML (1998) Internal structures containing transcriptase-related proteins in top component particles of mammalian orthoreovirus. Virology 245:33–46
Duncan R (1999) Extensive sequence divergence and phylogenetic relationships between the fusogenic and nonfusogenic orthoreoviruses: a species proposal. Virology 260:316–328
Ebert DH, Wetzel JD, Brumbaugh DE, Chance SR, Stobie LE, Baer GS, Dermody TS (2001) Adaptation of reovirus to growth in the presence of protease inhibitor E64 segregates with a mutation in the carboxy terminus of viral outer-capsid protein sigma3. J Virol 75:3197–3206
Ebert DH, Deussing J, Peters C, Dermody TS (2002) Cathepsin L and cathepsin B mediate reovirus disassembly in murine fibroblast cells. J Biol Chem 277:24609–24617
Enami M, Sharma G, Benham C, Palese P (1991) An influenza virus containing 9 different RNA segments. Virology 185:291–298
Estes MK (2001) Rotaviruses and their replication. In: Knipe DM, Howley M, Griffen DE et al (eds) Fields virology. Lippincott Williams & Wilkins, Philadelphia, pp 1747–1785
Ewing J (1905) The structure of vaccine bodies in isolated cells. J Med Res 13:233–251
Fausnaugh J, Shatkin AJ (1990) Active site localization in a viral mRNA capping enzyme. J Biol Chem 265:7669–7672
Fields BN, Joklik WK (1969) Isolation and preliminary genetic and biochemical characterization of temperature-sensitive mutants of reovirus. Virology 37:335–342
Fields BN, Raine CS, Baum SG (1971) Temperature-sensitive mutants of reovirus type 3: defects in viral maturation as studied by immunofluorescence and electron microscopy. Virology 43:569–578
Fields BN, Laskov R, Scharff MD (1972) Temperature-sensitive mutants of reovirus type 3: studies on the synthesis of viral peptides. Virology 50:209–215
Fraser RD, Furlong DB, Trus BL, Nibert ML, Fields BN, Steven AC (1990) Molecular structure of the cell-attachment protein of reovirus: correlation of computer-processed electron micrographs with sequence-based predictions. J Virol 64:2990–3000
Fujii Y, Goto H, Watanabe T, Yoshida T, Kawaoka T (2003) Selective incorporation of influenza virus RNA segments into virions. Proc Natl Acad Sci U S A 100:2002–2007

Furuichi Y, Morgan M, Muthukrishnan S, Shatkin AJ (1975) Reovirus messenger RNA contains a methylated, blocked 5′-terminal structure: m-7G(5′)ppp(5′)G-MpCp-. Proc Natl Acad Sci U S A 72:362–366

Giantini M, Shatkin AJ (1989) Stimulation of chloramphenicol acetyltransferase mRNA translation by reovirus capsid polypeptide sigma 3 in cotransfected COS cells. J Virol 63:2415–2421

Giantini M, Seliger LS, Furuichi Y, Shatkin AJ (1984) Reovirus type 3 genome segment S4: nucleotide sequence of the gene encoding a major virion surface protein. J Virology 52:984–987

Gillian AL, Nibert ML (1998) Amino terminus of reovirus nonstructural protein sigma NS is important for ssRNA binding and nucleoprotein complex formation. Virology 240:1–11

Gillian AL, Schmechel SC, Livny J, Schiff LA, Nibert ML (2000) Reovirus protein sigmaNS binds in multiple copies to single-stranded RNA and shares properties with single-stranded DNA binding proteins. J Virol 74:5939–5948

Golden JW, Bahe JA, Lucas WT, Nibert ML, Schiff LA (2004) Cathepsin S supports acid-independent infection by some reoviruses. J Biol Chem 279:8547–8557

Gomatos PJ, Stamatos NM, Sarkar NH (1980) Small reovirus-specific particle with polycytidylate-dependent RNA polymerase activity. J Virol 36:556–565

Gomatos PJ, Prakash O, Stamatos NM (1981) Small reovirus particle composed solely of sigma NS with specificity for binding different nucleic acids. J Virol 39:115–124

Guarnieri G (1893) Recherches sur la pathologie et étiologie de l'infection vaccinique et varioleuse. Arch Ital Biol 19:195–209

Haller BL, Barkon ML, Vogler GP, Virgin HW (1995) Genetic mapping of reovirus virulence and organ tropism in severe combined immunodeficient mice: organ-specific virulence genes. J Virol 69:357–364

Harrison SJ, Farsetta DL, Kim J, Noble S, Broering TJ, Nibert ML (1999) Mammalian reovirus L3 gene sequences and evidence for a distinct amino-terminal region of the lambda1 protein. Virology 258:54–64

Hazelton PR, Coombs KM (1995) The reovirus mutant tsA279 has temperature-sensitive lesions in the M2 and L2 genes: the M2 gene is associated with decreased viral protein production and blockade in transmembrane transport. Virology 207:46–58

Hazelton PR, Coombs KM (1999) The reovirus mutant tsA279 L2 gene is associated with generation of a spikeless core particle: implications for capsid assembly. J Virol 73:2298–2308

Huismans H, Joklik WK (1976) Reovirus-coded polypeptides in infected cells: isolation of two native monomeric polypeptides with affinity for single-stranded and double-stranded RNA, respectively. Virology 70:411–424

Hundley F, Biryahwaho B, Gow M, Desselberger U (1985) Genome rearrangements of bovine rotavirus after serial passage at high multiplicity of infection. Virology 143:88–103

Ikegami N, Gomatos PJ (1968) Temperature-sensitive conditional-lethal mutants of reovirus 3. I. Isolation and characterization. Virology 36:447–458

Imani F, Jacobs BL (1988) Inhibitory activity for the interferon-induced protein kinase is associated with the reovirus serotype 1 sigma 3 protein. Proc Natl Acad Sci U S A 85:7887–7891

Ito Y, Joklik WK (1972) Temperature-sensitive mutants of reovirus. I. Patterns of gene expression by mutants of groups C, D, and E. Virology 50:189–201
Jané-Valbuena J, Nibert ML, Spencer SM, Walker SB, Baker TS, Chen Y, Centonze VE, Schiff LA (1999) Reovirus virion-like particles obtained by recoating infectious subvirion particles with baculovirus-expressed sigma3 protein: an approach for analyzing sigma3 functions during virus entry. J Virol 73:2963–2973
Jané-Valbuena J, Breun LA, Schiff LA, Nibert ML (2002) Sites and determinants of early cleavages in the proteolytic processing pathway of reovirus surface protein sigma 3. J Virol 76:5184–5197
Jayaram H, Estes MK, Prasad BVV (2004) Emerging themes in rotavirus cell entry, genome organization, transcription and replication. Virus Res 101:67–81
Jayasuriya AK, Nibert ML, Fields BN (1988) Complete nucleotide sequence of the M2 gene segment of reovirus type 3 Dearing and analysis of its protein product mu 1. Virology 163:591–602
Joklik WK (1983) The reoviridae. Plenum Press, New York
Joklik WK (1985) Recent progress in reovirus research. Annu Rev Genet 19:537–575
Joklik WK (1998) Assembly of the reovirus genome. Curr Top Microbiol Immunol 233:57–68
Joklik WK, Roner MR (1995) What reassorts when reovirus genome segments reassort? J Biol Chem 270:4181–4184
Joklik WK, Roner MR (1996) Molecular recognition in the assembly of the segmented reovirus genome. Prog Nucleic Acids Res Mol Biol 53:249–281
Kainov DE, Butcher SJ, Bamford DH, Tuma R (2003) Conserved intermediates on the assembly pathway of double-stranded RNA bacteriophages. J Mol Biol 328:791–804
Kapikian AZ, Hoshino Y, Chanock RM (2001) Rotaviruses. In: Knipe DM, Howley M, Griffen DE et al (eds) Fields virology. Lippincott Williams & Wilkins, Philadelphia, pp 1787–1833
Kedl R, Schmechel S, Schiff L (1995) Comparative sequence analysis of the reovirus S4 genes from 13 serotype 1 and serotype 3 field isolates. J Virol 69:552–559
Kim J, Zhang X, Centonze VE, Bowman VD, Noble S, Baker TS, Nibert ML (2002) The hydrophilic amino-terminal arm of reovirus core shell protein lambda1 is dispensable for particle assembly. J Virol 76:12211–12222
Kim J, Tao Y, Reinisch KM, Harrison SC, Nibert ML (2004) Orthoreovirus and aquareovirus core proteins: conserved enzymatic surfaces, but not protein–protein interfaces. Virus Res 101:15–28
Koonin EV, Gorbalenya AE, Chumakov KM (1989) Tentative identification of RNA-dependent RNA polymerases of dsRNA viruses and their relationship to positive strand RNA viral polymerases. FEBS Lett 252:42–46
Lamb RA, Krug RM (2001) Orthomyxoviridae: the viruses and their replication. In: Knipe DM, Howley M, Griffen DE et al (eds) Fields virology. Lippincott Williams & Wilkins, Philadelphia, pp 1487–1531
Larson SM, Antczak JB, Joklik WK (1994) Reovirus exists in the form of 13 particle species that differ in their content of protein sigma 1. Virology 201:303–311
Lee PW, Hayes EC, Joklik WK (1981a) Characterization of anti-reovirus immunoglobulins secreted by cloned hybridoma cell lines. Virology 108:134–146

Lee PW, Hayes EC, Joklik WK (1981b) Protein sigma 1 is the reovirus cell attachment protein. Virology 108:156–163

Lemay G, Danis C (1994) Reovirus lambda 1 protein: affinity for double-stranded nucleic acids by a small amino-terminal region of the protein independent from the zinc finger motif. J Gen Virol 75:3261–3266

Lemieux R, Zarbl H, Millward S (1984) mRNA discrimination in extracts from uninfected and reovirus-infected L-cells. J Virol 51:215–222

Lemieux R, Lemay G, Millward S (1987) The viral protein sigma 3 participates in translation of late viral mRNA in reovirus-infected L cells. J Virol 61:2472–2479

Liddington RC, Yan Y, Moulai J, Sahli R, Benjamin TL, Harrison SC (1991) Structure of simian virus-40 at 3.8 Å resolution. Nature 354:278–284

Liemann S, Chandran K, Baker TS, Nibert ML, Harrison SC (2002) Structure of the reovirus membrane-penetration protein, mu1, in a complex with is protector protein, Sigma3. Cell 108:283–295

Lucia-Jandris P, Hooper JW, Fields BN (1993) Reovirus M2 gene is associated with chromium release from mouse L cells. J Virol 67:5339–5345

Luftig RB, Kilham SS, Hay AJ, Zweerink HJ, Joklik WK (1972) An ultrastructural study of virions and cores of reovirus type 3. Virology 48:170–181

Luongo CL (2002) Mutational analysis of a mammalian reovirus mRNA capping enzyme. Biochem Biophys Res Commun 291:932–938

Luongo CL, Contreras CM, Farsetta DL, Nibert ML (1998) Binding site for S-adenosyl-L-methionine in a central region of mammalian reovirus lambda2 protein. Evidence for activities in mRNA cap methylation. J Biol Chem 273:23773–23780

Luongo CL, Reinisch KM, Harrison SC, Nibert ML (2000) Identification of the guanylyltransferase region and active site in reovirus mRNA capping protein lambda2. J Biol Chem 275:2804–2810

Luongo CL, Zhang X, Walker SB, Chen Y, Broering TJ, Farsetta DL, Bowman VD, Baker TS, Nibert ML (2002) Loss of activities for mRNA synthesis accompanies loss of lambda2 spikes from reovirus cores: an effect of lambda2 on lambda1 shell structure. Virology 296:24–38

Lymperopoulos K, Wirblich C, Brierley I, Roy P (2003) Sequence specificity in the interaction of Bluetongue virus non-structural protein 2 (NS2) with viral RNA. J Biol Chem 278:31722–31730

Mabrouk T, Lemay G (1994) Mutations in a CCHC zinc-binding motif of the reovirus sigma 3 protein decrease its intracellular stability. J Virol 68:5287–5290

Mabrouk T, Danis C, Lemay G (1995) Two basic motifs of reovirus sigma 3 protein are involved in double-stranded RNA binding. Biochem Cell Biol 73:137–145

Matoba Y, Colucci WS, Fields BN, Smith TW (1993) The reovirus M1 gene determines the relative capacity of growth of reovirus in cultured bovine aortic endothelial cells. J Clin Invest 92:2883–2888

Matsuhisa T, Joklik WK (1974) Temperature-sensitive mutants of reovirus. V. Studies on the nature of the temperature-sensitive lesion of the group C mutant ts447. Virology 60:380–389

Mbisa JL, Becker MM, Zou S, Dermody TS, Brown EG (2000) Reovirus mu2 protein determines strain-specific differences in the rate of viral inclusion formation in L929 cells. Virology 272:16–26

McCown MF, Pekosz A (2005) The influenza A virus M2 cytoplasmic tail is required for infectious virus production and efficient genome packaging. J Virol 79:3595–3605
McCrae MA, Joklik WK (1978) The nature of the polypeptide encoded by each of the 10 double-stranded RNA segments of reovirus type 3. Virology 89:578–593
McPhillips TH, Ramig RF (1984) Extragenic suppression of temperature-sensitive phenotype in reovirus: mapping suppressor mutations. Virology 135:428–439
Mendez II, She Y-M, Ens W, Coombs KM (2003) Digestion pattern of reovirus outer capsid protein sigma3 determined by mass spectrometry. Virology 311:289–304
Mertens PPC, Attoui H, Duncan R, Dermody TS (2005) Reoviridae. In: Fauquet CM, Mayo MA, Maniloff J et al (eds) Virus taxonomy. Eighth report of the International Committee on Taxonomy of Viruses Elsevier/Academic Press, London, pp 447–454
Metcalf P, Cyrklaff M, Adrian M (1991) The three-dimensional structure of reovirus obtained by cryo-electron microscopy. EMBO J 10:3129–3136
Middleton JK, Severson TF, Chandran K, Gillian AL, Yin J, Nibert ML (2002) Thermostability of reovirus disassembly intermediates (ISVPs) correlates with genetic, biochemical, and thermodynamic properties of major surface protein mu1. J Virol 76:1051–1061
Miller CL, Broering TJ, Parker JS, Arnold MM, Nibert ML (2003) Reovirus sigma NS protein localizes to inclusions through an association requiring the mu NS amino terminus. J Virol 77:4566–4576
Miller CL, Parker JSL, Dinoso JB, Piggott CDS, Perron MJ, Nibert ML (2004) Increased ubiquitination and other covariant phenotypes attributed to a strain- and temperature-dependent defect of reovirus core protein mu 2. J Virol 78:10291–10302
Moody MD, Joklik WK (1989) The function of reovirus proteins during the reovirus multiplication cycle: analysis using monoreassortants. Virology 173:437–446
Morgan EM, Zweerink HJ (1974) Reovirus morphogenesis. Corelike particles in cells infected at 39 degrees with wild-type reovirus and temperature-sensitive mutants of groups B and G. Virology 59:556–565
Morgan EM, Zweerink HJ (1975) Characterization of transcriptase and replicase particles isolated from reovirus-infected cells. Virology 68:455–466
Morozov SY (1989) A possible relationship of reovirus putative RNA polymerase to polymerases of positive-strand RNA viruses. Nucleic Acids Res 17:5394
Mustoe TA, Ramig RF, Sharpe AH, Fields BN (1978) A genetic map of reovirus. III. Assignment of the double-stranded RNA-positive mutant groups A, B, and G to genome segments. Virology 85:545–556
Nason EL, Samal SK, Prasad BVV(2000) Trypsin-induced structural transformation in aquareovirus. J Virol 74:6546–6555
Nibert ML, Schiff LA (2001) Reoviruses and their replication. In: Knipe DM, Howley M, Griffen DE et al (eds) Fields virology. Lippincott Williams & Wilkins, Philadelphia, pp 1679–1728
Nibert ML, Schiff LA, Fields BN (1991) Mammalian reoviruses contain a myristoylated structural protein. J Virol 65:1960–1967
Nibert ML, Odegard AL, Agosto MA, Chandran K, Schiff LA (2005) Putative autocleavage of reovirus mu1 protein in concert with outer-capsid disassembly and activation for membrane permeabilization. J Mol Biol 345:461–474

Noad L, Shou J, Coombs KM, Duncan R (2005) Sequences of avian reovirus M1, M2, and M3 genes and predicted structure/function of the encoded μ proteins. Virus Res Nov 14 [epub ahead of print]

Noble S, Nibert ML (1997a) Characterization of an ATPase activity in reovirus cores and its genetic association with core-shell protein lambda1. J Virol 71:2182–2191

Noble S, Nibert ML (1997b) Core protein mu2 is a second determinant of nucleoside triphosphatase activities by reovirus cores. J Virol 71:7728–7735

Odegard AL, Chandran K, Liemann S, Harrison SC, Nibert ML (2003) Disulfide bonding among mu1 trimers in mammalian reovirus outer capsid: a late and reversible step in virion morphogenesis. J Virol 77:5389–5400

Odegard AL, Chandran K, Zhang X, Parker JSL, Baker TS, Nibert ML (2004) Putative autocleavage of outer capsid protein mu 1, allowing release of myristoylated peptide mu 1N during particle uncoating, is critical for cell entry by reovirus. J Virol 78:8732–8745

Offit PA (1994) Rotaviruses: immunological determinants of protection against infection and disease. Adv Virus Res 44:161–202

Olland AM, Jane-Valbuena J, Schiff LA, Nibert ML, Harrison SC (2001) Structure of the reovirus outer capsid and dsRNA-binding protein σ3 at 1.8 Å resolution. EMBO J 20:979–989

Parker JSL, Broering TJ, Kim J, Higgins DE, Nibert ML (2002) Reovirus core protein mu 2 determines the filamentous morphology of viral inclusion bodies by interacting with and stabilizing microtubules. J Virol 76:4483–4496

Patrick M, Duncan R, Coombs KM (2001) Generation and genetic characterization of avian reovirus temperature-sensitive mutants. Virology 284:113–122

Patton JT, Stacy-Phipps S (1986) Electrophoretic separation of the plus and minus strands of rotavirus SA11 double-stranded RNAs. J Virol Methods 13:185–190

Patton JT, Carpi RVD, Spencer E (2004) Replication and transcription of the rotavirus genome. Curr Pharma Design 10:3769–3777

Poranen MM, Tuma R (2004) Self-assembly of double-stranded RNA bacteriophages. Virus Res 101:93–100

Poranen MM, Paatero AO, Tuma R, Bamford DH (2001) Self-assembly of a viral molecular machine from purified protein and RNA constituents. Mol Cell 7:845–854

Qiu T, Luongo CL (2003) Identification of two histidines necessary for reovirus mRNA guanylyltransferase activity. Virology 316:313–324

Rabin ER, Jenson AB (1967) Electron microscopic studies of animal viruses with emphasis on in vivo infections. Prog Med Virol 9:392–450

Ramig RF (1998) Suppression and reversion of mutant phenotype in reovirus. Curr Top Microbiol Immunol 233:109–135

Ramig RF, Fields BN (1979) Revertants of temperature-sensitive mutants of reovirus: evidence for frequent extragenic suppression. Virology 92:155–167

Ramig RF, Fields BN (1983) Genetics of reovirus. In: Jolik WK (ed) The Reoviridae. Plenum, New York, pp 197–228

Ramig RF, Mustoe TA, Sharpe AH, Fields BN (1978) A genetic map of reovirus. II. Assignment of the double-stranded RNA-negative mutant groups C, D, and E to genome segments. Virology 85:531–534

Ramig RF, Ahmed R, Fields BN (1983) A genetic map of reovirus: assignment of the newly defined mutant groups H, I, and J to genome segments. Virology 125:299–313

Reinisch KM, Nibert ML, Harrison SC (2000) Structure of the reovirus core at 3.6 Å resolution. Nature 404:960–967

Rhim JS, Jordan LE, Mayor HD (1962) Cytochemical, fluorescent-antibody and electron microscopic studies on the growth of reovirus (Echo 10) in tissue culture. Virology 17:342–355

Rodgers SE, Connolly JL, Chappell JD, Dermody TS (1998) Reovirus growth in cell culture does not require the full complement of viral proteins: identification of a σ1s-null mutant. J Virol 72:8597–8604

Roner MR (1999) Rescue systems for dsRNA viruses of higher organisms. Adv Virus Res 53:355–367

Roner MR, Joklik WK (2001) Reovirus reverse genetics: Incorporation of the CAT gene into the reovirus genome. Proc Natl Acad Sci U S A 98:8036–8041

Roner MR, Sutphin LA, Joklik WK (1990) Reovirus RNA is infectious. Virology 179:845–852

Roner MR, Lin PN, Nepluev I, Kong LJ, Joklik WK (1995) Identification of signals required for the insertion of heterologous genome segments into the reovirus genome. Proc Natl Acad Sci U S A 92:12362–12366

Roner MR, Neplioueev I, Sherry B, Joklik WK (1997) Construction and characterization of a reovirus double temperature-sensitive mutant. Proc Natl Acad Sci U S A 94:6826–6830

Roner MR, Bassett K, Roehr, J (2004) Identification of the 5′ sequences required for incorporation of an engineered ssRNA into the reovirus genome. Virology 329:348–360

Rouault E, Lemay G (2003) Incorporation of epitope-tagged viral sigma 3 proteins to reovirus virions. Can J Microbiol 49:407–417

Roy P (2001) Orbiviruses. In: Knipe DM, Howley M, Griffen DE et al (eds) Fields virology. Lippincott Williams & Wilkins, Philadelphia, pp 1835–1869

Schiff LA (1998) Reovirus capsid proteins sigma 3 and mu 1: interactions that influence viral entry, assembly, and translational control. Curr Top Microbiol Immunol 233:167–183

Schiff LA, Nibert ML, Co MS, Brown EG, Fields BN (1988) Distinct binding sites for zinc and double-stranded RNA in the reovirus outer capsid protein sigma 3. Mol Cell Biol 8:273–283

Schildgen O, Graper S, Blumel J, Matz B (2005) Genome replication and progeny virion production of herpes simplex virus type 1 mutants with temperature-sensitive lesions in the origin-binding protein. J Virol 79:7273–7278

Schmechel S, Chute M, Skinner P, Anderson R, Schiff L (1997) Preferential translation of reovirus mRNA by a sigma3-dependent mechanism. Virology 232:62–73

Schwartzberg PL, Roth MJ, Tanese N, Goff SP (1993) Analysis of a temperature-sensitive mutation affecting the integration protein of Moloney murine leukemia virus. Virology 192:673–678

Sekellick MJ, Carra SA, Bowman A, Hopkins DA, Marcus PI (2000) Transient resistance of influenza virus to interferon action attributed to random multiple packaging and activity of NS genes. J Interferon Cytokine Res 20:963–970

Sharpe AH, Fields BN (1981) Reovirus inhibition of cellular DNA synthesis: role of the S1 gene. J Virol 38:389–392
Sharpe AH, Fields BN (1982) Reovirus inhibition of cellular RNA and protein synthesis: role of the S4 gene. Virology 122:381–391
Shatkin AJ (1974) Methylated messenger RNA synthesis in vitro by purified reovirus. Proc Natl Acad Sci U S A 71:3204–3207
Shatkin AJ, Kozak M (1983) Biochemical aspects of reovirus transcription and translation. In: Jolik WK (ed) The Reoviridae. Plenum, New York, pp 79–106
Shatkin AJ, LaFiandra AJ (1972) Transcription by infectious subviral particles of reovirus. J Virol 10:698–706
Shepard DA, Ehnstrom JG, Schiff LA (1995) Association of reovirus outer capsid proteins sigma 3 and mu 1 causes a conformational change that renders sigma 3 protease sensitive. J Virol 69:8180–8184
Shepard DA, Ehnstrom JG, Skinner PJ, Schiff LA (1996) Mutations in the zinc-binding motif of the reovirus capsid protein delta 3 eliminate its ability to associate with capsid protein mu 1. J Virol 70:2065–2068
Sherry B, Fields BN (1989) The reovirus M1 gene, encoding a viral core protein, is associated with the myocarditic phenotype of a reovirus variant. J Virol 63:4850–4856
Shing M, Coombs KM (1996) Assembly of the reovirus outer capsid requires mu 1/sigma 3 interactions which are prevented by misfolded sigma 3 protein in temperature-sensitive mutant tsG453. Virus Res 46:19–29
Silverstein SC, Schonberg M, Levin DH, Acs G (1970) The reovirus replicative cycle: conservation of parental RNA and protein. Proc Natl Acad Sci U S A 67:275–281
Silverstein SC, Astell C, Levin DH, Schonberg M, Acs G (1972) The mechanisms of reovirus uncoating and gene activation in vivo. Virology 47:797–806
Skup D, Millward S (1980) Reovirus-induced modification of cap-dependent translation in infected L cells. Proc Natl Acad Sci U S A 77:152–156
Smith JA, Schmechel SC, Williams BR, Silverman RH, Schiff LA (2005) Involvement of the interferon-regulated antiviral proteins PKR and RNase L in reovirus-induced shutoff of cellular translation. J Virol 79:2240–2250
Smith RE, Zweerink HJ, Joklik WK (1969) Polypeptide components of virions, top component and cores of reovirus type 3. Virology 39:791–810
Spandidos DA, Krystal G, Graham AF (1976) Regulated transcription of the genomes of defective virions and temperature-sensitive mutants of reovirus. J Virol 18:7–19
Spencer SM, Sgro JY, Dryden KA, Baker TS, Nibert ML (1997) IRIS explorer software for radial-depth cueing reovirus particles and other macromolecular structures determined by cryoelectron microscopy and image reconstruction. J Struct Biol 120:11–21
Stamatos NM, Gomatos PJ (1982) Binding to selected regions of reovirus mRNAs by a nonstructural reovirus protein. Proc Natl Acad Sci U S A 79:3457–3461
Starnes MC, Joklik WK (1993) Reovirus protein lambda 3 is a poly(C)-dependent poly(G) polymerase. Virology 193:356–366
Strong JE, Leone G, Duncan R, Sharma RK, Lee PW (1991) Biochemical and biophysical characterization of the reovirus cell attachment protein sigma 1: evidence that it is a homotrimer. Virology 184:23–32

Sturzenbecker LJ, Nibert M, Furlong D, Fields BN (1987) Intracellular digestion of reovirus particles requires a low pH and is an essential step in the viral infectious cycle. J Virol 61:2351–2361

Tao Y, Farsetta DL, Nibert ML, Harrison SC (2002) RNA synthesis in a cage—structural studies of reovirus polymerase lambda3. Cell 111:733–745

Taraporewala ZF, Patton JT (2004) Nonstructural proteins involved in genome packaging and replication of rotaviruses and other members of the Reoviridae. Virus Res 101:57–66

Tillotson L, Shatkin AJ (1992) Reovirus polypeptide sigma 3 and N-terminal myristoylation of polypeptide mu 1 are required for site-specific cleavage to mu 1C in transfected cells. J Virol 66:2180–2186

Tosteson MT, Nibert ML, Fields BN (1993) Ion channels induced in lipid bilayers by subvirion particles of the nonenveloped mammalian reoviruses. Proc Natl Acad Sci U S A 90:10549–10552

Tyler KL (2001) Mammalian reoviruses. In: Knipe DM, Howley M, Griffen DE et al (eds) Fields virology. Lippincott Williams & Wilkins, Philadelphia, pp 1729–1745

Tyler KL, McPhee DA, Fields BN (1986) Distinct pathways of viral spread in the host determined by reovirus S1 gene segment. Science 233:770–774

Tyler KL, Squier MK, Rodgers SE, Schneider BE, Oberhaus SM, Grdina TA, Cohen JJ, Dermody TS (1995) Differences in the capacity of reovirus strains to induce apoptosis are determined by the viral attachment protein sigma 1. J Virol 69:6972–6979

Ward RL, Shatkin AJ (1972) Association of reovirus mRNA with viral proteins: a possible mechanism for linking the genome segments. Arch Biochem Biophys 152:378–384

Ward R, Banerjee AK, LaFiandra A, Shatkin AJ (1972) Reovirus-specific ribonucleic acid from polysomes of infected L cells. J Virol 9:61–69

Watanabe T, Watanabe S, Noda T, Fujii Y, Kawaoka Y (2003) Exploitation of nucleic acid packaging signals to generate a novel influenza virus-based vector stably expressing two foreign genes. J Virol 77:10575–10583

Watanabe Y, Kudo H, Graham AF (1967) Selective inhibition of reovirus ribonucleic acid synthesis by cycloheximide. J Virol 1:36–44

Watanabe Y, Millward S, Graham AF (1968) Regulation of transcription of the reovirus genome. J Mol Biol 36:107–123

Weiner HL, Drayna D, Averill D-RJ, Fields BN (1977) Molecular basis of reovirus virulence: role of the S1 gene. Proc Natl Acad Sci U S A 74:5744–5748

Weiner HL, Ramig RF, Mustoe TA, Fields BN (1978) Identification of the gene coding for the hemagglutinin of reovirus. Virology 86:581–584

Weiner HL, Powers ML, Fields BN (1980) Absolute linkage of virulence and central nervous system cell tropism of reoviruses to viral hemagglutinin. J Infect Dis 141:609–616

White CK, Zweerink HJ (1976) Studies on the structure of reovirus cores: selective removal of polypeptide lambda 2. Virology 70:171–180

Wiener JR, Joklik WK (1987) Comparison of the reovirus serotype 1, 2, and 3 S3 genome segments encoding the nonstructural protein sigma NS. Virology 161:332–339

Wiener JR, Joklik WK (1989) The sequences of the reovirus serotype 1, 2, and 3 L1 genome segments and analysis of the mode of divergence of the reovirus serotypes. Virology 169:194–203

Wiener JR, Bartlett JA, Joklik WK (1989a) The sequences of reovirus serotype 3 genome segments M1 and M3 encoding the minor protein mu 2 and the major nonstructural protein mu NS, respectively. Virology 169:293–304

Wiener JR, McLaughlin T, Joklik WK (1989b) The sequences of the S2 genome segments of reovirus serotype 3 and of the dsRNA-negative mutant ts447. Virology 170:340–341

Wilson GA, Morrison LA, Fields BN (1994) Association of the reovirus S1 gene with serotype 3-induced biliary atresia in mice. J Virol 68:6458–6465

Xu P, Miller SE, Joklik WK (1993) Generation of reovirus core-like particles in cells infected with hybrid vaccinia viruses that express genome segments L1, L2, L3, and S2. Virology 197:726–731

Xu W, Patrick MK, Hazelton PR, Coombs KM (2004) Avian reovirus temperature-sensitive mutant tsA12 has a lesion in major core protein sigma A and is defective in assembly. J Virol 78:11142–11151

Xu W, Tran AT, Patrick MK, Coombs KM (2005) Assignment of avian reovirus temperature-sensitive mutant recombination groups B, C, and D to genome segments. Virology 338:227–235

Yeager M, Weiner SG, Coombs KM (1996) Transcriptionally active reovirus core particles visualized by electron cryo-microscopy and image reconstruction. Biophys J 70:484

Yin P, Cheang M, Coombs KM (1996) The M1 gene is associated with differences in the temperature optimum of the transcriptase activity in reovirus core particles. J Virol 70:1223–1227

Yin P, Keirstead ND, Broering TJ, Arnold MM, Parker JSL, Nibert ML, Coombs KM (2004) Comparisons of the M1 genome segments and encoded μ2 proteins of different reovirus isolates. Virol J 1:6

Zhang X, Walker SB, Chipman PR, Nibert ML, Baker TS (2003) Reovirus polymerase lambda 3 localized by cryo-electron microscopy of virions at a resolution of 7.6 angstrom. Nature Struct Biol 10:1011–1018

Zhang X, Tang J, Walker SB, O'Hara D, Nibert ML, Duncan R, Baker TS (2005) Structure of avian orthoreovirus virion by electron cryomicroscopy and image reconstruction. Virology 343:25–35

Zou S, Brown EG (1992) Identification of sequence elements containing signals for replication and encapsidation of the reovirus M1 genome segment. Virology 186:377–388

Zou S, Brown EG (1996) Stable expression of the reovirus mu2 protein in mouse L cells complements the growth of a reovirus ts mutant with a defect in its M1 gene. Virology 217:42–48

CTMI (2006) 309:169–187

Rotavirus Genome Replication and Morphogenesis: Role of the Viroplasm

J. T. Patton (✉) · L. S. Silvestri · M. A. Tortorici · R. Vasquez-Del Carpio · Z. F. Taraporewala

Laboratory of Infectious Diseases, National Institutes of Allergy and Infectious Diseases, National Institutes of Health, 50 South Drive, MSC 8026, Room 6314, Bethesda, MD 20892-8026, USA
jpatton@niaid.nih.gov

Abstract The rotaviruses, members of the family *Reoviridae*, are icosahedral triple-layered viruses with genomes consisting of 11 segments of double-stranded (ds)RNA. A characteristic feature of rotavirus-infected cells is the formation of large cytoplasmic inclusion bodies, termed viroplasms. These dynamic and highly organized structures serve as viral factories that direct the packaging and replication of the viral genome into early capsid assembly intermediates. Migration of the intermediates to the endoplasmic reticulum (ER) initiates a budding process that culminates in final capsid assembly. Recent information on the development and organization of viroplasms, the structure and function of its components, and interactive pathways linking RNA synthesis and capsid assembly provide new insight into how these microenvironments serve to interface the replication and morphogenetic processes of the virus.

1 Introduction

A characteristic feature of rotavirus-infected cells is the presence of large cytoplasmic inclusion bodies, termed viroplasms. These structures represent viral factories that direct the packaging and replication of the viral genome into capsid intermediates. Migration of the intermediates to the endoplasmic reticulum (ER) initiates a budding process that culminates in final capsid assembly. Recent information on the development and organization of viroplasms, the structure and function of its components, and interactive pathways linking RNA synthesis and capsid assembly provide new insight into how these microenvironments serve to interface the replication and morphogenesis processes of the virus.

2 Rotavirus Replication: An Overview

The rotavirion is an icosahedron composed of three concentric layers of protein that contains eleven segments of double-stranded (ds)RNA [50]. The outer protein layer, formed by the spike protein, VP4, and the glycoprotein, VP7, is lost from the virion during entry, producing a double-layered particle (DLP). Each DLP consists of a T=1 symmetrical core surrounded by a protein layer consisting of VP6 [31]. The DLP functions as a transcriptional machine in the cytoplasm, producing eleven capped (+)RNAs [10]. The transcripts are synthesized by the viral RNA-dependent RNA polymerase (RdRP), VP1, and capped by the viral methyltransferase and guanylyltransferase, VP3 [13, 33, 64]. A copy of each of these proteins is situated at most if not all of the 12 vertices of the core. Pentamers comprised of five dimers of the RNA-binding protein, VP2, form the shell of the core, and serve as anchoring sites for VP1

Fig. 1A–C Viroplasm organization. **A** Electron-dense viroplasms (*VP*) are surrounded by ER vesicles in which TLPs accumulate during rotavirus infection. Note the ribosome-studded ER vesicles (*arrowhead*) and the DLP bound to the membrane exterior (*small arrow*). **B** High-magnification immunofluorescence analysis of proteins associated with viroplasms using specific antisera. The NSP2–NSP5 containing interior of viroplasms is surrounded by an exterior zone of VP6 and NSP4. Progeny cores formed in the interior migrate to the exterior zone where they acquire the VP6 shell and undergo NSP4-mediated budding into the lumen of the endoplasmic reticulum. **C** As shown using a gene 8-specific siRNA to knockdown NSP2 expression, NSP2 has an essential role in the formation of viroplasms

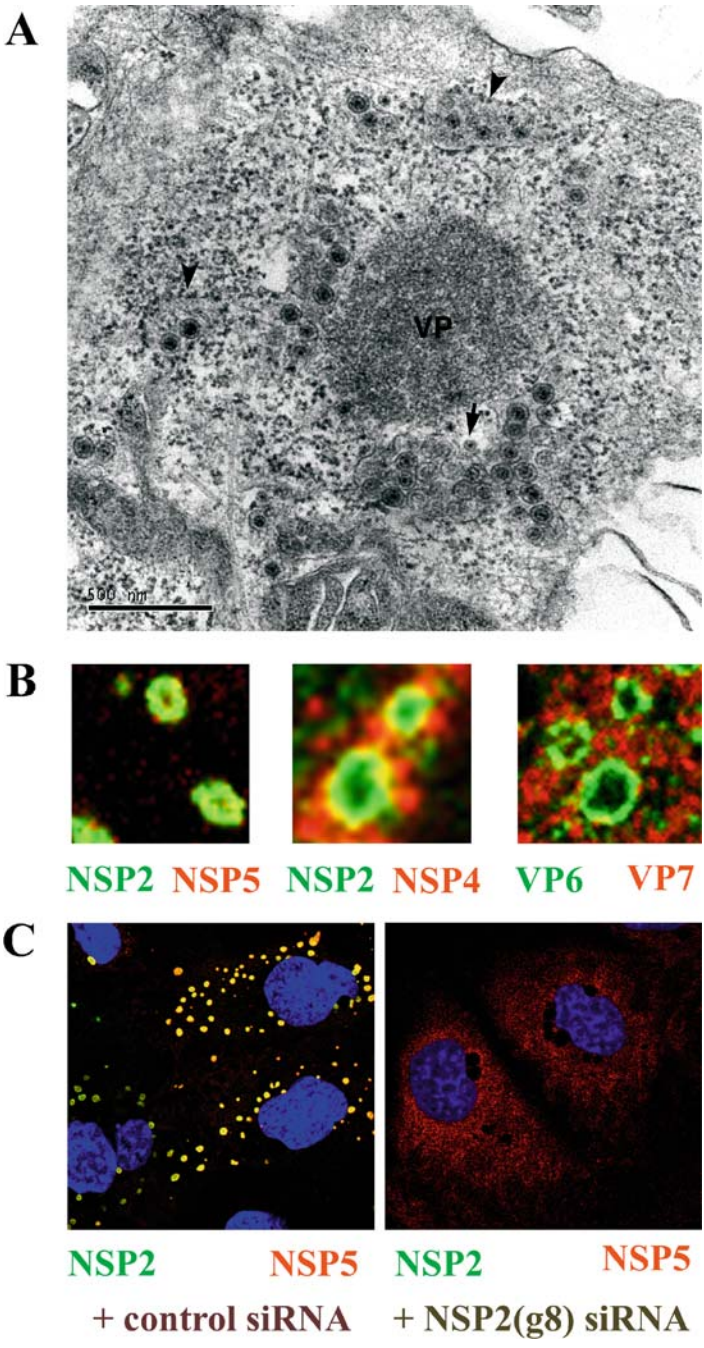
A
VP
500 nm
B
NSP2 NSP5 NSP2 NSP4 VP6 VP7
C
NSP2 NSP5 NSP2 NSP5
+ control siRNA + NSP2(g8) siRNA

and VP3 [31]. The genome segments are presumably organized inside the core such that each interacts with one particular VP1–VP3 complex [47, 51]. During transcription, nascent (+)RNAs are extruded from the DLP through aqueous channels located at the vertices that extend through both the VP2 and VP6 protein layers [30].

Translation of the viral (+)RNAs produces eleven or twelve viral proteins, of which six are structural (VP) and the remainder are nonstructural (NSP). Two of the proteins, NSP2 and NSP5, direct the formation of viroplasms and act as recruiters of the protein components of the core (Fig. 1) [6, 18, 27]. Concentrated fields of ribosomes that surround viroplasms are the likely source of proteins needed for the formation and function of the inclusions. Viroplasms are viral factories, serving as sites in which viral (+)RNAs are packaged into cores and simultaneously replicated to dsRNAs. The source of the (+)RNAs for these processes include DLPs associated with viroplasms [57]. The mechanism of genome packaging is poorly understood. However, the process must include the gene-specific recognition of viral RNAs, as progeny viruses contain a complete and equimolar constellation of dsRNAs [41]. Given that the interaction of (+)RNAs with newly formed cores precedes replication of the (+)RNAs to dsRNAs, it follows that the gene-specific recognition signals promoting packaging must reside within the (+)RNAs. Packaging and replication are intertwined by the VP2-dependent catalytic activity of the viral RdRP [46]. As a consequence, dsRNA synthesis is linked to core assembly, thereby precluding the formation of naked dsRNAs in the infected cell.

An enriched zone of VP6 is present at the periphery of viroplasms (Fig. 1). This VP6 zone serves as the site at which cores assembled within the viroplasm are subsequently converted to DLPs. Such newly formed DLPs may amplify the viral replication cycle by directing the synthesis of additional (+)RNAs. Alternatively, the DLPs may migrate to the ER via the affinity of their VP6 capsid shell for the ER-transmembrane protein NSP4 [5, 63]. The DLP-NSP4 interaction triggers budding of the DLP through VP7-containing membrane patches, an event associated with the appearance of membrane-bound particles within the lumen of the ER (Fig. 1) [37]. By an undefined mechanism, the VP7 component of the envelope coalesces to yield the triple-layered virion.

The stage at which the VP4 spike protein becomes incorporated into progeny virions is not certain, and may be, to some extent, cell-type dependent. The initial hypothesis on VP4 assembly was based on studies suggesting that VP4 was associated with VP7–NSP4 complexes located in ER membranes [37]. Budding of DLPs through these VP4-containing complexes was predicted to result in the co-assembly of VP4 and VP7 into the outer capsid in the lumen of the ER. However, more recent studies showing that VP4 accumulates in raft microdomains located in the plasma membrane has

led to an alternative hypothesis for the assembly of VP4 [54]. In this model, DLPs are proposed to migrate from the viroplasm to the ER, where by budding through NSP4–VP7 complexes, the particles acquire the VP7 destined to form the outer capsid [14]. ER-derived vacuoles containing maturing particles then interact with rafts, to yield an environment in which VP4 can be integrated with VP7 into the outer capsid shell. This model presumes that VP7 and VP4 interact sequentially with the DLP, as opposed to the concurrent interaction of these proteins with DLPs proposed by the earlier model.

3
Viroplasms: Interface Between Replication and Morphogenesis

The rotavirus structural proteins have inherent affinities for one another that drive the assembly of virion-like particles (VLPs) even in the absence of viroplasms. For example, co-expression of the inner capsid components VP1, VP2, VP3, and VP6 by recombinant baculoviruses is efficient in producing empty DLPs in insect cells [68]. Likewise, co-expression of inner and outer capsid shell proteins (e.g., VP2, VP6, VP4, and VP7) leads to the production of empty virion-like triple-layered particles (TLPs) [28]. If the formation of RNA-containing progeny virus is to occur, the tendencies of the capsid proteins to self-assemble must be coordinated with genome packaging and replication in the infected cell. Such coordination is the domain of the viroplasm. To achieve this function, the viroplasm must not only recruit the inner capsid proteins but also spatially and temporally regulate their interactions. The burden of recruiting and mediating the interaction of the capsid proteins most likely falls on one or more nonstructural proteins. Without the appropriate development and function of the viroplasm, morphogenesis becomes unregulated leading to the assembly of empty particles. As one example, cells infected with *tsE*, a rotavirus mutant with a temperature-sensitive (*ts*) lesion in NSP2, fail to develop mature viroplasms at the nonpermissive temperature, but accumulate excessive numbers of empty particles [53]. Given the role for the viroplasm in linking replication and morphogenesis, it may be reasoned that the subset of empty particles typically arising during productive rotavirus infection are the consequence of unregulated capsid assembly events occurring outside the viroplasm.

3.1
Spatial Organization

Beginning at 3–4 h postinfection (p.i.), numerous small punctate inclusions appear throughout the cytoplasm of rotavirus-infected cells. With time, the

punctate inclusions appear to give way to the 10–20 large (10–20 μm) viroplasms that are typical of late stages of infection [3, 21, 32]. The temporal transition in number and sizes of inclusions may result from coalescence of the early small inclusions into larger ones or by the selected support of a few of the inclusions for further growth and development [16].

Electron microscopy has shown that viroplasms are electron-dense inclusions, as though rich in nucleic acids and proteins (Fig. 1) [3, 48]. Regions surrounding the viroplasms often contain numerous polysomes, the likely source of proteins used in supporting the maturation of the viroplasms and the replication and assembly processes occurring within them. Closely associated with viroplasms are membranous vacuoles of the ER, many studded with ribosomes, that contain TLPs (Fig. 1). Detectable between viroplasms and the ER vacuoles are DLPs, likely representing newly assembled particles in the process of migrating to the ER where they undergo budding.

Immunofluorescence staining of infected cells using monospecific antisera has revealed much about the distribution of viral proteins in and around viroplasms. Such an analysis indicates that viroplasms can be subdivided into interior and exterior domains based on their antibody-accessible protein content (Fig. 1). The interior domain is highlighted by the presence of the nonstructural proteins, NSP2 and NSP5, and the core proteins, VP1 and VP2 [3, 21, 32]. Pulse-labeling of infected cells with the nucleotide analog, BrUTP, indicates that the interior domain is the site of accumulation of newly made (+)RNA [57]. Its protein and RNA composition is consistent with the interior domain serving as the site of progeny core formation, implying that this also represents the site in which genome packaging and replication occurs. The interior domain likely corresponds to the electron-dense inclusions noted in infected cells by electron microscopy. The exterior domain is characterized by the presence of an antibody-accessible continuum of VP6 that surrounds the relatively VP6-free interior domain of the viroplasm. Given the relative scarcity of accumulated DLPs within the exterior domain as judged by electron microscopy (Fig. 1), the VP6 continuum detected by immunofluorescence most likely reflects an accumulation of unassembled VP6. The exterior domain is also characterized by the presence of NSP4, which through its affinity for VP6, may be instrumental in recruiting unassembled VP6 to this site, and producing the necessary environment for morphogenesis of cores to DLPs [21, 32]. Immunofluorescence assays reveal that viroplasms are collectively embedded in discontinuous VP7-rich zones of the cytoplasm. Such zones reflect locations of unassembled VP7 on the ER and/or assembled TLPs within membrane-bound vacuoles, depending on the specificity of VP7 antibody used in immunofluorescence analysis.

3.2 Contribution of NSP2 and NSP5

Viroplasm formation is dependent on the nonstructural proteins, NSP2 and NSP5. This has been demonstrated by siRNA-mediated knockdown experiments where the loss of NSP2 or NSP5 expression has been tied to the lack of viroplasm formation in the infected cell (Fig. 1) [57] (unpublished results). Moreover, the essential role of these proteins in viroplasm development has been illustrated by experiments showing that transient expression of NSP2 and NSP5 together in uninfected cells generates viroplasm-like inclusions [18]. Given evidence that NSP2 has affinity for VP1 and that NSP5 has affinity for VP2 [4, 6, 27], NSP2 and NSP5 may be critical for recruiting the appropriate inner capsid proteins to viroplasms necessary to support core assembly. Indeed, when either VP1 or VP2 are co-expressed with NSP2 and NSP5, these core proteins will accumulate with the viroplasm-like inclusions formed by NSP2 and NSP5 (unpublished results).

3.2.1 NSP2 Structure–Function

NSP2 is a highly conserved basic protein of 317 amino acids that is expressed at high levels in infected cells. Early sedimentation analyses established that the NSP2 exists as large approximately 12S homomultimeric structures in infected cells [27]. Through the study of purified recombinant NSP2 by analytical ultracentifugation and dynamic light scattering, the protein was found to have the intrinsic ability to self-assemble into octamers [56]. These octamers represent the functional form of the protein in infected cells [60], possessing sequence-independent affinity for single-stranded (ss)RNA and affinity for nucleotides [26, 56]. Interaction with NTPs causes the octamer to undergo a conformation shift to a more condensed form [56]. Such ligand-dependent conformational shifts are hallmark features of packaging proteins and molecular motors.

The structure of the octamer has been determined to a resolution of 2.6 Å by X-ray crystallography [25]. The octamer has a novel 4-2-2 symmetry and consists of two doughnut-shaped NSP2 tetramers stacked tail-to-tail. Running diagonally across the tetramer–tetramer interface are four prominent grooves, highly electropositive in nature. These grooves likely represent the binding sites for ssRNA. The octamer also possesses an NTP-independent helix-destabilizing activity capable of disrupting short-stretches of duplex RNA [58], a property likely intertwined with the RNA-binding activity of NSP2. The structure and activities of the octamer suggest that it may serve as a platform for organizing and relaxing (+)RNAs in preparation of packaging

into newly formed cores. This would be akin to the known roles that the multimeric structures formed by single-stranded DNA-binding proteins (SSBs) play in the replication of cellular DNA and various viral genomic DNAs [20, 52].

In addition to its other activities, the NSP2 octamer was noted several years ago to have an associated NTPase activity (NTP → NDP + P_i) [59]. The active site for this activity resides within a deep cleft created by the folding of the structurally distinct N- and C-terminal domains of the NSP2 monomer [25]. The location of the NTP-binding site was initially extrapolated from superposition of the C-terminal domain of NSP2 with the catalytic core of protein kinase C-interacting protein (PKCI), a prototypic member of the histidine triad (HIT) family of nucleotide-interacting proteins [9]. Although NSP2 lacks the classic HIT motif (HϕHϕHϕϕ, where ϕ is a hydrophobic residue), the cleft of NSP2 includes an arrangement of His residues reminiscent of such a motif. Mutagenesis has demonstrated that residues of this HIT-like motif are indeed involved in the binding and hydrolysis of NTPs [65]. Nucleophilic attack on the β-γ linkage of the NTP generates a short-lived phosphorylated form of NSP2, a phenomenon accounting for the occasional reports of autokinase activity associated with the protein [59]. To date, NSP2 is the only viral protein identified with a HIT-like fold.

Molecular docking programs that simulate the interaction of an NTP with NSP2 suggest that NTP-binding into the cleft is guided by the phosphate backbone of the ligand and not by its nucleoside component [65]. Such an interaction would explain the ability of NSP2 to hydrolyze any of the four NTPs. The fact that the sole basis driving the interaction of an NTP with the active site of the cleft may be its phosphate groups suggests that NSP2 may hydrolyze the phosphoanhydride bonds of other polyphosphate-containing moieties. Indeed, recent studies have revealed that the HIT-like motif can hydrolyze the 5′ β-γ phosphoanhydride bond (and not the α-β bond) of RNA (Patton et al., unpublished data). Thus, the NSP2 octamer can function as an RTPase. Interestingly, early studies on rotavirus genomic dsRNAs indicated that the (–) strand lacks the 5′ γ-phosphate [24, 39], a characteristic raising the possibility of an involvement of NSP2 in the initiation of (–) strand synthesis. The concept that NSP2 may be involved in initiation is further supported by the fact that NSP2 accumulates at the site of genome replication (i.e., the viroplasm), is a component of replication intermediates (RIs) with replicase activity [4, 19], and can interact with the viral RdRP [27]. Given that genomic dsRNAs do not exist in the infected cell in a nonpackaged (naked) form and that NSP2 has poor affinity for dsRNA, it is doubtful that the protein would mediate removal of the γ-phosphate from a dsRNA following completion of (–) strand synthesis.

3.2.2 NSP5 Structure–Function

NSP5 is a highly conserved 198-amino acid protein that is acidic and rich in serine and threonine residues. The protein forms dimers [49], binds ss and dsRNA [66], and undergoes phosphorylation [67] and *O*-glycosylation [22] in the infected cell. Variation in the extent of phosphorylation produces NSP5 isomers, ranging in size from the 28-kDa hypophosphorylated form to the 32- to 34-kDa hyperphosphorylated forms [1, 8]. Burrone and colleagues have dissected the pathway of NSP5 phosphorylation by analyzing modifications made to mutant species of the protein transiently expressed in mammalian cells [17]. Their results indicate that phosphorylation is a multi-step process in which specific serine residues of NSP5 are modified by casein kinase 1 (CK1) or a CK1-like activity. The conclusion was drawn from the observation that the phosphorylated serine residues in the various isomers of NSP5 fall within sequences with similarity to CK1 consensus phosphorylation sites and that recombinant CK1 is able to phosphorylate the relevant Ser residues in NSP5-specific peptides [17]. These recent findings suggesting the involvement of CK1 or a CK1-like activity are contrary to earlier reports that raised the possibility that CK2 or a CK2-like activity was responsible for NSP5 phosphorylation [15].

Burrone and colleagues propose that the initial step in the phosphorylation pathway of NSP5 is dependent on NSP2, and leads to phosphorylation of Ser-67 [17]. NSP2 is suggested to exert this effect by interacting with NSP5 in such a way as to induce a structural transition in NSP5 that renders Ser-67 accessible to a cellular kinase. The hypophosphorylated NSP5 isomer produced by modification of Ser-67 appears to have an activator function that triggers the phosphorylation of multiple serine residues near the C-terminus of the protein. This second wave of modifications yields the hyperphosphorylated isomers of NSP5. The importance of Ser-67 phosphorylation to the eventual hyper-phosphorylation of the protein was revealed by experiments showing that mutation of the serine to alanine produced a form of NSP5 unable to undergo phosphorylation even in the presence of NSP2 [17]. In contrast, conversion of Ser-67 to the phosphomimetic residue, aspartic acid, conveyed activator function to NSP5 even in the absence of NSP2.

Despite recent evidence from transient expression assays that the hypo- and hyperphosphorylation of NSP5 is mediated by CK1 or CK1-like kinases [17], the results of several in vitro studies, including some using purified recombinant protein, indicate the presence of a low-level autokinase activity associated with NSP5 that stimulates the basal phosphorylation of the protein [2, 49, 66]. Related experiments have shown that the phosphorylation of NSP5 is stimu-

lated several-fold by co-incubation with NSP2 [49, 66]. Transient-expression assays conducted with NSP2 mutants indicate that in vivo the NSP2-induced phosphorylation of purified NSP5 is not directly linked to the NTPase activity of NSP2 [65]. Instead, the results of in vitro assays suggest that NSP2 upregulates an autokinase activity that is associated with NSP5. Whether this activity results in the phosphorylation of the same residue of NSP5 that undergoes NSP2-dependent modification (i.e., Ser-67) in transient expression assays [17] remains to be determined. The results of the in vitro assays also leave open the possibility that the phosphorylated isoforms of NSP5 detected in the infected cell are the consequence of not only host CK- or CK-like activities but also of an NSP5-associated kinase activity.

While there can be little doubt that phosphorylation is important to the function of NSP5 in the infected cell, the nature of that function remains obscure. For that matter, we do not know if all NSP5 isomers, or only a subset of them, have biological activity in the cell. But given the additional negative charge that serine phosphorylation imparts to a protein, the NSP5 isomers can be expected to vary in their ability to interact with RNA and other proteins, and thus, to vary in function. Since the hypophosphorylated form of NSP5 is the most abundant isomer in the infected cell [7, 65], it is tempting to speculate that this form must represent an active species. However, this may not be true given the numerous examples whereby it is the relative minor population of a phosphorylated or hyperphosphorylated protein that has primary effector function, as opposed to a more predominant but less phosphorylated form (e.g., IRF3 [34]). Treatment of rotavirus-infected cells with inhibitors of protein kinases and phosphatases have indicated that the hyperphosphorylated isomers of NSP5 may be re-cycled to hypophosphorylated isomers through the activity of cellular phosphatases [8]. Thus, NSP5 phosphorylation is likely a dynamic event in the infected cell with isomers constantly transitioning from one form to another.

With the accumulation of large amounts of NSP5 in viroplasms of infected cells, it can be assumed that the protein is involved in genome replication or core assembly. Certainly, the affinity of NSP5 for VP2 and ss and dsRNA is consistent with such a hypothesis [6, 66]. However, we cannot exclude the possibility that its RNA-binding activity is primarily connected to suppressing the dsRNA-dependent activation of antiviral host factors such as the protein kinase PKR by sequestering viral dsRNAs generated within viroplasms [55, 66]. This would give NSP5 a function similar to that reported previously for the σA protein of reovirus [23]. Moreover, the sequestering RNA-binding activity of NSP5 may be responsible for the inability of siRNA-induced RNases to degrade viral RNAs located within viroplasms [57].

While NSP5 is the primary product of genome segment 11, for many rotaviruses this segment encodes a second protein through an alternative out-of-phase open reading frame [38]. This protein, NSP6 (92 amino acids), accumulates in viroplasms, and interacts with the C-terminus of NSP5 [61]. Although the function of the protein is not known, the fact that only some rotaviruses encode the protein indicates that it has nonessential function.

3.3 Nucleation and Maturation

Studies using RNA interference (RNAi) technology have shown that gene-specific RNases induced by short-interfering RNAs (siRNAs) can target for degradation those (+)RNAs that direct protein synthesis but not those (+)RNAs that direct dsRNA synthesis [57]. These and related findings have indicated that (+)RNAs used as templates for dsRNA synthesis are made within viroplasms, and are not translocated to such inclusions from outside sites. Thus, the development of viroplasms as sites of genome replication and core assembly is dependent on the presence of transcriptionally-active DLPs within the inclusions. Given this conclusion, it follows that transcriptionally active DLPs, generated from infecting virions, may act as nucleation points for the formation of viroplasms at least at early times of infection when progeny DLPs are yet to be formed.

The viral proteins localizing to the interior domain of the viroplasm all have affinity for single-stranded RNA [26, 29, 42, 43, 66]. With the high concentration of these proteins in the viroplasm, the capacity of the inclusions to retain (+)RNAs produced from DLPs can be predicted to be quite large and to produce an environment favoring the efficient packaging and replication of the viral genome. Those (+)RNAs generated by DLPs in the viroplasm that exceed the retention capacity of the RNA-binding proteins forming the inclusion may be expected to migrate to nearby polysomes. Translation of the (+)RNAs would in turn produce additional viroplasm-resident proteins (e.g., NSP2, NSP5, VP1, VP2) which would support further growth of the viroplasm. Such growth would allow for additional retention of newly made (+)RNAs in the viroplasm, an event enhancing levels of genome replication and core assembly. Thus, viroplasm growth and activity may be regulated by two factors: numbers of (+)RNAs escaping from the inclusion and numbers of transcriptionally active DLPs present in the inclusion.

The application of RNAi technology has provided surprising findings concerning the role of the ER-transmembrane protein NSP4 in the development of viroplasms [32]. Notably, knockdown of NSP4 expression by siRNAs was found to have multiple effects on upstream events in the replication cycle,

including causing a severe reduction in the assembly of DLPs and preventing the maturation of viroplasms beyond that typical of the early inclusions formed in the infected cell. Not only were the viroplasms immature in size, but they also lacked the pronounced exterior zone of VP6 characteristic of fully formed viroplasms. Instead, NSP4 knockdown caused an aberrant distribution of VP6 in the cytoplasm, such that the protein no longer localized to viroplasms, but rather aggregated into large filamentous arrays [32]. The results of the siRNA experiments indicate that NSP4 plays a critical role in the appropriate distribution of VP6 in the infected cell, which if not accomplished, precludes VP6 from interacting with viroplasms in a manner that supports DLP assembly. Thus, while the function of NSP4 may include recruiting DLPs to the ER through the affinity of NSP4 for the assembled VP6 capsid layer, the function of NSP4 also includes supporting the maturation and function of viroplasms by directing the localization of unassembled VP6 to the periphery of these inclusions. From this, it may be predicted that the mechanism of VP6 recruitment to viroplasms differs fundamentally from that of VP1 and VP2, with the former dependent on NSP4 and the latter two dependent on NSP2 and NSP5. Given the likelihood that unassembled VP6 is bound to ER-associated NSP4, it follows that the conversion of cores to DLPs may occur on the ER membrane. In this scenario, the interaction of packaged capsid intermediates would be mediated by the affinity of the VP2 shell of the core for VP6–NSP4 complexes anchored to the ER.

Molecular events occurring at the ER that lead to the conversion of DLPs to TLPs are poorly understood. Nonetheless, there have been proposals suggesting that NSP4 is essential for recruiting DLPs to the ER and that the interaction of NSP4 with VP7 produces protein complexes in the ER membrane through which DLPs bud to produce TLPs [5, 37, 63]. The weakness of these concepts is that TLPs can be efficiently produced in the absence of NSP4 by infecting insect cells with recombinant baculoviruses expressing VP2, VP6, and VP7 [28]. Also, large numbers of empty TLPs are formed in rotavirus-infected cells in which NSP4 expression has been suppressed using siRNA. Thus, there is not an absolute requirement for NSP4 in generating the VP7 outer capsid of rotavirus. This raises the possibility that the primary role of NSP4 in the replication cycle is tied to recruitment and localization of unassembled VP6, and that NSP4 has at best an indirect or nonessential role in DLP budding.

3.4 Genome Replication and Early Morphogenesis

Characterization of the protein and RNA content, biophysical properties, and enzymatic activities of subviral particles (SVPs) recovered from rotavirus-

infected cells has provided information on the features of viral replication intermediates (RIs). Such studies have indicated that the simplest intermediates with replicase activity (ss →dsRNA polymerase activity) are core-like in their structure and protein content (core RI) [19]. Pulse-chase experiments indicate that core RIs serve as precursors of double-layered RIs, the latter representing structures with replicase activity that appear to be cores surrounded by a partial or complete layer of VP6. These and related findings indicate that as RIs carry out dsRNA synthesis, they concurrently undergo morphogenesis from cores to DLPs with the assembly of the VP6 shell having the effect of neither inhibiting nor promoting replicase activity [44]. That VP6 is not needed for replicase activity is further supported by studies on *tsG*, a mutant rotavirus with a temperature-sensitive lesion in VP6 [36]. At the nonpermissive temperature, *tsG*-infected cells continue to form RIs with replicase activity despite a defect in the ability of VP6 to assemble into a capsid shell. In addition to the structural proteins, the viroplasm-resident protein NSP2 is a component of RIs with replicase activity. Its presence supports the belief that RIs are located in viroplasms and that viroplasms are sites of genome replication, and core and DLP assembly.

Treatment of RIs with RNases specific for ssRNA destroys the associated (+) templates for (–) strand synthesis, rendering the RIs incapable of synthesizing dsRNAs [44]. RNase treatment also has the parallel effect of reducing the overall size of the RIs, such that they migrate electrophoretically between cores and DLPs on agarose gels, depending on their VP6 content. The impact of RNase treatment on the replicase activity and size of RIs indicates that at least a portion of each (+) template passes from the exterior (RNase accessible) to the interior (RNase inaccessible) of the intermediate during dsRNA synthesis. Moreover, the data indicate that the (+) templates are not packaged into cores prior to their replication to dsRNAs, but rather are replicated concurrently with their translocation into the cores. This process differs fundamentally from that reported for φ6, a well-studied segmented dsRNA-containing bacteriophage, which appears to complete the packaging of its three (+) strand template RNAs into cores prior to initiating dsRNA synthesis [40]. The φ6 (+)RNAs are sequentially packaged into its cores through channels located at each of the five-fold vertices [35]. The gene-specific recognition and insertion of the (+)RNAs into the core mediates the assortment process, yielding φ6 progeny that have the complete constellation of the three viral RNAs.

In a manner analogous to φ6, the eleven (+)RNAs of rotavirus may be predicted to enter into preformed cores through the central channels located in each of the VP2 pentamers. Given that VP1 anchors to the interior side of each VP2 pentamer [69] and that the replicase activity of VP1 is dependent on its interaction with VP2 [46], it may also be suggested that the VP2-bound

form of VP1 catalyzes (–) strand synthesis on the (+)RNA templates to form dsRNAs. In this scenario, the same VP1–VP2 complexes in DLPs that direct transcription would act during the packaging of (+)RNAs into cores, to direct (–)strand synthesis. The energy produced from nucleotide hydrolysis during (–) strand elongation may be critical for driving the translocation of (+)RNAs into the cores. Alternatively, NSP2 may generate the necessary energy through its associated NTPase activity.

Although we have some insight into the properties of the core RI, our understanding of the steps in its assembly is poor, particularly regarding the mechanism governing the gene-specific association (assortment) of viral (+)RNAs with the intermediate. Perhaps most importantly, does the assortment process occur prior to or after the formation of the VP2 shell of the core? If the process mimics that of φ6, then the empty preformed core of rotavirus would have to display eleven different packaging signals. Intuitively, such a requirement seems complex to the point of being unlikely. Instead, it may be that the various (+)RNAs interact with viral proteins to form RNA–protein complexes that then interact with one another to form the core RI. Evidence of the existence of a precore complex consisting of RNA, VP1, and VP3 is in fact consistent with the idea that core RIs are formed from preexisting RNA–protein complexes [19].

Irrespective of the assembly pathway for the core RI, the protein components and (+)RNAs must interact in such a way to produce initiation complexes for (–) strand synthesis. The required protein components of such complexes include VP1 and VP2, the same two proteins shown before to be essential for dsRNA synthesis [62]. The optimal molar ratio of VP1:VP2 required to support formation of the initiation complex approximately 1:10, which is the same ratio of VP1:VP2 contained within each pentamer of the viral core. Thus, it can be proposed that an initiation complex is the structural equivalent of one of the vertices of the core and that the core RI is formed by the interaction of multiple initiation complexes differing only in their (+)RNA content.

Even though VP1 can bind specifically to viral (+)RNAs in the absence of any other protein [42], the fact that the polymerase requires VP2 for catalytic activity couples the processes of genome replication and core assembly [46]. The mechanism by which VP2 induces polymerase activity is not known, but deletion mutagenesis has shown that the N-terminus of VP2 is essential for the activity [46, 68]. This region of VP2 is multifunctional, contributing to the interaction of VP1 with the VP2 shell and conveying RNA-binding activity to the protein [29, 69].

Additional factors affecting the formation of (–) strand initiation complexes include the sequence and structure of the (+)RNA template [62]. In par-

ticular, cis-acting signals located at both the 5′ and 3′-ends of the (+)RNAs are needed for the efficient formation of initiation complexes [11, 45]. This characteristic likely assures that dsRNA synthesis is initiated on intact (+)RNAs that can appropriately serve as templates for transcription following elongation of the (–) strand. Formation of functional initiation complexes is also dependent on the presence of the divalent cations, Mg^{2+} and Mn^{2+}, and the initiating nucleotide GTP [12].

3.5 Compendium

Viroplasms are dynamic highly organized inclusions that support genome replication and the assembly of cores and DLPs. These processes are intertwined by the VP2-dependent nature of the catalytic activity of the viral RdRP. The formation of viroplasms and the recruitment of core proteins to viroplasms are mediated by the multifunctional RNA-binding proteins, NSP2 and NSP5. The (+)RNAs that serve as templates for genome replication in viroplasms are the products of transcriptionally-active DLPs associated with these inclusions. Besides providing environments designed to promote viral-specific events, viroplasms also serve as safe houses that protect these events from interference by the innate antiviral responses of the host [57].

Our advances in understanding the properties and function of the viroplasm provide a possible explanation for the difficulties that have been encountered in developing a reverse genetics system for the rotaviruses. Most notably, recent studies indicate that (+)RNAs used in dsRNA synthesis are made in viroplasms, and are not transported to these inclusions from outside locations of the cytosol [57]. If this is the case, then those approaches for establishing a reverse genetics system that are simply based on transfection of (+)RNAs into infected cells may be inefficient, since there appears to be no pathways within the cell for transporting the (+)RNAs to the site of genome replication, vis-à-vis, the viroplasm. Alternative approaches that may be helpful in developing a reverse genetics system include transfection of (+)RNA–protein complexes into cells that nucleate viroplasm formation or the assembly of infectious particles in vitro. Given the complexities of events and processes taking place within the viroplasm, the potential for recreating a functioning viroplasm-like environment within in a test tube seems daunting. Nonetheless, the importance of such a system in elucidating the mechanism of RNA packaging and assortment makes it a worthwhile endeavor.

References

1. Afrikanova I, Miozzo MC, Giambiagi S, Burrone O (1996) Phosphorylation generates different forms of rotavirus NSP5. J Gen Virol 77:2059–2065
2. Afrikanova I, Fabbretti E, Miozzo MC, Burrone OR (1998) Rotavirus NSP5 phosphorylation is up-regulated by interaction with NSP2. J Gen Virol 79:2679–2686
3. Altenburg BC, Graham DY, Estes MK (1980) Ultrastructural study of rotavirus replication in cultured cells. J Gen Virol 46:75–85
4. Aponte C, Poncet D, Cohen J (1996) Recovery and characterization of a replicase complex in rotavirus-infected cells by using a monoclonal antibody against NSP2. J Virol 70:985–991
5. Au KS, Chan WK, Burns JW, Estes MK (1989) Receptor activity of rotavirus nonstructural glycoprotein NS28. J Virol 63:4553–4562
6. Berois M, Sapin C, Erk I, Poncet D, Cohen J (2003) Rotavirus nonstructural protein NSP5 interacts with major core protein VP2. J Virol 77:1757–1763
7. Blackhall J, Fuentes A, Hansen K, Magnusson G (1997) Serine protein kinase activity associated with rotavirus phosphoprotein NSP5. J Virol 71:138–144
8. Blackhall J, Munoz M, Fuentes A, Magnusson G (1998) Analysis of rotavirus nonstructural protein NSP5 phosphorylation. J Virol 72:6398–6405
9. Brenner C, Bieganowski P, Pace HC, Huebner K (1999) The histidine triad superfamily of nucleotide-binding proteins. J Cell Physiol 181:179–187
10. Charpilienne A, Lepault J, Rey F, Cohen J (2002) Identification of rotavirus VP6 residues located at the interface with VP2 that are essential for capsid assembly and transcriptase activity. J Virol 76:7822–7831
11. Chen D, Patton JT (1998) Rotavirus RNA replication requires a single-stranded 3′ end for efficient minus-strand synthesis. J Virol 72:7387–7396
12. Chen D, Patton JT (2000) De novo synthesis of minus strand RNA by the rotavirus RNA polymerase in a cell-free system involves a novel mechanism of initiation. RNA 6:1455–1467
13. Chen D, Luongo CL, Nibert ML, Patton JT (1999) Rotavirus open cores catalyze 5′-capping and methylation of exogenous RNA: evidence that VP3 is a methyltransferase. Virology 265:120–130
14. Delmas O, Gardet A, Chwetzoff S, Breton M, Cohen J, Colard O, Sapin C, Trugnan G (2004) Different ways to reach the top of a cell. Analysis of rotavirus assembly and targeting in human intestinal cells reveals an original raft-dependent, Golgi-independent apical targeting pathway. Virology 327:157–161
15. Eichwald C, Vascotto F, Fabbretti E, Burrone OR (2002) Rotavirus NSP5: mapping phosphorylation sites and kinase activation and viroplasm localization domains. J Virol 76:3461–3470
16. Eichwald C, Rodriguez JF, Burrone OR (2004) Characterization of rotavirus NSP2/NSP5 interactions and dynamics of viroplasm formation. J Gen Virol 85:625–634
17. Eichwald C, Jacob G, Muszynski B, Allende JE, Burrone OR (2004) Uncoupling substrate and activation functions of rotavirus NSP5: phosphorylation of Ser-677 by casein kinase 1 is essential for hyperphosphorylation. Proc Natl Acad Sci U S A 101:16304–16309

18. Fabbretti E, Afrikanova I, Vascotto F, Burrone OE (1999) Two non-structural rotavirus proteins, NSP2 and NSP5, form viroplasm-like structures in vivo. J Gen Virol 80:333–339
19. Gallegos CO, Patton JT (1989) Characterization of rotavirus replication intermediates: a model for the assembly of single-shelled particles. Virology 172:616–627
20. Gascon I, Gutierrez C, Salas M (2000) Structural and functional comparative study of the complexes formed by viral ϕ29, Nf and GA-1 SSB proteins with DNA. J Mol Biol 296:989–999
21. Gonzalez RA, Espinosa R, Romero P, Lopez S, Arias CF (2000) Relative localization of viroplasmic and endoplasmic reticulum-resident rotavirus proteins in infected cells. Arch Virol 145:1963–1973
22. Gonzalez SA, Burrone OR (1991) Rotavirus NSP6 is modified by addition of single O-linked residues of N-acetylglucosamine. Virology 182:8–16
23. Gonzalez-Lopez C, Martinez-Costas J, Esteban M, Benavente J (2003) Evidence that avian reovirus sigma A protein is an inhibitor of the double-stranded RNA-dependent protein kinase. J Gen Virol 84:1629–1639
24. Imai M, Akatani K, Ikegami N, Furuchi Y (1983) Capped and conserved terminal structures in human rotavirus genome double-stranded RNA segments. J Viol 47:125–136
25. Jayaram H, Taraporewala Z, Patton JT, Prasad BV (2002) Rotavirus protein involved in genome replication and packaging exhibits a HIT-like fold. Nature 417:311–315
26. Kattoura M, Clapp LL, Patton JT (1992) The rotavirus non-structural protein, NS35, is a nonspecific RNA-binding protein. Virology 191:698–708
27. Kattoura MD, Chen X, Patton JT (1994) The rotavirus RNA-binding protein NS35 (NSP2) forms 10S multimers and interacts with the viral RNA polymerase. Virology 202:803–813
28. Kim Y, Chang KO, Kim WY, Saif LJ (2002) Production of hybrid double- or triple-layered virus-like particles of group A and C rotaviruses using a baculovirus expression system. Virology 302:1–8
29. Labbe M, Baudoux P, Charpilienne A, Poncet D, Cohen J (1994) Identification of the nucleic acid binding domain of the rotavirus VP2 protein. J Gen Virol 75:3423–3430
30. Lawton JA, Estes MK, Prasad BV (1997) Three-dimensional visualization of mRNA release from actively transcribing rotavirus particles. Nat Struct Biol 4:118–121
31. Lawton JA, Zeng CQ, Mukherjee S, Cohen J, Estes MK, Prasad BV (1997) Three-dimensional structural analysis of recombinant rotavirus-like particles with intact and amino-terminal-deleted VP2: implications for the architecture of the VP2 capsid layer. J Virol 71:7353–7360
32. Lopez T, Camacho M, Zayas M, Najera R, Sanchez R, Arias CF, Lopez S (2005) Silencing the morphogenesis of rotavirus. J Virol 79:184–192
33. Lui M, Mattion NM, Estes MK (1992) Rotavirus VP3 expressed in insect cells possesses guanylyltransferase activity. Virology 188:77–84
34. Malmgaard L (2004) Induction and regulation of IFNs during viral infections. J Interferon Cytokine Res 24:439–454

35. Mancini EJ, Kainov DE, Grimes JM, Tuma R, Bamford DH, Stuart DI (2004) Atomic snapshots of an RNA packaging motor reveal conformational changes linking ATP hydrolysis to RNA translocation. Cell 118:743–755
36. Mansell EA, Ramig RF, Patton JT (1994) Temperature-sensitive lesions in the capsid proteins of the rotavirus mutants *tsF* and *tsG* that affect virion assembly. Virology 204:69–81
37. Maass DR, Atkinson PH (1990) Rotavirus proteins VP7, NS28, and VP4 form oligomeric structures. J Virol 64:2632–2641
38. Mattion NM, Mitchell DB, Both GW, Estes MK (1991) Expression of rotavirus proteins encoded by alternative open reading frames of genome segment 11. Virology 181:295–304
39. McCrae MA, McCorquodale JG (1983) Molecular biology of rotaviruses. V. Terminal structure of viral RNA species. Virology 126:204–212
40. Mindich L (2004) Packaging, replication and recombination of the segmented genome of bacteriophage phi6 and its relatives. Virus Res 101:83–92
41. Patton JT (1990) Evidence for equimolar synthesis of double-strand RNA and minus-strand RNA in rotavirus-infected cells. Virus Res 17:199–208
42. Patton JT (1996) Rotavirus VP1 alone specifically binds to the 3′-end of viral mRNA but the interaction is not sufficient to initiate minus-strand synthesis. J Virol 70:7940–7947
43. Patton JT, Chen D (1999) RNA-binding and capping activities of proteins in rotavirus open cores. J Virol 73:1382–1391
44. Patton JT, Gallegos CO (1990) Rotavirus RNA replication: single-strand RNA extends from the replicase particle. J Gen Virol 71:1087–1094
45. Patton JT, Wentz M, Xiaobo J, Ramig RF (1996) Cis-acting signals that promote genome replication in rotavirus mRNA. J Virol 70:3961–3971
46. Patton JT, Jones MT, Kalbach AN, He Y-W, Xiaobo J (1997) Rotavirus RNA polymerase requires the core shell protein to synthesize the double-stranded RNA genome. J Virol 71:9618–9626
47. Pesavento JB, Lawton JA, Estes MK, Prasad BVV (2001) The reversible condensation and expansion of the rotavirus genome. Proc Natl Acad Sci U S A 98:1381–1386
48. Petrie B L, Greenberg HB, Graham DY, Estes MK (1984) Ultrastructural localization of rotavirus antigens using colloidal gold. Virus Res 1:133–152
49. Poncet D, Lindenbaum P, L'Haridon R, Cohen J (1997) In vivo and in vitro phosphorylation of rotavirus NSP5 correlates with its localization in viroplasms. J Virol 71:34–41
50. Prasad BVV, Wang GJ, Clerx JPM, Chiu W (1988) Three-dimensional structure of rotavirus. J Mol Biol 199:269–275
51. Prasad BVV, Rothnagel R, Zeng CQ-Y, Jakana J, Lawton JA, Chiu W, Estes MK (1996) Visualization of ordered genomic RNA and localization of transcriptional complexes in rotavirus. Nature 382:471–473
52. Raghunathan S, Kozlov AG, Lohman TM, Waksman G (2000) Structure of the DNA binding domain of the E. coli SSB bound to ssDNA. Nat Struct Biol 7:648–652
53. Ramig RF, Petrie BL (1984) Characterization of temperature-sensitive mutants of simian rotavirus SA11: protein synthesis and morphogenesis. J Virol 49:665–673

54. Sapin C, Colard O, Delmas O, Tessier C, Breton M, Enouf V, Chwetzoff S, Ouanich J, Cohen J, Wolf C, Trugnan G (2002) Rafts promote assembly and atypical targeting of a nonenveloped virus, rotavirus, in Caco-2 cells. J Virol 76:4591–4602
55. Saunders LR, Barber GN (2003) The dsRNA binding protein family: critical roles, diverse cellular functions. FASEB J 17:961–983
56. Schuck P, Taraporewala Z, McPhie P, Patton JT (2001) Rotavirus nonstructural protein NSP2 self-assembles into octamers that undergo ligand-induced conformational changes. J Biol Chem 276:9679–9687
57. Silvestri LS, Taraporewala ZF, Patton JT (2004) Rotavirus replication: plus-sense templates for double-stranded RNA synthesis are made in viroplasms. J Virol 78:7763–7774
58. Taraporewala ZF, Patton JT (2001) Identification and characterization of the helix-destabilizing activity of rotavirus nonstructural protein NSP2. J Virol 75:4519–4527
59. Taraporewala Z, Chen D, Patton JT (1999) Multimers formed by the rotavirus nonstructural protein NSP2 bind to RNA and have nucleoside triphosphatase activity. J Virol 73:9934–9943
60. Taraporewala ZF, Schuck P, Ramig RF, Patton JT (2002) Analysis of a rotavirus temperature-sensitive mutant indicates that NSP2 octamers are the functional form of the protein. J Virol 76:7082–7093
61. Torres-Vega MA, González RA, Duarte M, Poncet D, López S, Arias CF (2000) The C-terminal domain of rotavirus NSP5 is essential for its multimerization, hyperphosphorylation and interaction with NSP6. J Gen Virol 81:821–830
62. Tortorici MA, Broering TJ, Nibert ML, Patton JT (2003) Template recognition and formation of initiation complexes by the replicase of a segmented double-stranded RNA virus. J Biol Chem 278:32673–32682
63. Taylor JA, O'Brien JA, Yeager M (1996) The cytoplasmic tail of NSP4, the endoplasmic reticulum-localized nonstructural glycoprotein of rotavirus, contains distinct virus binding and coiled coil domains. EMBO J 15:4469–4476
64. Valenzuela S, Pizarro J, Sandino AM, Vasquez M, Fernandez J, Hernandez O, Patton J, Spencer E (1991) Photoaffinity labeling of rotavirus VP1 with 8-azido-ATP: identification of the viral RNA polymerase. J Virol 65:3964–3967
65. Vasquez-Del Carpio R, Gonzalez-Nilo FD, Jayaram H, Spencer E, Venkataram Prasad BV, Patton JT, Taraporewala ZF (2004) Role of the histidine triad-like motif in nucleotide hydrolysis by the rotavirus RNA-packaging protein NSP2. J Biol Chem 279:10624–10633
66. Vende P, Taraporewala ZF, Patton, JT (2002) RNA-binding activity of the rotavirus phosphoprotein NSP5 includes affinity for double-stranded RNA. J Virol 76:5291–5299
67. Welch SK, Crawford SE, Estes MK (1989) Rotavirus SA11 genome segment 11 protein is a nonstructural phosphoprotein. J Virol 63:3974–3982
68. Zeng CQ, Wentz MJ, Cohen J, Estes MK, Ramig RF (1996) Characterization and replicase activity of double-layered and single-layered rotavirus-like particles expressed from baculovirus recombinants. J Virol 70:2736–2742
69. Zeng CQ-Y, Estes MK, Charpilienne A, Cohen J (1998) The N terminus of rotavirus VP2 is necessary for encapsidation of VP1 and VP3. J Virol 72:201–208

CTMI (2006) 309:189–219

Rotavirus Proteins: Structure and Assembly

J. B. Pesavento[1] · S. E. Crawford[2] · M. K. Estes[2] ·
B. V. Venkataram Prasad[1] (✉)

[1]Verna and Marrs McLean Department of Biochemistry and Molecular Biology, Baylor College of Medicine, Houston, TX 77030, USA
vprasad@bcm.tmc.edu

[2]Department of Molecular Virology and Microbiology, Baylor College of Medicine, Houston, TX 77030, USA

Abstract Rotavirus is a major pathogen of infantile gastroenteritis. It is a large and complex virus with a multilayered capsid organization that integrates the determinants of host specificity, cell entry, and the enzymatic functions necessary for endogenous transcription of the genome that consists of 11 dsRNA segments. These segments encode six structural and six nonstructural proteins. In the last few years, there has been substantial progress in our understanding of both the structural and functional aspects of a variety of molecular processes involved in the replication of this virus. Studies leading to this progress using of a variety of structural and biochemical techniques including the recent application of RNA interference technology have uncovered several unique and intriguing features related to viral morphogenesis. This review focuses on our current understanding of the structural basis of the molecular processes that govern the replication of rotavirus.

1 Introduction

Rotavirus is a major cause of gastroenteritis in young children (under age 5) worldwide. It is responsible for an estimated 600,000–870,000 annual deaths worldwide (Cohen 2001; Kapikian 2002; Midthun and Kapikian 1996; Parashar et al. 2003). Deaths from rotavirus are most prevalent in developing nations, where patients may not always receive adequate medical attention quickly enough. Rotavirus infection occurs primarily in the differentiated enterocytes of the jejunum in the small intestine, which are responsible for digestion and absorption (Moon 1994). Destruction of these cells results in the loss of nutrient and water absorption, followed by dehydration and malnutrition that ultimately can lead to death. An increasing number of reports indicate that rotavirus escapes the gastrointestinal tract resulting in antigenemia in children and viremia in animal models (Blutt et al. 2003) and the detection of rotavirus antigen or RNA in tissues of infected children and adults (Cioc and Nuovo 2002; Hongou et al. 1998; Iturriza-Gomara et al. 2002; Lynch et al. 2001, 2003; Morrison et al. 2001; Pager et al. 2000). The full clinical significance of such extraintestinal virus remains to be determined.

Rotavirus is a member of the *Reoviridae* family, which consists of 11 genera (Fields 1996). Members of this family of viruses have multilayered, nonenveloped, icosahedral capsids with a diameter ranging from approximately 600 to 1000 Å. Each member of this family encapsidates between 10–12 segments of dsRNA. In these viruses, the enzymatic machinery necessary for transcription is housed within an intact core, where the genome is transcribed. Transcriptionally active particles of these viruses are capable of repeated cycles of transcription. These viruses replicate in the cytoplasm of the cell and encode several nonstructural proteins to aid in their replication and morphogenesis inside the host cell.

Biochemical studies on rotaviruses have established much of our basic understanding of rotavirus infectivity, genome transcription, morphogenesis, and virus–cell interactions. The lack of a reverse genetics system for rotavirus, as for all members of the *Reoviridae*, has hampered a detailed understanding of the intracellular functional roles of the virally encoded proteins. In lieu of this, recombinant proteins and virus-like particles (VLPs) have been very useful, not only in rotavirus but also in other dsRNA viruses, for the understanding of both biochemical and structural properties of rotaviral structural and nonstructural proteins. All rotaviral genes of several rotavirus strains have been cloned (Estes and Cohen 1989). These genes have been successfully expressed, and co-expression of specific structural proteins has been shown to result in the spontaneous formation of virus-like particles (VLPs) and other functional complexes (Cohen et al. 1989; Crawford et al. 1994; Estes et al. 1987; Labbe et al. 1991; Mattion et al. 1991, 1992; Zeng et al. 1994). In parallel, structural studies have played an important role to help understand the virus functions in the context of the three-dimensional structures of the virus and virus-encoded individual proteins. An exciting development in the field of rotavirus biology in recent years is the application of RNA interference techniques to study the functional roles of rotaviral proteins during the process of infection (Arias et al. 2004; Campagna et al. 2005; Dector et al. 2002; Lopez et al. 2005; Silvestri et al. 2004).

Until recently, much of our understanding of the structure–function relationships in rotaviruses has come from using electron cryomicroscopy (cryo-EM) techniques (Prasad and Estes 2000). Determination of the overall low-resolution structure of rotavirus using cryo-EM techniques in 1988 (Prasad et al. 1988) began paving the way for more elaborate structural characterization of this virus (Prasad et al. 1990, 1996; Shaw et al. 1993; Yeager et al. 1990, 1994). In addition to providing a detailed description of the architectural features of this large and complex virus, including the topographical locations of all the structural proteins and their stoichiometric proportions, these structural studies using cryo-EM techniques also provided more insight into some of the biological functions of the virus such as trypsin-enhanced infectivity (Crawford et al. 2001), cell entry (Dormitzer et al. 2004, Pesavento et al. 2005), antibody interactions (Prasad et al. 1990; Tihova et al. 2001), endogenous transcription (Lawton et al. 1997a, 2000), and genome organization (Pesavento et al. 2001, 2003b).

More recently, X-ray crystallography has been successfully applied to determine the atomic structures of several of the structural and nonstructural proteins of rotavirus (Deo et al. 2002; Dormitzer et al. 2002, 2004; Groft and Burley 2002; Jayaram et al. 2002; Mathieu et al. 2001). With the lack of an X-ray structure of the rotavirus particle or any of its subassemblies, cryo-EM

reconstructions in combination with X-ray structural information have filled the void to some extent and provided more in-depth structural characterization of the particles at atomic resolution (Dormitzer et al. 2004; Mathieu et al. 2001). With the spectacular success in determining near atomic resolution structures of the bluetongue virus (BTV) core (Grimes et al. 1998) and orthoreovirus core (Reinisch et al. 2000), there is the expectation that the entire rotavirus or homologous subassemblies of rotavirus can be addressed using X-ray crystallography. The status of our current understanding of the three-dimensional structure of this important medical pathogen and some of its proteins in the context of its replication cycle is the main focus of this review.

2 Rotavirus Proteins

The 11 dsRNA segments of the rotavirus genome code for six structural and six nonstructural proteins (Fig. 1a). The naming of the structural proteins is based on their molecular weights, with VP1, the largest at 125 kDa, and VP8*, one of the two proteolytic fragments of VP4, the smallest at 28 kDa. The six structural proteins form the multi-layered capsid of the mature rotavirus particle. The nonstructural proteins, except for NSP1, are essential for virus replication. NSP1 is an RNA-binding protein that directly interacts with IRF-3 (Graff et al. 2002). The loss of NSP1 does not seem to negatively affect rotavirus replication in cultured cells (Silvestri et al. 2004). However, it plays a role in pathogenesis in some animal models (reviewed in Desselberger 1997), likely by antagonizing the type I interferon response to increase viral pathogenesis (Barro and Patton 2005). In this regard, NSP1 shares some similarities with NS1 of influenza virus, although the mechanism of action appears to be unique. The function and roles that the rest of the rotaviral proteins play in the structure and replication of rotavirus are discussed below. A brief summary of the properties of the rotavirus structural and nonstructural proteins is given in Table 1.

3 Capsid Architecture

The architectural features of the mature rotavirus along with the positions of various structural proteins are shown in Fig. 1b and c. The mature infectious rotavirus particle 1000 Å in diameter (including the spikes), is made of three concentric icosahedral protein layers that encapsidate the genome of

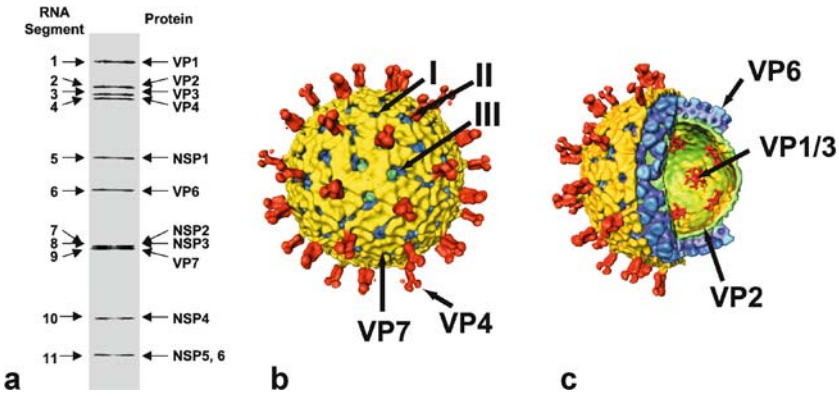

Fig. 1a–c **a** PAGE showing rotavirus RNA segments and gene–protein assignments. The RNA segments are numbered in order of gel migration on the *left* and their encoded protein products are indicated on the *right*. Gene segments 7, 8, and 9 are very close in length and tend to migrate nearly on top of one another. Gene 11 is alternatively processed to produce NSP5 and NSP6. (Torres-Vega et al. 2000; Welch et al. 1989). For protein molecular weights, see Table 1. **b** Surface representation of the mature rotavirus particle (TLP). *Arrows* indicate the three types of aqueous channels, labeled *I*, *II*, and *III*. The 60 VP4 spikes are colored *red* and the 780 copies of VP7 forming the outer capsid layer are shown in *yellow*. (Adapted from Pesavento et al. 2003b). **c** Cut-away of the TLP structure showing the internal structural features. The density due to genomic RNA is removed for clarity. The internal VP6 protein layer is in *blue* and the core VP2 layer in *green*. The flower-shaped VP1–VP3 transcription complex is attached to the inside of the VP2 layer at the five-fold icosahedral axes directly below the type I channels and is colored *red*. (Adapted from Prasad et al. 1996)

11 dsRNA segments. The complete virion is called a triple-layered particle (TLP). Like many of the members of the *Reoviridae,* the capsid architecture is predominantly based on T=13 icosahedral symmetry.

3.1 VP7 Layer and VP4 Spikes

The outer layer of the TLP is composed of two structural proteins: VP7 and VP4. VP7, the major constituent of the outer layer, is a glycoprotein in most rotavirus strains although glycosylation is not required for capsid assembly (Estes 2001). Seven hundred eighty copies of VP7 are grouped as 260 trimers at all the icosahedral and local three-fold axes of a T=13 icosahedral lattice surrounding 132 channels. The outer layer is decorated by 60 spikes, each of which is formed by a dimer of VP4 (Fig. 1b). Thus each rotavirus particle has 120 copies of VP4. The composition of the spike was confirmed by cryo-EM

Table 1 Properties of rotavirus structural and nonstructural proteins[a]

Gene segment	Protein	Mass (kDa)[b]	Post-translational modification(s)	Location (no. of copies)	Functional properties
1	VP1	125	–	SLP (12)	RNA-dependent RNA polymerase, RNA binding, interacts with VP2 and VP3
2	VP2	95	Cleaved	SLP (120)	RNA binding, interacts with VP1
3	VP3	88	–	SLP (12)	Guanylyl and methyl transferase, ssRNA binding, interacts with VP1
4	VP4 (VP5* + VP8*)	85 (58+27)	Cleaved	TLP (120)	Hemagglutinin, neutralization antigen, virulence, protease-enhanced infectivity, cell attachment, fusion region
5	NSP1	53	–	Nonstructural	RNA binding, antagonist of interferon response
6	VP6	45	–	DLP (780)	Hydrophobic trimer, group and subgroup antigen
7	NSP3	34	–	Nonstructural	Important for viral mRNA translation, PABP homologue, RNA binding, interacts with eIF4G
8	NSP2	35	–	Nonstructural	Important for genome replication/packaging, main constituent of viroplasm, NTPase, RNA binding, interacts with NSP5
9	VP7	34	Cleaved signal sequence, high mannose glycosylation and trimming	TLP (780)	RER integral membrane glycoprotein, neutralization antigen, Ca^{++} binding
10	NSP4	20	Uncleaved signal sequence, high mannose glycosylation and trimming	Nonstructural	RER transmembrane glycoprotein, role in morphogenesis, viral enterotoxin
11	NSP5	26	Phosphorylated, *O*-glycosylated	Nonstructural	Constituent of viroplasm, interacts with NSP2, RNA binding, Protein kinase
11	NSP6	11	–	Nonstructural	Constituent of the viroplasm, interacts with NSP5

[a]A number of known functional properties were added, many taken from Estes 2001
[b]Molecular weights based on apparent molecular weights by SDS-PAGE analysis

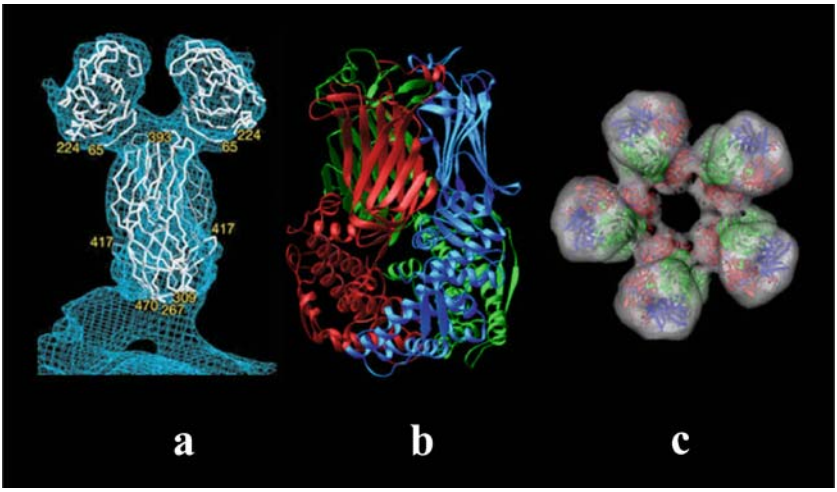

Fig. 2a–c X-ray structure of the VP8*, VP5*, and VP6. **a** X-ray structures of VP5* and VP8* (shown in the backbone representation) fitted into the cryo-EM envelope of the VP4 spike derived from a 12-Å resolution map. (Adapted from Dormitzer et al. 2004). **b** X-ray structure of the VP6 trimer (monomers in *red, green, and blue*) shown in ribbon representation. (Mathieu et al. 2001). **c** Fitting of the X-ray structure of the VP6 trimers into the trimers around the type I channel in the cryo-EM map of the DLP

studies of the rotavirus complexed with VP4-specific monoclonal antibodies (Prasad et al. 1990; Tihova et al. 2001).

The VP4 spike exhibits a distinct structure with two distal globular domains, a central body, and an internal globular domain that is tucked inside the VP7 layer in the peripentonal channel of the T=13 icosahedral lattice (Shaw et al. 1993; Yeager et al. 1994). X-ray structures of proteolytic fragments of VP4, VP8*, and VP5* have been determined (Dormitzer et al. 2002, 2004), and provide strong evidence that the distal globular domain of the VP4 spike is composed of VP8* with the remaining body of the spike consisting of VP5* (Fig. 2a). The crystallographic studies on VP5*, as discussed in connection with cell entry below, have also indicated the possibility of an alternate oligomerization state of VP4 (Dormitzer et al. 2004).

3.2 Aqueous Channels

One of the distinctive features of the rotavirus architecture is the presence of large channels that penetrate through the VP7 and VP6 layers. These channels allow for the passage of aqueous materials and biochemical substrates into

and out of the capsid. The 132 channels at the five-fold and quasi six-fold positions of the T=13 lattice are grouped into three distinct types. Twelve type I channels are located at the five-fold vertices of the capsid (arrows, Fig. 1b). There are 60 type II channels at each of the pentavalent locations surrounding the type I channels, near which VP4 is attached to VP7 and VP6 (Fig. 1b). The 60 type III channels are located at the remaining hexavalent positions on the capsid surrounding the icosahedral three-fold axes (Fig. 1b).

3.3 VP6 Layer

The intermediate layer is formed by the VP6 protein, and is in direct contact with the VP7 later. Particles carrying VP6 on the outside are called double-layered particles (DLPs). The VP6 layer maintains the same icosahedral symmetry as the VP7 layer with 780 copies of VP6 arranged as 260 trimers on a T=13 icosahedral lattice (Fig. 1c). These trimers are located right below the VP7 trimers such that the channels in the VP7 and VP6 layers are in register. The DLP is the transcriptionally competent form of the virus during the replication cycle. VP6 is the major protein of the rotavirus particle by weight. It plays a key role in the overall organization of the rotavirus architecture by interacting with the outer layer proteins, VP7 and VP4, and the inner most layer protein VP2. Thus, it may integrate two principal functions of the virus: cell entry (outer layer) and endogenous transcription (inner layer). The X-ray structure of VP6 has been determined and it shows that VP6 has two domains (Fig. 2b, c) (Mathieu et al. 2001). It its overall structure, VP6 is similar to the VP7 of BTV (Grimes et al. 1997, 1998) and to the μ1 protein of orthoreovirus (Liemann et al. 2002). The distal domain with an eight-stranded antiparallel β-sandwich fold makes contact with the VP7 layer, and the lower domain, consisting of a cluster of α-helices, makes contact with the inner VP2 layer. Fitting of the X-ray structure of VP6 into the cryo-EM structure of the DLP shows that the VP6 trimers interact laterally to form the T=13 layer (Mathieu et al. 2001). There appear to be two types of contacts between the trimers. The contacts, across the quasi two-fold axes and closer to the icosahedral three-fold axis are similar, whereas the contacts are varied as the trimers approach the icosahedral five-fold axis. In contrast to VP7 of BTV (Grimes et al. 1998), the VP6 trimer exhibits extensive lateral interactions involving charged residues.

3.4 VP2 Layer and Transcription Enzyme Complex

Underneath the VP6 layer is the innermost protein layer of the rotavirus structure. The particle structure at this level is referred to as the single-layer

particle (SLP). The SLP houses the dsRNA genome within a protein layer composed of 120 copies of VP2 (Fig. 3a) arranged in an unusual T=1 icosahedral lattice with two molecules in the icosahedral asymmetric unit (Lawton et al. 1997b). All the structurally characterized members of the *Reoviridae* and of other dsRNA viruses such as phi6 and LA viruses exhibit this unique

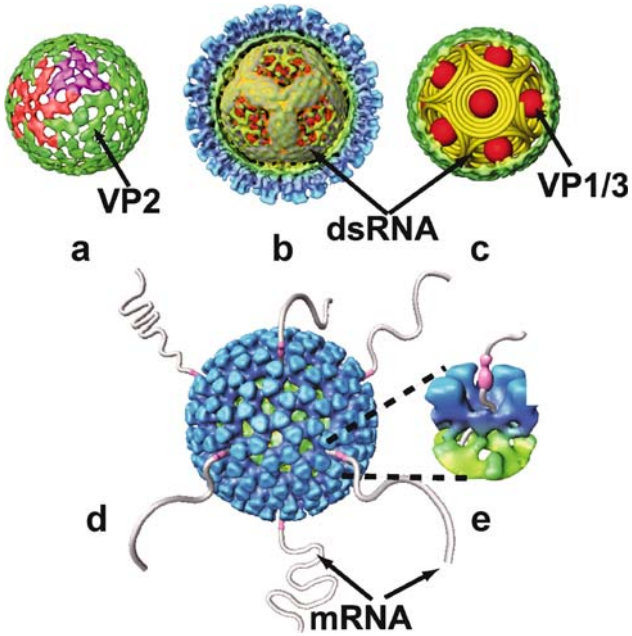

Fig. 3a–e Structural organization of the VP2 layer, genomic dsRNA, and transcription by the rotavirus DLP. **a** Surface representation of the outer portion of VP2. In one of the 60 dimers that constitute this layer, the VP2 subunits are colored in *red and purple* to indicate their orientations and connections to one another. (Adapted from Lawton et al. 1997b). **b** Cut-away view of the DLP. The VP6 and VP2 layers were peeled halfway to expose the outermost layer of genomic organization. The outer layer of RNA has a dodecahedral appearance and surrounds each of the VP1–VP3 star-shaped complexes at the five-fold vertices. (Adapted from Prasad et al. 1996). **c** Model for genome organization around the VP1/3 transcription enzyme complex. The outer *green* portions represent a cut-away view of the VP2 layer. The *yellow spirals* indicate dsRNA gene segments and the *red spheres* represent the VP1/3 transcription complexes. (Adapted from Pesavento et al. 2003). **d** A DLP is shown with mRNA transcripts exiting out by the proposed pathway through the type I channel at a five-fold vertex. The transcripts are colored as *gray strands*. **e** Close-up view of a transcribing DLP. The *pink bowling-pin-shaped density* is the result of the exiting transcript seen in the reconstructions of actively transcribing DLPs. (Lawton et al. 1997a)

organization of the core protein (reviewed in Prasad and Prevelige 2003). The structural organization of the corresponding layers in three of the *Reoviridae* members—BTV (Grimes et al. 1998), orthoreovirus (Reinisch et al. 2000), and rice dwarf virus (Nakagawa et al. 2003)—have been visualized at the atomic level. From the X-ray structure of the BTV core particle, which closely resembles the rotavirus DLP, Grimes et al. (1998) have argued that the pentameric caps of VP3 (equivalent of rotavirus VP2) dimers are building blocks in the assembly of this layer. VP2 expressed using the baculovirus expression system, forms helix-like structures that can form spherical particles at lower concentrations (Zeng et al. 1994) and co-expression of VP2 with VP1 and/or VP3 results in the self-assembly of these proteins into VP1/2, VP2/3, and VP1/2/3 virus-like particles (VLPs) (Wentz et al. 1996). Comparative cryo-EM analysis of these particles showed that 12 copies of the VP1/VP3 transcription enzyme complexes are attached to the inner surface of the VP2 layer at each of the five-fold vertices of the SLP and surrounding each of the transcription complexes is genomic dsRNA (Fig. 1c). Similar structural localization of the enzymes, particularly the polymerase, required for endogenous transcription is found in other members of the *Reoviridae* such as BTV (Gouet et al. 1999; Nason et al. 2004), rice dwarf virus (Nakagawa et al. 2003; Zhou et al. 2001), aquareovirus (Nason et al. 2000), orthoreoviruses (Zhang et al. 2003), and cypovirus (Zhang et al. 1999). Such structural conservation is not surprising given that in all these viruses endogenous transcription of multiple segments is a common and necessary phenomenon. However, a contrasting feature is in regard to the location of the capping enzyme. In viruses such as rotavirus, BTV, and rice dwarf virus, the capping enzyme is suggested to be inside the core layer, whereas in viruses such as the orthoreovirus, aquareovirus, and cypovirus, the capping enzyme forms a distinctive turret structure with a central hole localized at the virion five-fold axis (Hill et al. 1999).

3.5 Genome Organization

The question of how the dsRNA segments are arranged inside the capsid is particularly interesting considering that they are transcribed simultaneously and repeatedly within the confines of the capsid. By analyzing the structural differences between empty virus-like particles (VLPs) and native rotavirus particles, Prasad et al. (1996) showed that a significant portion of the genome is statistically ordered and manifests as concentric layers of density inside the icosahedrally averaged reconstructions of the rotavirus particles (Fig. 3b). Similar structural manifestation of the genome is indeed seen in the X-ray structure of the BTV core and cryo-EM reconstructions of several

other dsRNA viruses. However, because of the implicit use of icosahedral symmetry averaging in the structure determination of these viruses, either by crystallography and or cryo-EM, the precise organization of the individual genome segments is lost. Interestingly, in rotavirus, using a combination of biochemical and cryo-EM techniques, Pesavento et al. (2001) showed that the rotavirus genome can undergo reversible condensation and expansion without affecting the integrity of the surrounding capsid layers. A plausible model that emerges from the available biochemical and structural data for rotaviruses and other dsRNA viruses, is that each genome segment is spooled around a transcription complex (consisting of VP1 and VP3) that is anchored to the inner surface of the VP2 layer at the five-fold axis (Gouet et al. 1999; Pesavento et al. 2003b). Such a model (Fig. 3c) allows for up to 12 independent transcription complexes, each associated with an individual dsRNA segment for concurrent transcription.

4 Reassortants

Although most of the cryo-EM structural studies have been performed on a few selected strains of rotavirus, these studies clearly indicate that the general architectural features are generalizable and independent of the strains. Cryo-EM structural studies have been reported on several rotavirus reassortants. These structural studies indicate that the capsid structure remains unaltered except for the VP4 spikes. Rotavirus reassortment occurs widely in nature and represents a major force for genetic diversity along with point mutations and gene rearrangements (Desselberger 1996; Iturriza-Gomara et al. 2001). The structures of reassortants show that while VP4 generally maintains the parental structure, when moved to a heterologous protein background, in certain reassortants there are subtle alterations in the conformation of VP4 (Pesavento et al. 2003a). The alterations in the VP4 conformation correlated with the observation of unexpected VP4-associated phenotypes. Interactions between heterologous VP4 and VP7 in reassortants expressing unexpected phenotypes appear to induce the conformational alterations seen in VP4.

5 Protease-Enhanced Infectivity

From their locations in the structure of rotavirus, VP7 and VP4 are obvious candidates to be implicated in the cell entry processes. Although early studies

implicated VP7 in the cell entry process (Fukuhara et al. 1988; Sabara et al. 1985), subsequent studies have increasingly indicated the involvement of VP4 not only in cell attachment and cell penetration, but also in hemagglutination, neutralization, virulence, and host range (Burns et al. 1988; Fiore et al. 1991; Kirkwood et al. 1998; Lopez et al. 1985; Ludert et al. 1996, 1998; Mackow et al. 1988). Prior to its interaction with the host cell, VP4 is proteolytically cleaved for efficient internalization of rotaviruses into cells. This is particularly relevant considering that rotavirus replication takes place in enterocytes in the small intestine, an environment rich in proteases. Proteolytic cleavage of VP4 enhances viral infectivity by several fold (Arias et al. 1996; Estes et al. 1981) and facilitates virus entry into cells (Kaljot et al. 1988). Proteolysis of VP4 generates two fragments, VP8* (aa 1–247) and VP5* (248–776) and these fragments remain associated with the virion (Fiore et al. 1991; Lopez et al. 1985). Trypsinized viruses enter cells more efficiently without using the endosomal pathway, compared to particles that are not trypsinized (Kaljot et al. 1988; Keljo et al. 1988). In vitro experiments have shown that proteolytically activated particles, as well as recombinant VP5*, possess lipophilic activity (Dowling et al. 2000; Nandi et al. 1992; Ruiz et al. 1994). Although rotavirus is a nonenveloped virus, it is interesting to note some parallels between rotavirus VP4 and cell attachment proteins in enveloped viruses such as influenza viruses. Proteolytic cleavage is as essential for infection in influenza virus as it is for rotavirus, because it primes the HA (hemagglutinin) protein for an ensuing irreversible conformational change, which occurs in the low-pH environment of endosomes prior to membrane fusion. The rotavirus VP5* and VP8* trypsin cleavage products are analogous to the proteolytically cleaved fragments of the influenza virus hemagglutinin, HA1 and HA2. Much like rotavirus VP8*, the HA1 subunit plays an accessory role by providing initial binding to the cell via sialic acid containing receptors. HA2 functions more like VP5*, as it is required and sufficient on its own for cell fusion (Wiley and Skehel 1987).

5.1 Trypsin-Induced Unique Order-to-Disorder Transition in the Spike

The molecular mechanism of increased infectivity by proteolysis is not well understood. To understand the structural basis of trypsin-enhanced infectivity in rotaviruses, Crawford et al. (2001) examined the biochemical and structural properties of rotaviruses grown in the absence (nontrypsinized rotavirus, NTR) or presence (trypsinized rotavirus, TR) of trypsin. The infectivity of the NTR particles is drastically reduced, as anticipated. Exogenous addition of trypsin to NTR particles increased their infectivity but to nowhere

near the level of infectivity seen with TR particles. Despite clear biochemical indications for the presence of uncleaved VP4 in correct stoichiometric proportion in the NTR particles, the spikes in the cryo-EM reconstruction of these particles are not visualized in contrast to the well defined spike structure seen in the particles that are grown in the presence of trypsin (Fig. 4a , b).

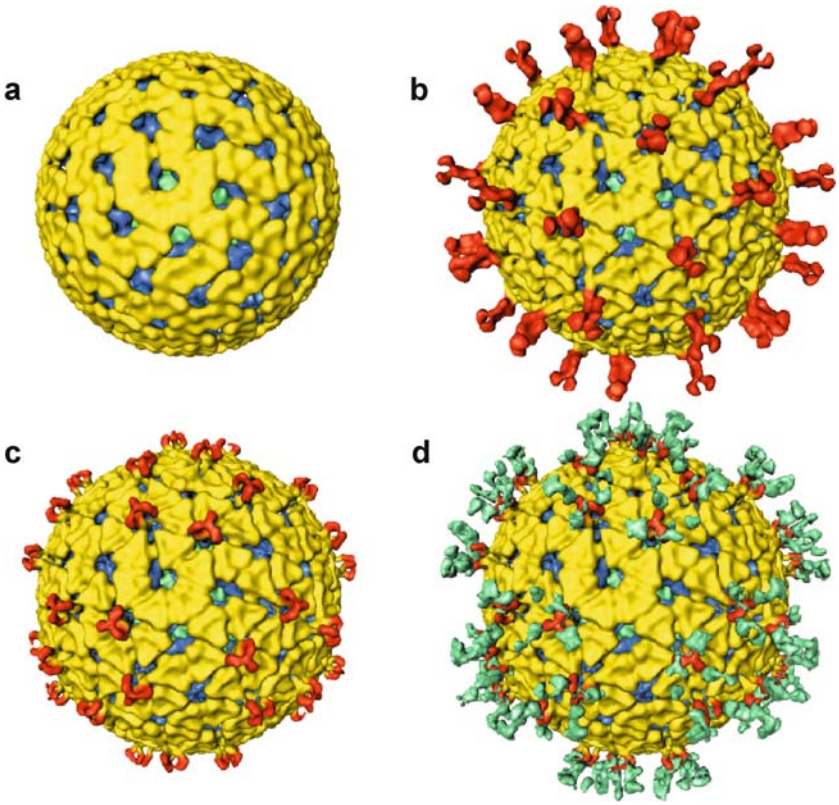

Fig. 4a–d Effects of trypsin and pH on the spike structure. The highly flexible VP4 spike protein on rotavirus assumes altered conformations due to proteolytic cleavage or encountering high pH. **a** Rotavirus grown in the absence of trypsin (*upper panel*) has low infectivity and the VP4 spike is disordered on particles (i.e., not represented in cryo-EM reconstructions). (Crawford et al. 2001). **b** Proteolytically cleaved rotavirus has high infectivity and a well-ordered spike appearing dimeric at the top. **c** Treatment of rotavirus with ~pH 11 induces a conformational change in the spike resulting in a trilobed stunted spike and unmasks a cell binding domain that appears to be involved in infection of cells by a sialic acid-independent mechanism. (Pesavento et al. 2005). **d** The high-pH-altered short spikes are recognized by VP5*-specific 2G4-Fab fragments, and three Fab fragments are seen binding to each altered spike (Pesavento et al. 2005)

These results thus indicate that trypsin cleavage imparts structural order to the VP4 spikes on de novo synthesized virus particles and that these ordered spikes make virus entry into cells more efficient (Crawford et al. 2001).

The idea of a trypsin-induced disorder-to-order transition is indeed unique and has not been documented with any other virus thus far. Does trypsin act from within or outside of cells? One possibility is that during virus infection, trypsin acts outside cells on the newly formed VP4 and that this trypsinized VP4 is able to assemble properly onto the rotavirus particles. This hypothesis is consistent with the finding, using confocal microscopy of virus-infected MA104 cells, that high amounts of VP4 are present at the plasma membrane approximately 3 h after infection and that the N-terminal region, i.e., VP8*, is accessible to antibodies (Nejmeddine et al. 2000). Similar results were obtained with cells transfected with a VP4 plasmid, suggesting that VP4 targeting depends on signals in the protein rather than on the presence of virus particles. Targeting of VP4 to the plasma membrane appears to be a general phenomenon as it is seen in both polarized and nonpolarized cells (Sapin et al. 2002). Further structural and biochemical studies are needed to provide a better understanding of how and where trypsin affects spike assembly.

6 Cell Entry

The consensus opinion that has emerged from several recent studies is that rotavirus cell entry is a coordinated multistep process involving sequential interactions with sialic acid (SA) -containing receptors in the initial cell attachment step. Next, interactions are throught to occur with hsp70, and integrins such as αvβ3, α4β1, α2β1 during the subsequent postattachment steps (reviewed in Lopez and Arias 2004). In the entry process, the VP8* domain is involved in the interactions with SA, whereas VP5* is implicated in the interactions with integrins. Involvement of VP8* in cell attachment is further supported by studies that show that several VP8*-specific neutralizing mAbs block cell attachment. The X-ray structure of the VP8*–SA complex has shown that VP8* has a beta-sandwich fold similar to that of galectins, whose natural ligands are carbohydrates (Dormitzer et al. 2002). The SA binds to a shallow pocket between the two β-sheets, a region that is distinct from the carbohydrate binding pocket in the galectins, which is blocked in the VP8*. Involvement of SA during rotavirus infections is not an essential step in all rotavirus strains. For many of the rotavirus strains, including human rotaviruses, cell entry is SA-independent (Ciarlet et al. 2001). In these viruses, the majority of neutralizing mAbs select mutations in VP5* (Kirkwood et al.

1996, 1998; Padilla-Noriega et al. 1995), suggesting that cell entry is mediated mainly by the VP5*. An interesting question is what the role of VP8* might be in these SA-independent viruses.

6.1 Possible Structural Alterations in VP4 During Cell Entry

How does VP4 facilitate such multistep entry processes in rotavirus? It is possible that VP4 undergoes distinct conformational changes at various stages during cell entry to mask certain epitopes and reveal others in order to optimally interact with different receptors and the cellular membrane. Such distinct conformational states during cell entry processes have been observed in viruses such as influenza virus (Bullough et al. 1994), flavivirus (Modis et al. 2004; Mukhopadhyay et al. 2003), alphavirus (Gibbons et al. 2004) and picornaviruses (Belnap et al. 2000). Recent studies on rotavirus clearly point to conformational changes of VP4 during cell entry. In addition to the drastic conformational change from a flexible to a rigid-bilobed spike structure upon trypsinization, as discussed above (Crawford et al. 2001), recent X-ray crystallographic studies of VP5* (Dormitzer et al. 2004) and cryo-EM studies in high-pH-treated rotaviruses suggest the possibility of further structural changes in the spike structure that may be relevant during rotavirus cell entry.

6.1.1 Is the VP4 Spike a Trimer?

In the crystal structure, VP5* is a trimer with substantial intersubunit interactions (Dormitzer et al. 2004). That is, by itself, VP5* has a propensity to form strong trimers. Why, then, in the cryo-EM structures is the spike a dimeric structure? Two individual monomers of VP5* clearly fit into the main body of the spike in the cryo-EM structure (Fig. 2a). A proposed possibility is that each spike is indeed a trimer of VP4, and upon trypsinization, two of them form the visible spike, as seen in the cryo-EM reconstruction of the trypsinized rotavirus particles, with the other monomer being floppy and not visible in the reconstruction (Dormitzer et al. 2004). During cell entry, by a yet unknown entry-associated event, the floppy VP4 monomer together with the other two molecules, trimerizes as seen in the VP5* crystal structure.

6.1.2 pH-Induced Changes of the Spike: Implication for Cell Entry and Antibody Neutralization

Recent studies on high-pH-treated rotavirus have uncovered an interesting phenomenon that appears to substantiate the above proposal (Pesavento et al.

2005). At elevated pH, the spike undergoes a drastic irreversible conformational change and becomes stunted with a pronounced tri-lobed appearance (Fig. 4c). Biochemical analysis of pH-treated particles indicates that VP4 is present in the same amount as in native particles. Three Fab fragments of the VP5*-specific neutralizing monoclonal antibody, 2G4, are seen to bind to the altered spike structure (Fig. 4d). One strong possibility from these observations is that VP4 has undergone a dimer to trimer transition. Despite the loss of infectivity and the ability to hemagglutinate, the high-pH-treated particles surprisingly exhibit SA-independent cell binding, in contrast to native virions, which exhibit SA-dependent cell binding. These studies have also shown that the binding of 2G4-Fab to native particles completely protects the spikes from undergoing pH-induced conformational changes and preserves the SA-dependent cell binding and hemagglutinating functions of the virion. However, when 2G4 is bound to the pH-altered particles, cell binding is completely lost. A hypothesis that emerges from this study is that high-pH treatment triggers a conformational change that mimics a post-SA attachment step to expose an epitope recognized by one of the downstream receptors in the rotavirus cell entry process, and the mechanism by which the 2G4 antibody neutralizes infectivity is by preventing this conformational change.

In their cell attachment, the pH-treated particles appear to resemble the nar3 mutant of rhesus rotavirus (RRV) (Graham et al. 2003; Zarate et al. 2000a). This mutant exhibits SA-independent cell binding in contrast to its parental strain and has been shown to attach to the cell surface by interacting with integrin $\alpha 2\beta 1$ through the DGE motif in VP5*. As in the high-pH-treated particles, 2G4 antibody binding to the nar3 mutant inhibits cell binding (Zarate et al. 2000b). A distinct possibility is that the DGE motif (residues 308–310) becomes exposed in the pH-treated particles, and the 2G4-Fab inhibits cell binding of the pH-treated particles by sterically hindering the accessibility of this motif. In the studies by Pesavento et al. (2005), pH was used to trigger the conformational changes. During a natural infection process, it is not known what triggers the conformational changes necessary to interact with downstream receptors. As yet there are no structural studies reported of rotavirus complexed with any of the multiple, proposed receptors molecules.

7
Endogenous Transcription

The next stage in the replication cycle of the virus is the transcription of dsRNA segments into viable mRNA molecules that can be processed for

template generation and viral protein production. During the process of cell entry, the outer layer is removed and the resulting DLPs in the cytoplasm become transcriptionally competent (Estes et al. 2001). The dsRNA segments are transcribed within the structural confines of the DLP. Cryo-EM structural studies have shown that DLPs remain structurally intact during the process of transcription, and the nascent transcripts exit through the type I channels that penetrate the inner VP2 and outer VP6 capsid layers of the DLP at the five-fold vertices (Fig. 3d) (Lawton et al. 1997a). The DLP possesses the complete enzymatic activities needed to synthesize not only mRNA transcripts but also to properly guanylate and methylate the cap structure at the 5′ end of each mRNA to facilitate translation by the cellular translation machinery. These enzymatic functions are carried out by VP1, the RNA-dependent-RNA polymerase (Valenzuela et al. 1991), and VP3, a guanylyltransferase and methyltransferase (Chen et al. 1999). While DLPs are transcriptionally competent both in vitro and in vivo, the TLPs are transcriptionally incompetent. Certain monoclonal antibodies, which bind to the distal end of VP6, almost 140 Å away from the site of transcription initiation, inhibit transcription (Ginn et al. 1992; Kohli et al. 1993; Thouvenin et al. 2001). From cryo-EM studies of DLPs complexed with these antibodies, it has been proposed that binding of ligand, such as an antibody or VP7, induces a conformation change at the interface of the VP2 and VP6 layers to inhibit sustained elongation and translocation of the transcripts (Lawton et al. 1999). Further higher-resolution structural analysis of TLPs and DLPs is necessary to understand the structural basis of transcriptional activation and inhibition.

8
Genome Replication and Packaging

Following endogenous transcription and release of the transcripts, the rotavirus replication cycle may be viewed as having three subsequent major stages: (1) translation and synthesis of the viral proteins; (2) replication, genome packaging, and DLP assembly; (3) budding of the newly formed DLPs into the ER and assembly of the outer layer to form mature TLPs (reviewed in Estes 2001). The positive-stranded RNA transcripts encode the rotaviral proteins and function as templates for production of negative strands to make the progeny dsRNA. Recent studies with siRNA have indicated that there are likely to be two separate pools of mRNA for these distinct functions (Silvestri et al. 2004).

8.1
NSP3 and Genome Translation

The nonstructural protein NSP3 is implicated in the specific recognition of the rotaviral mRNAs and in facilitating their translation using the cellular machinery (Piron et al. 1998, 1999; Vende et al. 2000). NSP3 is a functional homologue of cellular poly(A) binding protein (PABP). While the N-terminal domain of NSP3 interacts with the 3′-consensus sequence of the rotaviral viral mRNAs, the C-terminal domain interacts with eIF4G to enable circularization of viral mRNA and its delivery to the ribosomes for viral protein synthesis. The X-ray structures of both the N-terminal domain complexed with the consensus rotaviral mRNA sequence, and that of the C-terminal domain bound to a peptide that corresponds to the binding site on eIF4G have been determined (Deo et al. 2002; Groft and Burley 2002). These studies clearly indicate that NSP3 functions as a homodimer. Both the domains have novel folds. While the RNA binding domain forms a heart-shaped asymmetric dimer, the C-terminal domain forms a rod-shaped symmetric dimer. The dimeric N-terminal domain tightly binds to the consensus 3′-end of the mRNA inside a tunnel formed at the dimeric interface. The binding of NSP3 to the mRNA had also been proposed as a possible mechanism to transport newly made mRNAs to viroplasms for subsequent replication.

8.2
NSP2 and NSP5

Replication, genome packaging and assembly of the DLP occur in perinuclear, nonmembrane-bound, electron dense inclusions called viroplasms, which appear 2–3 h after infection. Several in vivo and in vitro studies have strongly implicated two of the nonstructural proteins NSP2 and NSP5, not only in the formation of the viroplasm, but also in genome replication and packaging (Afrikanova 1998; Aponte et al. 1996; Gallegos and Patton 1989; Kattoura et al. 1994; Petrie et al. 1984). Co-expression of NSP2 and NSP5 in uninfected cells form viroplasm-like structures (Fabbretti et al. 1999). NSP5 is a dimeric phosphoprotein rich in Ser and Thr residues that undergoes O-linked glycosylation (Afrikanova et al. 1996; Poncet et al. 1997) . In co-transfection experiments with NSP5 and NSP2, NSP2 has been shown to upregulate phosphorylation of NSP5 (Afrikanova 1998). In vivo studies have shown that these two proteins along with VP1, the viral RNA polymerase, are co-localized in the viroplasms and that they are the main constituents of the replication intermediates (reviewed in Taraporewala and Patton 2004). Further evidence for the involvement of NSP2 and NSP5 in the formation of viroplasms, genome replication, and virion assembly is provided by recent studies using siRNA

techniques, which showed that suppression of either NSP2 or NSP5 expression inhibits the formation of viroplasms, genome replication, and viral assembly (Campagna et al. 2005; Silvestri et al. 2004). Noting that the viral mRNA located outside the viroplasms that are involved in translation are susceptible to siRNA-induced degradation, while the mRNA in the viroplasms that undergo replication are not, Silvestri et al. (2004) have suggested that the transcriptionally active progeny DLPs form foci for the formation of the viroplasms, thus eliminating the necessity for two spatially distinct locations for transcription and replication. This model eliminates the necessity of having to transport viral mRNAs and viral proteins, as per an earlier model, to the viroplasms for negative strand synthesis and subsequent DLP assembly and genome packaging.

Biochemical studies on recombinant NSP2 have shown that it readily forms an octamer and has NTPase (nucleotide triphosphatase), ssRNA-binding, and helix destabilizing activities (Taraporewala et al. 1999, 2001; Taraporewala and Patton 2001). Based on these properties, it has been suggested that NSP2 may function as a molecular motor using the energy derived from NTP hydrolysis to facilitate genome packaging. The X-ray structure of NSP2 has provided some insights into the locations of NTP and RNA binding sites (Jayaram et al. 2002). NSP2 is a two-domain α/β protein. The two domains are separated by a deep cleft. The N-terminal domain is predominantly α-helical with only a few β-strands, whereas the C-terminal domain has a twisted antiparallel β-sheet with flanking α-helices. Despite any detectable sequence similarity, the polypeptide fold in this domain is highly similar to that observed in the HIT (histidine triad) family of nucleotidyl hydrolases (Lima 1997). Based on this similarity, it was suggested that this domain contains the NTP binding pocket. Recent mutational analysis based on the structural observations is consistent with such a prediction (Carpio et al. 2004). NSP2 forms a doughnut-shaped octamer with a 35-Å-wide central hole, and four grooves related by a four-fold axis on the sides of the octamer. These grooves, lined with basic residues, are suggested to be the sites for RNA binding. Thus while the NTPase activity is localized in the monomeric subunit, the ability to bind RNA and other proteins such as NSP5 and VP1 may require the formation of the octamer.

Based on the structure of NSP2 and its functional properties, it is tempting to speculate that the replication complex is organized around the NSP2 octamer providing a platform or a scaffold (Jayaram et al. 2004). It is possible that the hydrophobic side of the octamer, around the four-fold axis, may bind to VP1; given that NSP5 is an acidic protein, the basic grooves of the NSP2 octamer may be the binding sites for NSP5. Although the role of NSP5 in the overall replication process remains to be elucidated, it is plausible that by having its binding site on NSP2 overlap with that of the RNA binding site, the

function of NSP5 is to regulate the binding of RNA by NSP2 during replication and packaging. It is still unclear whether NSP6, which is encoded by an alternating open reading frame in the gene segment 11 along with NSP5 and is also present in the viroplasms, has any role in genome replication and/or packaging. NSP6 interacts with NSP5 and it is suggested that it might have a regulatory role in the self-association of NSP5 (Torres-Vega et al. 2000).

8.3 A Working Model for Genome Encapsidation in Rotavirus

How the correct set of 11 segments of dsRNA get encapsidated into each virion remains entirely unclear. Given that multiple segments of varied length have to be encapsidated, and that each one has to occupy different vertices to associate with a transcription enzyme complex, as per the current model of genome organization, it is unlikely that the dsRNA genome segments are encapsidated into preformed empty capsids as in some of the bacteriophages. Instead, the encapsidation could be concurrent with the capsid assembly as proposed by Pesavento et al. (2003). In this model (Fig. 5), the capsid assembly begins with the association of 12 units, each unit consisting of pentamers of VP2 dimers in complex with a transcription enzyme complex (VP1/VP3) and a genome segment, to form the SLP and provide a scaffold for the subsequent assembly

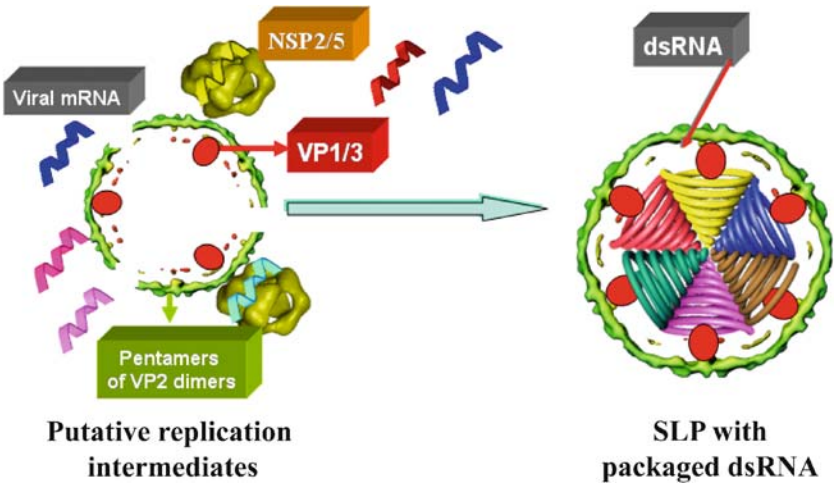

Fig. 5 A working model for genome encapsidation in rotavirus. Based on the available biochemical and structural data, one possible model for genome encapsidation is shown. All the components that are likely to be involved in this process are indicated. See Sect. 8.3 in the text for details

of the VP6 trimers leading to the assembly of a DLP. The proteinaceous parts of each of these units may represent the replicase complex in which mRNA, brought in with the aid of nonstructural proteins (NSP2/NSP5), is fed into the enzyme complex for the synthesis of the negative strand and the formation of the duplex RNA, which gets spooled around the enzyme complex. In such a process, NSP5 may function as an adapter, with its ability to interact with VP2 and to facilitate interactions between NSP2 and the VP1–VP3–VP2 complex (Berois et al. 2003). This model raises an important question as to how a correct set of 11 (as in rotavirus) distinct segments is brought together. It is possible that specific RNA–RNA interactions coordinate this process.

9
Maturation and Release

Maturation and release represent the final steps of the rotavirus replication cycle. Once formed, DLPs bud from the viroplasms into the proximally located ER (Estes 2001), and by a mechanism that is not clear DLPs acquire the outer layer consisting of VP7 and VP4. This budding process is facilitated by the nonstructural proteins NSP4, which has a binding site for VP6 (Au et al. 1989, 1993; Meyer et al. 1989; Tian et al. 1996). Both NSP4 and the outer layer protein VP7 are synthesized on the ER-associated ribosomes and co-translationally inserted into the ER membrane. NSP4 is a predominantly α-helical glycoprotein that forms a tetramer with its C-terminal 131 residues on the cytoplasmic side of the ER. The C-terminal residues form a binding site for VP6 (O'Brien et al. 2000; Taylor et al. 1992, 1993). As yet there is no structural information on NSP4, except that of a small region that is responsible for tetramerization (Bowman et al. 2000). Recent studies using RNA interference have shown that accumulation of rotaviral proteins and indeed, DLPs and TLPs, are blocked by silencing the expression of the NSP4 gene (Lopez et al. 2005). This result indicates that NSP4 may have previously unexpected functions related to virus maturation. Aside from its role in viral morphogenesis, NSP4 is a viral enterotoxin capable of inducing diarrhea on its own in mice (Ball et al. 1996; Estes 2001, 2003; Sasaki et al. 2001).

During the budding process, DLPs get enveloped transiently in the ER. This may be an intermediate stage during acquisition of the VP7 layer. Silencing the expression of VP7 does not affect the assembly of DLPs but leads to the accumulation of enveloped DLPs in the ER, thereby suggesting that VP7 is required for removal of the lipid envelope (Lopez et al. 2005). Although the assembly of the VP7 layer onto the DLPs, as generally agreed, takes place in the ER, where and how the spike protein VP4, which is synthesized on free

cytosolic ribosomes, is assembled onto the particles is unclear. The cryo-EM structure of the particles produced by silencing the VP4 gene during virus infection clearly shows all the features of the native TLP structure except for the VP4 spikes (Arias et al. 2004; Dector et al. 2002). These results suggest that neither the proper assembly of VP7 nor the budding of the DLPs into the ER require VP4. Based on the results that indicate VP4 alone can traffic to the plasma membrane of the infected cells (Nejmeddine et al. 2000; Sapin et al. 2002), a likely possibility is that assembly of VP4 onto viral particles may take place at the plasma membrane shortly before particle release and that VP4 may be involved in the early stages of virus release. The presence of trypsin or a protease outside of cells may access the VP4 and bring about appropriate structural alterations for its proper assembly on the particles with the VP7 layer already assembled.

10 Conclusion

In last few years, there has been tremendous progress in our understanding of the structural and biochemical aspects of a variety of the molecular processes involved in rotavirus morphogenesis, including protease enhanced infectivity, cell entry, antibody neutralization, genome replication, and maturation. This has been made possible by the appropriate use of structural techniques such as cryo-EM and X-ray crystallography either independently or in combination. Particularly noteworthy are the insights provided by the atomic structures of several of the rotaviral proteins, including VP4, VP6, NSP3, NSP4, and NSP2. In parallel, this progress was facilitated by equally important advances in the molecular biology of rotaviruses, resulting in recombinant proteins and virus-like particles, along with the successful application of RNA interference techniques. These studies have uncovered several unique aspects of rotavirus morphogenesis and as always raise several intriguing new questions about these viruses such as:

1. How and where does the assembly of VP4 take place in infected cells?
2. How does trypsin facilitate proper assembly of the VP4 spike?
3. How does VP4 facilitate interactions with the variety of proposed receptors?
4. How is the endogenous transcription controlled by the addition or the removal of the outer capsid layer?

5. How is the process of genome replication, packaging and assembly orchestrated and controlled by the interplay between structural and nonstructural proteins?
6. What is the structural and molecular basis of NSP4 function both in relation to viral pathogenesis and morphogenesis?

Dissecting the rotavirus functions in terms of its individual proteins would have been much easier if a reverse genetics system was available. Given the complexity of this virus, or any other member of the *Reoviridae* for that matter, establishing such a system is indeed a daunting task. A major achievement in the near future, as a result of continued and better understanding of the processes that control rotavirus morphogenesis, could be the establishment of a reverse genetics system.

Acknowledgements This work was supported by NIH grants AI-36040 (B.V.V.P.) and DK-30144 (M.K.E.) and a grant from R. Welch foundation (B.V.V.P). J.B.P. acknowledges the support of NSF training grant BIR-9256580.

References

Afrikanova I, Miozzo MC, Giambiagi S, Burrone O (1996) Phosphorylation generates different forms of rotavirus NSP5. J Gen Virol 77:2059–2065

Afrikanova I, Fabbretti E, Miozzo MC, Burrone OR (1998) Rotavirus NSP5 phosphorylation is up-regulated by interaction with NSP2. J Gen Virol 79:2679–2686

Aponte C, Poncet D, Cohen J (1996) Recovery and characterization of a replicase complex in rotavirus-infected cells by using a monoclonal antibody against NSP2. J Virol 70:985–991

Arias CF, Romero P, Alvarez V, Lopez S (1996) Trypsin activation pathway of rotavirus infectivity. J Virol 70:5832–5839

Arias CF, Dector MA, Segovia L, Lopez T, Camacho M, Isa P, Espinosa R, Lopez S (2004) RNA silencing of rotavirus gene expression. Virus Res 102:43–51

Au KS, Chan WK, Burns J W, Estes MK (1989) Receptor activity of rotavirus nonstructural glycoprotein NS28. J Virol 63:4553–4562

Au KS, Mattion NM, Estes MK (1993) A subviral particle binding domain on the rotavirus nonstructural glycoprotein NS28. Virology 194:665–673

Ball JM, Tian P, Zeng CQ, Morris AP, Estes MK (1996) Age-dependent diarrhea induced by a rotaviral nonstructural glycoprotein. Science 272:101–104

Barro M, Patton J T (2005) Rotavirus nonstructural protein 1 subverts innate immune response by inducing degradation of IFN regulatory factor 3. Proc Natl Acad Sci U S A 102:4114–4119

Belnap DM, Filman DJ, Trus BL, Cheng N, Booy FP, Conway JF, Curry S, Hiremath CN, Tsang SK, Steven AC, Hogle JM (2000) Molecular tectonic model of virus structural transitions: the putative cell entry states of poliovirus. J Virol 74:1342–1354

Berois M, Sapin C, Erk I, Poncet D, Cohen J (2003) Rotavirus nonstructural protein NSP5 interacts with major core protein VP2. J Virol 77:1757–1763

Blutt SE, Kirkwood CD, Parreno V, Warfield KL, Ciarlet M, Estes MK, Bok K, Bishop RF, Conner ME (2003) Rotavirus antigenaemia and viraemia: a common event? Lancet 362:1445–1449

Bowman GD, Nodelman IM, Levy O, Lin SL, Tian P, Zamb TJ, Udem SA, Venkataraghavan B, Schutt CE (2000) Crystal structure of the oligomerization domain of NSP4 from rotavirus reveals a core metal-binding site. J Mol Biol 304:861–871

Bullough PA, Hughson FM, Skehel JJ, Wiley DC (1994) Structure of influenza haemagglutinin at the pH of membrane fusion. Nature 371:37–43

Burns JW, Greenberg HB, Shaw RD, Estes MK (1988) Functional and topographical analyses of epitopes on the hemagglutinin (VP4) of the simian rotavirus SA11. J Virol 62:2164–2172

Campagna M, Eichwald C, Vascotto F, Burrone OR (2005) RNA interference of rotavirus segment 11 mRNA reveals the essential role of NSP5 in the virus replicative cycle. J Gen Virol 86:1481–1487

Carpio RV, Gonzalez-Nilo FD, Jayaram H, Spencer E, Prasad BV, Patton JT, Taraporewala ZF (2004) Role of the histidine triad-like motif in nucleotide hydrolysis by the rotavirus RNA-packaging protein NSP2. J Biol Chem 279:10624–10633

Chen D, Luongo CL, Nibert ML, Patton J T (1999) Rotavirus open cores catalyze 5′-capping and methylation of exogenous RNA: evidence that VP3 is a methyltransferase. Virology 265:120–130

Ciarlet M, Crawford SE, Estes MK (2001) Differential infection of polarized epithelial cell lines by sialic acid-dependent and sialic acid-independent rotavirus strains. J Virol 75:11834–11850

Cioc AM, Nuovo GJ (2002) Histologic and in situ viral findings in the myocardium in cases of sudden, unexpected death. Mod Pathol 15:914–922

Cohen J (2001) Rethinking a vaccine's risk. Science 293:1576–1577

Cohen J, Charpilienne A, Chilmonczyk S, Estes MK (1989) Nucleotide sequence of bovine rotavirus gene 1 and expression of the gene product in baculovirus. Virology 171:131–140

Crawford SE, Labbe M, Cohen J, Burroughs MH, Zhou YJ, Estes MK (1994) Characterization of virus-like particles produced by the expression of rotavirus capsid proteins in insect cells. J Virol 68:5945–5922

Crawford SE, Mukherjee SK, Estes MK, Lawton JA, Shaw AL, Ramig RF, Prasad BV (2001) Trypsin cleavage stabilizes the rotavirus VP4 spike. J Virol 75:6052–6061

Dector MA, Romero P, Lopez S, Arias CF (2002) Rotavirus gene silencing by small interfering RNAs. EMBO Rep 3:1175–1180

Deo RC, Groft CM, Rajashankar KR, Burley SK (2002) Recognition of the rotavirus mRNA 3′ consensus by an asymmetric NSP3 homodimer. Cell 108:71–81

Desselberger U (1996) Genome rearrangements of rotaviruses. Arch Virol Suppl 12:37–51

Desselberger U (1997) Viral factors determining rotavirus pathogenicity. Arch Virol Suppl 13:131–139

Dormitzer PR, Sun ZY, Wagner G, Harrison SC (2002) The rhesus rotavirus VP4 sialic acid binding domain has a galectin fold with a novel carbohydrate binding site. EMBO J 21:885–897

Dormitzer PR, Nason EB, Prasad BV, Harrison SC (2004) Structural rearrangements in the membrane penetration protein of a non-enveloped virus. Nature 430:1053–1058

Dowling W, Denisova E, LaMonica R, Mackow ER (2000) Selective membrane permeabilization by the rotavirus VP5* protein is abrogated by mutations in an internal hydrophobic domain. J Virol 74:6368–6376

Estes MK (2001) Rotaviruses and their replication. In: Fields BN, Knipe RM, Chanock MS et al (eds) Virology. Lippincott-Raven, Philadelphia, pp 1747–1785

Estes MK (ed) (2003) The rotavirus NSP4 enterotoxin: Current status and challenges. Elsevier, Amsterdam

Estes MK, Cohen J (1989) Rotavirus gene structure and function. Microbiol Rev 53:410–449

Estes MK, Graham DY, Mason BB (1981) Proteolytic enhancement of rotavirus infectivity: molecular mechanisms. J Virol 39:879–888

Estes MK, Crawford SE, Penaranda ME, Petrie BL, Burns JW, Chan WK, Ericson B, Smith GE, Summers MD (1987) Synthesis and immunogenicity of the rotavirus major capsid antigen using a baculovirus expression system. J Virol 61:1488–1494

Estes MK, Kang G, Zeng CQ, Crawford SE, Ciarlet M (2001) Pathogenesis of rotavirus gastroenteritis. Novartis Found Symp 238:82–96; discussion 96–100

Fabbretti E, Afrikanova I, Vascotto F, Burrone OR (1999) Two non-structural rotavirus proteins, NSP2 and NSP5, form viroplasm-like structures in vivo. J Gen Virol 80:333–339

Fields BN (1996) The Reoviridae. In: Fields BN, Knipe RM, Chanock MS et al (eds) Virology. Lippincott-Raven, Philadelphia, pp 1553–1555

Fiore L, Greenberg HB, Mackow ER (1991) The VP8 fragment of VP4 is the rhesus rotavirus hemagglutinin. Virology 181:553–563

Fukuhara N, Yoshie O, Kitaoka S, Konno T (1988) Role of VP3 in human rotavirus internalization after target cell attachment via VP7. J Virol 62:2209–2218

Gallegos CO, Patton JT (1989) Characterization of rotavirus replication intermediates: a model for the assembly of single-shelled particles. Virology 172:616–627

Gibbons DL, Vaney MC, Roussel A, Vigouroux A, Reilly B, Lepault J, Kielian M, Rey FA (2004) Conformational change and protein-protein interactions of the fusion protein of Semliki Forest virus. Nature 427:320–325

Ginn DI, Ward RL, Hamparian VV, Hughes JH (1992) Inhibition of rotavirus in vitro transcription by optimal concentrations of monoclonal antibodies specific for rotavirus VP6. J Gen Virol 73:3017–3022

Gouet P, Diprose JM, Grimes JM, Malby R, Burroughs JN, Zientara S, Stuart DI, Mertens PP (1999) The highly ordered double-stranded RNA genome of bluetongue virus revealed by crystallography. Cell 97:481–490

Graff JW, Mitzel DN, Weisend CM, Flenniken ML, Hardy ME (2002) Interferon regulatory factor 3 is a cellular partner of rotavirus NSP1. J Virol 76:9545–9550

Graham KL, Halasz P, Tan Y, Hewish MJ, Takada Y, Mackow ER, Robinson MK, Coulson BS (2003) Integrin-using rotaviruses bind alpha2beta1 integrin alpha2 I domain via VP4 DGE sequence and recognize alphaXbeta2 and alphaVbeta3 by using VP7 during cell entry. J Virol 77:9969–9978

Grimes JM, Jakana J, Ghosh M, Basak AK, Roy P, Chiu W, Stuart DI, Prasad BV (1997) An atomic model of the outer layer of the bluetongue virus core derived from X-ray crystallography and electron cryomicroscopy. Structure 5:885–893

Grimes JM, Burroughs JN, Gouet P, Diprose JM, Malby R, Zientara S, Mertens PP, Stuart DI (1998) The atomic structure of the bluetongue virus core. Nature 395:470–478

Groft CM, Burley SK (2002) Recognition of eIF4G by rotavirus NSP3 reveals a basis for mRNA circularization. Mol Cell 9:1273–1283

Hill CL, Booth TF, Prasad BV, Grimes JM, Mertens PP, Sutton GC, Stuart DI (1999) The structure of a cypovirus and the functional organization of dsRNA viruses. Nat Struct Biol 6:565–568

Hongou K, Konishi T, Yagi S, Araki K, Miyawaki T (1998) Rotavirus encephalitis mimicking afebrile benign convulsions in infants. Pediatr Neurol 18:354–357

Iturriza-Gomara M, Isherwood B, Desselberger U, Gray J (2001) Reassortment in vivo: driving force for diversity of human rotavirus strains isolated in the United Kingdom between 1995 and 1999. J Virol 75:3696–3705

Iturriza-Gomara M, Auchterlonie IA, Zaw W, Molyneaux P, Desselberger U, Gray J (2002) Rotavirus gastroenteritis and central nervous system (CNS) infection: characterization of the VP7 and VP4 genes of rotavirus strains isolated from paired fecal and cerebrospinal fluid samples from a child with CNS disease. J Clin Microbiol 40:4797–4799

Jayaram H, Taraporewala Z, Patton JT, Prasad BV (2002) Rotavirus protein involved in genome replication and packaging exhibits a HIT-like fold. Nature 417:311–315

Jayaram H, Estes MK, Prasad BV (2004) Emerging themes in rotavirus cell entry, genome organization, transcription and replication. Virus Res 101:67–81

Kaljot KT, Shaw RD, Rubin DH, Greenberg HB (1988) Infectious rotavirus enters cells by direct cell membrane penetration, not by endocytosis. J Virol 62:1136–1144

Kapikian AZ (2002) Ecological studies, rotavirus vaccination, and intussusception. Lancet 359:1065–1066; author reply 1066

Kattoura M, Chen X, Patton J (1994) The rotavirus RNA-binding protein NS35 (NSP2) forms 10S multimers and interacts with the viral RNA polymerase. Virology 202:803–813

Keljo DJ, Kuhn M, Smith A (1988) Acidification of endosomes is not important for the entry of rotavirus into the cell. J Pediatr Gastroenterol Nutr 7:257–263

Kirkwood CD, Bishop RF, Coulson BS (1996) Human rotavirus VP4 contains strain-specific, serotype-specific and cross-reactive neutralization sites. Arch Virol 141:587–600

Kirkwood CD, Bishop RF, Coulson BS (1998) Attachment and growth of human rotaviruses RV-3 and S12/85 in Caco-2 cells depend on VP4. J Virol 72:9348–9352

Kohli E, Pothier P, Tosser G, Cohen J, Sandino AM, Spencer E (1993) In vitro reconstitution of rotavirus transcriptional activity using viral cores and recombinant baculovirus expressed VP6. Arch Virol 133:451–458

Labbe M, Charpilienne A, Crawford SE, Estes MK, Cohen J (1991) Expression of rotavirus VP2 produces empty corelike particles. J Virol 65:2946–2952

Lawton JA, Estes MK, Prasad BV (1997a) Three-dimensional visualization of mRNA release from actively transcribing rotavirus particles. Nat Struct Biol 4:118–121

Lawton JA, Zeng CQ, Mukherjee SK, Cohen J, Estes MK, Prasad BV (1997b) Three-dimensional structural analysis of recombinant rotavirus-like particles with intact and amino-terminal-deleted VP2: implications for the architecture of the VP2 capsid layer. J Virol 71:7353–7360

Lawton JA, Estes MK, Prasad BV (1999) Comparative structural analysis of transcriptionally competent and incompetent rotavirus-antibody complexes. Proc Natl Acad Sci U S A 96:5428–5433

Lawton JA, Estes MK, Prasad BV (2000) Mechanism of genome transcription in segmented dsRNA viruses. Adv Virus Res 55:185–229

Liemann S, Chandran K, Baker TS, Nibert ML, Harrison SC (2002) Structure of the reovirus membrane-penetration protein, Mu1, in a complex with is protector protein, Sigma3. Cell 108:283–295

Lima CD, Klein MG, Hendrickson WA (1997) Structure-based analysis of catalysis and substrate definition in the HIT protein family. Science 278:286–290

Lopez S, Arias CF (2004) Multistep entry of rotavirus into cells: a Versaillesque dance. Trends Microbiol 12:271–278

Lopez S, Arias CF, Bell JR, Strauss J H, Espejo RT (1985) Primary structure of the cleavage site associated with trypsin enhancement of rotavirus SA11 infectivity. Virology 144:11–19

Lopez T, Camacho M, Zayas M, Najera R, Sanchez R, Arias CF, Lopez S (2005) Silencing the morphogenesis of rotavirus. J Virol 79:184–192

Ludert JE, Feng N, Yu JH, Broome RL, Hoshino Y, Greenberg HB (1996) Genetic mapping indicates that VP4 is the rotavirus cell attachment protein in vitro and in vivo. J Virol 70:487–493

Ludert JE, Mason BB, Angel J, Tang B, Hoshino Y, Feng N, Vo PT, Mackow EM, Ruggeri FM, Greenberg HB (1998) Identification of mutations in the rotavirus protein VP4 that alter sialic-acid-dependent infection. J Gen Virol 79:725–729

Lynch M, Lee B, Azimi P, Gentsch J, Glaser C, Gilliam S, Chang HG, Ward R, Glass RI (2001) Rotavirus and central nervous system symptoms: cause or contaminant? Case reports and review. Clin Infect Dis 33:932–938

Lynch M, Shieh WJ, Tatti K, Gentsch JR, Ferebee-Harris T, Jiang B, Guarner J, Bresee J S, Greenwald M, Cullen S et al (2003) The pathology of rotavirus-associated deaths, using new molecular diagnostics. Clin Infect Dis 37:1327–1333

Mackow ER, Shaw RD, Matsui SM, Vo PT, Dang MN, Greenberg HB (1988) The rhesus rotavirus gene encoding protein VP3: location of amino acids involved in homologous and heterologous rotavirus neutralization and identification of a putative fusion region. Proc Natl Acad Sci U S A 85:645–649

Mathieu M, Petitpas I, Navaza J, Lepault J, Kohli E, Pothier P, Prasad BV, Cohen J, Rey FA (2001) Atomic structure of the major capsid protein of rotavirus: implications for the architecture of the virion. EMBO J 20:1485–1497

Mattion NM, Mitchell DB, Both GW, Estes MK (1991) Expression of rotavirus proteins encoded by alternative open reading frames of genome segment 11. Virology 181:295–304

Mattion NM, Cohen J, Aponte C, Estes MK (1992) Characterization of an oligomerization domain and RNA-binding properties on rotavirus nonstructural protein NS34. Virology 190:68–83

Meyer JC, Bergmann CC, Bellamy AR (1989) Interaction of rotavirus cores with the nonstructural glycoprotein NS28. Virology 171:98–107

Midthun K, Kapikian AZ (1996) Rotavirus vaccines: an overview. Clin Microbiol Rev 9:423–434

Modis Y, Ogata S, Clements D, Harrison SC (2004) Structure of the dengue virus envelope protein after membrane fusion. Nature 427:313–319

Moon HW (1994) Pathophysiology of viral diarrhea. In: Kapikian AZ (ed) Viral infections of the gastrointestinal trac. Marcel Dekker, New York, pp 27–52

Morrison C, Gilson T, Nuovo GJ (2001) Histologic distribution of fatal rotaviral infection: an immunohistochemical and reverse transcriptase in situ polymerase chain reaction analysis. Hum Pathol 32:216–221

Mukhopadhyay S, Kim BS, Chipman PR, Rossmann MG, Kuhn RJ (2003) Structure of West Nile virus. Science 302:248

Nakagawa A, Miyazaki N, Taka J, Naitow H, Ogawa A, Fujimoto Z, Mizuno H, Higashi T, Watanabe Y, Omura T et al (2003) The atomic structure of rice dwarf virus reveals the self-assembly mechanism of component proteins. Structure (Camb) 11:1227–1238

Nandi P, Charpilienne A, Cohen J (1992) Interaction of rotavirus particles with liposomes. J Virol 66:3363–3367

Nason EL, Samal SK, Venkataram Prasad BV (2000) Trypsin-induced structural transformation in aquareovirus. J Virol 74:6546–6555

Nason EL, Rothagel R, Mukherjee SK, Kar AK, Forzan M, Prasad BV, Roy P (2004) Interactions between the inner and outer capsids of bluetongue virus. J Virol 78:8059–8067

Nejmeddine M, Trugnan G, Sapin C, Kohli E, Svensson L, Lopez S, Cohen J (2000) Rotavirus spike protein VP4 is present at the plasma membrane and is associated with microtubules in infected cells. J Virol 74:3313–3320

O'Brien JA, Taylor JA, Bellamy AR (2000) Probing the structure of rotavirus NSP4: a short sequence at the extreme C terminus mediates binding to the inner capsid particle. J Virol 74:5388–5394

Padilla-Noriega L, Dunn SJ, Lopez S, Greenberg HB, Arias CF (1995) Identification of two independent neutralization domains on the VP4 trypsin cleavage products VP5* and VP8* of human rotavirus ST3. Virology 206:148–154

Pager C, Steele D, Gwamanda P, Driessen M (2000) A neonatal death associated with rotavirus infection-detection of rotavirus dsRNA in the cerebrospinal fluid. S Afr Med J 90:364–365

Parashar UD, Hummelman EG, Bresee JS, Miller MA, Glass RI (2003) Global illness and deaths caused by rotavirus disease in children. Emerg Infect Dis 9:565–572

Pesavento JB, Lawton JA, Estes ME, Venkataram Prasad BV (2001) The reversible condensation and expansion of the rotavirus genome. Proc Natl Acad Sci U S A 98:1381–1386

Pesavento JB, Billingsley AM, Roberts EJ, Ramig RF, Prasad BV (2003a) Structures of rotavirus reassortants demonstrate correlation of altered conformation of the VP4 spike and expression of unexpected VP4-associated phenotypes. J Virol 77:3291–3296

Pesavento JB, Estes MK, Prasad BV (2003b) Structural organization of the genome in rotavirus. In: Desselberger U (ed) Perspectives in medical virology 9: viral gastroenteritis Elsevier, London, pp 115–127

Pesavento J, Crawford SE, Roberts E, Estes MK, Prasad BV (2005) pH-Induced conformational change of the rotavirus VP4 spike: implications for cell entry and antibody neutralization. J Virol 79:8572–8580

Petrie BL, Greenberg HB, Graham DY, Estes MK (1984) Ultrastructural localization of rotavirus antigens using colloidal gold. Virus Res 1:133–152

Piron M, Vende P, Cohen J, Poncet D (1998) Rotavirus RNA-binding protein NSP3 interacts with eIF4GI and evicts the poly(A) binding protein from eIF4F. EMBO J 17:5811–5821

Piron M, Delaunay T, Grosclaude J, Poncet D (1999) Identification of the RNA-binding, dimerization, and eIF4GI-binding domains of rotavirus nonstructural protein NSP3. J Virol 73:5411–5421

Poncet D, Lindenbaum P, L'Haridon R, Cohen J (1997) In vivo and in vitro phosphorylation of rotavirus NSP5 correlates with its localization in viroplasms. J Virol 71:34–41

Prasad BVV, Estes MK (2000) Electron cryomicroscopy and computer image processing techniques: use in structure-function studies of rotavirus. Human Press, Totowa, NJ

Prasad BV, Prevelige PE Jr (2003) Viral genome organization. Adv Protein Chem 64:219–258

Prasad BV, Wang GJ, Clerx JP, Chiu W (1988) Three-dimensional structure of rotavirus. J Mol Biol 199:269–275

Prasad BV, Burns JW, Marietta E, Estes MK, Chiu W (1990) Localization of VP4 neutralization sites in rotavirus by three-dimensional cryo-electron microscopy. Nature 343:476–479

Prasad BV, Rothnagel R, Zeng CQ, Jakana J, Lawton JA, Chiu W, Estes MK (1996) Visualization of ordered genomic RNA and localization of transcriptional complexes in rotavirus. Nature 382:471–473

Reinisch KM, Nibert ML, Harrison SC (2000) Structure of the reovirus core at 3.6 Å resolution. Nature 404:960–967

Ruiz MC, Alonso-Torre SR, Charpilienne A, Vasseur M, Michelangeli F, Cohen J, Alvarado F (1994) Rotavirus interaction with isolated membrane vesicles. J Virol 68:4009–4016

Sabara M, Gilchrist JE, Hudson GR, Babiuk LA (1985) Preliminary characterization of an epitope involved in neutralization and cell attachment that is located on the major bovine rotavirus glycoprotein. J Virol 53:58–66

Sapin C, Colard O, Delmas O, Tessier C, Breton M, Enouf V, Chwetzoff S, Ouanich J, Cohen J, Wolf C, Trugnan G (2002) Rafts promote assembly and atypical targeting of a nonenveloped virus, rotavirus, in Caco-2 cells. J Virol 76:4591–4602

Sasaki S, Horie Y, Nakagomi T, Oseto M, Nakagomi O (2001) Group C rotavirus NSP4 induces diarrhea in neonatal mice. Arch Virol 146:801–806

Shaw AL, Rothnagel R, Chen D, Ramig RF, Chiu W, Prasad BV (1993) Three-dimensional visualization of the rotavirus hemagglutinin structure. Cell 74:693–701

Silvestri LS, Taraporewala ZF, Patton JT (2004) Rotavirus replication: plus-sense templates for double-stranded RNA synthesis are made in viroplasms. J Virol 78:7763–7774

Taraporewala ZF, Patton JT (2001) Identification and characterization of the helix-destabilizing activity of rotavirus nonstructural protein NSP2. J Virol 75:4519–4527

Taraporewala ZF, Patton JT (2004) Nonstructural proteins involved in genome packaging and replication of rotaviruses and other members of the Reoviridae. Virus Res 101:57–66

Taraporewala Z, Chen D, Patton JT (1999) Multimers formed by the rotavirus nonstructural protein NSP2 bind to RNA and have nucleoside triphosphatase activity. J Virol 73:9934–9943

Taraporewala ZF, Chen D, Patton JT (2001) Multimers of the bluetongue virus nonstructural protein, NS2, possess nucleotidyl phosphatase activity: similarities between NS2 and rotavirus NSP2. Virology 280:221–231

Taylor JA, Meyer JC, Legge MA, O'Brien JA, Street JE, Lord VJ, Bergmann CC, Bellamy AR (1992) Transient expression and mutational analysis of the rotavirus intracellular receptor: the C-terminal methionine residue is essential for ligand binding. J Virol 66:3566–3572

Taylor JA, O'Brien JA, Lord VJ, Meyer JC, Bellamy AR (1993) The RER-localized rotavirus intracellular receptor: a truncated purified soluble form is multivalent and binds virus particles. Virology 194:807–814

Thouvenin E, Schoehn G, Rey F, Petitpas I, Mathieu M, Vaney MC, Cohen J, Kohli E, Pothier P, Hewat E (2001) Antibody inhibition of the transcriptase activity of the rotavirus DLP: a structural view. J Mol Biol 307:161–172

Tian P, Ball JM, Zeng CQ, Estes MK (1996) Rotavirus protein expression is important for virus assembly and pathogenesis. Arch Virol Suppl 12:69–77

Tihova M, Dryden KA, Bellamy AR, Greenberg HB, Yeager M (2001) Localization of membrane permeabilization and receptor binding sites on the VP4 hemagglutinin of rotavirus: implications for cell entry. J Mol Biol 314:985–992

Torres-Vega MA, Gonzalez RA, Duarte M, Poncet D, Lopez S, Arias CF (2000) The C-terminal domain of rotavirus NSP5 is essential for its multimerization, hyperphosphorylation and interaction with NSP6. J Gen Virol 81:821–830

Valenzuela S, Pizarro J, Sandino AM, Vasquez M, Fernandez J, Hernandez O, Patton J, Spencer E (1991) Photoaffinity labeling of rotavirus VP1 with 8-azido-ATP: identification of the viral RNA polymerase. J Virol 65:3964–3967

Vende P, Piron M, Castagne N, Poncet D (2000) Efficient translation of rotavirus mRNA requires simultaneous interaction of NSP3 with the eukaryotic translation initiation factor eIF4G and the mRNA 3′ end. J Virol 74:7064–7071

Welch SK, Crawford SE, Estes MK (1989) Rotavirus SA11 genome segment 11 protein is a nonstructural phosphoprotein. J Virol 63:3974–3982

Wentz MJ, Zeng CQ, Patton JT, Estes MK, Ramig RF (1996) Identification of the minimal replicase and the minimal promoter of (–)-strand synthesis, functional in rotavirus RNA replication in vitro. Arch Virol Suppl 12:59–67

Wiley DC, Skehel JJ (1987) The structure and function of the hemagglutinin membrane glycoprotein of influenza virus. Annu Rev Biochem 56:365–394

Yeager M, Dryden KA, Olson NH, Greenberg HB, Baker TS (1990) Three-dimensional structure of rhesus rotavirus by cryoelectron microscopy and image reconstruction. J Cell Biol 110:2133–2144

Yeager M, Berriman JA, Baker TS, Bellamy AR (1994) Three-dimensional structure of the rotavirus haemagglutinin VP4 by cryo-electron microscopy and difference map analysis. EMBO J 13:1011–1018

Zarate S, Espinosa R, Romero P, Guerrero CA, Arias CF, Lopez S (2000a) Integrin alpha2beta1 mediates the cell attachment of the rotavirus neuraminidase-resistant variant nar3. Virology 278:50–54

Zarate S, Espinosa R, Romero P, Mendez E, Arias CF, Lopez S (2000b) The VP5 domain of VP4 can mediate attachment of rotaviruses to cells. J Virol 74:593–599

Zeng CQ, Labbe M, Cohen J, Prasad BVV, Chen D, Ramig RF, Estes MK (1994) Characterization of rotavirus VP2 particles. Virology 201:55–65

Zhang H, Zhang J, Yu X, Lu X, Zhang Q, Jakana J, Chen DH, Zhang X, Zhou ZH (1999) Visualization of protein-RNA interactions in cytoplasmic polyhedrosis virus. J Virol 73:1624–1629

Zhang X, Walker SB, Chipman PR, Nibert ML, Baker TS (2003) Reovirus polymerase lambda 3 localized by cryo-electron microscopy of virions at a resolution of 7.6 A. Nat Struct Biol 10:1011–1018

Zhou ZH, Baker ML, Jiang W, Dougherty M, Jakana J, Dong G, Lu G, Chiu W (2001) Electron cryomicroscopy and bioinformatics suggest protein fold models for rice dwarf virus. Nat Struct Biol 8:868–873

CTMI (2006) 309:221–244

Structural Studies on Orbivirus Proteins and Particles

D. I. Stuart (✉) · J. M. Grimes

Division of Structural Biology, The Henry Wellcome Building for Genomic Medicine, University of Oxford, Roosevelt Drive, Oxford OX3 7BN, UK
dave@strubi.ox.ac.uk

Abstract X-ray and electron microscopy analysis of *Bluetongue* virus (BTV), the type species of the *Orbivirus* genus within the family *Reoviridae*, have revealed various aspects of the organisation and structure of the proteins that form the viral capsid. Orbiviruses have a segmented dsRNA genome, which imposes constraints on their structure and life cycle. The atomic structure of the BTV core particle, the key viral component which transcribes the viral mRNA within the cell cytoplasm, revealed the architecture and assembly of the major core proteins VP7 and VP3. In addition, these studies formed the basis for a plausible model for the organisation of the dsRNA viral genome and the arrangement of the viral transcriptase complex (composed of the RNA-dependent RNA polymerase, the viral capping enzyme and RNA helicase) that resides within the core particle. Electron cryo-microscopy of the viral particle has shown how the two viral proteins VP2 and VP5 are arranged to form the outer capsid, with distinct packing arrangements between them and the core protein VP7. By comparison of the outer capsid proteins of orbiviruses with those of other nonturreted members of the family *Reoviridae*, we are able to propose a more detailed model of these structures

and possible mechanisms for cell entry. Further structural results are also discussed including the atomic structure of an N-terminal domain of nonstructural protein NS2, a protein involved in virus genome assembly and morphogenesis.

1 Introduction

Structural studies have provided insights into the biological functions of many viruses (Abrescia et al. 2004; Chiu et al. 1997; Cockburn et al. 2004; Wikoff et al. 2000). In comparison to other viruses, orbiviruses and the other members of the family *Reoviridae* (Mertens et al. 2005) have additional constraints on their life cycle, due to their dsRNA genome. Since dsRNA would trigger the host's defence mechanisms if it were released into the cytoplasm of an infected cell, the orbivirus genome must be retained within the viral capsid. In the absence of host cell transcriptases which can use dsRNA as template for mRNA synthesis, the naked virus genome will be transcriptionally and translationally inert within the cell cytoplasm and therefore be unable to initiate replication. The orbivirus core particle provides a compartment within which the ten genome segments can be repeatedly transcribed by core-associated enzymes. mRNA copies of each of the segments are synthesised simultaneously and released from the core particle into the host cell cytoplasm, to function as templates for translation, as well as for negative strand viral RNA synthesis within nascent progeny virus particles. This requires the efficient co-ordination of some half a dozen enzyme activities required for helicase, polymerase and RNA capping actions.

Bluetongue virus (BTV) is the type species (one of 21 different species) of the genus *Orbivirus*, within the family *Reoviridae*. The *Reoviridae* includes a total of ten distinct genera, some of which infect or are pathogenic for humans (*Orthoreovirus*, *Rotavirus*, *Coltivirus* and *Seadornavirus*) (Mertens et al. 2005). Orbiviruses are nonturreted members of the family which are characterised by infecting both insect and mammalian cells, with transmission via insect vectors. The intact BTV virion possesses seven structural proteins (Burroughs et al. 1994; Huismans et al. 1987; Mertens et al. 1987; Van Dijk and Huismans 1988), and in addition the genome encodes three nonstructural proteins (Table 1). Three of the structural proteins are present in relatively small numbers in each particle [minor proteins: VP1(Pol), VP4(Cap) and VP6(Hel)] and have enzymatic functions associated with the synthesis and capping of the viral mRNA (Mertens et al. 1987; Ramadevi et al. 1998; Roy et al. 1988; Stauber et al. 1997; Urakawa et al. 1989). Two relatively more abundant proteins (major proteins: VP2 and VP5) form the outer shell of the intact virus particle (Burroughs et al. 1994; Mertens et al. 1987). Under suitable conditions,

Table 1 Orbivirus genome, gene products and their functions, as exemplified by BTV (data from Stuart et al. 1998)

Genome segment (size: bp)	Protein nomenclature	Location	Copy number/ particle	No. of amino acids	Properties and functions
1 (3954)	VP1 (Pol)	Within the subcore at the five-fold axis	10	1,302	RNA-dependent RNA polymerase
2 (2926)	VP2	Outer capsid	180	956	Trimeric outer capsid protein, serotype specific antigen, cell attachment protein, cleaved by trypsin
3 (2770)	VP3 (T2)	Inner layer of the core particle	120	901	Innermost protein capsid shell, subcore capsid layer, T=2 symmetry, interacts with internal minor proteins
4 (1981)	VP4 (Cap)	Within the subcore at the five-fold axis	20	644	Capping enzyme, guanylyltransferase, methyltransferase
5 (1769)	NS1 (TuP)	Cytoplasm forms tubules	–	552	Forms tubules in the cell cytoplasm, characteristic of orbivirus replication
6 (1638)	VP5	Outer capsid	360	526	Trimeric outer capsid protein, implicated in membrane fusion
7 (1156)	VP7 (T13)	Outer layer of the core particle	780	349	Trimer forms outer core surface, T=13 symmetry
8 (1124)	NS2 (ViP)	Cytoplasm, viral inclusion bodies	–	357	Important viral inclusion body matrix protein, binds ssRNA
9 (1046)	VP6 (Hel)	Within the subcore at the five-fold axis	72	329	Helicase
10 (822)	NS3/NS3a	Cell membranes	–	229/216	Membrane glycoproteins involved in viral cell exit

Pol, RNA polymerase; Cap, capping enzyme (guanylyltransferase, methyltransferase, etc.); Hel, helicase enzyme; T2, protein with pseudo T=2 symmetry; T13, protein with T=13 symmetry; ViP, viral inclusion body matrix protein; TuP, tubule protein

this outer capsid can be released (Burroughs et al. 1994; Mertens et al. 1987), and it can also be modified by treatment with proteases (such as trypsin, chymotrypsin, or plasmin), which results in cleavage of VP2 and modification of the biological properties and solubility of the particle. The remaining two major proteins [VP3(T2) and VP7(T13)] form the inner and outer layers, respectively, of the core particle, which is central to the process of transcription and genome replication and is the cornerstone of the virus particle assembly process (Brookes et al. 1993; Eaton et al. 1990). The nonstructural proteins NS1–NS3 are found in the cell cytoplasm and are thought to play roles in viral assembly, transport and egress from the cell (Brookes et al. 1993).

2
The Architecture of the Core Particle

The structures of the core of bluetongue virus serotypes 1 (BTV-1) and 10 (BTV-10) have been determined to resolutions of 3.5 Å and 6.5 Å, respectively (Gouet et al. 1999; Grimes et al. 1998). These structures revealed the organisation of the protein bilayer that makes up the icosahedral capsid of the core and demonstrated that it was feasible to analyse crystals with a unit cell mass of approximately half a billion daltons.

Fig. 1A–D BTV-1 core architecture. **A** Diagramme showing the structure of the VP7(T13) trimer. A single subunit has been coloured from the N-terminus to the C-terminus *blue to red*, whilst the other subunits are in *grey*. The trimer sits on the exterior surface of the VP3(T2) subcore, making contact through the bottom surface (in this view), whilst inter-VP7(T13) contacts are mediated through the sides of the lower domain of the molecule. **B** Diagramme showing the core structure. The icosahedral asymmetric unit (which is a triangular area delineated by the symmetry axes marked on the icosahedron) contains 13 copies of VP7(T13) arranged as five trimers, P, Q, R, S and T, coloured *red*, *orange*, *green*, *yellow* and *blue*, respectively. Trimer T sits on the icosahedral three-fold axis and thus contributes a monomer to the unique portion. **C** Diagramme showing the domain structure of VP3(T2), colouring is by domain: apical is *blue* (residues 297–588), carapace is *green* (residues 7–297, 588–698 and 855–901) and dimerization is *red* (residues 698–855). The *left image* shows the molecule as if it were in the subcore when viewed from outside the particle looking towards the centre, with secondary structural elements labelled as defined in Grimes et al. (1998). The *right* image is an orthogonal view. **D** The BTV subcore, made up of 120 copies of VP3(T2). The icosahedrally unique molecules A and B are coloured *green* and *red*, respectively. Note the different structural environment of the A and B molecules. The icosahedral five-fold, three-fold and two-fold symmetry axes have been marked. One decamer, a putative assembly intermediate, has been highlighted. Figure adapted from Grimes et al. (1998)

The core is made up of an outer surface composed of 260 trimers of VP7(T13) (38 kDa), sitting on a skin of 120 copies of VP3(T2) (100 kDa), which form a subcore layer (Fig. 1). The monomer of VP7(T13) has a two-domain structure composed an outer and an inner domain (where the outer domain lies at a greater radius from the centre of the core particle) (Fig. 1A). The outer domain consists of about 130 residues, representing the central portion of the molecule's amino acid chain and has a jelly-roll topology common to many viral structural proteins (Stuart 1993). This structure has characteristics common of an upright jelly roll (such as that seen in the P domain of tomato bushy stunt virus (TBSV), rather than the in-plane jelly roll [such as the S domain of TBSV (Harrison et al. 1978); data not shown]. The inner domain

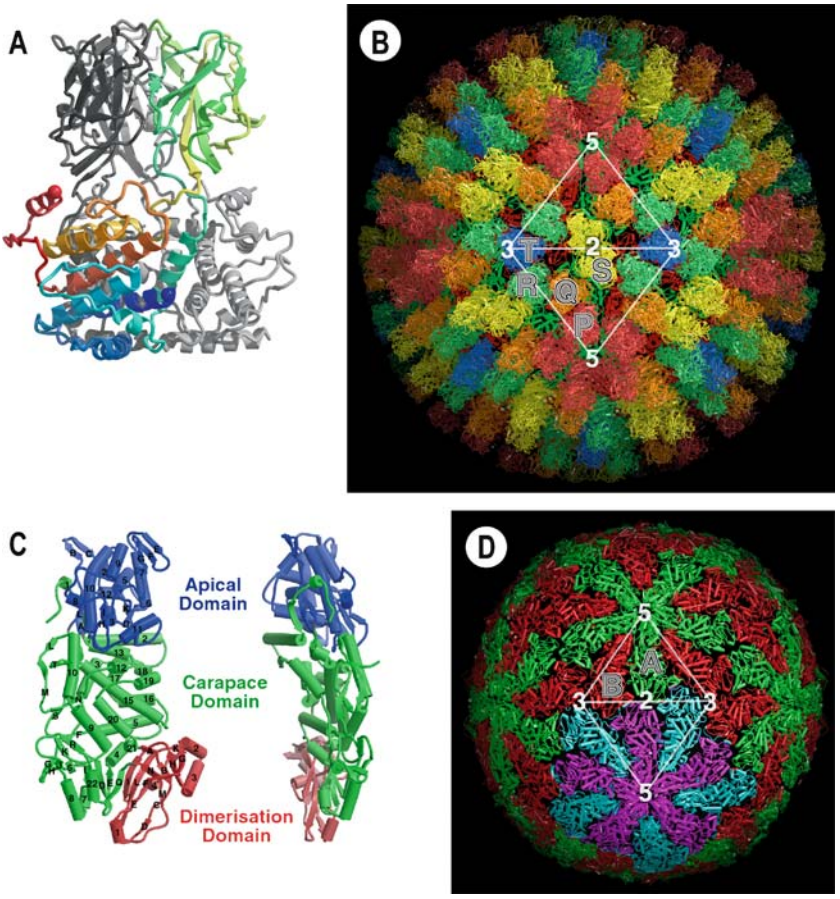

is entirely α-helical, and has a topology seen only in homologous T13 proteins of the members of the *Reoviridae* (Mathieu et al. 2001). The relative disposition of these domains is such that they wrap around the molecular three-fold axis in a right-handed sense (Fig. 1A) (Grimes et al. 1995). The trimers themselves are arranged on a pseudo-hexagonal T=13*l* lattice and are all very similar to each other. These quasi-equivalent (Caspar and Klug 1962; Johnson and Speir 1997) trimers build up the core surface layer, such that they form pairs related by almost exact two-fold symmetry (Fig. 1B). This is achieved by the unique architecture of this layer: the contact regions between the different VP7(T13) trimers are located in a thin band within the lower α-helical domain and are essentially one-dimensional in nature. This region is formed in large part by a short hydophobic α-helix, that seems to act as a greasy hinge, about which the trimers are able to roll, as they pack onto the surface of the inner core of VP3(T2). This rolling enables the same mode of interaction to be used between the different trimers (P-T; see Fig. 1B) with minimal distortion (Grimes et al. 1998).

The inner core protein VP3(T2) is arranged as 120 copies per particle, with icosahedral symmetry, on a pseudo T=2 lattice, as shown in Fig. 1D. VP3(T2) possesses a highly unusual structure, with its 901 amino acids organised into a structure that resembles a triangular wedge (130 Å by 75 Å), with a thickness varying between 13 Å and 35 Å (Fig. 1C). Three domains make up the VP3(T2) molecule: an apical domain that sits nearest to the icosahedral five-fold axis; a carapace domain, which forms a rigid plate; and a dimerisation domain that is involved in forming the quasi two-fold interaction between the different molecules of VP3(T2) (Fig. 1C). The VP3(T2) subcore is believed to be of particular significance in the process of orbivirus replication and morphogenesis. VP3(T2) is the only viral protein which can assemble, when expressed by itself, to form icosahedral particles similar in appearance to the authentic sub core (French and Roy 1990; Moss and Nuttall 1994). The subcore layer is also sufficiently stable that it can retain the particle size and structure after removal of the outer capsid layer and the VP7(T13) layer of the core surface (Huismans et al. 1987; Loudon and Roy 1991, 1992). During assembly of progeny virus particles within the viral inclusion bodies (VIB) in infected cells, the smallest particles, which are thought to contain viral RNA, are equivalent in size to subcores (Brookes et al. 1993; Eaton et al. 1990). The subcore is therefore thought to be involved both in genome packaging and in defining the size and overall morphology of the outer layers of the capsid, which are added later.

The icosahedral building block of the subcore shell contains two chemically identical molecules of VP3(T2), which have different structural environments and are therefore denoted A and B (Fig. 1D). These two molecules fit together

in a manner seen only for dsRNA viruses (Bamford et al. 2005). Conceptually the 60 A subunits define the size of the subcore by forming a continuous scaffold of pairs, which span icosahedral two-fold axes and link adjacent five-fold axes. This scaffold is sealed off by the 60 B subunits, which cluster at the icosahedral three-fold axes to form triangular plugs (Fig. 1D). A tightly packed, almost hermetic, shell is achieved by rotations within these VP3(T2) molecular building blocks, primarily at the dimerisation domain (which is intimately involved in forming the quasi two-fold interface between molecules A and B) and between the carapace and apical domains. These rotations combine to swing the tip of the apical domain some 35 Å. Additional small changes ensure that the molecules fit snugly around each five-fold axis, in the form of a decamer. This quasi two-fold relationship between the A and B molecules in adjacent decamers (which breaks down beyond the dimerisation domains) may be thought of as a subtriangulation of the icosahedron into a T=2 structure. The molecular contacts between the A and B subunits within VP3(T2) decamers surrounding the five-fold axes of the subcore are very extensive and it seems plausible that this is a building block for virus assembly (Grimes et al. 1998), as supported by mutational analysis (Kar et al. 2004) (Fig. 1D).

The VP7(T13) and VP3(T2) layers interact through flat, largely hydrophobic, surfaces. Given the symmetry mismatch between the two layers, there are 13 different sets of contacts between the 13 subunits of VP7(T13) packed onto the two copies of VP3(T2). Remarkably the VP3(T2) A and VP3(T2) B molecules make completely different yet extensive contacts with the various VP7(T13) molecules, whose structures are virtually identical to one another and to the structure of the protein in isolation (Grimes et al. 1995, 1998). The VP7(T13) subunits form trimers, even in solution, which in some orbiviruses (e.g. African horse sickness virus, AHSV) assemble into flat sheets of hexameric rings (Burroughs et al. 1994). One may think of the completion of the outer core layers as the crystallisation of 260 preformed trimers of VP7(T13) onto the fragile VP3(T2) subcore. The driving force for this assembly is the adhesion of these two relatively flat surfaces. The relative orientation of adjacent trimers of VP7(T13) being determined by their mutual side-to-side interactions, thus avoiding the requirement for control by conformational switching. Analysis of the adhesion surfaces suggests the order for this assembly process, whereby trimers attach first to the icosahedral three-fold axes, with the peripentonal trimers being the last to attach and the first to be released (Grimes et al. 1998). This model is supported by EM analysis (Hewat et al. 1992a) and appears to hold for other dsRNA viruses (Lu et al. 1998; Nakagawa et al. 2003).

3
The Transcription Complex and Genome Organisation of the Core Particle

The atomic structure of the principle proteins of the core was derived from the analysis of BTV-1; however, a careful comparative study of the structures of BTV-10 and BTV-1 allowed analysis of those components of the core which are not arranged with icosahedral symmetry (see Fig. 2A). There is density positioned directly under the icosahedral five-fold axes, which is attributable to the minor proteins of the transcriptase complex (TC) (Fig. 2A, B). These proteins are reported to possess helicase (Stauber et al. 1997), polymerase (Roy et al. 1988; Urakawa et al. 1989) and RNA capping activity (Ramadevi et al. 1998). It has been estimated that the TC is formed from one subunit of VP1 (polymerase), a dimer of VP4 (capping enzyme) and the hexameric VP6 (helicase) (Stuart et al. 1998), and it seems that such a complex is arranged at each of the five-fold apices of the icosahedrally symmetric subcore during assembly of the virus. This location of the TC appears to be general to all members of the family *Reoviridae* (Bartlett et al. 1974; Gillies et al. 1971; Gouet et al. 1999; Lawton et al. 1997; Nason et al. 2004; Reinisch et al. 2000).

In the orbivirus core, each of the ten segments of genomic dsRNA will be intimately associated with a TC. This is in agreement with the data for both BTV-1 and BTV-10 shown in Fig. 2A, B where four layers of electron density line the VP3(T2) shell and are closely associated with the density for the TC. This demonstrates that genomic RNA is packaged in a rather structured way,

Fig. 2A–E The ordered dsRNA genome. **A, B** Slices through the electron density in the BTV-10 core (**A**) and BTV-1 (**B**). The icosahedral five-fold and two-fold axes are marked by *red lines with a pentagon and oval*, respectively. The density is coloured by the number of standard deviations above the mean density in the map, with *black* at or below the mean and *purple* at or greater than 1 standard deviation. The strong density of the capsid layer is visible in *purple*. Within the capsid, three layers of density are visible away from the five-fold axis. These layers are of thickness and spacing consistent with their being due to dsRNA. **C** Diagramme showing dsRNA following shallow grooves on the underside of the VP3(T2) layer. The grooves are in roughly the same place on both the A (*green*) and B (*red*) molecules. When assembled into the subcore layer, A and B are offset, and the grooves on one molecule feed into a groove further from the five-fold on the next, giving rise to the spiral pattern**. D** Model of the external layer of dsRNA as a spiral around the five-fold axis. The strands shown in *orange* are related to the strands shown in *blue* by icosahedral symmetry. **E** Cartoon of the arrangement of the RNA genome. The RNA is shown as a *blue coil* around the transcription complex (coloured *green*), indicating the disposition of the RNA within the core with respect to the five-fold vertices. Figure adapted from Gouet et al. (1999)

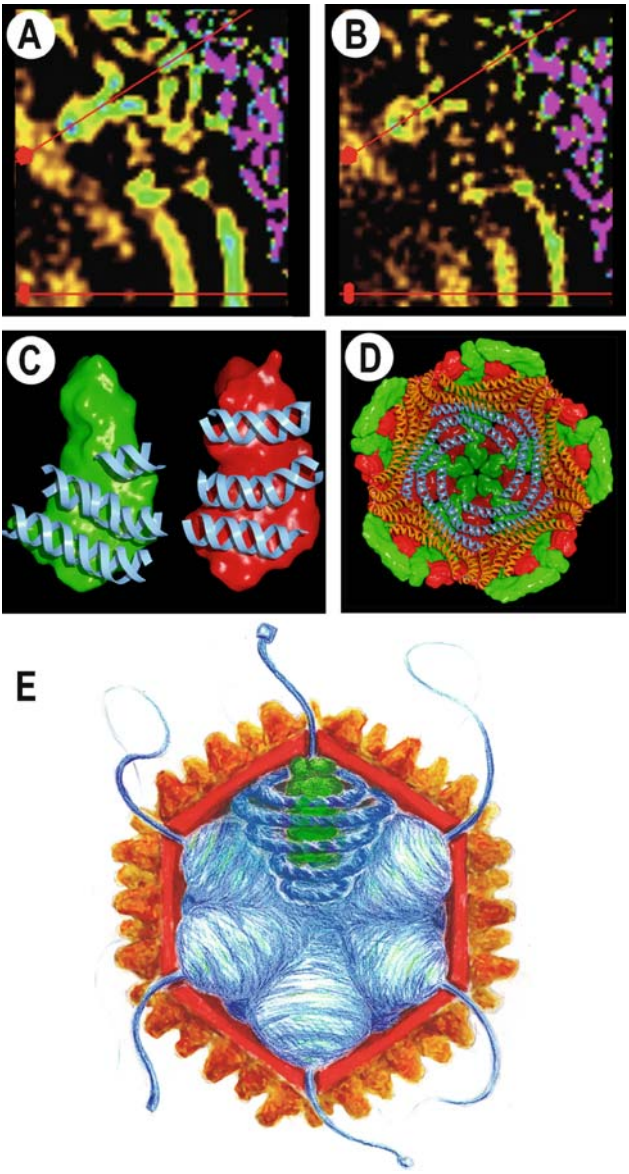
A
B
C
D
E

with a liquid crystalline array of RNA strands following, to a surprising extent, the icosahedral symmetry of the core. This order is imposed by the VP3(T2) layer, which possesses, on its inner surface, shallow, chemically bland grooves that form tracks along which tubes of dsRNA lie. The peculiar architecture of the VP3(T2) layer means that the A and B molecules of VP3(T2) generate a spiral of grooves for the RNA around each five-fold apex (Fig. 2C, D) (Gouet et al. 1999). The RNA lies in layers, separated by 26–30 Å, and a plausible model for the overall layout of the separate gene segments has been proposed (Fig. 2E) (Gouet et al. 1999), which explains how RNA can be tightly packed within the core and yet remain sufficiently fluid for efficient, repeated, and independent transcription of the ten segments of dsRNA (totalling about 19,200 base pairs of RNA). Each RNA segment is wound around its associated TC, until it hits a neighbouring segment. At this point, because of steric hindrance, it may flip down to form the next layer, and wind back in towards the TC, like rope coiled up on a ship's deck, stored in an orderly fashion yet ready for action. Note that the genome segments differ substantially in length and so the size of these coils will, naturally, reflect this. This model is also in agreement with observations of other members of the family *Reoviridae* made by electron cryo-microscopy (cryo-EM) (Hill et al. 1999; Moss and Nuttall 1994; Prasad et al. 1996; Zhou et al. 2003). The logistics of organising the genome for repeated transcription in a fully conservative way are assisted by tethering to the TC [demonstrated for cytoplasmic polyhedrosis virus (Yazaki and Miura 1980) and reovirus (Gillies et al. 1971)]. A detailed model of how this might be achieved (and how the process might differ from other dsRNA viruses, such as bacteriophage phi6, which proceed by semi-conservative transcription) was proposed by Butcher et al. (2001).

A more detailed understanding of the transcription complex requires atomic level structural information for the minor proteins VP1(Pol), VP4(Cap), and VP6(Hel). No published data are available for any of these proteins from an *Orbivirus*. Some information on the polymerase can be inferred from the published structure of reovirus λ1 (Tao et al. 2002). Although the sequence similarity between BTV and reovirus polymerases is too low to allow meaningful automatic alignments, by fixing conserved residues and using secondary structure predictions it appears that, as expected, the proteins show some overall similarity in their structures, being highly elaborated versions of the common right-hand polymerase fold seen in a much simpler form in the polymerase of the dsRNA bacteriophage phi6 (Butcher et al. 2001).

Despite the likely similarity of the polymerases across members of the family *Reoviridae*, there are also major differences in the non-structural proteins, most notably between the turreted viruses (e.g. *Orthoreovirus*, *Cypovirus*) and

the nonturreted viruses (e.g. *Orbivirus*, *Rotavirus*). The turreted viruses possess an elaborate five-fold symmetric cage at the icosahedral vertices which contains the enzymatic activities required to cap the RNA transcript as it leaves the particle (Cleveland et al. 1986; Fausnaugh and Shatkin 1990). In contrast, the nonturreted viruses possess fewer copies of their capping enzyme [VP4(Cap)] (Stuart et al. 1998), and these appear to reside within the core particle (Gouet et al. 1999). Although there is structural information for the capping enzyme for a representative turreted virus (Reinisch et al. 2000), we have not been able to produce convincing alignments of the sequences between the two classes of viruses. Capping activity would seem to be an absolute requirement for a dsRNA virus infecting eukaryotic hosts (there is no evidence for the use of alternative translation initiation mechanisms); hence it will be interesting to see if the capping enzymes are in fact closely related structurally or are radically different, since this might indicate if the bifurcation of the family *Reoviridae* into turreted and nonturreted viruses occurred before or after the emergence of the cellular capping machinery in their hosts.

The final component of the TC is VP6(Hel). This is thought to be a hexameric helicase; however, its exact role in transcription is not certain (Butcher et al. 2001) and there are, for now, no structural data to illuminate its function.

4 Translocation Portals for Entry and Exit of Substrate and Product

Crystallographic experiments, based on soaking BTV-1 core particles in transcription buffers have shown how substrates are localised and sequestered at the capsid barrier, and how mRNA product and by-products are released (Diprose et al. 2001) (Fig. 3). A prerequisite of such analysis is that the particles are activated by immersion in a buffer containing magnesium at approximate cytoplasmic concentration. This results in an overall expansion of the capsid, particularly around the five-fold axes (Diprose et al. 2001). The capsid expansion is likely to have biological relevance and may be greater in solution, allowing the looser viral shell to become more permeable to nucleotide substrates and ions, as well as facilitating the release of mRNA and by-products.

The pore at the icosahedral five-fold axis (Fig. 3) is the largest opening through the VP3(T2) subcore layer. Cryo-EM studies suggested that mRNA exited close to, but not at, the five-fold axis of actively transcribing rotavirus particles (Lawton et al. 1997). In contrast, crystallographic analysis of the binding of nucleotides and oligonucleotides demonstrated that the pore at the five-fold axis is the site of exit of mRNA from BTV core particles (indicated by a column of electron density extending upwards along the five-fold axis from

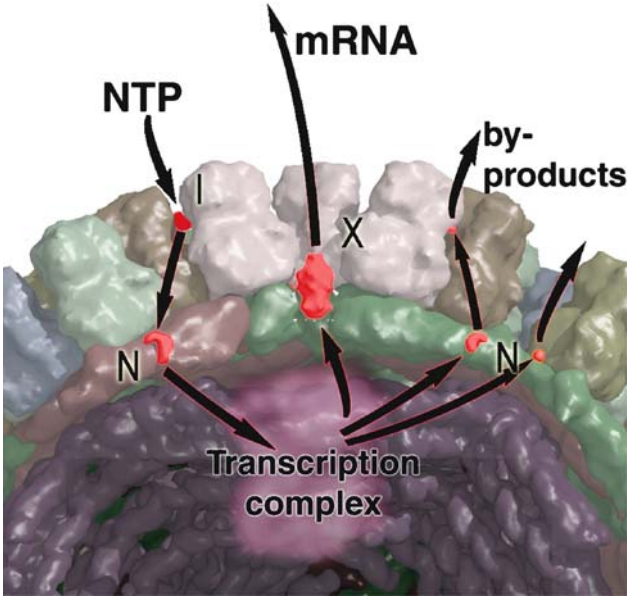

Fig. 3 The translocation portals. Diagramme showing the movement of NTP raw material into the core particle, and the site of egress of the product mRNA transcript and by-products PPi, Pi and NDPs. NTPs are sequestered at inter-trimer sites I. NTPs are thought to cross the protein barrier via the pore at site N. The product of transcription leaves via the pore at the five-fold axis of the particle, site X. By-products leave via the pores at sites X and N. Figure taken from Diprose et al. (2001)

the subcore) (Diprose et al. 2001) (site X in Fig. 3). This polar pore formed by the apical domains of VP3(T2) is lined with a set of three arginine residues. The constriction of the pore will prevent the formation of RNA secondary structure, so that the major conformational determinants imposed on the RNA are the connectivity of the RNA backbone itself, base stacking and the interaction of the backbone phosphates with the amino acid side chains that line the pore (Diprose et al. 2001).

Transcription of ssRNA occurs simultaneously from each genome segment (Gillies et al. 1971; Lawton et al. 1997; Yazaki and Miura 1980), presumably blocking the pores at the five-fold axes. Other routes are therefore necessary for the entry of substrates (NTPs and S-adenosyl-methionine) and for the release of reaction by-products (Pi, PPi, S-adenosyl-homocysteine and ADP). A pore between the A and B molecules of VP3(T2) (site N in Fig. 3) serves the role of nucleotide transport (Diprose et al. 2001). Re-orientation of arginine and lysine side chains switch the chemical nature of the entrance to the pore

between hydrophobic and charged. This, together with a small hydrophobic patch approximately halfway through the pore and a negatively charged side chain, appears to optimise the pore for the rapid transport of nucleotides, explaining how the BTV core selectively imports the substrates required for mRNA synthesis (Diprose et al. 2001).

A number of additional binding sites have been mapped within the VP7(T13) layer (site I in Fig. 3) (Diprose et al. 2001). These occur at local two-fold axes between trimers of VP7(T13), and are defined by four arginine residues, two from each monomer. Once again, flexible arginine side chains are important. The delocalised positively charged nitrogens at the end of arginine side chains allows the negative charge of the nucleoside phosphates to be balanced, whilst the hydrophobic nature of the aliphatic carbon side chain facilitates binding of the nucleoside base. The presence of relatively large numbers of nucleotides on the particle surface may act as a substrate sink, increasing the local concentration so that the core particles can compete effectively with other cellular activities for limited nucleotide resources.

5
The Core Particle Sequesters dsRNA

The BTV core appears to use two mechanisms to prevent its genomic dsRNA activating the apoptotic host responses, firstly it passively compartmentalises the dsRNA from the cytoplasm; secondly it sequesters any dsRNA inadvertently released into the cytoplasm (Diprose et al. 2002). X-ray analysis revealed that the exterior of the core particle was festooned with long ropes of A-form dsRNA, with the major and minor grooves clearly delineated (Fig. 4A, B) (Diprose et al. 2002). In total, some 2,000 base pairs are associated with each core particle in the crystal. Ropes of dsRNA are passed from one particle to another so that the crystal lattice is largely held together by RNA–protein interactions. The strands of RNA form 39 different interactions with the VP7(T13) layer in the crystal. Over half of these are strikingly similar and involve contact with two subunits of the trimer (Fig. 4C). The 780 independent binding sites presented on the core surface make use of polar residues which are conserved across BTVs (primarily Asn 164, Asn 200, Gln 202, Gln 239 and Asn 240). This provides immense scope for the amplification of binding strength by avidity effects facilitated by the arrangement of the BTV trimers on the T=13 surface lattice, which present the most favoured dsRNA-binding sites aligned, zipper-like, along great circles of the core surface. This gently bent structure for the RNA is in line with the observed persistence length of approximately 1,100 Å for rotavirus genome segments (Kapahnke et al. 1986).

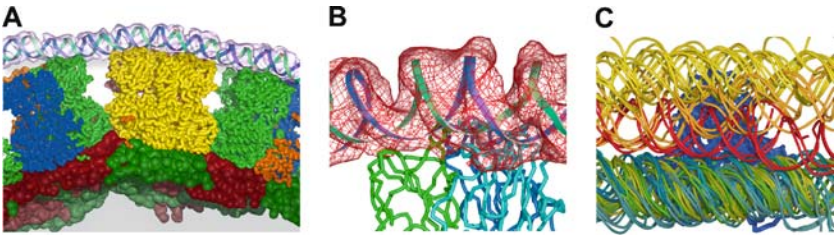

Fig. 4A–C Ropes of RNA within BTV core crystals. **A** View of the interaction of the parts of one RNA rope with the BTV core. The RNA model and electron density are shown (the density is rendered semitransparent). The VP7 trimers and underlying VP3 molecules are coloured as described for Fig. 1. **B** Image of the fit of the dsRNA model, with a portion of the difference electron density map in *red*, showing the typical disposition of the RNA on the top surface of a VP7 trimer. The strands of the RNA model are shown as *green and blue ribbons*, and the three polypeptide chains of VP7 are drawn in *green*, *cyan*, and *blue*. **C** The modes of binding of the 39 crystallographically independent interactions between the dsRNA and VP7 trimers are drawn superimposed, so as to best align the RNA trajectories. The RNA is coloured according to binding mode. The principal mode (24 members, lower bundle) is coloured *green-yellow to cyan*. The next most populous mode (eight members, upper bundle) is coloured *yellow*. Two minor intermediate modes (three and four members) are coloured *red* and *orange*. Figure adapted from Diprose et al. (2002)

Thus the core itself seems capable of soaking up free dsRNA [this is supported by RNA pull-down experiments (Diprose et al. 2002)]. Specific sequestration of dsRNA is seen also in other members of the *Reoviridae*; for example, the Orthoreovirus sigma 3 protein and the avian σA protein both bind dsRNA (Bergeron et al. 1998; Jacobs and Langland 1998; Martinez-Costas et al. 2000).

6
The Outer Capsid Proteins VP2 and VP5

Cryo-EM has revealed the structure and organisation of the outer capsid layer in BTV (Fig. 5 maps these results onto the X-ray structure of the core) (Nason et al. 2004). Two distinct density features make up the rather porous outer layer of the virus, consisting of VP2 and VP5. VP2 (111 kDa) is the larger protein, possesses hemagglutination activity and has been shown to be the receptor-binding protein (Hassan and Roy 1999). VP2 is also the protein most variable in sequence of the seven structural proteins of BTV across all serotypes and carries neutralisation-specific epitopes. These properties support the assignment (Hewat et al. 1992b) of VP2 to triskelions on the outer surface, and VP5 (~59 kDa), which has membrane fusion activity, to more

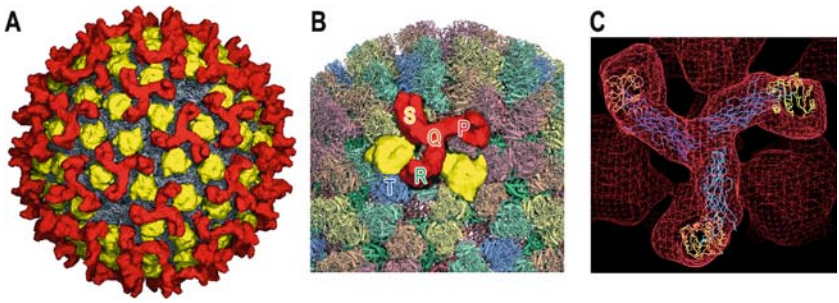

Fig. 5A–C The outer capsid proteins VP2 and VP5. **A** Arrangement of outer capsid proteins VP2 and VP5 on the core surface. The 60 trimers of the VP2 triskelion are shown in *red* and the 120 copies of the globular VP5 density is shown in *yellow*. **B** The arrangement of the icosahedral asymmetric portion of VP2 and VP5 (in *grey*) on the core (coloured as in Fig. 1). The positions of the icosahedrally unique trimers of VP7(T13) are labelled (*P-T*) to help clarify the positions of VP2 and VP5. **C** Illustrative fit of rotavirus VP5 core domain (*blue*) (Dormitzer et al. 2004) and Banna virus VP9 core domain (*yellow*) (Mohd Jaafar et al. 2005) into 24-Å reconstruction of BTV (Nason et al. 2004). The triskelion density corresponds to a trimer of VP2, subunit MW 110 kDa, and the structure fitted corresponds to only two-thirds of this mass. The remaining structure appears to be an additional domain close to that modelled by Banna virus VP9

globular structures, nestled above pseudo-hexagonal rings of VP7 trimers (Hassan et al. 2001; Hewat et al. 1992b). This assignment was confirmed by a comparative analysis of Broadhaven virus (Schoehn et al. 1997).

Higher resolution (24 Å) cryo-EM studies provides a more precise picture of the BTV outer shell (Nason et al. 2004). The 60 triskelions extend to give the virus a maximum diameter of approximately 880 Å. Interspersed between the triskelions lie the 120 copies of the globular VP5, at a maximum diameter of roughly 820 Å. Based on the volume of the density features, both the VP2 triskelions and VP5 globules appear to represent trimers. At present there are, unfortunately, no X-ray analyses of either VP2 or VP5, and so functional inference depends on comparisons with viruses for which such information is available, as discussed below.

7
Cell Entry Mechanisms

It appears that there are multiple cell entry mechanisms for BTV (Mertens et al. 1996). The intact virus particle is required for the efficient infection of mammalian cells, although the core particles appear to possess some residual infectivity (Mertens et al. 1987). Furthermore, treatment by proteases, to produce

the poorly characterised (compared to, for instance the analogous particles of Orthoreovirus) infectious subviral particle (ISVP) does not enhance infectivity in mammalian cells. In contrast, viral cores can infect insect cells with an efficiency within approximately 1 log of intact viruses, whilst ISVPs are considerably more infectious than either cores or intact virions (Mertens et al. 1996).

The mechanism by which cores enter cells is not known, although the observation of a putative integrin-binding RGD motif in an exposed position on VP7(T13), ideally placed to bind receptor, suggested a possible route of interaction (Grimes et al. 1995). The involvement of the RGD peptide was confirmed by cell-binding assays for wild-type and mutant core-like particles, which showed reduced binding when the RGD tripeptide was mutated (Tan et al. 2001). Whilst there are no direct data available to address the issue of conformational changes in the core that might lead to, or accompany, cell entry, structural studies of the outer protein of the core, VP7(T13), have demonstrated that the two domains of this molecule can flex and that its twisted architecture provides a natural mechanism for large-scale conformational change. VP7(T13)s from both BTV and AHSV undergo proteolytic cleavage at a point between the two domains (Basak et al. 1996; Basak et al. 1997). This may simply reflect inherent flexibility in the molecule which is manifest in a low-resolution structure of BTV VP7(T13) and reveals that the α-helical domains can rotate by roughly 160° to produce to a massive unwinding of the trimer (Basak et al. 1997). It is interesting to note that all known viral fusion machines employ large-scale conformational rearrangements of trimeric molecules, and although there is no direct evidence that such mechanisms are employed by nonenveloped viruses, a very similar proposal has been made for the μ1 protein of reovirus (Liemann et al. 2002), whose fold is noticeably similar to BTV VP7(T13).

The architecture of the core of non-turreted members of the *Reoviridae* family appears to be rather well conserved; however, the outer layers of the virus particles are much more variable. Recent analyses have revealed the fold of the proteins for several outer shell components (Dormitzer et al. 2002, 2004; Mohd Jaafar et al. 2005), raising the question of whether these results have implications for our understanding of the outer layer of orbiviruses. We have compared the positioning of the outer proteins in the low-resolution structures of different nonturreted viruses, on the basis of which we propose that it is useful to view certain proteins as orthologues (Fig. 5C). In particular we propose that VP2 of BTV and VP4 of rotavirus may possess similarities in structure as well as function. In line with this, we find that the core structure of rotavirus VP5 (the larger of the two protein fragments that remain attached to the virus on proteolytic activation of VP4) derived by X-ray crystallography fits well into the corresponding portion of BTV VP2. Furthermore, despite

the radically different copy numbers of BTV VP5 (120 trimers) and rotavirus VP7 (260 trimers) comparison of low resolution cryo-EM reconstructions of the two molecules reveals similarities which suggest that the somewhat larger (59-kDa vs 37-kDa) BTV VP5 subunit may consist of two domains, arranged in a twisted stack with the lower portion resembling rotavirus VP7. The argument for drawing such speculative parallels between the different viruses becomes stronger when one takes into account the similar biological functions attributed to the pair of molecules in the two viruses, the growing convergence in structure [VP5 of rotavirus, long thought to exist on the virus particle as dimers is now known to be trimeric (Dormitzer et al. 2004)], and the distant, but detectable, similarity between rotavirus VP8 (the second cleavage product of VP4, a structure involved in receptor interactions) and the trimeric receptor binding protein VP9 of Banna virus (a virus belonging to the genus *Seadornavirus,* a genus of nonturreted viruses of the *Reoviridae* which constitute an emerging threat to human health) (Mohd Jaafar et al. 2005). In summary, we propose that BTV VP2 may be thought of as a relative of rotavirus VP4 in which the preactivation state is well ordered by interactions with the virus core (in rotavirus the VP7 outer layer proteins prevent such stabilisation) and cryo-EM results (Dormitzer et al. 2004) demonstrate that the three arms of VP4 are disordered prior to proteolytic activation. On this basis, by combining data from cryo-EM analyses of BTV and rotavirus with X-ray data on the structures of rotavirus VP5 and VP8 and on Banna virus VP9 (Dormitzer et al. 2002, 2004; Mohd Jaafar et al. 2005, Nason et al 2004), we propose a generic quasi-atomic model for these molecular systems which appear to mediate receptor interactions and cell entry (Fig. 5C). As noted by Dormitzer et al. (2004), the recent structural results suggest that there might be mechanistic similarities between the cell entry mechanisms of dsRNA viruses and the fusion machinery of enveloped viruses.

8 The Nonstructural Proteins

The three nonstructural proteins, NS1, NS2 and NS3, are relatively poorly characterised functionally, but clearly play important roles in the co-ordination of viral assembly, virus translocation within the cell and egress through the cell membrane (Brookes et al. 1993). Just as cell entry remains largely a matter of speculation, the structural basis for the exquisite selectivity shown by orbiviruses in packaging one copy of each of their ten genome segments, and also how such large assemblies might leave the host cell without causing disruption, is unknown. It is likely that the nonstructural

proteins hold the key to these processes; however, our structural knowledge remains pitifully limited. Until very recently, the only structural information available was low-resolution microscopy (Brookes et al. 1993); however, this has recently been supplemented by the first atomic level information on a portion of NS2 (Butan et al. 2004). It can only be hoped that this will stimulate further work. NS2 of bluetongue virus is a nonspecific ssRNA binding protein that forms large homomultimers (Taraporewala et al. 2001). The protein is synthesised in large amounts throughout the replication cycle of BTV and accumulates in large, dense perinuclear structures called viral inclusion bodies in BTV-infected mammalian cells. The protein is of particular interest because of its possible involvement in genome recognition (preference for viral ssRNA over cellular ssRNA), which is a key early step in the assembly of the viruses. Deletion mutagenesis studies have indicated that the N-terminal half, which is the most conserved part of the protein across all BTV serotypes, is an RNA binding domain.

The structure of the N-terminal domain of NS2 has been determined by X-ray crystallography and is composed predominantly of two β-sheets arranged as a sandwich. These structures form tight oligomeric complexes with two distinct sets of oligomeric interactions (Butan et al. 2004). The net effect of applying the crystallographic symmetry operators to this dimer is to produce a crystal lattice which is made up of broad, shallow spirals of NS2 molecules arranged with 12 subunits per turn of the 6_1 helix. This remarkable packing

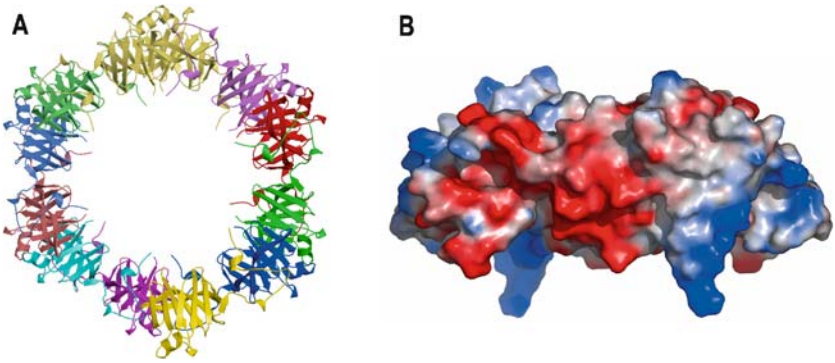

Fig. 6A, B NS2. **A** Diagramme showing the helical packing of the RNA-binding domains of NS2 observed in the crystals of Butan et al. (2004). Subunits are coloured individually and drawn as secondary structural cartoons. **B** Electrostatic potential of a putative dimer of NS2 showing the amphipathic nature of the molecule (negative potential: *red*, positive: *blue*, on an arbitrary scale). The putative RNA binding domain is towards the bottom of the molecule (as drawn)

is shown in Fig. 6A, from which it will be seen that the C-termini of the N-terminal fragments project into cylindrical voids within the crystal. The N-terminal domain visualised in the crystal contains the RNA binding motifs and the rough position of the interaction with RNA may be gauged from Fig. 6B, where we show the electrostatic surface potential for the NS2 N-terminal domain. Note that the motifs previously reported to be so-called RNA binding domains (Zhao et al. 1994) are disposed relatively close to each other in space, so that they are well positioned to collaborate in the formation of an RNA-binding surface. The mode of binding of ssRNA is reminiscent of other ssRNA-binding proteins where the RNA-binding surface is formed by β-sheets (Handa et al. 1999). Thus, the presentation of the RNA-binding surface suggests that the crystal packing observed for NS2 may recapitulate biologically relevant higher-order assemblies of this molecule.

9 Perspectives

Our structural understanding of orbiviruses has developed steadily over the last 10 years, so that, by making reasonable analogies with related proteins, we are now in the position of having structural insight into half of the proteins of the virus. The best-developed area of understanding is the viral core. When determined this was the largest structure visualised by crystallography and it still provides a paradigm for other members of the family *Reoviridae* (Grimes et al. 1998; Reinisch et al. 2000). In essence, by using an unusual association of two subunits of the VP3(T2) protein, the inner layers of the particles can assemble without further conformational switching. This mechanism is therefore not readily scaled to form more complex particles, and it may therefore be no coincidence that there are not substantially larger viruses belonging to the viral lineage that contains the *Reoviridae* (Bamford et al. 2002). This fragile internal VP3(T2) skin is rigidified by the cloak of 260 essentially identical trimers of VP7(T13). The BTV core particle is also an attractive model system for how a subcellular organelle orchestrates its structural and functional components and biochemical activities. Structural analysis has shed light on the logistics of the supply of raw materials and the removal of products and by-products from the transcription factory (Diprose et al. 2001). In addition, the analysis of the core has revealed that it is an effective sink, capable of sequestering some 2,000 base pairs of dsRNA per particle (Diprose et al. 2002); the BTV core particles themselves therefore probably scour infected cells of dsRNA released from damaged particles, which might otherwise trigger cellular responses preventing completion of the viral replication cycle.

Our understanding of the orbivirus outer layer, comprising in the case of BTV VP2 and VP5, is far more sketchy. However, we have indicated above how we believe structural information from other members of the family (Dormitzer et al. 2004; Mohd Jaafar et al. 2005; Nason et al 2004) can be mapped onto BTV to provide a rough working model for the structure of VP2. The structure of VP5, in contrast, remains obscure. Whilst these outer proteins are of potential interest as targets for the development of novel antiviral therapies, this will require a far deeper structural understanding than we possess at present.

The minor capsid proteins have enzymatic activity. VP1 is probably, for the most part, similar to the equivalent protein (λ1) from reovirus (Tao et al. 2002). In contrast to the turreted viruses (for instance reovirus), the various enzymatic activities (including the four capping functions which reside on VP4) are coordinated within the core. What will be particularly interesting is to learn how BTV and the other nonturreted members of the family *Reoviridae* orchestrate, in time and space, the various biochemical activities during conservative transcription to yield capped mRNA at high efficiency.

The final set of proteins, the nonstructurals, NS1, NS2 and NS3, are the least well understood. Our only structural information concerns the RNA binding domain of NS2 (Butan et al. 2004), and as indicated above, this only provides limited insights. Nevertheless, structures for these proteins would be very helpful, not least since, in the continued absence of a robust reverse genetics system, a series of chemical compounds targeted at individual proteins on the basis of their structure would be powerful probes of function.

Acknowledgements We thank the Royal Society and the Medical Research Council for personal support and the MRC, BBSRC & EU for supporting work on these viruses, in particular with our valued collaborators Professors Polly Roy and Peter Mertens.

References

Abrescia NG, Cockburn JJ, Grimes JM, Sutton GC, Diprose JM, Butcher SJ, Fuller SD, San Martin C, Burnett RM, Stuart DI, Bamford DH, Bamford JK (2004) Insights into assembly from structural analysis of bacteriophage PRD1. Nature 432:68–74

Bamford DH, Burnett RM, Stuart DI (2002) Evolution of viral structure. Theor Popul Biol 61:461–470

Bamford DH, Grimes JM, Stuart DI (2005) What does structure tell us about virus evolution? Curr Op Struct Biol 15:1–9

Bartlett NM, Gillies SC, Bullivant S, Bellamy AR (1974) Electron microscopy study of reovirus reaction cores. J Virol 14:315–326

Basak AK, Gouet P, Grimes J, Roy P, Stuart D (1996) Crystal structure of the top domain of African horse sickness virus VP7: comparisons with bluetongue virus VP7. J Virol 70:3797–3806

Basak AK, Grimes JM, Gouet P, Roy P, Stuart DI (1997) Structures of orbivirus VP7: implications for the role of this protein in the viral life cycle. Structure 5:871–883

Bergeron J, Mabrouk T, Garzon S, Lemay G (1998) Characterization of the thermosensitive ts453 reovirus mutant: increased dsRNA binding of sigma 3 protein correlates with interferon resistance. Virology 246:199–210

Brookes SM, Hyatt AD, Eaton BT (1993) Characterization of virus inclusion bodies in bluetongue virus-infected cells. J Gen Virol 74:525–530

Burroughs JN, O'Hara RS, Smale CJ, Hamblin C, Walton A, Armstrong R, Mertens PP (1994) Purification and properties of virus particles, infectious subviral particles, cores and VP7 crystals of African horsesickness virus serotype 9. J Gen Virol 75:1849–1857

Butan C, Van Der Zandt H, Tucker PA (2004) Structure and assembly of the RNA binding domain of bluetongue virus non-structural protein 2. J Biol Chem 279:37613–37621

Butcher SJ, Grimes JM, Makeyev EV, Bamford DH, Stuart DI (2001) A mechanism for initiating RNA-dependent RNA polymerization. Nature 410:235–240

Caspar DLD, Klug A (1962) Physical principles in the construction of regular viruses. Cold Spring Harbor Symp Quant Biol 27:1–24

Chiu W, Burnett R, Garcea RE (1997) Structural biology of viruses. Oxford University Press, New York

Cleveland DR, Zarbl H, Millward S (1986) Reovirus guanylyltransferase is L2 gene product lambda 2. J Virol 60:307–311

Cockburn JJ, Abrescia NG, Grimes JM, Sutton GC, Diprose JM, Benevides JM, Thomas GJ Jr, Bamford JK, Bamford DH, Stuart DI (2004) Membrane structure and interactions with protein and DNA in bacteriophage PRD1. Nature 432:122–125

Diprose JM, Burroughs JN, Sutton GC, Goldsmith A, Gouet P, Malby R, Overton I, Zientara S, Mertens PP, Stuart DI, Grimes JM (2001) Translocation portals for the substrates and products of a viral transcription complex: the bluetongue virus core. EMBO J 20:7229–7239

Diprose JM, Grimes JM, Sutton GC, Burroughs JN, Meyer A, Maan S, Mertens PP, Stuart DI (2002) The core of bluetongue virus binds double-stranded RNA. J Virol 76:9533–9536

Dormitzer PR, Sun ZY, Wagner G, Harrison SC (2002) The rhesus rotavirus VP4 sialic acid binding domain has a galectin fold with a novel carbohydrate binding site. EMBO J 21:885–897

Dormitzer PR, Nason EB, Prasad BV, Harrison SC (2004) Structural rearrangements in the membrane penetration protein of a non-enveloped virus. Nature 430:1053–1058

Eaton BT, Hyatt AD, Brookes SM (1990) The replication of bluetongue virus. Curr Top Microbiol Immunol 162:89–118

Fausnaugh J, Shatkin AJ (1990) Active site localization in a viral mRNA capping enzyme. J Biol Chem 265:7669–7672

French TJ, Roy P (1990) Synthesis of bluetongue virus (BTV) corelike particles by a recombinant baculovirus expressing the two major structural core proteins of BTV. J Virol 64:1530–1536

Gillies S, Bullivant S, Bellamy AR (1971) Viral RNA polymerases: electron microscopy of reovirus reaction cores. Science 174:694–696

Gouet P, Diprose JM, Grimes JM, Malby R, Burroughs JN, Zientara S, Stuart DI, Mertens PP (1999) The highly ordered double-stranded RNA genome of bluetongue virus revealed by crystallography. Cell 97:481–490

Grimes J, Basak AK, Roy P, Stuart D (1995) The crystal structure of bluetongue virus VP7. Nature 373:167–170

Grimes JM, Burroughs JN, Gouet P, Diprose JM, Malby R, Zientara S, Mertens PP, Stuart DI (1998) The atomic structure of the bluetongue virus core. Nature 395:470–478

Handa N, Nureki O, Kurimoto K, Kim I, Sakamoto H, Shimura Y, Muto Y, Yokoyama S (1999) Structural basis for recognition of the tra mRNA precursor by the Sex-lethal protein. Nature 398:579–585

Harrison SC, Olson AJ, Schutt CE, Winkler FK, Bricogne G (1978) Tomato bushy stunt virus at 2.9 Å resolution. Nature 276:368–373

Hassan SH, Wirblich C, Forzan M, Roy P (2001) Expression and functional characterization of bluetongue virus VP5 protein: role in cellular permeabilization. J Virol 75:8356–8367

Hassan SS, Roy P (1999) Expression and functional characterization of bluetongue virus VP2 protein: role in cell entry. J Virol 73:9832–9842

Hewat EA, Booth TF, Loudon PT, Roy P (1992a) Three-dimensional reconstruction of baculovirus expressed bluetongue virus core-like particles by cryo-electron microscopy. Virology 189:10–20

Hewat EA, Booth TF, Roy P (1992b) Structure of bluetongue virus particles by cryo-electron microscopy. J Struct Biol 109:61–69

Hill CL, Booth TF, Prasad BV, Grimes JM, Mertens PP, Sutton GC, Stuart DI (1999) The structure of a cypovirus and the functional organization of dsRNA viruses. Nat Struct Biol 6:565–568

Huismans H, van Dijk AA, Els HJ (1987) Uncoating of parental bluetongue virus to core and subcore particles in infected L cells. Virology 157:180–188

Jacobs BL, Langland JO (1998) Reovirus sigma 3 protein: dsRNA binding and inhibition of RNA-activated protein kinase. Curr Top Microbiol Immunol 233:185–196

Johnson JE, Speir JA (1997) Quasi-equivalent viruses: a paradigm for protein assemblies. J Mol Biol 269:665–675

Kapahnke R, Rappold W, Desselberger U, Riesner D (1986) The stiffness of dsRNA: hydrodynamic studies on fluorescence-labelled RNA segments of bovine rotavirus. Nucleic Acids Res 14:3215–3228

Kar AK, Ghosh M, Roy P (2004) Mapping the assembly pathway of bluetongue virus scaffolding protein VP3. Virology 324:387–399

Lawton JA, Estes MK, Prasad BV (1997) Three-dimensional visualization of mRNA release from actively transcribing rotavirus particles. Nat Struct Biol 4:118–121

Liemann S, Chandran K, Baker TS, Nibert ML, Harrison SC (2002) Structure of the reovirus membrane-penetration protein, Mu1, in a complex with is protector protein, Sigma3. Cell 108:283–295

Loudon PT, Roy P (1991) Assembly of five bluetongue virus proteins expressed by recombinant baculoviruses: inclusion of the largest protein VP1 in the core and virus-like proteins. Virology 180:798–802

Loudon PT, Roy P (1992) Interaction of nucleic acids with core-like and subcore-like particles of bluetongue virus. Virology 191:231–236

Lu G, Zhou ZH, Baker ML, Jakana J, Cai D, Wei X, Chen S, Gu X, Chiu W (1998) Structure of double-shelled rice dwarf virus. J Virol 72:8541–8549

Martinez-Costas J, Gonzalez-Lopez C, Vakharia VN, Benavente J (2000) Possible involvement of the double-stranded RNA-binding core protein sigmaA in the resistance of avian reovirus to interferon. J Virol 74:1124–1131

Mathieu M, Petitpas I, Navaza J, Lepault J, Kohli E, Pothier P, Prasad BV, Cohen J, Rey FA (2001) Atomic structure of the major capsid protein of rotavirus: implications for the architecture of the virion. EMBO J 20:1485–1497

Mertens PPC (2000) Orbiviruses and coltiviruses—general features. In: Webster RG, Granoff A (eds) Encyclopedia of virology. Academic Press, London

Mertens PPC, Burroughs JN, Anderson J (1987) Purification and properties of virus particles, infectious subviral particles, and cores of bluetongue virus serotypes 1 and 4. Virology 157:375–386

Mertens PP, Burroughs JN, Walton A, Wellby MP, Fu H, O'Hara RS, Brookes SM, Mellor PS (1996) Enhanced infectivity of modified bluetongue virus particles for two insect cell lines and for two Culicoides vector species. Virology 217:582–593

Mertens P, Attoui H, Duncan R, Dermody T (2005) Reoviridae. In: Fauquet C, Mayo J, Maniloff J, Desselberger U, Ball L (eds) Virus taxonomy. Eighth report of the International Committee on Taxonomy of Viruses. Elsevier/Academic Press, London, pp 447–454

Mohd Jaafar F, Attoui H, Bahar MW, Siebold C, Sutton G, Mertens PP, De Micco P, Stuart DI, Grimes JM, De Lamballerie X (2005) The structure and function of the outer coat protein VP9 of Banna virus. Structure 13:17–28

Moss SR, Nuttall PA (1994) Subcore- and core-like particles of Broadhaven virus (BRDV), a tick-borne orbivirus, synthesized from baculovirus expressed VP2 and VP7, the major core proteins of BRDV. Virus Res 32:401–407

Nakagawa A, Miyazaki N, Taka J, Naitow H, Ogawa A, Fujimoto Z, Mizuno H, Higashi T, Watanabe Y, Omura T, Cheng RH, Tsukihara T (2003) The atomic structure of rice dwarf virus reveals the self-assembly mechanism of component proteins. Structure 11:1227–1238

Nason EL, Rothagel R, Mukherjee SK, Kar AK, Forzan M, Prasad BV, Roy P (2004) Interactions between the inner and outer capsids of bluetongue virus. J Virol 78:8059–8067

Prasad BV, Rothnagel R, Zeng CQ, Jakana J, Lawton JA, Chiu W, Estes MK (1996) Visualization of ordered genomic RNA and localization of transcriptional complexes in rotavirus. Nature 382:471–473

Ramadevi N, Burroughs NJ, Mertens PP, Jones IM, Roy P (1998) Capping and methylation of mRNA by purified recombinant VP4 protein of bluetongue virus. Proc Natl Acad Sci U S A 95:13537–13542

Reinisch KM, Nibert ML, Harrison SC (2000) Structure of the reovirus core at 3.6 Å resolution. Nature 404:960–967

Roy P, Fukusho A, Ritter GD, Lyon D (1988) Evidence for genetic relationship between RNA and DNA viruses from the sequence homology of a putative polymerase gene of bluetongue virus with that of vaccinia virus: conservation of RNA polymerase genes from diverse species. Nucleic Acids Res 16:11759–11767

Schoehn G, Moss SR, Nuttall PA, Hewat EA (1997) Structure of Broadhaven virus by cryoelectron microscopy: correlation of structural and antigenic properties of Broadhaven virus and bluetongue virus outer capsid proteins. Virology 235:191–200

Stauber N, Martinez-Costas J, Sutton G, Monastyrskaya K, Roy P (1997) Bluetongue virus VP6 protein binds ATP and exhibits an RNA-dependent ATPase function and a helicase activity that catalyze the unwinding of double-stranded RNA substrates. J Virol 71:7220–7226

Stuart D (1993) Viruses. Curr Opin Struct Biol 3:167–174

Stuart DI, Gouet P, Grimes J, Malby R, Diprose J, Zientara S, Burroughs JN, Mertens PP (1998) Structural studies of orbivirus particles. Arch Virol Suppl 14:235–250

Tan BH, Nason E, Staeuber N, Jiang W, Monastryrskaya K, Roy P (2001) RGD tripeptide of bluetongue virus VP7 protein is responsible for core attachment to Culicoides cells. J Virol 75:3937–3947

Tao Y, Farsetta DL, Nibert ML, Harrison SC (2002) RNA synthesis in a cage—structural studies of reovirus polymerase lambda3. Cell 111:733–745

Taraporewala ZF, Chen D, Patton JT (2001) Multimers of the bluetongue virus non-structural protein, NS2, possess nucleotidyl phosphatase activity: similarities between NS2 and rotavirus NSP2. Virology 280:221–231

Urakawa T, Ritter DG, Roy P (1989) Expression of largest RNA segment and synthesis of VP1 protein of bluetongue virus in insect cells by recombinant baculovirus: association of VP1 protein with RNA polymerase activity. Nucleic Acids Res 17:7395–7401

Van Dijk AA, Huismans H (1988) In vitro transcription and translation of bluetongue virus mRNA. J Gen Virol 69:573–581

Wikoff WR, Liljas L, Duda RL, Tsuruta H, Hendrix RW, Johnson JE (2000) Topologically linked protein rings in the bacteriophage HK97 capsid. Science 289:2129–2133

Yazaki K, Miura K (1980) Relation of the structure of cytoplasmic polyhedrosis virus and the synthesis of its messenger RNA. Virology 105:467–479

Zhao Y, Thomas C, Bremer C, Roy P (1994) Deletion and mutational analyses of bluetongue virus NS2 protein indicate that the amino but not the carboxy terminus of the protein is critical for RNA–protein interactions. Virology 68:2179–2185

Zhou ZH, Zhang H, Jakana J, Lu XY, Zhang JQ (2003) Cytoplasmic polyhedrosis virus structure at 8 Å by electron cryomicroscopy: structural basis of capsid stability and mRNA processing regulation. Structure 11:651–663

CTMI (2006) 309:245–261

Rotavirus Assembly: An Alternative Model That Utilizes an Atypical Trafficking Pathway

S. Chwetzoff · G. Trugnan (✉)

INSERM-UPMC UMR 538, "Membrane traffic and signalization in epithelial cells", CHU Saint-Antoine, 27 rue de Chaligny, 75012 Paris, France
trugnan@ccr.jussieu.fr

Abstract We review here recent advances in our knowledge on trafficking and assembly of rotavirus and rotaviral proteins in intestinal cells. Assembly of rotavirus has been extensively studied in nonpolarized kidney epithelial MA104 cells, where several data indicate that most if not all the steps of rotavirus assembly take place within the endoplasmic reticulum (ER) and that rotavirus is release upon cell lysis. We focus here on data obtained in intestinal cells that argue for another scheme of rotavirus

assembly, where the final steps seem to take place outside the ER with an apically polarized release of rotavirus without significant cell lysis. One of the key observations made by different groups is that VP4 and other structural proteins interact substantially with specialized membrane microdomains enriched in cholesterol and sphingolipids termed rafts. In addition, recent data point to the fact that VP4 does not localize within the ER or the Golgi apparatus in infected intestinal cells. The mechanisms by which VP4, a cytosolic protein, may be targeted to the apical membrane in these cells and assembles with the other structural proteins are discussed. The identification of cellular proteins such as Hsp70, flotillin, rab5, PRA1 and cytoskeletal components that interact with VP4 may help to define an atypical polarized trafficking pathway to the apical membrane of intestinal cells that will be raft-dependent and by-pass the classical exocytic route.

1 Introduction

1.1 Rotavirus Structure

Rotavirus is a relatively large (75-nm) icosahedral, nonenveloped double-stranded RNA (dsRNA)-containing virus (reviewed in Lawton et al. 2000). Its capsid encloses 11 segments of dsRNA, each segment encoding for one protein except for segment 11, which encodes two proteins. Six out of these 12 proteins are structural proteins (VP1–VP4, VP6, and VP7) and the six others are nonstructural proteins (NSP1–NSP6). The capsid is composed of three concentric protein layers (reviewed in Jarayam et al. 2004). The inner layer is mostly made of 60 dimers of VP2 to which are associated small quantities of VP1, an RNA-dependent RNA polymerase, and VP3, a guanylyl and methyl transferase required for the synthesis of capped mRNA transcripts. The intermediate layer consists exclusively of 260 trimers of VP6 that interact with VP2 and with the two remaining structural proteins of the external layer of the capsid, VP7 and VP4 (Mathieu et al. 2001).

1.2 Rotavirus Mainly Targets Enterocytes

It has been shown that rotaviruses can infect a number of cell types in vitro (Ciarlet et al. 2001), and recent work suggests that rotavirus provokes viremia, thus transgressing the epithelial barrier (Blutt et al. 2003). Several studies, however, indicate that in vivo rotaviruses mainly target enterocytes from the small intestine of young animals, infants, and young children. Rotaviruses are the major causative agent of acute infantile gastroenteritis responsible for

nearly 600,000 deaths annually worldwide (Parashar et al. 2003). Most of the clinical symptoms are restricted to the gut, suggesting that progeny virions follow a pathway that limits widespread dissemination. Indeed, it has been shown that the vast majority of progeny virions are released through an ill-defined process at the apical pole of infected intestinal cells (Jourdan et al. 1997).

1.3 The Polarized Trafficking Machinery of Intestinal Epithelial Cells

Intestinal epithelial cells display a polarized phenotype and possess an apical membrane consisting of a brush border oriented towards the lumen of the gut. The apical membrane is separated from the basolateral membrane by a sophisticated junction system containing tight and adherent junctions that strictly control and limit the dissemination through the epithelial barrier and laterally between the apical and the basolateral domain. To support this organization, epithelial cells have developed sophisticated intracellular trafficking pathways able to sort and target molecules destined to the apical or the basolateral domains (Mostov et al. 2003). Proteins synthesized on endoplasmic reticulum (ER) -associated ribosomes enter the ER and follow a common route through the Golgi apparatus to the trans-Golgi network (TGN). The polarized traffic of lipids has been less studied, but recent data indicate that similar sorting and targeting processes are also at work for several lipid species (Hoekstra and van Ijzendoorn 2000). It is now an established fact that a first sorting event takes place in the TGN, where a subset of proteins will be targeted to the apical membrane, whereas other proteins are targeted to the basolateral membrane. Several data have shown that a second sorting event takes place at the basolateral membrane where proteins containing specific, as yet unidentified targeting signals will be readdressed to the apical domain using the endosomal system through a process called transcytosis (Polishchuk et al. 2004). It is also generally accepted that proteins bear sorting and/or targeting signals that are recognized by a complex intracellular machinery and help to incorporate proteins into specific intracellular vesicles equipped to address these proteins to the correct compartment. Unequivocal basolateral targeting signals have been identified (Mostov et al. 2000), but apical targeting signals remain to be more clearly defined. It has thus been proposed that the glycosylphosphatidylinositol (GPI) anchor (Mayor and Riezman 2004), protein glycosylation (Ait Slimane et al. 2001), or some specific transmembrane domains (Ait Slimane et al. 2001) may be involved in apical targeting, although these results are challenged by other experimental data (Rajho Meerson et al. 2000; Ait Slimane et al. 2000; Lipardi et al. 2000).

2
What Is Known About Rotavirus and Rotaviral Protein Trafficking?

Although it has been clearly established that intestinal cells are the main in vivo target of rotavirus, most of the studies on virus assembly and release have been carried out in nonpolarized and nonintestinal cells, mainly MA104 cells originating from monkey embryo kidney cells (Estes 2001). The picture emerging from these studies can be summarized as follows. After rotavirus entry into cells through a process that continues to be debated (endocytosis or direct entry; for details see Lopez and Arias 2004), the external layer of the capsid (VP4 and VP7) is removed through a calcium binding process (Ruiz et al. 2000), leading to a transcriptionally competent particle (called the double-layered particle or DLP; see Jarayam et al. 2004), producing segmented mRNAs which are capped at the 5′ end but not polyadenylated at the 3′ end (Estes 2001). Most of the encoded viral proteins are then thought to be synthesized on free ribosomes, except for VP7 and NSP4, which possess signal peptides and are therefore targeted to ER-associated ribosomes (Au et al. 1993; Stirzaker et al. 1990). All the cytosolic viral proteins except VP4 have been found in an ill-defined cytoplasmic organite, the viroplasm, considered to be a viral factory from which immature particles, containing the viral genome protected by the inner and the intermediate layer of the capsid (DLPs), emerge and enter within the ER lumen through an NSP4-dependent process (Taylor et al. 1993). Electron microscopy studies have shown that these DLPs have a transient membrane envelope (Suzuki et al. 1993). It is still not clear whether VP7 is associated with the virus particles at this stage. When VP7, a glycoprotein, is incorporated into viral particles of rotavirus SA11 strain in infected MA104 cells, the protein displays a glycosylation content consisting mostly of six mannose molecules (Kabcenell et al. 1988). This would suggest that VP7 remains accessible to glycan-processing enzymes localized in a post-ER compartment. The nonstructural protein NSP4, a viral glycoprotein associated with the ER membrane, is involved in DLP entry within the ER (Taylor et al. 1993) and has also been described as part of a complex with VP4 and VP7 (Maass and Atkinson 1990). This finding, together with the fact that NSP4 never reaches the Golgi apparatus (Xu et al. 2001), has favored the hypothesis that rotavirus final assembly takes place within the ER. It is generally accepted that new rotavirus virions are released through cell lysis in MA104.

3
Rotavirus and Intestinal Cells

Few studies have been conducted on the mechanisms by which rotavirus infects intestinal cells, despite the availability, since the early 1980s, of cell systems such as HT-29 or Caco-2 cells able to reproduce a significant part of the polarization and differentiation programs of human intestinal cells in culture (Chantret et al. 1988). Interestingly, these cell lines, when grown in a very precise manner, are able to form a regular monolayer with functional tight junctions, displaying a high electrical transepithelial resistance and expressing intestinal specific markers, such as apical brush border enzymes (Trugnan et al. 1987; Darmoul et al. 1992). Harry Greenberg's group was the first to demonstrate that polarized Caco-2 cells are fully susceptible to rotavirus infection (Svensson et al. 1991). We then showed that rotavirus infection of Caco-2 cells displays three major differences as compared to nonpolarized MA104 cells: (a) the time needed for virus morphogenesis appears to be significantly longer than in MA104 since a rise in virus titer is only observed at 12–15 h postinfection (pi), suggesting a more complex assembly process and/or a delayed entry (Jourdan et al. 1997, 1998); (b) intestinal cells do not lyse upon completion of the true viral replication cycle and remained viable for at least 48 h pi; and (c) in agreement with (b), progeny virions are selectively released through the apical membrane, suggesting that the general architecture of intestinal cells was maintained and that virus was assembled using polarized sorting and targeting mechanisms (Jourdan et al. 1997). Since then, additional work has been carried out to describe the pathway used by rotavirus and rotaviral protein for assembly and release in intestinal cells (see below). The main starting point for these studies was based on the idea that apical targeting may be mediated by specialized membrane microdomains, namely rafts, known to be enriched in cholesterol and sphingolipids (Simons and Ikonnen 1997).

4
Rotavirus and Rafts

4.1
Revisiting the Fluid Mosaic Model of Biological Membrane

The classical model of Singer and Nicolson (1972) predicted that cell membranes behave like a fluid mosaic in which proteins float within a sea of

lipids. This model has proven very useful for several generations of researchers. However, using either membrane models or biological systems, several other results have shown that lipids have specific capacities to self-assemble within microdomains, and therefore membranes should be heterogeneous in composition and structure (Simons and Vaz 2004). Proteins may choose a specific lipid environment, as shown, for example, for GPI-linked proteins, and this in turn may induce lipids to reorganize (Helms and Zurzolo 2004). The concept of rafts remains, however, a matter of debate, mostly because of the lack of accurate identification methodologies (Munro 2003). Most of the studies are based on a unique biochemical property of these microdomains: they are resistant to detergent extraction (detergent resistant membranes, DRM) and can therefore be floated on density gradients, because of their high lipid content. The raft hypothesis has been largely used to explain the number of biological and pathophysiological processes, including the involvement of rafts in the interaction of enveloped viruses with their target cells (Chazal and Gerlier 2003). In contrast, until recently, there were no data available on interactions of rafts with nonenveloped viruses.

4.2
Evidence for Raft Involvement in Rotavirus Assembly

Evidence that rotavirus and rotaviral proteins become associated with rafts was demonstrated using various approaches. The group of Carlos Arias and Susana Lopez demonstrated that some particular rafts of MA104 cells may be involved in rotavirus entry (Lopez and Arias 2004; Isa et al. 2004; Sanchez-San Martin et al. 2003) (see the chapter by S. Lopez and C. Arias in this volume). Using differentiated Caco-2 cells, our group showed that VP4 associated very early after infection with detergent-resistant membranes. We also demonstrated that the other rotaviral structural proteins associated later with DRMs in a time sequence that was compatible with a role of rafts for rotavirus assembly. This was confirmed using an X-ray diffraction approach with VP4 and a lipid mixture that resemble raft composition (Sapin et al. 2002). Finally, we showed that detergent-resistant membranes extracted from infected cells were able to infect naive Caco-2 cells (Sapin et al. 2002). A direct interaction between rotavirus, rotaviral proteins, and detergent-resistant membranes was confirmed by Harry Greenberg's group, which demonstrated that in vivo rotavirus also associated with lipid rafts in infected mice (Cuadras and Greenberg 2003). Interestingly, some discrepancies between the two sets of data were noted, mainly concerning the kinetics of rotavirus protein association with rafts, which was much more rapid and simultaneous in the

latter data (Cuadras and Greenberg 2003). This may at least in part be attributable to the fact that Caco-2 cells were grown in conditions in which they do not fully differentiate (Cuadras and Greenberg 2003). In the meantime, it was shown that NSP4 also associates with microdomains (Huang et al. 2001). Other recent data seem to indicate, however, that when VP5 fragments, derived from VP4, including the putative hydrophobic domain (residues 248–274) were transfected into Cos 7 or HEK293 cells, no association with DRMs was observed (Golantsova et al. 2004), suggesting that VP4 may not interact with rafts using this hydrophobic domain and/or that VP4 interaction with DRMs is not direct, as expected for a peripheral protein that requires additional membrane factor(s) to interact. This fit very well with preliminary data from our lab suggesting that VP4 may interact with cellular raft-associated proteins (Gardet et al., Delmas et al., unpublished data; Broquet et al. 2003, unpublished data).

5
Rotavirus Assembly Needs an Extra-Reticular Step

5.1
Rational for the Extra-Reticular Hypothesis

In an attempt to understand how rafts may be involved in the final assembly of rotavirus particles, it was necessary to comprehend how these rafts interact with the ER, since DLPs enter the ER when they emerge from the viroplasm and rafts are classically known to be excluded from this compartment. In eucaryotic cells, the synthesis of sphingolipids, which are essential raft components, takes place in the Golgi apparatus (Holthuis et al. 2001) from a ceramide precursor made in the ER and transported directly to the TGN via a nonvesicular pathway, catalyzed by a recently discovered protein called CERT (Hanada et al. 2003). If rotavirus uses rafts as an assembly platform, then it can be hypothesized that immature particles (containing VP1–VP3 and VP6) emerging from the ER associate with VP7, which is already present within the ER membrane, and with VP4, which is synthesized on free ribosomes. If this is true, then VP4 must be ER-associated and therefore sensitive to drugs affecting ER exit.

5.2
The Tunicamycin Effect

Experiments have recently been conducted in our laboratory in which tunicamycin was used to perturb ER exit. Tunicamycin is known to block the

first N-glycosylation step, resulting in the accumulation of nonglycosylated proteins within the ER (Struck and Lennarz 1977). This drug has already been used to study rotavirus assembly in MA104 cells and it has been shown that virus morphogenesis is strongly perturbed (Petrie et al. 1983; Mirazimi and Svensson 1998). Our experiments revealed a similar decrease in rotavirus final assembly in Caco-2 cells in the presence of tunicamycin. In addition, these experiments demonstrated that VP4 biosynthesis and trafficking were insensitive to tunicamycin, suggesting that VP4 does not interact with the ER (Delmas et al. 2004a).

5.3
VP4 Is an Extra-ER Protein: Consequences for Rotavirus Assembly

A major consequence of these observations is that VP4 must assemble with the other structural proteins outside the ER. This conclusion is also strengthened by previous data indicating that although rotavirus and rotaviral proteins never transit through the Golgi apparatus (Jourdan et al. 1997; Xu et al. 2001), perturbation of Golgi trafficking using either brefeldin A (Mirazimi et al. 1996) or monensin (Jourdan et al. 1997) leads to an abnormal assembly or a mistargeting of the virus. Finally, recent elegant experiments using the siRNA strategy to inhibit VP4 expression have shown that rotavirus particles that contained all structural proteins except VP4 can be assembled and detected in the cell cytoplasm (Dector et al. 2002). Altogether these data suggest that an alternative model for rotavirus final assembly can be proposed that includes both ER and extra-ER steps (Delmas et al. 2004b) as shown in Fig. 1.

Fig. 1A–F A new proposal for Rotavirus assembly in polarized Caco-2 cells. **A** Rotavirus enters Caco-2 cells through a ill-defined process. The external layer of the viral capsid (VP4 and VP7) is removed. Double layered particles are released and are competent to deliver viral dsRNA within the cytosol. **B** Viral protein synthesis starts on free ribosomes form most of structural and nonstructural proteins except NSP4 and VP7, which are synthesized on ribosomes associated with the rough endoplasmic reticulum. Several structural and nonstructural proteins are found in the viroplasm, an ill-defined cytoplasmic organelle. **C** Double-layered particles are assembled within the viroplasm in the vicinity of the ER. Early after infection, VP4 is found associated with the cytoskeleton. **D** During the endoplasmic reticulum assembly step, DLP enters the ER. Double-layered particles are surrounded with a transient lipid envelope. **E** VP7 is recruited on the external layer of the virus capsid. The viral particles lacking VP4 exit the ER. The VP4 present in the cytosol, mostly associated with the cytoskeleton, is assembled on the viral particles. **F** Virus exits the cells through a mechanism that requires lipid rafts and the cytoskeleton

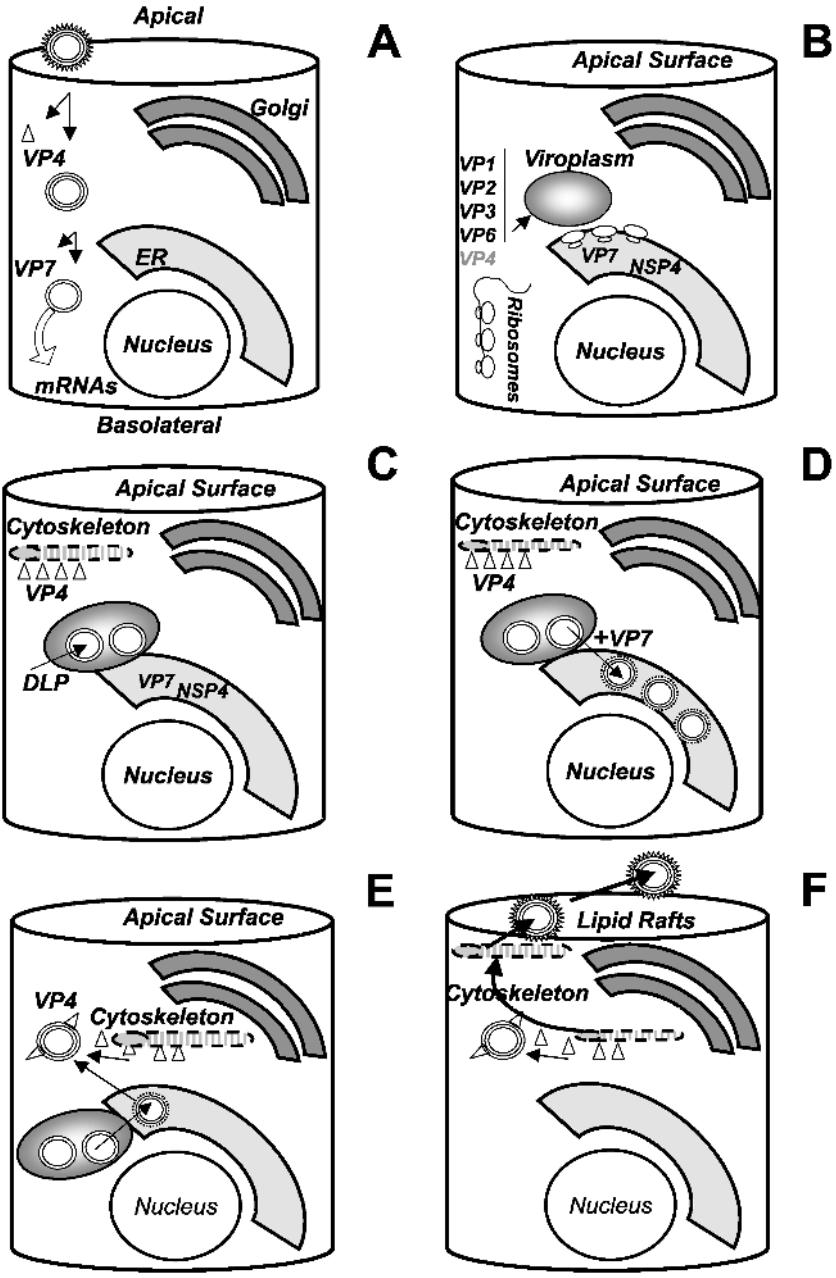
A
Apical
Golgi
VP4
VP7
ER
Nucleus
mRNAs
Basolateral
B
Apical Surface
VP1
VP2
VP3
VP6
VP4
Viroplasm
VP7
NSP4
Ribosomes
Nucleus
C
Apical Surface
Cytoskeleton
VP4
DLP
VP7
NSP4
Nucleus
D
Apical Surface
Cytoskeleton
VP4
+VP7
Nucleus
E
Apical Surface
VP4
Cytoskeleton
Nucleus
F
Lipid Rafts
Cytoskeleton
Nucleus

6
Unanswered Questions

6.1
How Does VP4, a Cytosolic Protein, Associate with Rafts?

As mentioned above, VP4 is synthesized on free cytosolic ribosomes, but it has been shown that this protein never displays a cytosolic pattern but rather localizes on subcellular, still unidentified structures (Petrie et al. 1982; Gonzalez et al. 2000). One of the major questions is how this protein is recruited on cell membranes. Several plasma membrane proteins have already been suggested as partners, such as the cognate heat shock protein Hsc70 (Zarate et al. 2003), which mostly localizes at the cell surface, but not on intracellular membranes. Analysis of the primary structure of VP4 (Bremont et al. 1992) provided some additional clues to this issue. Several VP4 strains display a putative caveolin-1 scaffolding-binding motif within residues 289–296 (Couet et al. 1997) that may account for interaction with lipid microdomains. However, it is important to note that Caco-2 cells do not express caveolin (Mirre et al. 1996). An integrin L-binding domain has been described and recently shown to be correctly exposed at the protein surface and to play a role in rotavirus interactions (Dormitzer et al. 2004). However, it is expected that integrins will be associated with the external leaflet of membrane bilayers within cells and thus cannot be the first partner for VP4, which is produced within the cytosol. Rotavirus VP4 protein also presents a conserved coiled-coil domain, able to mediate protein–protein interactions. The functionality of this domain has not been demonstrated and site-directed mutagenesis experiments have to be carried out in order to confirm that this domain plays a role in VP4–membrane interactions. A peroxisomal targeting signal has been predicted at the C-terminal part of VP4, and a recent paper has suggested that VP4 may interact with peroxisomes (Mohan et al. 2002). However, we were unable to confirm a peroxisomal localization of rotavirus particles and of VP4, suggesting that this signal may be not functional. We have already mentioned that a fusion domain has been described and that this domain does not seem to be involved in VP4 interactions with membrane microdomains. The identification of a galectin-like domain on the VP8 part of VP4 suggests that glycans may represent an interesting membrane target for VP4 (Dormitzer et al. 2002). However, this would suggest highly specific interactions of VP4 with sugars, which does not seem likely if one considers the large variation in sugar interactions of several rotavirus strains (Delorme et al. 2002). Cytoskeletal proteins may also be an interesting tool to mediate VP4 interactions with membrane components. It is well established that rotavirus infection induces early cytoskeleton changes (Brunet

et al. 2000a, 2000b; Obert et al. 2000). Recently, the N-terminal part of VP4 (VP8*) has been shown to directly interact with tight junctions (Nava et al. 2004). Transfected VP4 was detected on cytoskeletal elements in Cos 7 cells (Nejmeddine et al. 2000). Further studies are in progress to analyze whether these cytoskeletal components are instrumental to promoting VP4 interactions with cell membranes and microdomains (Gardet et al., unpublished data).

6.2 In Which Subcellular Compartment Does VP4 Associate with DLPs?

Our current model proposes that VP4 does not assemble with the viral particles within the ER but that this assembly takes place within rafts. It must be definitively demonstrated that ER does not participate in this final step, since it cannot be fully ruled out that an atypical subcompartment of the ER is involved. Recent data seem to indicate that some particular rafts may form in the ER vicinity (Sarnatero et al. 2004). Electron microscopy and cryo-electron microscopy studies will be required to answer these questions. We favor an alternative hypothesis that involves the presence of microdomains within the membrane of an intracellular organelle that is not the Golgi apparatus or the ER. Using two-hybrid and co-immunoprecipitation strategies, it was recently found that VP4 may interact with rab5 and PRA1, two proteins associated with the endosomal system (Enouf et al. 2003). Whether these interactions are instrumental for rotavirus assembly must be further explored. Other intracellular compartments have not received enough attention, for example, autophagosomes or exosomes that have been shown to participate in the assembly of other viruses (Prentice et al. 2004; Nguyen et al. 2003). Finally, it will be interesting to analyze the fine composition of the raft subset that specifically associates with VP4, since this composition may provide insights into their origin. Indeed, it is now recognized that there are several subtypes of cholesterol–sphingolipid-enriched membrane microdomains that may be characterized by their differential solubility in various detergents (Schuck et al. 2003). It has also been shown that some raft subsets are resistant to cholesterol removal by methyl β cyclodextrin, suggesting that they display a different molecular organization. This is particularly true for rafts extracted from the apical membrane of intestinal cells (Danielsen and Hansen 2003). Preliminary results from our laboratory indicate that VP4 containing rafts are also resistant to methyl β cyclodextrin (Delmas et al., unpublished data).

6.3
Is There a Cellular Route Between the ER and the Plasma Membrane That Bypasses the Golgi Apparatus and That Can Be Used by Endogenous Proteins?

As mentioned above, rotavirus and its main structural proteins behave very differently in the final stages of morphogenesis in comparison to other viruses and do not seem to follow a classical exocytic route, although the virus is specifically delivered to the apical pole of intestinal cells (Jourdan et al. 1997). Indeed, some intermediate molecules are present within the ER and others are detected within various intracellular organelles, except the Golgi apparatus. It should be pointed out that most of the proteins of this virus are cytosolic and have no specific signals to enter the exocytic pathway. These proteins are synthesized on free ribosomes and directly released within the cytosol. Little is known on the mechanisms that control their sorting and targeting. In a recent review, Walter Nickel summarized the data on what is called the nonclassical protein secretion, a pathway that bypasses ER and Golgi compartments (Nickel 2003). Four mechanisms have been suggested for this atypical plasma membrane targeting: (1) a re-entry from the cytosol into the endosomal compartment (used for example by interleukin 1β); (2) the use of specific transporters at the cell surface (used by fibroblast growth factors 1 and 2); (3) a translocation at the membrane that probably needs a flip-flop mechanism (used by the *Leishmania* cell surface protein HASBP); and (4) exosomes that form through a membrane blebbing process (probably involved in galectin secretion). At least three such proteins that use the nonclassical protein secretion have recently been described as also being associated with rafts. One is the above-mentioned galectin family, a group of endogenous lectins that have been shown to reach the apical cell membrane through their association with particular DRMs, i.e., rafts (Braccia et al 2003; Hansen et al. 2001). The second one is annexin II, which has been proposed to be secreted through a hemi-fusion process (Danielsen et al. 2003; Faure et al. 2002). The last example is Hsp70, which has recently been shown in our laboratory to be targeted to the plasma membrane of intestinal Caco-2 cells and released in the extracellular medium through specific association with rafts, a process that is greatly increased when cells experienced heat shock (Broquet et al. 2003). Whether rotavirus and/or rotaviral proteins use one of these nonclassical protein secretion pathways remains to be demonstrated.

References

Aït Slimane T, Lenoir C, Sapin C, Maurice M, Trugnan G (2000) Apical secretion and sialylation of soluble dipeptidyl-peptidase-IV are two related events. Exp Cell Res 257:184–194

Aït Slimane T, Lenoir C, Bello V, Delaunay J-L, Goding JW, Chwetzoff S, Maurice M, Fransen JAM, Trugnan G (2001) The cytoplasmic/transmembrane domain of DP-PIV, a type II glycoprotein, contains an apical targeting signal that does not specifically interact with lipid rafts. Exp Cell Res 270:45–55

Au KS, Mattion NM, Estes MK (1993) A subviral particle binding domain on the rotavirus nonstructural glycoprotein NS28. Virology 194:665–673

Blutt SE, Kirkwood CD, Parreno V, Warfield KL, Ciarlet M, Estes MK, Bok K, Bishop RF, Conner ME (2003) Rotavirus antigenaemia and viraemia: a common event? Lancet 362:1445–1449

Braccia A, Villani M, Immerdal,L, Niels-Christiansen LL, Nystrom BT, Hansen GH, Danielsen EM (2003) Microvillar membrane microdomains exist at physiological temperature. Role of galectin-4 as lipid raft stabilizer revealed by superrafts. J Biol Chem 278:15679–15684

Bremont M, Juste-Lesage P, Chabanne-Vautherot D, Charpilienne A, Cohen J (1992) Sequences of the four larger proteins of a porcine group C rotavirus and comparison with the equivalent group A rotavirus proteins. Virology 186:684–692. Erratum in: Virology (1992) 189:402

Broquet AH, Thomas G, Masliah J, Trugnan G, Bachelet M (2003) Expression of the molecular chaperone Hsp70 in detergent-resistant microdomains correlates with its membrane delivery and release. J Biol Chem 278:21601–21606

Brunet JP, Cotte-Laffitte J, Linxe C, Quero AM, Geniteau-Legendre M, Servin A (2000a) Rotavirus infection induces an increase in intracellular calcium concentration in human intestinal epithelial cells: role in microvillar actin alteration. J Virol 74:2323–2332

Brunet JP, Jourdan N, Cotte-Laffitte J, Linxe C, Geniteau-Legendre M, Servin A, Quero AM (2000b) Rotavirus infection induces cytoskeleton disorganization in human intestinal epithelial cells: implication of an increase in intracellular calcium concentration. J Virol 74:10801–10806

Chantret I, Barbat A, Dussaulx E, Brattain MG, Zweibaum A (1988) Epithelial polarity, villin expression, and enterocytic differentiation of cultured human colon carcinoma cells: a survey of twenty cell lines. Cancer Res 48:1936–1942

Chazal N, Gerlier D (2003) Virus entry, assembly, budding, and membrane rafts. Microbiol Mol Biol Rev 67:226–237

Ciarlet M, Crawford SE, Estes MK (2001) Differential infection of polarized epithelial cell lines by sialic acid-dependent and sialic acid-independent rotavirus strains. J Virol 75:11834–11850

Couet J, Li S, Okamoto T, Ikezu T, Lisanti MP (1997) Identification of peptide and protein ligands for the caveolin-scaffolding domain. Implications for the interaction of caveolin with caveolae-associated proteins. J Biol Chem 272:6525–6533

Cuadras MA, Greenberg HB (2003) Rotavirus infectious particles use lipid rafts during replication for transport to the cell surface in vitro and in vivo. Virology 313:308–321

Danielsen EM, Hansen GH (2003) Lipid rafts in epithelial brush borders: atypical membrane microdomains with specialized functions. Biochim Biophys Acta 1617:1–9

Danielsen EM, van Deurs B, Hansen GH, (2003). Nonclassical secretion of annexin A2 to the lumenal side of the enterocyte brush border membrane. Biochemistry 42:14670–14676

Darmoul D, Lacasa M, Baricault L, Marguet D, Sapin C, Trotot P, Trugnan G (1992) Dipeptidylpeptidase IV (DPP IV,CD26) gene expression in enterocyte-like colon cancer cell lines HT-29 and Caco-2. Cloning of the complete human coding sequence and changes of DPP IV mRNA levels during cell differentiation. J Biol Chem 267:4824–4833

Dector MA, Romero P, Lopez S, Arias CF (2002) Rotavirus gene silencing by small interfering RNAs. EMBO Rep 3:1175–1180

Delmas O, Durand-Schneider AM, Cohen J, Colard O, Trugnan G (2004a) Spike protein VP4 assembly with maturing rotavirus requires a postendoplasmic reticulum event in polarized caco-2 cells. J Virol 78:10987–10994

Delmas O, Gardet A, Chwetzoff S, Breton M, Cohen J, Colard O, Sapin C, Trugnan G (2004b) Different ways to reach the top of a cell. Analysis of rotavirus assembly and targeting in human intestinal cells reveals an original raft-dependent, Golgi-independent apical targeting pathway. Virology 327:157–161

Delorme C, Brüssow H, Sidoti J, Roche N, Karlsson KA, Neeser JR, Teneberg S (2001) Glycosphingolipid binding specificities of rotavirus: identification of a sialic acid-binding epitope. J Virol 75:2276–2287

Dormitzer PR, Sun ZY, Wagner G, Harrison SC (2002) The rhesus rotavirus VP4 sialic acid binding domain has a galectin fold with a novel carbohydrate binding site. EMBO J 21:885–897

Dormitzer PR, Nason EB, Prasad BV, Harrison SC (2004) Structural rearrangements in the membrane penetration protein of a non-enveloped virus. Nature 430:1053–1058

Enouf V, Chwetzoff S, Trugnan G, Cohen J (2003) Interactions of rotavirus VP4 spike protein with the endosomal protein Rab5 and the prenylated Rab acceptor PRA1. J Virol 77:7041–7047

Estes MK (2001) Rotaviruses and their replication. In: Knipe DM, Howley PM, Griffin DE, Lamb RA, Martin MA, Roizman B, Strauss SE (eds) Fields virology, 4th edn. Lippincott Williams and Wilkins, Philadelphia, pp 1747–1785

Faure AV, Migne C, Devilliers G, Ayala-Sanmartin J (2002) Annexin 2 "secretion" accompanying exocytosis of chromaffin cells: possible mechanisms of annexin release. Exp. Cell Res 276:79–89

Golantsova NE, Gorbunova EE, Mackow ER (2004) Discrete domains within the rotavirus VP5 direct peripheral membrane association and membrane permeability. J Virol 78:2037–2044

Gonzalez RA, Espinosa R, Romero P, Lopez S, Arias CF (2000) Relative localization of viroplasmic and endoplasmic reticulum-resident rotavirus proteins in infected cells. Arch Virol 145:1963–1973

Hanada K, Kumagai K, Yasuda S, Miura Y, Kawano M, Fukasawa M, Nishijima M (2003) Molecular machinery for non-vesicular trafficking of ceramide. Nature 426:803–809

Hansen GH, Immerdal L, Thorsen E, Niels-Christiansen LL, Nystrom BT, Demant EJ, Danielsen EM (2001) Lipid rafts exist as stable cholesterol-independent microdomains in the brush border membrane of enterocytes. J Biol Chem 276:32338–32344

Helms JB, Zurzolo C (2004) Lipids as targeting signals: lipid rafts and intracellular trafficking Traffic 5:247–254

Hoekstra D, van Ijzendoorn SCD (2000) Lipid trafficking and sorting: how cholesterol is filling gaps. Curr Opin Cell Biol 12:496–502

Holthuis JC, Pomorski T, Raggers RJ, Sprong H, Van Meer G (2001) The organizing potential of sphingolipids in intracellular membrane transport. Physiol Rev 81:1689–1723

Huang H, Schroeder F, Zeng C, Estes MK, Schoer JK, Ball JM (2001) Membrane interactions of a novel viral enterotoxin: rotavirus nonstructural glycoprotein NSP4. Biochemistry 40:4169–4180

Isa P, Realpe M, Romero P, Lopez S, Arias CF (2004) Rotavirus RRV associates with lipid membrane microdomains during cell entry. Virology 322:370–381. Erratum in: Virology (2004) 328:158

Jayaram H, Estes MK, Prasad BV (2004) Emerging themes in rotavirus cell entry, genome organization, transcription and replication. Virus Res 101:67–81

Jourdan N, Maurice M, Delautier D, Quero AM, Servin AL, Trugnan G (1997) Rotavirus is released from the apical surface of cultured human intestinal cells through nonconventional vesicular transport that bypasses the Golgi apparatus. J Virol 71:8268–8278

Jourdan N, Brunet JP, Sapin C, Blais A, Cotte-Laffitte J, Forestier F, Quero AM, Trugnan G, Servin AL (1998) Rotavirus infection reduces sucrase-isomaltase expression in human intestinal epithelial cells by perturbing protein targeting and organization of microvillar cytoskeleton. J Virol 72:7228–7236

Kabcenell AK, Poruchynsky MS, Bellamy AR, Greenberg HB, Atkinson PH (1988) Two forms of VP7 are involved in assembly of SA11 rotavirus in endoplasmic reticulum. J Virol 62:2929–2941

Lawton JA, Estes MK, Prasad BV (2000) Mechanism of genome transcription in segmented dsRNA viruses. Adv Virus Res 55:185–229

Lipardi C, Nitsch L, Zurzolo C (2000) Detergent-insoluble GPI-anchored proteins are apically sorted in Fischer rat thyroid cells, but interference with cholesterol or sphingolipids differentially affects detergent insolubility and apical sorting. Mol Biol Cell 11:531–542

Lopez S, Arias CF (2004) Multistep entry of rotavirus into cells: a Versaillesque dance. Trends Microbiol 12:271–278

Maass DR, Atkinson PH (1990) Rotavirus proteins VP7, NS28, and VP4 form oligomeric structures. J Virol 64:2632–2641

Mathieu M, Petitpas I, Navaza J, Lepault J, Kohli E, Pothier P, Prasad BV, Cohen J, Rey FA (2001) Atomic structure of the major capsid protein of rotavirus: implications for the architecture of the virion. EMBO J 20:1485–1497

Mayor S, Riezman H (2004) Sorting GPI anchored proteins. Nat Rev Mol Cell Biol 5:110–120

Mirazimi A, Svensson L (1998) Carbohydrates facilitate correct disulfide bond formation and folding of rotavirus VP7. J Virol 72:3887–3892

Mirazimi A, von Bonsdorff CH, Svensson L (1996) Effect of brefeldin A on rotavirus assembly and oligosaccharide processing. Virology 217:554–563

Mirre C, Monlauzeur L, Garcia M, Delgrossi MH, Le Bivic A (1996) Detergent-resistant membrane microdomains from Caco-2 cells do not contain caveolin. Am J Physiol 271:C887–C889

Mohan KV, Som I, Atreya CD (2002) Identification of a type 1 peroxisomal targeting signal in a viral protein and demonstration of its targeting to the organelle. J Virol 76:2543–2547

Mostov KE, Verges M, Altschuler Y (2000) Membrane traffic in polarized epithelial cells. Curr Opin Cell Biol 12:483–490

Mostov K, Su T, ter Beest M (2003) Polarized epithelial membrane traffic: conservation and plasticity. Nat Cell Biol 5:287–293

Munro S (2003) Lipid rafts: elusive or illusive? Cell 115:377–388

Nava P, Lopez S, Arias CF, Islas S, Gonzalez-Mariscal L (2004) The rotavirus surface protein VP8 modulates the gate and fence function of tight junctions in epithelial cells. J Cell Sci 117:5509–5519

Nejmeddine M, Trugnan G, Sapin C, Kohli E, Svensson L, Lopez S, Cohen J (2000) Rotavirus spike protein VP4 is present at the plasma membrane and is associated with microtubules in infected cells. J Virol 74:3313–3320

Nickel W, (2003) The mystery of non classical protein secretion. A current view on cargo proteins and potential export routes. Eur J Biochem 270:2109–2119

Nguyen DG, Booth A, Gould SJ, Hildreth JE (2003) Evidence that HIV budding in primary macrophages occurs through the exosome release pathway. J Biol Chem 278:52347–52354

Obert G, Peiffer I, Servin AL (2000) Rotavirus-induced structural and functional alterations in tight junctions of polarized intestinal Caco-2 cell monolayers. J Virol 74:4645–4651

Parashar UD, Hummelman EG, Bresee JS, Miller MA, Glass RI (2003) Global illness and deaths caused by rotavirus disease in children. Emerg Infect Dis 9:565–572

Petrie BL, Graham DY, Hanssen H, Estes MK (1982) Localization of rotavirus antigens in infected cells by ultrastructural immunocytochemistry. J Gen Virol 63:457–467

Petrie BL, Estes MK, Graham DY (1983) Effects of tunicamycin on rotavirus morphogenesis and infectivity. J Virol 46:270–274

Polishchuk R, Di Pentima A, Lippincott-Schwartz J (2004) Delivery of raft-associated, GPI-anchored proteins to the apical surface of polarized MDCK cells by a transcytotic pathway. Nat Cell Biol 6:297–307

Prentice E, Jerome WG, Yoshimori T, Mizushima N, Denison MR (2004) Coronavirus replication complex formation utilizes components of cellular autophagy. J Biol Chem 279:10136–10141

Rajho Meerson N, Bello V, Delaunay J-L, Aït Slimane T, Delautier D, Lenoir C, Trugnan G, Maurice M (2000) Intracellular traffic of the ecto-nucleotide pyrophosphatase/phosphodiesterase NPP3 to the apical plasma membrane of MDCK and Caco-2 cells: apical targeting occurs in the absence of N-glycosylation. J Cell Sci 113:4193–4202

Ruiz MC, Cohen J, Michelangeli F (2000) Role of Ca 2+ in the replication and pathogenesis of rotavirus and other viral infections. Cell Calcium 28:137–149

Sanchez-San Martin C, Lopez T, Arias CF, Lopez S (2004) Characterization of rotavirus cell entry. J Virol 78:2310–2318

Sapin C, Colard O, Delmas O, Tessier C, Breton M, Enouf V, Chwetzoff S, Ouanich J, Cohen J, Wolf C, Trugnan G (2002) Rafts promote assembly and atypical targeting of a nonenveloped virus, rotavirus, in Caco-2 cells. J Virol 76:4591–4602

Sarnataro D, Campana V, Paladino S, Stornaiuolo M, Nitsch L, Zurzolo C (2004) PrP(C) association with lipid rafts in the early secretory pathway stabilizes its cellular conformation. Mol Biol Cell 15:4031–4042

Schuck S, Honsho M, Ekroos K, Shevchenko A, Simons K (2003) Resistance of cell membranes to different detergents. Proc Natl Acad Sci U S A 100:5795–5800

Simons K, Ikonnen E (1997) Functional rafts in cell membranes. Nature 387:569–572

Simons K, Vaz WLC (2004) Model systems, lipid rafts, and cell membranes. Annu Rev Biophys Biomol Struct 33:269–295

Singer SJ, Nicolson GL (1972) The fluid mosaic model of cell membranes. Science 175:720–731

Stirzaker SC, Poncet D, Both GW (1990) Sequences in rotavirus glycoprotein VP7 that mediate delayed translocation and retention of the protein in the endoplasmic reticulum. J Cell Biol 111:1343–1350

Struck DK, Lennarz WJ (1977) Evidence for the participation of saccharide-lipids in the synthesis of the oligosaccharide chain of ovalbumin. J Biol Chem 252:1007–1013

Suzuki H, Konno T, Numazaki Y (1993) Electron microscopic evidence for budding process-independent assembly of double-shelled rotavirus particles during passage through endoplasmic reticulum membranes. J Gen Virol 74:2015–2018

Svensson L, Finlay BB, Bass D, von Bonsdorff CH, Greenberg HB (1991) Symmetric infection of rotavirus on polarized human intestinal epithelial (Caco-2) cells. J Virol 65:4190–4197

Taylor JA, O'Brien JA, Lord VJ, Meyer JC, Bellamy AR (1993) The RER-localized intracellular rotavirus receptor: a truncated soluble form is multivalent and bind rotavirus particles. Virology 194:807–814

Trugnan G, Rousset M, Chantret I, Barbat A, Zweibaum A (1987) The posttranslational processing of sucrase-isomaltase in HT-29 cells is a function of their state of enterocytic differentiation. J Cell Biol 104:1199–1205

Xu A, Bellamy AR, Taylor JA (2000) Immobilization of the early secretory pathway by a virus glycoprotein that binds to microtubules. EMBO J 19:6465–6474

Zarate S, Cuadras MA, Espinosa R, Romero P, Juarez KO, Camacho-Nuez M, Arias CF, Lopez S (2003) Interaction of rotaviruses with Hsc70 during cell entry is mediated by VP5. J Virol 77:7254–7260

Subject Index

Current Topics in Microbiology and Immunology

Volumes published since 1989 (and still available)

Vol. 264/II: **Hacker, Jörg; Kaper, James B. (Eds.):** Pathogenicity Islands and the Evolution of Microbes. 2002. 24 figs. XVIII, 228 pp. ISBN 3-540-42682-5

Vol. 265: **Dietzschold, Bernhard; Richt, Jürgen A. (Eds.):** Protective and Pathological Immune Responses in the CNS. 2002. 21 figs. X, 278 pp. ISBN 3-540-42668X

Vol. 266: **Cooper, Koproski (Eds.):** The Interface Between Innate and Acquired Immunity, 2002. 15 figs. XIV, 116 pp. ISBN 3-540-42894-X

Vol. 267: **Mackenzie, John S.; Barrett, Alan D. T.; Deubel, Vincent (Eds.):** Japanese Encephalitis and West Nile Viruses. 2002. 66 figs. X, 418 pp. ISBN 3-540-42783X

Vol. 268: **Zwickl, Peter; Baumeister, Wolfgang (Eds.):** The Proteasome-Ubiquitin Protein Degradation Pathway. 2002. 17 figs. X, 213 pp. ISBN 3-540-43096-2

Vol. 269: **Koszinowski, Ulrich H.; Hengel, Hartmut (Eds.):** Viral Proteins Counteracting Host Defenses. 2002. 47 figs. XII, 325 pp. ISBN 3-540-43261-2

Vol. 270: **Beutler, Bruce; Wagner, Hermann (Eds.):** Toll-Like Receptor Family Members and Their Ligands. 2002. 31 figs. X, 192 pp. ISBN 3-540-43560-3

Vol. 271: **Koehler, Theresa M. (Ed.):** Anthrax. 2002. 14 figs. X, 169 pp. ISBN 3-540-43497-6

Vol. 272: **Doerfler, Walter; Böhm, Petra (Eds.):** Adenoviruses: Model and Vectors in Virus-Host Interactions. Virion and Structure, Viral Replication, Host Cell Interactions. 2003. 63 figs., approx. 280 pp. ISBN 3-540-00154-9

Vol. 273: **Doerfler, Walter; Böhm, Petra (Eds.):** Adenoviruses: Model and Vectors in VirusHost Interactions. Immune System, Oncogenesis, Gene Therapy. 2004. 35 figs., approx. 280 pp. ISBN 3-540-06851-1

Vol. 274: **Workman, Jerry L. (Ed.):** Protein Complexes that Modify Chromatin. 2003. 38 figs., XII, 296 pp. ISBN 3-540-44208-1

Vol. 275: **Fan, Hung (Ed.):** Jaagsiekte Sheep Retrovirus and Lung Cancer. 2003. 63 figs., XII, 252 pp. ISBN 3-540-44096-3

Vol. 276: **Steinkasserer, Alexander (Ed.):** Dendritic Cells and Virus Infection. 2003. 24 figs., X, 296 pp. ISBN 3-540-44290-1

Vol. 277: **Rethwilm, Axel (Ed.):** Foamy Viruses. 2003. 40 figs., X, 214 pp. ISBN 3-540-44388-6

Vol. 278: **Salomon, Daniel R.; Wilson, Carolyn (Eds.):** Xenotransplantation. 2003. 22 figs., IX, 254 pp. ISBN 3-540-00210-3

Vol. 279: **Thomas, George; Sabatini, David; Hall, Michael N. (Eds.):** TOR. 2004. 49 figs., X, 364 pp. ISBN 3-540-00534X

Vol. 280: **Heber-Katz, Ellen (Ed.):** Regeneration: Stem Cells and Beyond. 2004. 42 figs., XII, 194 pp. ISBN 3-540-02238-4

Vol. 281: **Young, John A. T. (Ed.):** Cellular Factors Involved in Early Steps of Retroviral Replication. 2003. 21 figs., IX, 240 pp. ISBN 3-540-00844-6

Vol. 282: **Stenmark, Harald (Ed.):** Phosphoinositides in Subcellular Targeting and Enzyme Activation. 2003. 20 figs., X, 210 pp. ISBN 3-540-00950-7

Vol. 283: **Kawaoka, Yoshihiro (Ed.):** Biology of Negative Strand RNA Viruses: The Power of Reverse Genetics. 2004. 24 figs., IX, 350 pp. ISBN 3-540-40661-1

Vol. 284: **Harris, David (Ed.):** Mad Cow Disease and Related Spongiform

Encephalopathies. 2004. 34 figs., IX, 219 pp. ISBN 3-540-20107-6

Vol. 285: **Marsh, Mark (Ed.):** Membrane Trafficking in Viral Replication. 2004. 19 figs., IX, 259 pp. ISBN 3-540-21430-5

Vol. 286: **Madshus, Inger H. (Ed.):** Signalling from Internalized Growth Factor Receptors. 2004. 19 figs., IX, 187 pp. ISBN 3-540-21038-5

Vol. 287: **Enjuanes, Luis (Ed.):** Coronavirus Replication and Reverse Genetics. 2005. 49 figs., XI, 257 pp. ISBN 3-540-21494-1

Vol. 288: **Mahy, Brain W. J. (Ed.):** Foot-and-Mouth-Disease Virus. 2005. 16 figs., IX, 178 pp. ISBN 3-540-22419X

Vol. 289: **Griffin, Diane E. (Ed.):** Role of Apoptosis in Infection. 2005. 40 figs., IX, 294 pp. ISBN 3-540-23006-8

Vol. 290: **Singh, Harinder; Grosschedl, Rudolf (Eds.):** Molecular Analysis of B Lymphocyte Development and Activation. 2005. 28 figs., XI, 255 pp. ISBN 3-540-23090-4

Vol. 291: **Boquet, Patrice; Lemichez Emmanuel (Eds.)** Bacterial Virulence Factors and Rho GTPases. 2005. 28 figs., IX, 196 pp. ISBN 3-540-23865-4

Vol. 292: **Fu, Zhen F (Ed.):** The World of Rhabdoviruses. 2005. 27 figs., X, 210 pp. ISBN 3-540-24011-X

Vol. 293: **Kyewski, Bruno; Suri-Payer, Elisabeth (Eds.):** CD4+CD25+ Regulatory T Cells: Origin, Function and Therapeutic Potential. 2005. 22 figs., XII, 332 pp. ISBN 3-540-24444-1

Vol. 294: **Caligaris-Cappio, Federico, Dalla Favera, Ricardo (Eds.):** Chronic Lymphocytic Leukemia. 2005. 25 figs., VIII, 187 pp. ISBN 3-540-25279-7

Vol. 295: **Sullivan, David J.; Krishna Sanjeew (Eds.):** Malaria: Drugs, Disease and Post-genomic Biology. 2005. 40 figs., XI, 446 pp. ISBN 3-540-25363-7

Vol. 296: **Oldstone, Michael B. A. (Ed.):** Molecular Mimicry: Infection Induced Autoimmune Disease. 2005. 28 figs., VIII, 167 pp. ISBN 3-540-25597-4

Vol. 297: **Langhorne, Jean (Ed.):** Immunology and Immunopathogenesis of Malaria. 2005. 8 figs., XII, 236 pp. ISBN 3-540-25718-7

Vol. 298: **Vivier, Eric; Colonna, Marco (Eds.):** Immunobiology of Natural Killer Cell Receptors. 2005. 27 figs., VIII, 286 pp. ISBN 3-540-26083-8

Vol. 299: **Domingo, Esteban (Ed.):** Quasispecies: Concept and Implications. 2006. 44 figs., XII, 401 pp. ISBN 3-540-26395-0

Vol. 300: **Wiertz, Emmanuel J.H.J.; Kikkert, Marjolein (Eds.):** Dislocation and Degradation of Proteins from the Endoplasmic Reticulum. 2006. 19 figs., VIII, 168 pp. ISBN 3-540-28006-5

Vol. 301: **Doerfler, Walter; Böhm, Petra (Eds.):** DNA Methylation: Basic Mechanisms. 2006. 24 figs., VIII, 324 pp. ISBN 3-540-29114-8

Vol. 302: **Robert N. Eisenman (Ed.):** The Myc/Max/Mad Transcription Factor Network. 2006. 28 figs. XII, 278 pp. ISBN 3-540-23968-5

Vol. 303: **Thomas E. Lane (Ed.):** Chemokines and Viral Infection. 2006. 14 figs. XII, 154 pp. ISBN 3-540-29207-1

Vol. 304: **Stanley A. Plotkin (Ed.):** Mass Vaccination: Global Aspects -- Progress and Obstacles. 2006. 40 figs. IX, ... pp. ISBN 3-540-29382-5

Vol. 305: **Radbruch, Andreas; Lipsky, Peter E. (Eds.):** Current Concepts in Autoimmunity. 2006. 29 figs. IIX, 276 pp. ISBN 3-540-29713-8

Vol. 306: **William M. Shafer (Ed.):** Antimicrobial Peptides and Human Disease. 2006. 12 figs. XII, 262 pp. ISBN 3-540-29915-7

Vol. 307: **John L. Casey (Ed.):** Hepatitis Delta Virus. 2006. 22 figs. XII, 228 pp. ISBN 3-540-29801-0

Vol. 308: **Honjo, Tasuku; Melchers, Fritz (Eds.):** Gut-Associated Lymphoid Tissues. 2006. 24 figs. XII, 206 pp. ISBN 3-540-30656-0